

**OPTIMIZATION OF
SOLIDIFICATION/STABILIZATION FOR
PETROLEUM-BASED WASTE USING BLENDED
CEMENT**

ASNA BINTI MOHD ZAIN

**FACULTY OF ENGINEERING
UNIVERSITY OF MALAYA
KUALA LUMPUR**

2013

**OPTIMIZATION OF SOLIDIFICATION/STABILIZATION FOR
PETROLEUM-BASED WASTE USING BLENDED CEMENT**

ASNA BINTI MOHD ZAIN

**THESIS SUBMITTED IN FULFILMENT OF THE
REQUIREMENTS FOR THE DEGREE OF DOCTOR OF
PHILOSOPHY**

**FACULTY OF ENGINEERING
UNIVERSITY OF MALAYA
KUALA LUMPUR**

2013

UNIVERSITY OF MALAYA
ORIGINAL LITERARY WORK DECLARATION

Name of Candidate: Asna Binti Mohd Zain

Registration/Matric No.: KHA 080009

Name of Degree: Doctor of Philosophy (Thesis)

Title of Dissertation ("this Work"): **Optimization of solidification/stabilization of petroleum-based waste using blended cement.**

Field of Study: Hazardous Waste Management

I do solemnly and sincerely declare that:

- (1) I am the sole author/writer of this Work;
- (2) This Work is original;
- (3) Any use of any work in which copyright exists was done by way of fair dealing and for permitted purposes and any excerpt or extract from, or reference to or reproduction of any copyright work has been disclosed expressly and sufficiently and the title of the Work and its authorship have been acknowledge in this work;
- (4) I do not have any actual knowledge nor I ought reasonably to know that the making of this work constitutes an infringement of any copyright work;
- (5) I hereby assign all and every rights in the copyright to this Work to the University of Malaya ("UM"), who henceforth shall be owner of the copyright in this Work and that any reproduction or use in any form or by any means whatsoever is prohibited without the written consent of UM having been first had and obtained;
- (6) I hereby declare that the Work is based on my original work except for quotations and citation which have been duly acknowledge;
- (7) I also declare that it has not been previously or concurrently submitted for any other degree at UM or other institutions.

Candidate's Signature

Date

Subscribed and solemnly declared before,

Witness's Signature

Date

Name:

Designation:

ABSTRACT

Petroleum waste is categorized as scheduled waste, one of the hazardous wastes that must be disposed at a licensed treatment plant. Refinery sludge produced in bulk quantity requires substantial cost for treatment. Toxic substance in the waste can be immobilized using stabilization and solidification method to reduce contaminant solubility and leachability using Portland cement as a main binder. Solidified waste with contaminants release in leachate below the standard levels can be disposed off on-site or recovered with limited utilization for construction materials. The petroleum sludge contained significant volatiles organics and oil and grease forming oily globules in thick sludge. Portland cement mainly composed of tricalcium silicate and dicalcium silicate. The cement to the sludge and water to cement ratios of 8 and 0.45 accordingly was used as the design parameters to investigate the effect of cement replacement materials at 5, 10 and 15 % weight. The cement replacement materials are condensed silica fume (CSF), fly ash (FA), activated carbon (AC), rice husk ash (RHA) and metakaolin (MK). RHA was the best binder of all cement replacement materials with 5 % weight achieved optimum strength of 28.34 N/mm². Similarly, other binders' strengths were optimized at 5 % weight. The increase in permeable porosity was in tandem with the rise of cement to the sludge ratio, while a contradictory effect was observed in the lower water to cement ratio. Isostrength peak was maximized at higher water to cement ratio of 0.45 in tandems with porosity but reversing effect occurs at the lower ratio. Prominent isostrength peak was observed with the inclusion of 5 % weight of cement replacement material for all binders. Inclusion of 5 % weight CSF, FA and MK in solidified sludge have resulted in the increased of micropore volume. Average pore size was also increased with cement replacement materials except FA. Minimum metals were leached out from of solidified sludge and solidified sludge with

cement replacement materials as determined by TCLP U.S. EPA SW-846 Method 1311. All toxic metals were below the applicable standard. Semi-dynamic leaching test of ANS 16.1 was employed as long term landfill leaching to determine leaching rate, diffusion coefficient and leachability index. Leaching rate of metals signify the diffusion leaching. Dynamic leaching of metal diffusion was pH control. Leaching achieved equilibrium at pH 9.5 whereby acetate ions are dominating the solution in reducing redox potential. Leachability indexes of most metal were above 6 as a guidance limit for landfill application of the monolith. Leaching mechanisms were governed by wash-off and diffusion. All semi-dynamic metals released were below the applicable standard. The solidified OPC sludge has exhibited ettringite and amorphous C-S-H surface. Inclusion of sludge has changed the surface into more C-S-H and less ettringite with calcium as the main element. Cement replacement material has affected reduction in the calcium content due to the concurrent rise in carbon. Pozzolanic reaction in the solidified sludge has caused the reduction in silica. The main crystal in the solidified sludge was rhombohedron calcite, which were formed by carbonation reaction of C-S-H and C-H with CO₂ in the cement hydration product. Thermogravimetry analysis of solidified sludge has exhibited the active pozzolanic reaction at temperature of 300 to 500°C shown by the weight loss of Ca(OH)₂. Another significant weight loss was due to decomposition of carbonation product at temperature 500 to 800°C. Solidified sludge contained linear or branched aliphatic hydrocarbon. The reaction of silica and carboxylic acid with hydrocarbon formed cyclic siloxane and acid ester. ¹H-NMR exhibits alkyl group's hydrogen in the solidified sludge. Similar ¹H groups were present in the leachate but inclusive of aromatic proton. ¹³C-NMR indicates the presence of straight chain alkane's carbon in the solidified sludge. As a conclusion, the stabilization/solidification of petroleum sludge containing metal and organic volatiles with Portland cement is effective by the formation of low organic and

metal leachability with moderate unconfined compressive. The leachability levels were below the toxicity characteristic of Environmental Quality Act 2009 and U.S.EPA standard. The solidified sludge unconfined compressive strength was above the satisfactory U.S.EPA of 0.34 MPa limit.

University of Malaya

ABSTRAK

Sisa petroleum diklasifikasikan sebagai sisa terjadual, salah satu dari sisa berbahaya yang mesti dilupuskan ditapak pelupusan berlesen. Sludge penyulingan dihasilkan dalam kuantiti pukal memerlukan kos rawatan yang tinggi. Bahan berbahaya dalam sisa toksik boleh diikat menggunakan kaedah penstabilan dan pemejalan untuk mengurangkan kelarutan dan kelarutresapan bahan toksik menggunakan semen Portland sebagai pengikat utama. Sludge yang telah dipejalkan yang mempunyai pelepasan pencemaran dalam turasan dibawah nilai piawai boleh dilupuskan di dalam tapak binaan, atau digunapakai secara terhad bagi tujuan pembinaan. Sludge petroleum mengandungi sejumlah bahan organik meruwap, dan minyak dan gris membentuk bebola minyak dalam sludge yang pekat. Semen Portland terdiri terutamanya dari kalsium trisilika dan kalsium disilika. Nisbah semen kepada sludge dan air kepada semen 8 dan 0.45 telah diguna sebagai parameter asas untuk menyiasat kesan bahan pengantian semen pada 5, 10 dan 15 % berat. Bahan penggantian semen yang diguna ialah wasap silika termendak, abu terbang, karbon teraktif, metakaolin dan abu sekam padi. Abu sekam padi adalah pengikat terbaik dalam semua bahan penganti semen pada 5 % berat yang mencapai nilai kekuatan optima 28.34 N/mm^2 . Begitu juga bahan pengikat yang lain menunjukkan kekuatan optima masing-masing pada 5 % berat. Peningkatan dalam resapan keliangan selaras dengan kenaikan nisbah semen kepada sludge, selain dari itu kesan yang bertentangan dilihat pada nisbah air kepada semen yang rendah. Kemuncak garis kekautan sama telah mencapai maksima pada nisbah air kepada semen yang tinggi iaitu pada 0.45 selaras dengan keliangan tetapi kesan yang berlawanan berlaku pada nisbah yang rendah. Kemuncak garis kekuatan sama yang jelas dilihat pada penggunaan 5 % berat bahan gentian semen untuk semua jenis pengikat. Kemasukan 5 % berat wasap silika termendak, abu terbang and metakaolin dalam sludge dipejalkan telah menghasilkan

peningkatan dalam jumlah isipadu liang mikro. Purata saiz liang juga meningkat dengan adanya bahan gentian semen kecuali abu terbang. Sejumlah kecil logam telah di rembes keluar dari sludge dipejalkan dan sludge dipejal bersama bahan gentian semen yang ditentukan dengan TCLP U.S.EPA SW-846 kaedah 1311. Semua logam berbahaya adalah dibawah nilai piawai ditetapkan. Larutresap separa dinamik ANS 16.1 telah digunakan sebagai larutresap jangka panjang untuk menentukan kadar larutresap, pemalar difusi dan indek larutresap. Kadar larutresap logam menunjukkan larutresap jenis difusi. Difusi logam larutresap dinamik adalah dikawal oleh pH. Larutresap mencapai keseimbangan pada pH 9.5 yang mana ion acetat mendominasi larutan dalam keupayaan redox yang mengurang. Indek larutresap kebanyakan logam adalah dibawah 6, sebagai nilai tunjuk untuk penggunaan monolith di dalam tapak pelupusan. Mekanisma larutresap dikawal oleh wash-off dan difusi. Kesemua aras logam dalam larutresap separa dinamik adalah dibawah nilai piawai. Sludge dipejal menunjukkan permukaan etringit dan amorphous C-S-H. Kemasukan sludge telah mengubah permukaan menjadi lebih banyak C-S-H dan berkurangnya etringit dengan kalsium sebagai unsur utama. Bahan ganti semen telah mengakibatkan berkurangnya kandungan kalsium disebabkan peningkatan karbon yang berlaku dimasa yang sama. Tindakbalas pozzolan telah mengurangkan kandungan silika dalam sludge dipejal. Kristal utama dalam sludge dipejal adalah kalsit berbentuk rombohedron yang terhasil dari tindakbalas penkarbonan C-S-H dan C-H dengan CO₂ dalam hasil penghidratan semen. Analisa termogravimetrik sludge dipejal menunjukkan reaksi pozzolan yang aktif pada suhu 300 ke 500 °C ditunjukkan oleh kehilangan berat Ca(OH)₂. Kehilangan berat yang ketara juga terhasil dari penguraian produk pengkarbonan pada suhu 500 ke 800 °C. Sludge dipejal mengandungi hidrokarbon alifatik lurus dan bercabang. Tindakbalas silika dan asid karboksilik dengan hidrokarbon membentuk bulatan siloksan dan asid ester. ¹H-NMR menunjukkan hidrogen kumpulan alkil dalam sludge

dipejal. Sama juga kumpulan ^1H hadir dalam turasan, tapi termasuk proton aromatik. ^{13}C -NMR menunjukkan kehadiran karbon alkane rantai lurus dalam sludge dipejal. Sebagai kesimpulan, penstabilan/ pemejalan sludge petroleum mengandungi logam dan organic meruwap dalam semen Portland adalah berkesan dengan membentuk larutresap organic dan logam yang rendah dengan nilai kekuatan tekanan tak terkurung yang sederhana. Nilai larutresap adalah dibawah sifat toksik pada nilai piawai Environmental Quality Act 2009 dan U.S.EPA. Kekuatan tekanan tak terkurung sludge dipejal adalah melebihi nilai memuaskan U.S.EPA iaitu 0.34 MPa.

ACKNOWLEDGEMENT

Alhamdulillah, praise to the Almighty for all the strength to carry out this work with the help of people as individuals or organizations that have contributed to the research in certain way.

The author wishes to express her sincere gratitude to the supervisors, Prof Dr Md Ghazaly Shaaban and Prof Dr Hilmi Mahmud for their constructive suggestions, encouragement and guidance throughout the course of this research. Each of them has contributed to the different field of expertise and areas of work for making meaningful research work.

Appreciation is acknowledged to the staff at concrete, SEM, safety, concrete material, GC, XRD laboratories, Ionic centre and Nanocens centre for the services and assistance in the experimental work. Very sincere thank to the staff at Civil Engineering Department, University of Malaya for the cooperation and assistance in the research work. Special thanks to Mrs Kalai for her helpful assistance in handling equipments and testing performance parameters.

The author also wishes to extend her gratitude to the IPS, University of Malaya and ExxonMobil for providing research grants, and Universiti Teknologi PETRONAS for granting the study leave and the financial support. The author wishes to express her gratitude to the industrial plants and manufacturers for providing the resource materials for the study which include PETRONAS Refinery, Lafarge Cement, BASF and TNB.

My honest appreciation to my parent and family members for their moral support and handfull spouse for bring the research work viable and fruitful. Last but not least, my sincerest thanks to all colleagues and friends, who have contributed directly and indirectly to the completion of this thesis.

TABLE OF CONTENTS

| | Page |
|---|--------|
| ORIGINAL LITERARY WORK DECLARATION | ii |
| ABSTRACT | iii |
| ABSTRAK | vi |
| ACKNOWLEDGEMENT | ix |
| TABLE OF CONTENTS | x |
| LIST OF FIGURES | xvi |
| LIST OF TABLES | xxi |
| LIST OF SYMBOLS AND ACRONYMS | xxiv |
| LIST OF APPENDICES | xxviii |
| | |
| CHAPTER 1.0 INTRODUCTION | |
| 1.1 Issues in Hazardous Waste from Petroleum Industry | 1 |
| 1.2 Problem Statements | 3 |
| 1.3 Objective of the Study | 4 |
| 1.4 Importance of the Study | 5 |
| 1.5 Limitation of the Study | 6 |
| 1.6 Outline of Thesis | 7 |
| | |
| CHAPTER 2.0 LITERATURE REVIEW | |
| 2.1 Hazardous Waste Management | 8 |
| 2.2 Stabilization and Solidification | 10 |
| 2.3 Binders Material | 12 |
| 2.3.1 Cement | 12 |
| 2.3.2 Modified clay | 13 |

| | | |
|---------|---|----|
| 2.3.3 | Pozzolans | 14 |
| 2.3.4 | Lime | 14 |
| 2.3.5 | Thermoplastics | 15 |
| 2.3.6 | Organic polymer | 15 |
| 2.4 | Cement Replacement Materials | 17 |
| 2.4.1 | Condensed silica fume | 19 |
| 2.4.2 | Fly ash | 20 |
| 2.4.3 | Activated carbon | 21 |
| 2.4.4 | Metakaolin | 22 |
| 2.4.5 | Rice husk ash | 23 |
| 2.5 | Petroleum Waste | 24 |
| 2.5.1 | Contaminant in refinery waste | 24 |
| 2.5.2 | Specific pollutants in refinery sludge | 24 |
| 2.6 | Mixing Water | 27 |
| 2.7 | OPC Stabilization/Solidification of Waste | 27 |
| 2.7.1 | Factors and mechanisms of cement immobilization | 29 |
| 2.7.2 | Interference in cement | 35 |
| 2.7.2.1 | Organic interference | 38 |
| 2.7.2.2 | Inorganic interference | 39 |
| 2.7.2.3 | Interference adjustment | 39 |
| 2.7.3 | Pretreatment or precondition of organic/inorganic waste | 40 |
| 2.7.4 | Performance of solidified cement | 41 |
| 2.7.4.1 | Leachability of solidified waste | 42 |
| 2.7.4.2 | Leaching mechanism | 45 |
| 2.7.4.3 | Strength and porosity | 47 |
| 2.8 | Regulatory Requirement of S/S | 50 |

| | | |
|------|--|----|
| 2.9 | Safety and Health Aspects | 51 |
| 2.10 | Long Term Durability of Solidified Waste | 53 |
| 2.11 | Critical Review | 54 |

CHAPTER 3.0 MATERIALS AND METHODS

| | | |
|---------|---|----|
| 3.1 | Introduction | 55 |
| 3.1 | Materials | 57 |
| 3.1.1 | Waste | 57 |
| 3.1.2 | Binders | 57 |
| 3.1.2.1 | Ordinary Portland cement | 57 |
| 3.1.2.2 | Rice husk ash | 57 |
| 3.1.2.3 | Metakaolin | 58 |
| 3.1.2.4 | Activated carbon | 58 |
| 3.1.2.5 | Fly ash | 58 |
| 3.1.2.6 | Condensed silica fume | 59 |
| 3.1.3 | Chemicals | 59 |
| 3.1.4 | Water | 59 |
| 3.1.5 | Mould | 59 |
| 3.2 | Methods | 60 |
| 3.2.1 | Characterization of sludge | 60 |
| 3.2.1.1 | Chemical properties | 60 |
| 3.2.1.2 | Physical properties | 61 |
| 3.2.1.3 | Microstructure analysis | 61 |
| 3.2.2 | Characterization of Portland cement and binders | 61 |
| 3.2.3 | Synthetic metals | 62 |
| 3.2.4 | Mix design of solidified OPC and waste | 62 |

| | | |
|---------|--|----|
| 3.2.5 | Leachability of solidified waste | 62 |
| 3.2.5.1 | Toxicity leaching characteristic procedure | 63 |
| 3.2.5.2 | Semi-dynamic leaching | 64 |
| 3.2.6 | Strength of solidified waste | 64 |
| 3.2.7 | Porosity of solidified waste | 65 |
| 3.2.8 | Microstructure of solidified waste | 65 |
| 3.2.9 | Organic analysis of solidified sludge | 66 |
| 3.2.10 | Experimental design | 67 |
| 3.2.11 | Statistical analysis | 69 |

CHAPTER 4.0 RESULTS AND DISCUSSION

| | | |
|---------|---------------------------------------|----|
| 4.1 | Waste Characterization | 70 |
| 4.1.1 | Physical properties of raw sludge | 70 |
| 4.1.2 | Chemical properties | 71 |
| 4.1.3 | Microstructure of petroleum sludge | 75 |
| 4.1.4 | Conclusions of waste characterization | 76 |
| 4.2 | Binders Characterization | 77 |
| 4.2.1 | Physical properties | 77 |
| 4.2.2 | Chemical properties | 78 |
| 4.2.3 | Microstructure | 81 |
| 4.2.3.1 | Ordinary Portland cement | 81 |
| 4.2.3.2 | Fly ash | 82 |
| 4.2.3.3 | Condensed silica fume | 82 |
| 4.2.3.4 | Rice husk ash | 83 |
| 4.2.3.5 | Metakaolin | 84 |
| 4.2.3.6 | Activated carbon | 84 |
| 4.2.3.7 | Conclusions | 86 |

| | | |
|---------|---|-----|
| 4.2.4 | Binders crystallization | 86 |
| 4.2.5 | Fourier Transform Infrared analysis | 89 |
| 4.2.6 | Thermogravimetry analysis of binders | 92 |
| 4.2.7 | Conclusions of binder characterization | 95 |
| 4.3 | Cement Paste Properties | 95 |
| 4.3.1 | Setting time | 96 |
| 4.3.1.1 | Effect of water to cement ratio | 96 |
| 4.3.1.2 | Effect of cement to sludge ratio | 99 |
| 4.3.1.3 | Effect of CRMs to solidified sludge | 100 |
| 4.3.2 | Workability | 103 |
| 4.3.3 | Conclusions of cement paste properties | 103 |
| 4.4 | Solidified Waste in OPC | 104 |
| 4.4.1 | Compressive strength | 104 |
| 4.4.1.1 | Baseline compressive strength | 104 |
| 4.4.1.2 | Compressive strength of OPC-sludge at different W/C | 107 |
| 4.4.1.3 | Strength of solidified OPC-sludge metal and RHA | 112 |
| 4.4.1.4 | Strength of solidified OPC-sludge with CRMs | 113 |
| 4.4.1.5 | Conclusions of UCS | 115 |
| 4.4.2 | Porosity | 116 |
| 4.4.2.1 | Porosity of OPC-sludge | 117 |
| 4.4.2.2 | Porosity of OPC-sludge with CRMs | 118 |
| 4.4.2.3 | Isostrength of solidified sludge with porosity and C/Sd | 120 |
| 4.4.2.4 | Isostrength of solidified sludge CRMs with porosity and CRMs | 124 |
| 4.4.2.5 | Pore size distribution of solidified waste | 127 |
| 4.4.2.6 | Conclusions of porosity | 134 |

| | | |
|---------|---|-----|
| 4.4.3 | Leachability of solidified sludge | 135 |
| 4.4.3.1 | Leachability simulated metals | 136 |
| 4.4.3.2 | Metals in TCLP of solidified OPC-sludge | 138 |
| 4.4.3.3 | Metals in TCLP of solidified OPC-sludge with CRMs | 141 |
| 4.4.3.4 | Semi-dynamic leaching test | 144 |
| 4.4.3.5 | Conclusions of leachability study | 172 |
| 4.4.4 | Microstructure of solidified sludge | 174 |
| 4.4.4.1 | SEM of solidified sludge, metal and RHA | 174 |
| 4.4.4.2 | FESEM of Solidified sludge with CRMs | 177 |
| 4.4.4.3 | X-Ray diffraction of solidified sludge | 181 |
| 4.4.4.4 | Thermogravimetry of solidified sludge | 187 |
| 4.4.4.5 | Conclusions of microstructure properties | 195 |
| 4.4.5 | Organic analysis | 196 |
| 4.4.5.1 | Microscale solvent extraction | 197 |
| 4.4.5.2 | Solid phase microextraction | 197 |
| 4.4.5.3 | Oil and grease | 203 |
| 4.4.5.4 | Nuclear magnetic resonance of ^1H and ^{13}C | 204 |
| 4.4.5.5 | Conclusions of organic analysis | 208 |
| 4.5 | Applications of Solidified Sludge and Commercialization Potential | 209 |
| 4.6 | Application of S/S to Organic or Mixed Waste | 215 |

CHAPTER 5.0 CONCLUSIONS AND RECOMMENDATIONS

| | | |
|-----|-----------------|-----|
| 5.1 | Conclusions | 217 |
| 5.2 | Recommendations | 222 |

REFERENCES

APPENDICES

LIST OF FIGURES

| | Page |
|---|------|
| Figure 1.1: Refinery sludges sources | 2 |
| Figure 2.1: Hazardous waste strategy | 8 |
| Figure 2.2: Hydration products of cement (a) Portlandite (b) Ettringite (c) C-S-H (d) Monosulfate hydrate (Mehta and Monteiro, 2005) | 13 |
| Figure 2.3: Organic waste adsorbed to an organophilic clay (La Grega et al, 2001) | 14 |
| Figure 2.4: Schematic representation of cement hydration (La Grega et al, 2001) | 28 |
| Figure 2.5: Solubilities of metal hydroxides as a function of pH (Grasso, 1993) | 31 |
| Figure 2.6: Contaminant removal by (a) solubilisation and (b) diffusion (Suthersan, 1999) | 42 |
| Figure 2.7: Conceptual leached model of cement based waste form | 43 |
| Figure 3.1: Performance tests of solidified waste | 55 |
| Figure 3.2: Experimental flowchart of stabilization and solidification | 56 |
| Figure 3.3: Experimental design of S/S | 68 |
| Figure 4.1: (a) Volatile organic material and (b) TPH organic fraction in the sludge | 74 |
| Figure 4.2: Structure of aromatic alkenes | 75 |
| Figure 4.3: Photomicrographs of dried petroleum sludge at (a) 990x and 3000x | 76 |
| Figure 4.4: Binder materials in powder form | 78 |
| Figure 4.5: Metal concentration in raw binder leachate | 79 |
| Figure 4.6: Photomicrographs of OPC at (a) 1000x and (b) 2000x | 81 |
| Figure 4.7: Photomicrographs of fly ash at (a) 1000x and (b) 4000x | 82 |
| Figure 4.8: Photomicrographs of silica fume at (a) 2000x and (b) 4000x | 83 |
| Figure 4.9: Photomicrographs of rice husk (a) raw at 1000x and (b) calcined at 1000x | 83 |
| Figure 4.10: Photomicrographs of metakaolin at (a) 1000x and (b) 5000x | 84 |

| | | |
|--------------|---|-----|
| Figure 4.11: | Photomicrographs of activated carbon at (a) 1000x and (b) 5000x | 85 |
| Figure 4.12: | Diffractograms of raw binder's spectrum for OPC, CSF and FA | 88 |
| Figure 4.13: | Diffractograms of raw binder's spectrum for AC, RHA and MK | 89 |
| Figure 4.14: | Infrared spectrum of binders (a) OPC, CSF, FA and (b) AC, MK and RHA | 90 |
| Figure 4.15: | Thermograms of binders (a) CSF (b) FA (c) AC (d) MK and (e) RHA | 92 |
| Figure 4.16: | OPC depth of penetration versus time | 97 |
| Figure 4.17: | Hydration of Portland cement (Cocke and Mollah, 1992; Mehta and Monteiro, 2006) | 98 |
| Figure 4.18: | OPC-sludge depth of penetration versus time | 99 |
| Figure 4.19: | CRM sludge depth of penetration versus time (a) CSF-Sd (b) FA-Sd (c) AC-Sd (d) MK-Sd and (e) RHA-Sd | 100 |
| Figure 4.20: | UCS of solidified petroleum sludge at different W/C ratio | 105 |
| Figure 4.21: | Contour and wireframe maps showing relationship of UCS with curing period and W/C ratio | 106 |
| Figure 4.22: | Contour and wireframe maps showing UCS of solidified petroleum sludge based on curing period and cement to sludge ratio | 106 |
| Figure 4.23: | UCS evolution for three batches of OPC-sludge at W/C (a) 0.4 (b) 0.45 and (c) 0.5 | 108 |
| Figure 4.24: | Residual plots of OPC-sludge mixed of W/C (a) 0.4 (b) 0.45 and (c) 0.5 | 111 |
| Figure 4.25: | Compressive strength of petroleum sludge with RHA | 113 |
| Figure 4.26: | UCS evolution of 5, 10 and 15 % OPC-sludge with CRMs (a) RHA (b) MK (c) AC (d) FA and (e) CSF | 114 |
| Figure 4.27: | Porosity of solidified OPC-sludge | 117 |
| Figure 4.28: | Porosity of solidified (a) RHA OPC-Sludge (b) MK OPC- Sludge (c) AC OPC Sludge (d) FA OPC-Sludge and (d) CSF | |

| | |
|---|-----|
| OPC-Sludge | 118 |
| Figure 4.29: Isostrength and its relationship with permeable porosity and cement to sludge ratio (a) W/C 0.4 (b) W/C 0.45 and (c) W/C | 122 |
| Figure 4.30: Isostrength and its relationship with percent CRMs and permeable porosity (a) CSF (b) FA (c) AC (d) MK and (e) RHA | 124 |
| Figure 4.31: Isotherm plot of solidified sludge | 127 |
| Figure 4.32: Isotherm plots of solidified sludge with 5 % weight CRMs (a) CSF (b) FA (c) AC (d) MK and (e) RHA | 128 |
| Figure 4.33: BJH cumulative adsorption pore volume of solidified sludge | 130 |
| Figure 4.34: BJH cumulative adsorption pore volume of solidified sludge with 5 % Weight CRMs (a) CSF (b) FA (c) AC (d) MK and (e) RHA | 131 |
| Figure 4.35: Leached metal in solidified sludge and RHA for (a) Cr and (b) Al | 137 |
| Figure 4.36: Oil and grease concentration leached from OPC-sludge | 138 |
| Figure 4.37: TCLP leachate of W/C 0.4 (a) metal concentration and (b) percent reduction | 139 |
| Figure 4.38: TCLP leachate of W/C 0.45 (a) metal concentration and (b) percent reduction | 140 |
| Figure 4.39: TCLP leachate of W/C 0.5 (a) metal concentration and (b) percent reduction | 140 |
| Figure 4.40: pH of solidified sludge | 141 |
| Figure 4.41: OPC-sludge TCLP metals leachate concentration for (a) CSF (b) FA (c) AC (d) RHA and (e) MK | 142 |
| Figure 4.42: pH of solidified sludge with CRMs | 144 |
| Figure 4.43: Solidified OPC-sludge 8045 leaching rate (a) Al, Cd and Cr (b) Cu, Mn and Fe (c) Ni, Pb and Zn | 146 |
| Figure 4.44: Leaching rate of solidified OPC-sludge CSF5 (a) Al, Cd and Cr (b) Cu, Fe and Mn (c) Ni, Pb and Zn | 147 |
| Figure 4.45: Leaching rate of solidified OPC-sludge FA5 (a) Al, Cd and | |

| | | |
|--------------|---|-----|
| | Cr (b) Cu, Fe and Mn (c) Ni, Pb and Zn | 148 |
| Figure 4.46: | Leaching rate of solidified OPC-sludge AC5 (a) Al, Cd and Cr (b) Cu, Fe and Mn (c) Ni, Pb and Zn | 149 |
| Figure 4.47: | Leaching rate of solidified OPC-sludge MK5 (a) Al, Cd and Cr (b) Cu, Fe and Mn (c) Ni, Pb and Zn | 150 |
| Figure 4.48: | Leaching rate of solidified OPC-sludge RHA5 (a) Al, Cd and Cr (b) Cu, Fe and Mn (c) Ni, Pb and Zn | 151 |
| Figure 4.49: | Cumulative fraction leached of metals in solidified sludge 8045 (a) Al, Cd and Cr (b) Cu, Fe and Mn (c) Ni, Pb and Zn | 159 |
| Figure 4.50: | Cumulative fraction leached of metals in solidified sludge CSF5 (a) Al, Cd and Cr (b) Cu, Fe and Mn (c) Ni, Pb and Zn | 160 |
| Figure 4.51: | Cumulative fraction leached of metals in solidified sludge FA5 (a) Al, Cd and Cr (b) Cu, Fe and Mn (c) Ni, Pb and Zn | 161 |
| Figure 4.52: | Cumulative fraction leached of metals in solidified sludge AC5 (a) Al, Cd and Cr (b) Cu, Fe and Mn (c) Ni, Pb and Zn | 162 |
| Figure 4.53: | Cumulative fraction leached of metals in solidified sludge MK5 (a) Al, Cd and Cr (b) Cu, Fe and Mn (c) Ni, Pb and Zn | 163 |
| Figure 4.54: | Cumulative fraction leached of metals in solidified sludge RHA5 (a) Al, Cd and Cr (b) Cu, Fe and Mn (c) Ni, Pb and Zn | 164 |
| Figure 4.55: | Accumulated leached metals concentration in solidified sludge 8045 (a) Al, Cd and Cr (b) Cu, Fe and Mn (c) Ni, Pb and Zn | 165 |
| Figure 4.56: | Accumulated leached metals concentration in solidified sludge CSF5 (a) Al, Cd and Cr (b) Cu, Fe and Mn (c) Ni, Pb and Zn | 166 |
| Figure 4.57: | Accumulated leached metals concentration in solidified sludge FA5 (a) Al, Cd and Cr (b) Cu, Fe and Mn (c) Ni, Pb and Zn | 167 |
| Figure 4.58: | Accumulated leached metals concentration in solidified sludge AC5 (a) Al, Cd and Cr (b) Cu, Fe and Mn (c) Ni, Pb and Zn | 168 |
| Figure 4.59: | Accumulated leached metals concentration in solidified sludge MK5 (a) Al, Cd and Cr (b) Cu, Fe and Mn (c) Ni, Pb and Zn | 169 |

| | | |
|--------------|--|-----|
| Figure 4.60: | Accumulated leached metals concentration in solidified sludge RHA5 (a) Al, Cd and Cr (b) Cu, Fe and Mn (c) Ni, Pb and Zn | 170 |
| Figure 4.61: | Photomicrographs of OPC-sludge at (a) 1000x and (b) 3000x | 175 |
| Figure 4.62: | Photomicrographs of OPC-sludge with metals at (a) 1000x and (b) 3000x | 175 |
| Figure 4.63: | Photomicrographs of OPC-sludge metals and RHA at (a) 1000x and (b) 3000x | 175 |
| Figure 4.64: | Photomicrographs of control OPC at W/C Of 0.45 at (a) 1000x and (b) 5000x | 176 |
| Figure 4.65: | Photomicrographs of solidified OPC-sludge 8045 at (a) 1000x and (b) 5000x | 177 |
| Figure 4.66: | Photomicrographs of OPC-sludge with CRMs and EDAX elemental analysis (a) CSF (b) FA (c) AC (d) RHA and (e) MK | 179 |
| Figure 4.67: | Diffractograms of solidified (a) OPC (b) OPC-sludge (c) OPC-CSF (d) OPC-FA (e) OPC-AC (f) OPC-MK and (g) OPC-RHA | 184 |
| Figure 4.68: | Thermograms of (a) Ca(OH) ₂ (b) OPC (c) hydrated OPC and (d) hydrated OPC-sludge | 188 |
| Figure 4.69: | Thermograms of hydrated OPC-sludge with (a) CSF (b) FA (c) AC (d) MK and (e) RHA | 191 |
| Figure 4.70: | Organic analysis flowchart | 196 |
| Figure 4.71: | SPME extraction and desorption of analyte | 198 |
| Figure 4.72: | Structure of leachate products (a) cyclonanosiloxane octadecamethyl (b) cyclooctasiloxane hexadecamethyl (c) propanoic acid, 2-methyl, 1-(1,1-dimethyl)-2 methyl 1-1,3-propanedyl ester and (d) heneicosane | 202 |
| Figure 4.73: | Oil and grease (a) concentration and (b) percent reduction in leachate | 204 |
| Figure 4.74: | Straight chain hydrocarbon with ¹³ C chemical shift in δ for AC5 | 208 |
| Figure 4.75: | The application of S/S on organic or mixed waste | 216 |

LIST OF TABLES

| | Page |
|--|-------------|
| Table 2.1: Centralized hazardous waste treatment facilities (adopted from Kualiti Alam S.B., 2003) | 9 |
| Table 2.2: Portland cement material (adopted from Mehta and Monteiro, 2006) | 12 |
| Table 2.3: Hydrated Portland cement and hydration product (adopted from Mehta and Monteiro, 2006) | 13 |
| Table 2.4: Waste compatibility with different types of binders (adopted from La Grega et al., 2001) | 16 |
| Table 2.5: CRMs and additives used in S/S processes (adopted from Paria and Yuet, 2006) | 18 |
| Table 2.6: Metal content found in crude oils (adopted from IPPP Bureau, 2001) | 25 |
| Table 2.7: Organic reactions in cement systems (adopted from Conner, 1990) | 35 |
| Table 2.8: Interference effects in cement (adopted from Conner, 1992; USEPA, 1993) | 37 |
| Table 2.9: Control measures in stabilization /solidification process (adopted from Conner, 1992) | 40 |
| Table 2.10: Extraction procedure for Crushed Block Leaching (CBL) | 44 |
| Table 2.11: U.S. EPA maximum TCLP extract and drinking water standard (adopted from Merit, 1996) | 50 |
| Table 2.12: Landfill criteria of Malaysian scheduled wastes (adopted from Kualiti Alam S.B., 2003) | 51 |
| Table 2.13: Lethal dose 50 % of volatile organics (adopted from IChemE, 2005) | 52 |
| Table 2.14: Toxicity rating of hazard levels (adopted from Martin et al, 2000) | 53 |
| Table 3.1: UK solidified waste performance characteristics (adopted from Sollars and Perry, 1989) | 68 |

| | | |
|-------------|--|-----|
| Table 4.1: | Sludge physical and chemical properties | 72 |
| Table 4.2: | Properties of detected volatiles contaminants in the sludge | 74 |
| Table 4.3: | Physical properties of selected binders | 77 |
| Table 4.4: | Composition of binders by EDAX analysis | 79 |
| Table 4.5: | Oxide of cement in percent weight and its abbreviation symbol | 80 |
| Table 4.6: | Potential cement composition | 80 |
| Table 4.7: | Microstructure properties of binders | 85 |
| Table 4.8: | Initial setting time for OPC | 97 |
| Table 4.9: | Initial setting time for the cement to sludge ratio | 100 |
| Table 4.10: | CRM-sludge initial setting time in minute | 103 |
| Table 4.11: | Maximum W/C ratio for various conditions (adopted from Beall and Jaffe, 2003) | 107 |
| Table 4.12: | Statistical analysis of OPC-sludge | 110 |
| Table 4.13: | Accumulated pore volume and average pore diameter | 134 |
| Table 4.14: | Average metals concentration leached in TCLP leachate of solidified OPC-sludge in mg/L | 139 |
| Table 4.15: | Average leached metal s concentration of solidified OPC-sludge CRMs in mg/L | 142 |
| Table 4.16: | Diffusion coefficient of metals leached in solidified OPC-sludge 8045 with CRMs in cm ² /sec in day 127 | 155 |
| Table 4.17: | Leachability index for solidified OPC-sludge | 156 |
| Table 4.18: | Regression analysis of log (B _t) versus log (t) for metals released | 171 |
| Table 4.19: | Percent reduction of solidified sludge with CRMs in semi-dynamic leaching | 172 |
| Table 4.20: | Elemental analysis of solidified sludge with 5 % weight CRMs | 181 |
| Table 4.21: | Thermogravimetry data for Ca(OH) ₂ , OPC and hydrated OPC | 190 |
| Table 4.22: | Thermogravimetry data for OPC-sludge with CRMs | 194 |
| Table 4.23: | SPME and GCMS operating parameters | 199 |
| Table 4.24: | Organic compound in the solidified sludge solid and leachate | 201 |

| | | |
|-------------|--|-----|
| Table 4.25: | Average chemical shifts of representative types of hydrogen (adopted from Brown, 2000) | 205 |
| Table 4.26: | ^1H -NMR proton chemical shifts in solidified sludge and leachate | 207 |
| Table 4.27: | ^{13}C -NMR in extracted solidified sludge | 208 |
| Table 4.28: | Cost estimation of waste S/S alternatives by Portland cement in U.S. dollar (adopted from Barth et al., 1990) | 214 |

University of Malaya

LIST OF SYMBOLS AND ACRONYMS

| | |
|-----------------------|---|
| AC | Activated carbon |
| ACGIH | American Conference of Governmental Industrial Hygienists |
| ANS | American Nuclear Society |
| APHA | American Public Health Association |
| API | American Petroleum Institute |
| ASTM | American Standard of Test Material |
| BET | Brunauer, Emmett and Teller |
| BTEX | Benzene, Toulene, Ethylbenzene, Xylene |
| CH | Calcium hydroxide, $\text{Ca}(\text{OH})_2$ |
| BJH | Barret-Joyner-Halenda |
| CaO | Lime |
| C_3A | Tricalcium aluminate, $3\text{CaOAl}_2\text{O}_3$ |
| C_4AF | Calcium alumina ferrite, $4\text{CaOAl}_2\text{O}_3\text{Fe}_2\text{O}_3$ |
| CBL | Crushed block leaching |
| CEC | Cation exchange capacity |
| CRMs | Cement replacement materials |
| C_3S | Tricalcium silicate, 3CaOSiO_2 |
| C_2S | Dicalcium silicate, 2CaOSiO |
| C/Sd | Cement to sludge ratio |
| CSF | Condensed silica fume |
| CP | Curing period |
| CPI | Corrugated plate interceptor |
| CRMs | Cement replacement materials |
| C-S-H | Hydrated calcium silicate |
| DAF | Dissolved air flotation unit |
| DEA | Diethanol amine |

| | |
|-------------------------------|---|
| DI | Deionize water |
| DMEA | Methyl diethanol amine |
| DWQA | Drinking water quality limit |
| EDAX | Energy dispersive X-ray |
| EPT | EP Tox |
| EU | European unions |
| FA | Fly ash |
| FCCU | Fluid catalytic cracker unit |
| FESEM | Field Environment Scanning Electron Microscope |
| FID | Flame Ionization Detector |
| FTIR | Fourier Transforms Infrared |
| FT-NMR | Fourier Transforms-Nuclear Magnetic Resonance |
| HA | Acetic acid solution |
| HCs | Hydrocarbons |
| HCB | Hexachlorobenzene |
| H ₂ O ₂ | Hydrogen peroxide |
| H ₂ S | Hydrogen sulphate |
| GC | Gas Chromatography |
| GCMS | Gas Chromatography Mass Spectrofotometer |
| ICP-OES | Inductively couple plasma atomic electronic spectrophotometer |
| LC ₅₀ | Lethal concentration 50 % |
| LD ₅₀ | Lethal dose 50 % |
| LPG | Liquefied petroleum gases |
| Li | Leachability index |
| LOI | Loss on ignition |
| MK | Metakaolin |
| MSE | Microscale solvent extraction |
| NMR | Nuclear magnetic resonance |

| | |
|-------|---|
| OPC | Ordinary Portland cement |
| ORP | Oxidation-reduction potential |
| OSHA | Occupational Safety and Health Act |
| PAH | Polycyclic Aromatic Hydrocarbons |
| PCBs | Polychlorinated Biphenyls |
| PDMS | Polymethylsiloxane |
| PEL | Permissible exposure limit |
| PC | Portland cement |
| PDI | Polydispersity index |
| PPE | Personal protective equipment |
| RHA | Rice husk ash |
| RCRA | Resource Conservation and Recovery Act |
| SEM | Scanning electron microscope |
| Sd | Sludge |
| SITE | Superfund Innovative Technology Evaluation |
| SPME | Solid phase microextraction |
| S/S | Stabilization and Solidification |
| TCE | Trichloroethylene |
| TMS | Tetramethylsilane |
| TPH | Total petroleum hydrocarbon |
| TCLP | Toxicity Characteristic Leaching Procedure |
| TTLC | Total threshold limit concentration |
| UCS | Unconfined compressive strength |
| UF | Urea formaldehyde |
| USEPA | United States Environmental Protection Agency |
| VOCs | Volatile organic compounds |
| SVOCs | Semi volatiles organic compounds |
| XRD | X-Ray Diffraction |

| | |
|-----|-----------------------|
| XRF | X-Ray Fluorescence |
| WBL | Whole block leaching |
| W/C | Water to cement ratio |
| WQL | Water quality limit |

University of Malaya

LIST OF APPENDICES

Appendix A: Physical properties of petroleum sludge

Appendix B: Chemical properties of petroleum sludge

Appendix C: Radar plots of TCLP

Appendix D: Calibration curve of volatile organic analysis

Appendix E: Toxicity characteristics of constituents

Appendix F: List of publications

University of Malaya

1.0 INTRODUCTION

1.1 Issues in Hazardous Waste from Petroleum Industry

Petroleum refining is one of the leading manufacturing industries. Worldwide there are in total about 700 refineries (IPPC Bureau, 2001) with 185 were located in the US and 100 in the EU countries, Switzerland and Norway. Oil and gas remain as the most important fuel in the economy to meet the energy demand although its important is declining in tandem with official policy to reduce the country's dependence on oil (Kamarudin and M Radzi, 2002).

As oil producer, Malaysia has five refineries for processing oil and gas into finished product of diesel, kerosene, jet oil, naphthalene and liquefied petroleum gas in peninsular Malaysia. Among the refineries stakeholder involves with oil processing are PETRONAS, Shell and ExxonMobil. According to Malaysian Investment Development Authority (MIDA), Malaysia has 100 trillion cubic feet of gas reserve at January 2007 (MIDA, 2007).

Source of the feed is local crude oil, mainly sweet and light crude with less sulfur compared to sour crude oil imported from gulf countries with more sulfur content. Processing of crude oil involve distillation of feed into different range hydrocarbon group which is extracted at different temperatures. The process use lots of water which form wastewater, namely oil-free water, accidentally contaminated wastewater from tank and process unit, and oil contaminated wastewater as illustrated in Figure 1.1. All of the wastewater is diverted to corrugated plate interceptor (CPI) except oil-free water to filter heavy material before pass-through oil skimmer forming grey water and recovered oil which is kept in slope oil tank. Grey water is pump to the dissolved air flotation unit (DAF)

for physically remove the remaining oil in water before wastewater is flowed to oxidation pond. Sludge is coming from slope oil tank, slump tank, which is stored in the sludge tank before sent to decanter 1 for moisture removal and decanter 2 to recover oil. Decanter 2 formed sludge cake, which is stored in drum awaiting collection to centralized treatment center. Sludge generation is estimated in range of 100 to 275 m³ per month for a refinery.

Every year large amount of waste is discharged from refinery, especially in form of sludge. The waste produced is classified under Quality Act (Scheduled Wastes) 1989 as hazardous waste and must be treated and disposed properly. The waste generation at refinery is estimated at 0.1 - 0.5 kg per tones of feed stock into the refinery plant (IPPC Bureau, 2001). The waste can be treated by stabilization and solidification (S/S) technology by immobilizes the toxic waste in cement matrix for final disposal in sanitary landfill or recovered as useful backfill materials. The application of S/S to industrial waste treatment helps to reduce the cost and toxicity simultaneously.

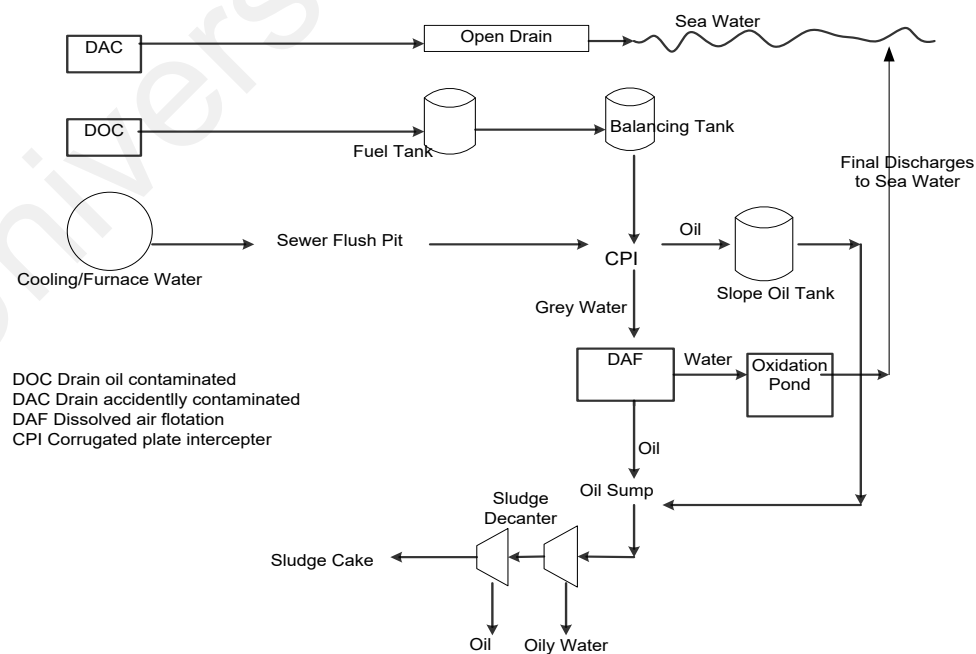


Figure 1.1: Refinery sludge sources

1.2 Problem Statements

The hazardous waste generation is produced in bulk quantity, which involves high cost for treatment, as the wastes are charge based on per ton basis. The waste should be treated and disposed of at a secured landfill. The facility for waste hazardous disposal is limited due to scarcity of available land plus public objection. Thermal destruction, the most efficient technology for organic waste becomes economically inconvenient as a formation of air pollution and inert ash residue still containing metals collected at the end of a long treatment process. The two faces of problem air and ash residue still need adoption of other cleaning systems like scrubber and leachate treatment. Leachate may contain highly toxic metals like mercury, lead, arsenic and volatiles compound such as benzene, toluene, ethyl benzene, xylene and polycyclic aromatic compounds that migrate into water bodies and this will cause the health problems to human beings. Air pollution may create global issues like ozone layer depletion causing global warming and weather changes as experienced by many countries. As a result lot of worst flood, extreme climate and disastrous wind turbulence recurs in so many regions that cause major damage to property, agriculture productivity and human loss.

The alternative of stabilization and solidification in hazardous waste for inorganic waste application was well established, but its application in organic waste require further investigation as it contains oil and grease and other organic compound that interfere with cement stabilization and solidification. Organic effect in cementation mechanism and its mixture with other additive is still a horizon for exploration albeit few researchers had put their effort to focus to certain pertaining aspects.

1.3 Objective of the Study

The objective of this study is to employ S/S method for the treatment of petroleum-based waste using blended cement. The main binder of ordinary Portland cement is blended with five cement replacement materials (CRMs) to enhance the S/S process. Experimental work involves characterization of the petroleum waste and binder materials properties. Treatability test was conducted to optimize the mix design parameters for the suitable binders/waste proportions. The performance of solidified waste form was investigated by unconfined compressive strength (UCS), leachability potential and porosity. The specific objectives of the study could be further defined as follows:

1. Characterize the physical, chemical and microstructure properties of sludge and binder materials.
2. Determine the optimum mix design parameters for S/S of waste. The design parameters used in the study include water to cement ratio, binder to sludge ratio and percentage of CRMs.
3. Determine the optimum composition of CRMs percentage to solidify and stabilized petroleum sludge using five CRMs namely condensed silica fume, fly ash, rice husk ash, metakaolin and activated carbon by referring to porosity and leachability.
4. Determine toxic substance immobilization of the solidified/stabilized waste by leachability study of toxicity characteristic leaching procedure (TCLP) and semi-dynamic leaching test. The leaching performance was evaluated based on the metals and organic contaminants' immobilization.

5. Investigate the microstructure properties of the solidified waste that contribute to high strength and low leachability monolithic.

1.4 Importance of the Study

Oil and hydrocarbon waste generation is one of the main hazardous waste generated in Malaysia (DOE, 2008). The waste contains metals, volatiles and semivolatiles organic compounds with toxic characteristics and referred to scheduled waste according to Environmental Quality Act 2005, which require proper treatment and disposal. The challenge of organic waste treatment is due to their properties of insolubility in water and other material due to the oil and grease content. The persistent of oily waste to the biodegradation process may prolong aquatic contamination. The stabilization and solidification process on oily waste as pretreatment may require adsorbent to enhance the fixation.

Organic waste has received less attention due to the interference effect to cement hydration as described by The Environmental Protection Agency (EPA) handbook (USEPA, 1986). Oil and grease affect cement reaction by inhibition and property alteration (Conner, 1990). Scientific study had been made to the organic waste stabilization and solidification as practices by EPA Superfund sites with 6 % organics and 31 % metal plus organic projects (USEPA, 2000). Previous research work focus to specific pollutant such as phenol (Vipulanandan, 1995; Vipulanandan and Krishnan, 1990), benzene, toluene, ethyl benzene and xylenes (Gitipour et al., 1997), chlorophenol compounds (Lo, 1996; Montgomery et al., 1991) and polycyclic aromatic hydrocarbon. Most of the previous works on organic stabilization and solidification have so far focus on the performance of solidified waste but fewer aspects of microstructure property were studied.

1.5 Limitation of the Study

Stabilization and solidification method is practically used for the treatment of industrial waste containing metals but the application for organic and mixed waste face difficulties due the interference effect from volatiles organic compounds. Other issues related to the organic waste associated with the toxic substance in the waste. Limitations of the S/S application for waste treatment are as follows:

1. The treated waste produced extensive waste volume. The binders used in the treatment process increase the requirement for final disposal space.
2. The application of waste treatment is subjected to the compatibility of waste and binder materials.
3. The application of S/S for hazardous waste requires approval or permission from the local authority.
4. The organic waste mechanism of interaction was not well discovered.
5. The long term effects of the solidified hazardous waste integrity is not been tested.
6. The performance of solidified waste was tested in laboratory environment may differ from the field test.

1.6 Outline of Thesis

The thesis was arranged by chapter sequence based on five main chapters. First chapter stated the introduction of the research which includes the issues in hazardous waste from petroleum industry, problem statement, objectives and importance of research study.

Chapter two presented literature reviews of the research topic covering the background information of hazardous waste management focus to research areas in stabilization and solidification. The fundamental theories lay behind the cementation process, factors involve and relevant binders applicable in stabilization and solidification are the gist in this chapter. The performance of treated waste and regulatory requirement from governing bodies is used to measure conformance of the finish products for industrial application.

Third chapter deliberated on the material used in conducting the research and method used in performing the sets of test parameters. The following chapter presents the result and discussion sought from the series of executed experimental work, which can be divided into four main sections, the waste and binder's characterization, durability and its leachability of solidified products, and the detail inspection of microstructure of solidified products. Durability of solidified waste was related to its porosity feature for finding its relationship with the waste content, and selected admixture incorporation.

Fifth chapter summarized the overall conclusion gathered from Chapter 4 for stabilization and solidification of petroleum waste in meeting the set objectives stated in Chapter 1. The recommendation was given to carry out further work on the related field for enhancement of the current work.

CHAPTER 2.0 LITERATURE REVIEW

2.1 Hazardous Waste Management

Rapid economic growth and industrialization have created toxic and hazardous substance pollution. The toxic substances may migrate to the receiving stream and contaminate drinking water if not properly treated and disposed. In considering waste management options the priority is in the following order:

Waste avoidance > waste reduction > waste separation/concentration > waste recovery >
waste treatment > secure ultimate disposal

Waste treatment strategies as in-plant alternatives are illustrated in Figure 2.1.

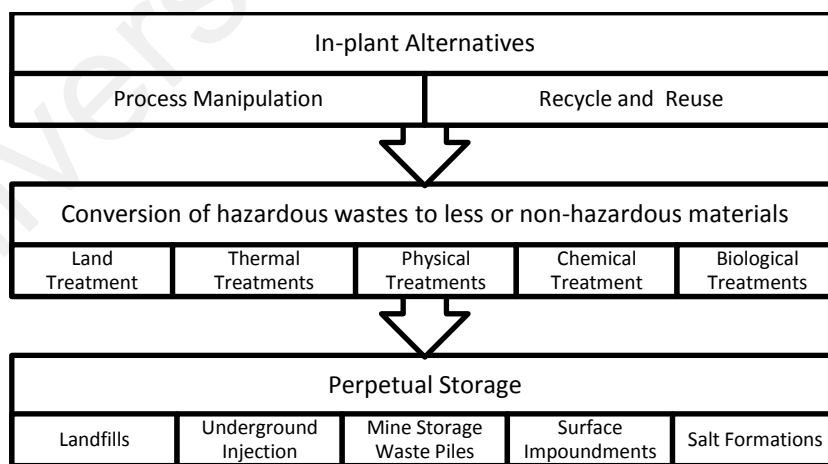


Figure 2.1: Hazardous waste strategy (Shaaban, 1993)

In order to prevent environmental degradation, Malaysian Department of Environment has introduced Scheduled Wastes regulation (Scheduled Wastes, 2005) to control the disposal of toxic wastes by adopting cradle to the grave tracking system on 107 scheduled waste classifications. In 2008, scheduled waste generation is exceeding one million metric ton, including the e-waste. Out of the total quantity, 45 % is treated onsite, less than 30 % (DOE, 2008) are being recycled and the remaining is treated offsite or sent to licensed disposal sites. Table 2.1 shows types of waste and criteria used for the treatment of hazardous waste.

Table 2.1: Centralized hazardous waste treatment facilities (adopted from Kualiti Alam S.B., 2003)

| <i>Method</i> | <i>Solidification plant</i> | <i>Incinerator plant</i> | <i>Physical/Chemical plant</i> | <i>Secure landfill</i> |
|---------------|--|--|---|--|
| Type of waste | 1. Sludge from oil storage tank with low oil and grease 2. Metal hydroxide sludge from wastewater treatment plant. 3. Residues from recovery of acid pickling liquor 4. Oxide or sulphate from wastewater treatment plant. 5. Fly ash trapped in fabric filter 6. Filter cake residue from physical /chemical plant | 1. Organic waste of mineral oil, solvent, pesticide and waste containing halogen /sulfur 2. Inorganic waste of metal hydroxide with high total organic carbon content | 1. Spent aqueous alkaline solution from metal and plastics surface 2. Spent aqueous alkaline solutions containing cyanide from metal and plastic surface 3. Spent aqueous chromic acid 4. Spent aqueous acid 5. Spent or discarded acid of $\text{pH} \leq 2$ | 1. Slag from rotary kiln 2. Solidification waste 3. External waste that fulfill the direct landfill criteria |

Based on a new clause in Regulation 7, Environmental Quality (Scheduled Wastes) 2005, a waste generator is allowed to apply to the Director General for permission to exclude scheduled wastes from being treated at prescribed premises if they are able to reduce scheduled waste according to specified maximum concentration TCLP, TTLC and hazards properties (DOE, 2005).

2.2 Stabilization and Solidification

Stabilization and solidification (S/S) have been widely used in hazardous waste treatment for industrial waste. It is used prior to land disposal to reduce toxic waste migration to soil and water table. The methods also been applied to contaminated soil in bulk quantity. Resource Conservation and Recovery Act (RCRA) in listed hazardous waste, identified S/S treatment as best demonstrated available technology for at least 57 commonly produced industrial waste and has selected the method for 26% of completed Superfund site remediation projects (USEPA, 1992). Stabilization may be used to treat hazardous waste prior to disposal (40 Code of Federal Regulation (CFR) Part 260). Land Disposal Restriction considered S/S as the required treatment for certain type of waste (40 CFR Part 268).

Stabilization is defined as the techniques that reduce the hazard potential of a waste by converting the contaminants into their least soluble, mobile or toxic (Conner, 1990). Stabilization is a process of binder and additives used with the objective to reduce the solubility or chemical reactivity of toxic waste by changing its chemical state or by physical entrapment (USEPA, 1986). Solidification refers to techniques that encapsulate the waste in a monolithic solid of high structural integrity. The encapsulation may involve

fine waste particles or large block of waste and encapsulation does not necessarily involve chemical interaction between waste and binder but mechanically bind the waste into the monolith (Conner, 1990). Solidification attempt to convert the waste into easily handled solid with reduced hazards from volatilization, leaching or spillage (USEPA, 1986). S/S is physicochemical process that can be combined in a process for hazardous waste treatment. S/S has been practiced long before 1970 in the primary four areas: (1) radioactive waste stabilization and disposal, (2) mine backfilling, (3) soil stabilization and grouting, and (4) production of stabilized base courses for road construction (Conner, 1994).

Radioactive waste which is classified as high-level waste and low-level waste is solidified by calcinations-solidification and cement/organic-solidification accordingly. Solidified radioactive waste will be disposed into final repository landfill overlay with impervious geomembrane layer to protect the leachate from migrating into the water table. Most of the low level radioactive waste was solidified by blended cement with other binders such as clay (Eskandar et al., 2011) or zeolite (El-Kamash et al, 2006). Mining activities deformed natural terrain and accumulate mine tailing with unstable soil condition. Land reclamation will induce sustainable development of the ex-mining area. Stabilization of the mining area can be made by mine backfilling using pozzolanic by-products such as fly ash (Senapati and Bishra, 2012) and cement (Peyronnard and Benzaazoua, 2012) as the material are abundant and economically feasible. Similarly soil stabilization and grouting used cement and pozzolanic material for soil improvement and reinforcement (Sina and Maassoumeh, 2012). Jet grouting is used for stabilization of soil underneath building or bridge (Ho, 1998). Asphalt, a mixture of bituminous material from refinery process is one of the base courses for road construction as well as blended cement, fly ash, slag and lime (Austroads, 2004).

2.3 Binder Materials

2.3.1 Cement

Ordinary Portland cement (OPC) is hydraulic cement capable of setting, hardening and remaining stable under water. Main component of OPC are tricalcium silicate (C_3S), dicalcium silicate (C_2S), tricalcium aluminate (C_3A) and tetracalcium aluminate ferric (C_4AF) as in Table 2.2. OPC reacts with water by forming calcium silicate hydrate (C-S-H), calcium hydroxide (CH), calcium sulfo-aluminate hydrate (ettringite of $C_6AS_3H_{32}$ or C_4ASH_{18}) and anhydrated clinker grain in solid forms shown by Table 2.3 and Figure 2.2 (Mehta and Monteiro, 2006). Cement is dissolved and precipitated when mixed with water and generate heat of hydration before hardens to monolithic mass.

Table 2.2: Portland cement material (adopted from Mehta and Monteiro, 2006)

| <i>Cement mineral</i> | <i>Structure</i> | <i>Percentage</i> | <i>Contribution</i> |
|-----------------------|----------------------|-------------------|---|
| C_3S | $3CaOSiO_2$ | 50 % | Reactive, high heat and high early strength |
| C_2S | $2CaOSiO$ | 25 % | Low heat and slow process |
| C_3A | $3CaOAl_2O_3$ | 10 % | High heat and high early strength |
| C_4AF | $4CaOAl_2O_3Fe_2O_3$ | 10 % | High early strength, set of cement |
| Gypsum, CSH_2 | $CaSO_4 \cdot 2H_2O$ | 5 % | |

Portland cement chemical reactions and heat of hydration (Equations 2-1 to 2-4):

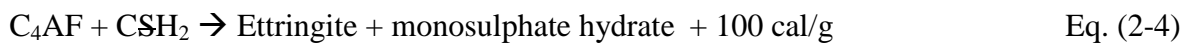
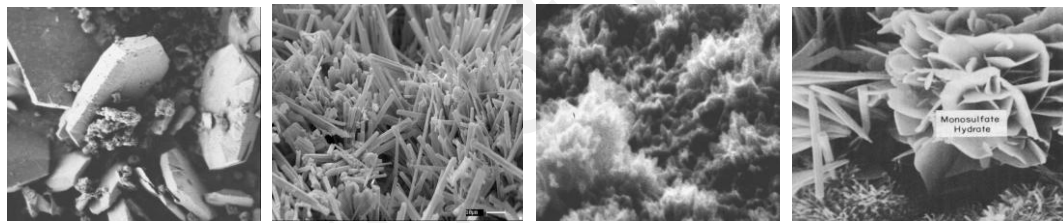


Table 2.3: Hydrated Portland cement hydration product (adopted from Mehta and Monteiro, 2006)

| <i>Hydrated products</i> | <i>Structure</i> | <i>Percent (%)</i> | <i>Significant property</i> |
|--|-------------------------|--------------------|---|
| C-S-H | Tobermorite gel | 50-60 | 100-700 m ² /g surface area, high strength |
| CH, portlandite | Large hexagonal-prism | 20-25 | Limited strength |
| Ettringite, C ₆ AS ₃ H ₃₂ | Needle shape crystal | 15-20 | Subject to sulphate attack, high early strength |
| Monosulfate hydrate, C ₄ ASH ₁₈ | Hexagonal plate crystal | | Final product of cement hydration containing > 5 % C ₃ A |



(a) Portlandite (b) Ettringite (c) C-S-H (d) Monosulfate hydrate

Figure 2.2: Hydration products of cement (a) Portlandite (b) Ettringite (c) C-S-H and (d) Monosulfate hydrate (Mehta and Monteiro, 2006)

2.3.2 Modified clay

Organically modified clays have been recently employed in conjunction with other stabilization reagents in order to entrap the organic portion of the waste to be stabilized. Microstructure study of organophilic clays containing organic waste and cement matrix inhibit early hydration product of ettringite (Montgomery, 1991). Organophilic clay is most promising option as an adsorbent for organics hazardous waste (Lo, 1996; Zhu et al., 2000;

La Grega et al., 2001) (Figure 2.3). Solidified samples prepared with Portland cement and modified clay improved the immobility of BTEX by 55 percent (Gitipour et al., 1997).

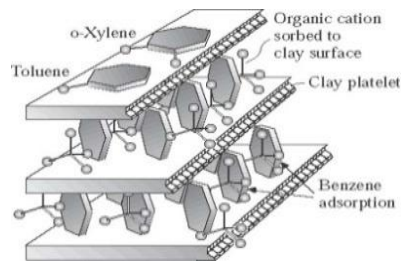


Figure 2.3: Organic waste adsorbed to an organophilic clay (La Grega et al., 2001)

2.3.3 Pozzolans

Pozzolan material reacts with lime in the presence of water to produce a cementitious material. The reaction of alumino-silicious material, lime and water results in the formation of concrete-like product termed pozzolanic concrete. Pozzolanic materials include fly ash, ground blast furnace slag and cement kiln dust. Pozzolans are more suitable for inorganic waste. Pozzolanic reactivity indicated by Ca(OH)_2 in mg contained per gram of pozzolan. Siddique (2008) quoted the pozzolanic activity by Asbridge et al. (2001) for silica fume, fly ash and metakaolin as 427, 875 and 1050 accordingly.

2.3.4 Lime

Calcium hydroxide, Ca(OH)_2 or lime, CaO , mixed with waste will form hydrates of calcium silicate, calcium alumina or calcium alumino-silicate. Lime is suitable for inorganic contaminant. Lime stabilization with waste material and water formed a chemically stable product when compacted has low water porosity that reduce leaching.

Lime-pozzolan cement had been used for treatment and delisting of hazardous waste containing metals such as hexavalent chromium, lead and cadmium (Shi, 2004).

2.3.5 Thermoplastics

Thermoplastic binders which include bitumen, paraffin and polyethylene are heated to disperse waste into the binder. The mixture is cooled to solidify the waste before it is buried in landfill. Thermoplastics involve no chemical reaction to form solid and not susceptible to failure. Bitumen was first used as binder for radioactive waste in 1960s (Kalb, 2004).

2.3.6 Organic polymer

Organic polymer trapped waste in sponge-like material in a wet or a dry batch treatment process. The commonly used polymer for the treatment is urea formaldehyde (UF). UF emulsion was used for low-level radioactive waste from the nuclear power plants with the additive of weak acid catalyst (Kalb, 2004).

The compatibility of waste component with four types of binders namely cement, pozzolan, thermoplastics and organic polymer are shown in Table 2.4 (La Grega et al., 2001). The table shows that oily waste may impede setting, and volatiles may escape during cementation process.

Table 2.4: Waste compatibility with different types of binders (adopted from La Grega, et al., 2001)

| <i>Waste component</i> | <i>Cement based</i> | <i>Pozzolan based</i> | <i>Thermoplastic</i> | <i>Organic polymer</i> |
|---|---|--|---|---|
| Nonpolar organics: oil & grease, aromatics HCs, halogenated HCs, PCBs | May impede setting, volatiles may escape | May impede setting, volatiles may escape | Organic may vaporize on heating | May impede setting, effective under certain condition |
| Polar organics: alcohols, phenols, organic acids, glycols | Phenol will retard setting | Phenol will retard setting | Organic may vaporize on heating | No effect on setting |
| Acids | Cement neutralize acid | Compatible | Can be neutralized before incorporation | Can be neutralized before incorporation |
| Oxidizers: Sodium hypochlorate, potassium permanganate, nitric acid, potassium dichromate | Compatible | Compatible | May cause matrix breakdown | May cause matrix breakdown |
| Salts: sulfates, halides, nitrates, cyanides | Increase setting time, decrease durability, sulphate may retard setting | Halides are easily leached and retard setting | Sulfate and halides may dehydrate and rehydrate, cause splitting | Compatible |
| Heavy metals: lead, chromium, cadmium, arsenic, mercury | Compatible, effective under certain condition | Compatible, effective on certain species, lead cadmium, chromium | Compatible, effective on certain species, copper, arsenic, chromium | Compatible, effective on arsenic |
| Radioactive materials | Compatible | Compatible | Compatible | Compatible |

2.4 Cement Replacement Materials

The usage of cement replacement materials (CRMs) can enhance or retard S/S process. S/S process must be cost effective by using low cost industrial byproduct in S/S (Stegemann and Zhou, 2008). S/S treatment offers the use of waste residue like coal power plant fly ash and kiln dust to treat hazardous waste. The chemical reactivity of the waste will determine the selection of binders and additives in S/S treatment.

Numerous CRMs used in S/S systems are activated carbon, organophilic clays (Montgomery, 1991), silica fumes (Asavapisit et al., 2001), slag, soluble silicates, fly ash, clays, and rice husk ash. CRMs blend with OPC will modify some properties of final product and normally used in range of 5 % to 20 %. Natural pozzolans and clays increase sorption of certain cation. The use of CRMs may give undesirable effect such as carbonaceous sorbent (carbon and cellulose) and oily waste may create pyrophoric waste.

Commercial binders are mixes of proprietary material use to bind specific types of waste. The proprietary material is formed by blending of CRMs, additives and OPC. Numerous proprietary material used in S/S process quoted by Paria and Yuet (2006) as reported by many researchers are presented in Table 2.5. CRMs and additives can increase compressive strength and reduce leachate metal concentration in industrial waste S/S (Tseng and Ho, 1986). The selection of suitable materials in the cement mixture depends on the nature of waste for stabilization and solidification process.

Table 2.5: CRMs and additives used in S/S processes (adopted from Paria and Yuet, 2006)

| <i>CRMs / Additives</i> | <i>References</i> |
|---|--|
| Gypsum + lime + fly ash | Gosh and Subbarao (1998) |
| Gypsum + lime + fly ash + H ₂ O ₂ | Dutre et al. (1999) |
| Pozzolan + lime; lime + kaolinite | Moon et al (2004) |
| Cement + lime | Dutre and Vandecasteele (1995); Dutree et al. (1998) |
| Cement + lime + H ₂ O ₂ | Vandecasteele et al. (2002) |
| Cement + H ₂ O ₂ | Fuessle and Taylor (2000) |
| Cement + iron | Miller et al. (2000); Leist et al. (2003); |
| Cement + lime + iron | Jing et al. (2003); Fuessle and Taylor (2004) |
| Cement + iron + H ₂ O ₂ | Voight et al. (1996) |
| Cement + fly ash | Palfy et al (1999) |
| Cement + Organophilic clay | Akhter et al. (1997) |
| | Shih and Lin (2003) |

Studies and demonstration project conducted on specific waste using commercial proprietary binders specifically formulated to achieve the S/S objective. The projects were conducted under EPA's Superfund Innovative Technology Evaluation (SITE) Program in December 1988. The application of OPC for waste S/S is summarized as follows:

1. Chemfix technologies tested on polychlorinated biphenyls (PCBs) and metals waste by using polysilicate of chemset c220 and dry calcium reagent (USEPA, 1991). Waste from petrochemical and industrial sludge was used with the content of below 15% oil and grease.
2. Geo-Con Inc. setup in-situ waste site cleanup of PCBs, volatile organics and metals contaminated soil (USEPA, 1990a). The proprietary used was HWT-20, which consist of modified smectite clay and soluble silicate at 15% and 5% accordingly to treat PCB and other volatile organics.

3. On-site treatment of soils contaminated with PCBs, metals and petroleum hydrocarbons (USEPA, 1990b) by Soliditech Inc. used Urrichem and proprietary additive, fly ash, kiln dust and cement to treat contaminated soil, filter cake and oily sludge. Portland cement was used to treat oily sludge by addition of 0.5 % Urrichem and 0.9 % proprietary additive.
4. Hazcon treated petroleum waste originated from American Petroleum Institute (API) separator sludge, slope oil emulsion and filter cake containing 9 to 10 % of trichloro-ethylene (TCE), toluene and benzene. Waste was stabilized by cement and chloranan (USEPA, 1989).

2.4.1 Condensed silica fume

Condensed silica fume (CSF) is non-crystalline silica in dry powder byproduct of silicon and ferrosilicon industries. CSF size is about 100 times finer than OPC with the average size of 0.1 to 0.2 μm spherical particles (ACI, 2006). CSF with high specific surface area will cause increase in water demand for concrete application. For every 1 m^3 of concrete, the increase in water demand per kilogram of silica fume added was about 1 liter (Malhotra and Mehta, 1996). CSF is found to accelerate cement hydration (FIP, 1988). CSF decreases permeability and increase sorption of metals and nonmetals (Mattus and Gilliam, 1994). Silica fume is used as cement replacement material and as addition to improve concrete properties (ACI, 2006; FIP, 1988).

Kuala Lumpur Twin Tower was build using high performance silica fume concrete which can received 80 MPa pressure. Higher SiO_2 content normally manufactured from silicon metal manufacturer. The incorporation of CSF of up to 15 % did not affect initial

setting but increase 50 % of final setting time (Ata and Vipulanandan, 1997). Ten percent by weight of CSF in OPC was found to increase the strength by 25 % at 29-day due to its pozzolanic beneficial effect (Asavapisit et al., 2001).

2.4.2 Fly ash

Fly ash grain size is 0.2 to 200 μm with most particles being larger than 1 μm with spherical, irregular or angular in shapes (Alonso and Wesche, 1991). Coal fly ash (FA) is a byproduct of pulverized coal combustion in thermal power plants. Major constituent of FA are silica, alumina, and oxides of calcium and iron. FA with class F exhibit pozzolanic properties whereas class C has pozzolanic and cementitious properties. According to ASTM C 618 Class F FA should have at least 70 % sum of the oxides ($\text{SiO}_2 + \text{Al}_2\text{O}_3 + \text{Fe}_2\text{O}_3$) and Class C FA has 50 % of the same oxides. FA is generally lower the setting of concrete (Malhotra and Mehta, 1996). FA can decrease permeability, increase mix fluidity and lower initial heat evolution (Mattus and Gilliam, 1994). FA suitable for concrete shall have not more than 34 % of the particles retained on the 45 μm sieve.

Low calcium class F FA application in concrete gives lower strength gain at early ages but increase in strength gain at final ages due to continuity of pozzolanic activity but high calcium class C FA strength development similar or more than OPC at early ages (Siddique, 2008). ACI report (2003) has quoted higher strength of FA compared to normal concrete recorded from 1 year (Lane and Best, 1982) which has made it suitable for application of high-performance concrete. Finer FA (3 % retained on sieve No. 325 with opening 45 μm) produced mortar with good strength and low porosity compared to coarse original FA (36 % retained on a sieve No. 325) when used as OPC replacement at 20 to 40 % by weight of binder (Rukzon and Chindaprasirt, 2008). Fly ash used in concrete

application should meet the fineness of 34 % weight retained on sieve No. 325 based on ASTM C 618 (U.S. Department of Transportation, 2012). Concrete with 50 % by weight of Class F FA achieved 40 MPa compressive strength at 28-day higher than the control mix with 26.4 MPa (Siddique, 2003). Generally, Portland cement-FA contained 30 % FA produced at the cement manufacturer. Aerated concrete using palm oil fuel ash as CRMs at 10 to 40 % in OPC produced significant strength development (Abdullah et al., 2006).

FA was also blended with lime, slag, gypsum for a wide application such as brick's wall, oil well cement, blocks production, aggregate and road construction (Bijen et al., 1991). Portland-FA cement containing 30 % FA with compressive strength of 40.7 MPa was used to stabilized/solidified lead and cadmium able to reduce leached metal ions to 0.1 mg/L and 0.005 mg/L accordingly (Ilic and Polic, 2005). A mix of 20 % FA and OPC able to prevent Cr (VI) leaching at 97.66 % efficiency within 48 hours (Pera et al., 1997).

2.4.3 Activated carbon

Activated carbon (AC) derived from carbonaceous material like coal, wood, coconut shell and peat. The activated carbon is thermally treated by steam at 800 to 1000°C to produce internal surface area from 500 to 1500 m²/g. The major portion of surface area is composed of micropore and mesopore. Coconut shell activated carbon exhibit a predominance of micropores of radius less than 20 Å. Powder activated carbon (PAC) has particle size smaller than 80 meshes U.S. sieve series.

Activated carbon was used to sorbs dissolved organics in hazardous waste (Barth et al., 1990), oil and grease or certain metals. Electric Power Research Institute (EPRI) treatability test program treated composites soil containing BTEX using a mix of 5 % and

10 % PAC with 12 % OPC resulted in approximately two orders of magnitude lower than the untreated soil. PAH concentration in the soil was also reduced by approximately 30 to 50 % (EPRI, 2004). Carbon is most commonly used stabilization agent for organics when using TCLP or other aqueous leaching test. Carbon OPC able to reduce 98 % of ethyl acetate in spike organic contaminated soil based on targeted constituent of 100 mg/kg (Conner, 1996).

2.4.4 Metakaolin

Metakaolin (MK) is a pozzolanic material formed from kaolinite clay by dehydroxylation under high temperature of 500°C to 800°C. Main constituents in MK are SiO₂ and Al₂O₃. Silica in MK reacts with Ca(OH)₂ to produce C-S-H gel whereas alumina reacts with CH to form alumina phase such as C₄AH₁₃, C₂ASH₈ and C₃AH₆ (Siddique, 2008). Malhotra and Mehta (1996) quoted commercial average particle size of MK is about 1.5 μm (Caldarone et al., 1994) and BET surface area of 20,000 m²/kg (Ambroise et al., 1994). Composition of 20 % MK OPC was found to prevent leaching of Cr (VI) with the efficiency of 98.95 % based on the initial weight 3.6 g Cr (VI) per kg of binders (Pera et al., 1997). Degree of pozzolanic reaction in 5 % MK cement is higher than 10 % or 15 % MK cement and in general is better than FA or CSF blended cement (Poon et al., 2001).

MK content in cement increase water demand and delay setting time can be seen at 20 % MK (Badogiannis et al., 2005). The inclusion of MK as cement replacement enhanced compressive strength at all ages, 20 % MK gives optimum long term strength with 82 MPa and 85 MPa for 28-day and 90-day accordingly (Wild et al., 1996).

Compressive strength increased with the increase of metakaolin content but the 10 % MK performing the best strength (Brooks and Johari, 2001; Poon et al., 2001).

Strength changes in MK cement were contributed by three factors namely filler effect, acceleration of OPC and pozzolanic effect (Wild et al., 1996). Filler effect act immediately and acceleration effect start within first 24 hours while pozzolanic effect occurred between 7 to 14 days where CH in cement was removed than generated by hydration. Reaction of MK with lime retarded in 14 to 28 days with the CH increased due to inhibiting layer formed at the MK particle.

2.4.5 Rice husk ash

Rice husk ash (RHA) is the agricultural byproduct from paddy planting activity. RHA is produced by high-temperature combustion forming amorphous silica. Out of 200 kg rice husk combusted only 25 % RHA is generated (Siddique, 2008). As agricultural waste, abundance rice husk is available at a cheaper cost to produce RHA it becomes an attractive cement replacement material. RHA is highly pozzolanic with average particle size of 6 to 10 μm and high internal surface area of 40,000 to 100,000 m^2/kg due to its microporous structure (Malhotra and Mehta, 1996). A higher burning temperature will produce higher silica content in RHA. Amorphous silica can be produced at temperature below 500°C under oxidized conditions for prolonged periods or up to 680°C with a hold times of less than a minute (Mehta, 1979).

It pozzolanic activity contributes to high strength and increase durability of concrete due to it silica content of more than 80 to 85 % (Siddique, 2008). RHA incorporation produce more C-S-H gel and less $\text{Ca}(\text{OH})_2$ due to reaction of RHA with Ca^+ and OH^- ions

(Yu et al., 1999). The 10 % RHA in Portland cement was found to reduce porosity and Ca(OH)_2 amounts in the interfacial zone compared to control cement (Zhang et al., 1996). Leaching and strength of OPC with 10, 20 and 30 % RHA for solidification/stabilization of lead contaminated soil at concentration 25,000 mg/kg was found in compliance the USEPA maximum concentration of 5 mg/kg and exceeding compressive strength limit of mortar (Yin et al., 2006).

2.5 Petroleum Waste

2.5.1 Contaminant in refinery waste

Refinery waste composed of two categories of materials:

1. Sludges

Combination of oily such as tanks bottoms, biotreatment sludges, interceptor sludges, wastewater treatment sludges, contaminated soils, desalter sludge; and oil spill debris, filter clay acid, tar rags, filter dust, packing, lagging, activated carbon.

2. Other refinery wastes

Other wastes include miscellaneous liquid, semi-liquid or solid wastes. Example of these waste are contaminated soil, spent catalysts from conversion processes, oily wastes, incinerator ash, spent caustic, spent clay, spent chemicals and acid tar.

2.5.2 Specific pollutants in refinery sludge

Refinery sludge is associated with hazardous substances due to the presence of identified pollutants under different classification, such as priority pollutant stipulated by legal requirement. The pollutants are deliberated as follows:

1. Metals

Toxic metals like cadmium, lead and mercury are found in final effluent. Highest cadmium recorded less than 5 µg/L is below the API guidelines of 26 mg/kg. Lead is found less than 50 µg/L compared to API guidelines of 300 mg/kg. Highest mercury in the final effluent is below 0.2 µg/L compared to the API guidelines of 17 mg/kg. Mercury is originated from crude oil with mean content of 1.98 ng/g of crude oil or 1.98 ppb (Jacob Consultancy Inc., 2002). Mercury is found in crude oil in form of elemental, dissolved organic mercury, inorganic mercury salt and adsorbed on suspended solid. Crude oil contained certain amount of metals as tabulated in Table 2.6.

Table 2.6: Metal content found in crude oils (adopted from IPPC Bureau, 2001)

| <i>Element</i> | <i>Concentration (ppm)</i> |
|----------------|----------------------------|
| V | 5.0 - 1500.0 |
| Ni | 3.0 - 120.0 |
| Fe | 0.04 - 120 |
| Cu | 0.2 - 12.0 |
| Co | 0.01 - 12.0 |
| Si | 0.1 - 5.0 |
| Ca | 1.0 - 2.5 |
| Mg | 1.0 - 2.5 |
| Zn | 0.5 - 1.0 |
| Al | 0.5 - 1.0 |
| Ce | 0.001 - 0.6 |
| Zr | 0.001 - 0.4 |
| Ti | 0.001 - 0.4 |
| Sn | 0.1 - 0.3 |
| Pb | 0.001 - 0.2 |
| Hg | 0.03 - 0.1 |
| B | 0.001 - 0.1 |
| Ga | 0.001 - 0.1 |
| Ba | 0.001 - .1 |
| Sr | 0.001 - 0.1 |

2. Polyaromatic hydrocarbons (PAH)

PAHs are inherent part of the overall refinery operations. Most of the PAH values were below the detectable limit.

3. Polychlorinated biphenyls (PCBs)

Most of refineries have tested PCBs below the detectable limit.

4. Miscellaneous wastewater pollutant loads

Miscellaneous pollutants like soil, catalyst, scale and rust and tank bottom are seasonal and it may sources from maintenance routine. Turnaround activity will produce fluid catalytic cracker unit (FCCU) catalyst residue, during offloading of spent catalyst or loading of fresh catalyst. Scale and rust from isolated areas or containment pad for exchanger bundle cleaning that are utilized in all refineries. Rust also generated from tank or vessel cleaning.

5. Other pollutants

Numerous pollutants in form of surfactants from cleaning material and antifoams, dissolved solid from boiler and cooling blow downs, salts from drier product and caustic from product treaters. Amines solvent used to remove H₂S in form of diethanol amine (DEA) and methyl diethanol amine (DMEA) from amine sump systems.

2.6 Mixing Water

Mixing water for the waste S/S similar for concrete or grout must be fit for drinking purposes. The impurities in water may affect strength development and setting of the cement paste. Slightly acidic or alkaline water are acceptable due to water shortage in many areas of the world (Mehta and Monteiro, 2006). Mixing water should be clean and free from substance which may affect concrete development and potable water is recommended or if not available distilled water should be used (ACI, 1995).

2.7 OPC Stabilization/Solidification of Waste

Cement based is used for slurry waste to form concrete. Schematic diagram of cement hydration is as shown in Figure 2.4. It used for spent catalytic cracker unit that form insoluble hydrates with the chalk present in cement mixture, which also gives beneficial fixation of heavy metals. Applicability of cement based is especially effective when the waste contained metals because at high pH, most metal compounds are converted into insoluble metal hydroxides. The insoluble products trapped by lattice incorporation into crystalline components of set cement (Glasser, 1993). Cement products, C-S-H gel has high surface area and responsible for the mechanical strength of hardened pastes (Shi, 2004). Cement based has various advantages (Spence and Caijun, 2004) which include low cost, long term stability, good impact and compressive strength. Cement, clay and lime based S/S of hazardous waste sludge is sufficiently and economically viable for small industrial waste generators (Marcos et al., 2007).

OPC and blended cement binders was used to study leaching behavior of alkanes and PAH in oil refinery sludge (Athenasious and Evangelos, 2007). Leaching behavior of

zinc, nickel and copper from refinery sludge was controlled by chemical equilibrium and surface complexation onto ferrihydrite at pH range of 2 to 12 (Karamalidis and Voudrias, 2007).

Characterization of tricalcium silicate hydration in the presence of heavy metals at different ages by X-ray diffraction (XRD), thermal analysis and nuclear magnetic resonance (NMR) found out that metal accelerate hydration process at an early period of C_3S hydration (Chen et al., 2007).

Sucrose additive gives retardation effect to waste-cement (containing 1% each of lead and zinc) mixture setting and sorbitol (alcohol) often employed as a water reducing plasticizer decrease the water needed to make the cement workable (Linghong et al., 2008). The immobilization of 56 % FA and 20 % waste sludge in cement matrix has increased the strength and stabilization rate of zinc, iron and manganese at pH 7 (Shefali et al., 2008).

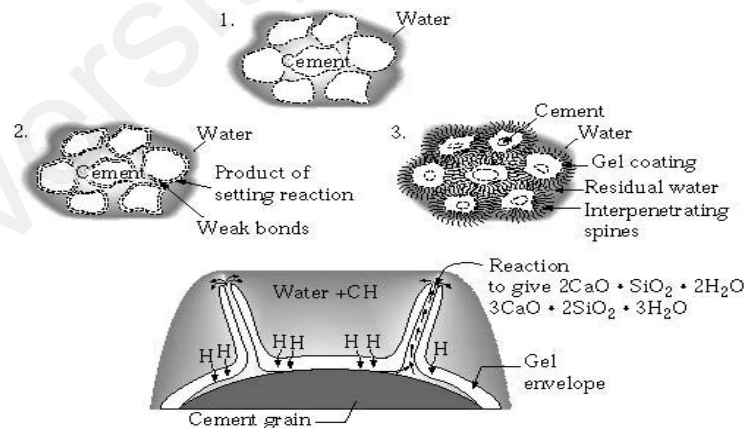


Figure 2.4: Schematic representation of cement hydration (La Grega et al., 2001)

Crude oil in kaolinite clay medium was stabilized by combination of additives which includes cement, lime, attapulgite clay and FA (Pamukcu, 1993). Based on his

finding the best highest UCS value of 115 kPa was reflected by the combination of 10 % cement, 10 % lime and 5 % attapulgite; and combination of 5 % cement, 10 % lime with 5 % FA also give high-strength value of 95.6 KPa. Another study based on synthetic sludge was tested with the present of organic interference with Portland cement, Portland cement with FA and lime with FA binders (Cullinane and Bricka, 1992).

Organic interferences incorporated in the study are phenol, oil, grease, trichloroethylene (TCE) and hexachlorobenzene (HCB). The addition of oil, grease and phenol reduce the strength of Portland cement binder, but addition of 0.08 of HCB to binder/sludge increased the UCS value. Higher concentration of the interference materials in cement/FA binders will reduce of the UCS value. Addition of 0.08 by weight ratio of phenol and oil individually reduced the UCS value by 90 % and 42 % accordingly. In lime/FA binders, the addition of interference material had a consistently negative impact on the UCS value except TCE and HCB. Concrete produced from refinery sludge has better strength at 10 % to 20 % of sludge mixing and in general, its strength is reduced after 20 % (Mohd Zain and Amran, 2008). The concrete developed (10 % sludge) are able to immobilize metals of Zn, Cu and Pb in a solidified cement matrix.

2.7.1 Factor and mechanisms of cement immobilization

Numerous factors affect immobilization of waste in Portland cement. Conner (1990) identified few important factors contributed to the immobilization process which include pH, redox potential, chemical reactions, adsorption, chemisorptions, passivation, ion exchange, diadochy, reprecipitation, encapsulation and alteration of physical change.

1. pH

pH directly control the fixation of waste during cement hydration, and thus control the leachability of the organic and inorganic species. The initial pH of aqueous cement solution is 12.4 at 18°C, which relate to the Ca:Si ratio of about 2.0, where the Ca(OH)_2 and C-S-H in solid mass was formed. In the mix of abundant silica from cementitious material like FA or CSF, the Ca(OH)_2 were consume by SiO_2 , which leads to reduction of Ca:Si ratio to about 1.0 (Spence, 1992). At this point, the pH was reduced to about 11 or less and abundant C-S-H and silica gel was formed. It was demonstrated that minimum leachability exist for Ca:Si ratio of 1.0, and increasing as the ratio is changed in either direction (Roy and Scheetz, 1992). The cement composition was governed by the ternary blend of CaO, SiO_2 and H_2O . The solubilities of metal hydroxides as a function of pH are illustrated in Figure 2.5 (La Grega et al., 2001). Metal that can be precipitated by hydrogen sulfide in acid solution is defined as heavy metal and have densities greater than 5 g/cm^3 (Radojevic and Baskin, 2006). Most of heavy metals are amphoteric. It is possible to produce minimum amount of metal in aqueous phase by adjusting pH. The optimum pH is usually in range of 8 to 11 (Cheng, 1991). Most of metal hydroxides have minimum dissolution at pH of 7.5 to 11.0 (Barth et al., 1990). The alkalinity in cement is controlled by lime, sodium carbonate, sodium hydroxide and magnesium hydroxide. Limestone and clay has an acid neutralizing capability that buffer the leachant pH changes (Conner, 1990).

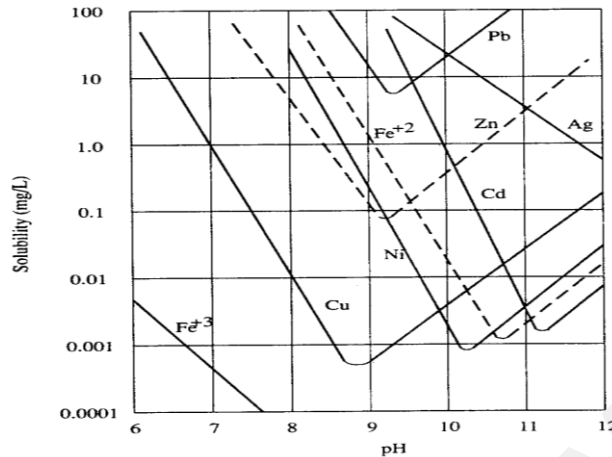


Figure 2.5: Solubility of metal hydroxides as a function of pH (Grasso, 1993)

2. Oxidation-reduction potential (ORP)

ORP in the waste was used to convert the valence state of metal species which affect their speciation and therefore their mobility. Metals were reduced to lower insoluble valence state for precipitation. Metals that have more than one valence state are As, Cr, Fe, Hg, Mn, Ni and Se, while non metal of sulfur have multiple valence state that affected the speciation of Ag, Cu, Cd and Zn. Usable reducing agent includes ferrous sulfate, sodium metabisulfite, sodium hydrosulfite and sulfides that help to reduce Cr^{6+} . Oxidizing agent like oxygen, ozone was rarely used for specific metals as organics like oil and grease also competing for the same oxidizing agent (Conner, 1990). Cement pore fluid has the internal oxidizing redox potential, E_h of +100 to +200 mV and addition of 40 to 50 % electroactive blast furnace slag in cement mix reduced the E_h to -350 to -450 mV (Spence, 1992). Similarly, waste containing organics and reactive metals able to reduce the E_h value. A low E_h provide favorable condition for immobilization of toxic wastes as well as in saturated landfill disposal.

3. Precipitation

Hydroxide precipitation occurs in cement hydration reaction is subject to pH control. Inorganic metal species are immobilized by forming carbonates, silicates, sulfates and non metal like cyanide, sulfate are precipitated as metal complexes. Fluoride can be immobilized as calcium salt. Lead waste in the calcite Portland cement produce lead precipitates identified as $\text{PbSO}_4(\text{CO}_3)_2(\text{OH})_2$, and $3\text{PbCO}_3 \cdot 2\text{Pb}(\text{OH})_2 \cdot \text{H}_2\text{O}$ that accumulated on surface solid waste forms, which hinder the ongoing hydration of underlying clinker material as detected by SEM/EDX and XRD analysis (Lee, 2004). Lead nitrate may alter the properties of solidified products and inhibit setting (Spence, 1992) or retard the waste and binder (Stegemann, 2005). Solubility of Al in the cement greatly reduced due to it preferentially bind with Ca to form hydrogarnet (Spence, 1992).

4. Adsorption/Chemisorption

C-S-H in cement provides adsorption by high specific surface area with a structure containing a block of calcium silicate layer with silicon at low state of polymerization. Irregular stacking of solid block, with each 10-100 nm create a large volume of micropores ranging from few to few tens of nanometer (Glasser, 1993). C-S-H surface area with high density of irregular hydrogen bonding, provide a strong potential for sorption. C-S-H with rich calcium has a positive surface charge and tends to adsorb anions but when Ca:Si ratio decrease, this surface charge gradually lessens until zero at Ca:Si ratio of 1.2 and become negative in lower Ca:Si ratio. This high SiO C-S-H is better sorbers for cationic species. Adsorption is commonly described in terms of Langmuir adsorption isotherm or Friedlich

isotherm. The adsorption of contaminant in forms of concentrated fluid on the surface of the cement matrix was greatly enhanced by activated carbon by chemical or physical forces. The molecule was held by a weak van der Waals force in physisorption. Chemisorption is binding of an adsorbate to the surface of solid by forces whose energy levels approximate those of a chemical bond, for example, organic compound on montmorillonite clay.

5. Passivation

Passivation is one of important mechanisms in cement fly ash system. Dissolved metal ions from solid surface precipitate on the surface after contacting anion in solution that forms a less soluble species. This mechanism is seen in reaction of gypsum with barium solution (Conner, 1990).

6. Ion exchange

Ion at the surface layer can exchange with other species in solution. Ion exchange occurs in natural or synthetic material and it is more important in cation exchangers as the ability of ion exchange is measured in cation exchange capacity (CEC). The magnitude is depended on the charge or hydrated cation and its size in solution. The surface charge may arise from ionization of hydroxyl groups attached to silicon atom or isomorphous substitution. Isomorphous substitution resulted from Al^{+3} , Fe^{+3} for Si^{-4} , or Mg^{+2} for Al^{+3} , forming fairly distributed surface charge of 2:1 clay particle of montmorillonite, beidellite and vermiculate. 1:1 clay particle has a lower surface charge coming from hydroxyl ionization (Conner, 1990).

7. Diadochy

Observe when one element substitutes for another similar size and charge in a crystalline lattice. The diadochy factor can be found in substitution of Zn or Mg for Ca in calcite.

8. Reprecipitation

Occurs when acid leachant dissolved alkali in solid matrix and cause localized acidic condition where metal hydroxide dissolved. Other mechanisms take place and reprecipitate the metal hydroxide. As a result of metal hydroxides dissolved, silica solubilized into silicate, and heavy metal competes with alkaline earth metal such as calcium for silicate and both precipitating heavy metal that interfere the cement setting (Conner, 1990).

9. Encapsulation

Most waste form in S/S treatment is hold by microencapsulation, and these particle occlusions and agglomeration can be easily viewed by scanning electron microscopy.

10. Alteration

Pretreatment to the waste by changing the properties of waste prior to the S/S to enhance the immobilization of waste, for example, the reduction of waste size, change of waste material into less soluble state or neutralize acidic waste.

The most likely reactions in organic S/S are adsorption, volatilization, reduction-oxidation, hydrolysis and salt formation (Conner, 1990). Some of the organic reactions occur in cement based system are listed in Table 2.7.

Table 2.7: Organic reactions in cement systems (adopted from Conner, 1990)

| <i>Reactions</i> | <i>Reactants</i> | <i>Products</i> |
|------------------|---|--|
| Hydrolysis | RX + H ₂ O | ROH + HX |
| | Organoaminos | Organics + NH ₃ |
| Oxidation | Phenol + 14H ₂ O ₂ + Fe ²⁺ | 6CO ₂ + 17H ₂ O |
| | R-CH ₃ | R-COOH |
| | R-CH ₂ OH | R-COOH |
| | RCHOH-CHOHR' | R-COOH + R'-COOH |
| | R-CHO | R-COOH |
| | R ₂ CH ₂ | R ₂ CO |
| | R ₂ CH(OH) | R ₂ CO |
| | R ₃ CH | R ₃ C(OH) |
| | R ₃ CH + HCR' ₃ | R ₃ -C-C-R' ₃ |
| | R ₂ N-H + H-NR' ₂ | R ₂ N-NR' ₂ |
| | RCH=CHR' | RCHOH-CHOHR' |
| | 2R-SH | R-S-S-R |
| | R-S-S-R' | R'SO ₃ H + RSO ₃ H |
| Reduction | Fe + 2H ₂ O + 2RCl | 2ROH + Fe ⁺² + 2Cl + H ₂ |
| Salt formation | Oxalic acid | Calcium oxalate |

2.7.2 Interference in cement

There are few groups of interference that act upon the cement reaction, physically or chemically. The action can be in forms of inhibition of bonding in waste material, retardation in setting, reduction in stability or reduction in physical strength of final product. Lists of interference's effects on the cement binders are given in Table 2.8. The interference must be carefully considered since the reaction may give significant impact to the final property of the concrete like strength, durability and leachability.

Specific study was conducted to find interference effect on cement-based waste forms. The interferences of numerous anionic and metallic species effect were summarized based on investigation of previous authors by Mattus and Gilliam (1994). Collective review of cement-based interference mechanisms has been done based on constituent, organic and inorganic (Abdul Majid et al., 1996); admixture effects on Portland cement/pozzolans products and waste effect on Portland cement/pozzolans process (Jones, 1990).

The interference effect may give adverse or beneficial outcome to the cement hydration. As the retardation of cement setting can provide time for cement paste application in the field work. On the contradictory the retardation to setting will expose the cement paste to leaching during wet season batching. The adverse interference requires solution viewed from many aspects such as composition of mixture, additional materials or pretreatment to the used waste material without compromise to the final solidified products quality or compliance to the legal requirement and at the same time should be cost effective.

Table 2.8: Interference effects to cement (adopted from Conner, 1992; USEPA, 1993)

| <i>Interference</i> | <i>Effect</i> |
|--|--|
| Semi volatile organic | Binding of waste |
| Oil and grease | Weaken the binding of waste and cement, inhibit setting and alteration of final product |
| Phenol, hexachlorobenzene, xylene | Weaken compressive strength, alteration of properties |
| Acid and bases | Retardation and property change |
| Chlorides | Accelerate by flocculation and disrupt matrix |
| Organics-nonpolar: Oil and grease, aromatic hydrocarbons, PCBs | Impede setting, retard setting, decrease durability, vaporization |
| Organics-polar: Alcohols, phenols, organic acids, glycols | Retard setting, decrease durability |
| Solid organics: plastics, tars, resins | Ineffective with UF polymers, retard setting of other polymer |
| Aliphatic and aromatic hydrocarbons | Increase setting time |
| Chlorinated organic/hydrocarbon | Increase set time, decrease durability, interfere cement hydration |
| Complex organics | Retard setting time |
| Presence of phenol and nitrates | Cannot be immobilize with lime/fly ash, cement, and soluble silicates; fly ash and cement; or bentonite and cement |
| Metals: Lead, chromium, cadmium, arsenic and mercury | May increase setting time of cement |
| Lead, tin and magnesium compound | Property change |
| Iron compounds | Retard and disrupt matrix |
| Metal salts and complexes | Increase set time and decrease durability for cement or clay/cement |
| Copper, lead and zinc | Detrimental effect on physical properties of cement-treated waste. |
| Copper nitrate | Retardation of set cement |
| Gypsum hydrate | Acceleration of set cement |
| Gypsum hemihydrates, lead nitrate | Inhibit setting |
| Silica | Setting/curing retardation |
| Sodium hydroxide, sodium sulfate and zinc nitrate | Property change interference |
| Halides | May retard setting, easily leach from cement and pozzolan waste, May dehydrate thermoplastics |

2.7.2.1 Organic interference

Petroleum waste has high oil and grease as well as other organics that hindered the setting or hydration of cement. The reactions observed are inhibition and alteration of physical properties of the cement paste. Oily waste requires sorbent to absorb the oil and practically the modified clay is used to carry this function. In neutral waste the pH is not a major concern, but the moisture content is very critical to ensure the waste is solidified. Organic waste also may remove volatile gases during the mixing, thus the pozzolans like fly ash able to delay the setting, moderate the heat of hydration and control the emission of vaporization. Interference mechanisms of organic compound in the solidified waste are identified as follows (Jones, 1990):

1. Adsorption of waste on surface that block normal hydration.
2. Complexation of the hydration product retards the setting.
3. Precipitation of phosphates, borates and oxalates at surface of hydrating material.
4. Nucleation inhibition by soluble silica and organic that retard tricalcium silicate hydration.

Some of the previous works on organic waste indicate the interference of organic in S/S, such as (Minocha et al., 2003) a range of organic compounds including oil and grease retarded setting and strength development and adversely influence the retention of metals in solidified metal sludge.

Trussel and Spence (1994) have identified potential interference of organic compound may be dependent on both concentration and the presence of other

contaminants. Organic acid has effect of acid attack on binders by solubilized their calcium salt from phenolic compounds, amines, amides and esters forming alcohol and carboxylic acids. Organic contaminants that purely bind by physical mechanism in cement may easily leach out especially if soluble in water and has low pKa. Organic interference of solidified/stabilized hazardous wastes using Portland cement was conducted based on SEM and XRD microstructure analysis (Eaton et al., 1987). They found that organic forms complex gel phase and revealed changes in the C-S-H relative peak height with the presence of organic.

2.7.2.2 Inorganic interference

Similar like organic, inorganic also give interference effect by affecting solidification process. Acids and heavy metal salts interfere with cement reaction, which alter properties of cured products (Spence, 1992). Inorganic contaminant such as metals and metal salts may increase setting time and alter properties of solidified waste (Jones, 1990). Retardation via adsorption onto C-S-H is due to the H-bonding (Taylor, 1997). Sulfate in waste can react with cement-hydrates to cause delayed ettringite formation, which may lead to problems of expansion. Metal hydroxide such as copper, lead and zinc hydroxide can inhibit cement reaction (Conner, 1990). Wilk (1997) tested S/S on five metals, namely Pb, Cr, Cd, As and Hg by sequential batch leaching on mature cement pastes, concluded that the metals' mobility was a function of pH.

2.7.2.3 Interference adjustment

Interference effects of waste in stabilized/solidified cement can be minimized or removed by identified the factors that contribute to the interference and suitable additive or proprietary chemical can be incorporated in the formulation of cement mixture proportions.

Based on the interference effects of specific contaminants in Portland cement, which influence the cementation process are described in Table 2.8. Therefore, possible control measures or additives and its effects in the cement mixture are described in Table 2.9.

Table 2.9: Control measures in stabilization /solidification process (adopted from Conner, 1992)

| <i>Additives/Control measures</i> | <i>Effects</i> |
|---|--|
| Flocculent agent | Aggregate fine particles and film former |
| Wetting agent | Dispersion of oil & grease and fine particle away from reacting surface |
| pH adjustment | Removal of interfering substance, destruction of gel and film former |
| Fe ²⁺ /Fe ³⁺ addition | Precipitation of interfering substances |
| Ion exchange | Removal of interfering substances from solution |
| Sorbent addition | Removal of interfering substance from reacting surface |
| Redox potential change | Destruction or conversion of interfering substances |
| Aeration modification | Alteration of morphology, removal of interfering volatiles |
| Temperature adjustment | Acceleration of reaction rate to counter retarding effect |
| Lime addition | Supplies additional calcium for reaction, reacts with certain interfering organics and pH adjustment |
| Sodium silicate | React with interfering metals cause acceleration of initial set |
| Calcium chloride | Accelerate setting in Portland cement system |
| Sodium hydroxide | pH adjustment may solubilize silica for a quicker reaction with calcium ion |

2.7.3 Pretreatment or precondition of organic/inorganic waste

The organic waste may be exposed to a different pretreatment or precondition such as the storage of waste in an open environment lead to weathering effect occur to the waste. The waste exposed to high temperature will reduce the volatile component and moisture as decomposition and vaporization occurred at once. Chemical conditioning will cause dissolution or precipitation of specific compound in the waste so as to facilitate the cementation process or change in the pH value.

2.7.4 Performance of solidified cement

Performance of solidified waste in cement can be measured by various physical and chemical tests. The tests were described by USEPA (USEPA, 1990a). Important performance tests include porosity, strength and leachability of solidified material. Series of performance test to stabilize/solidify the waste were conducted to access for full-scale treatment to judge for effectiveness of selected binders.

2.7.4.1 Leachability of solidified waste

Leaching is defined as the physical or chemical detachment of the waste into a solution medium. The rate of leaching process is governed by pertinent factors that lead to the degradation of solidified material. The relevance factors model (Caijun and Roger, 2004) is made by considering environmental impact to the solidified material. Identified factors include pH, liquid to solid ratio, temperature, porosity, permeability, leachant flowrate and complexation sorption, redox potential, geometry, biological and hydrological conditions. Mehta and Monterio also quoted the similar first three factors with additional factors of surface area (BET), nature of extraction vessel, nature of leachant, agitation techniques, number of elution used, contact time and separation of solid and liquid.

Leaching can occur by few mechanisms, such as diffusion, dissolution, ion exchange and precipitation. Diffusion leaching occurs in most of steady state thin film. As a rule of thumb, reactions are diffusion controlled if the rates of constant are faster than 10^9 l/mol.sec. Weathering is partial solubilization of elements in a mineral as it was a natural leaching process. The rate of contaminant removal of solubilization and diffusion curves is given in Figure 2.6 (a) and (b).

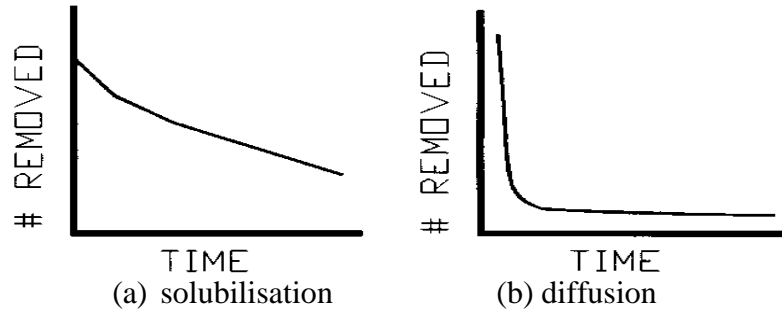


Figure 2.6: Contaminant removal by (a) solubilisation and (b) diffusion (Suthersan, 1999)

Fourier number as shown in Equation 2-5 can be used to decide which of the limits is more closely approached, thin film steady state or semi infinite slab which applicable for dilute solution. If the value is much larger than unity, it can be assumed semi infinite slab, but if it is much less than unity, it was expected a steady state or equilibrium (Cussler, 2009).

$$Fourier\ number = \frac{(Length\ h)^2}{(diffusion\ coefficient)(time)} \quad Eq. (2-5)$$

The leaching of solidified sludge is a heterogeneous chemical reaction, involving the diffuse of metal from solid into liquid by acetic acid or H^+ attack on the surface of cement. The conceptual leached model of the cement-based form subjected to acid attack was visualized for steady-state diffusion as shown in Figure 2.7 (Cheng, 1991).

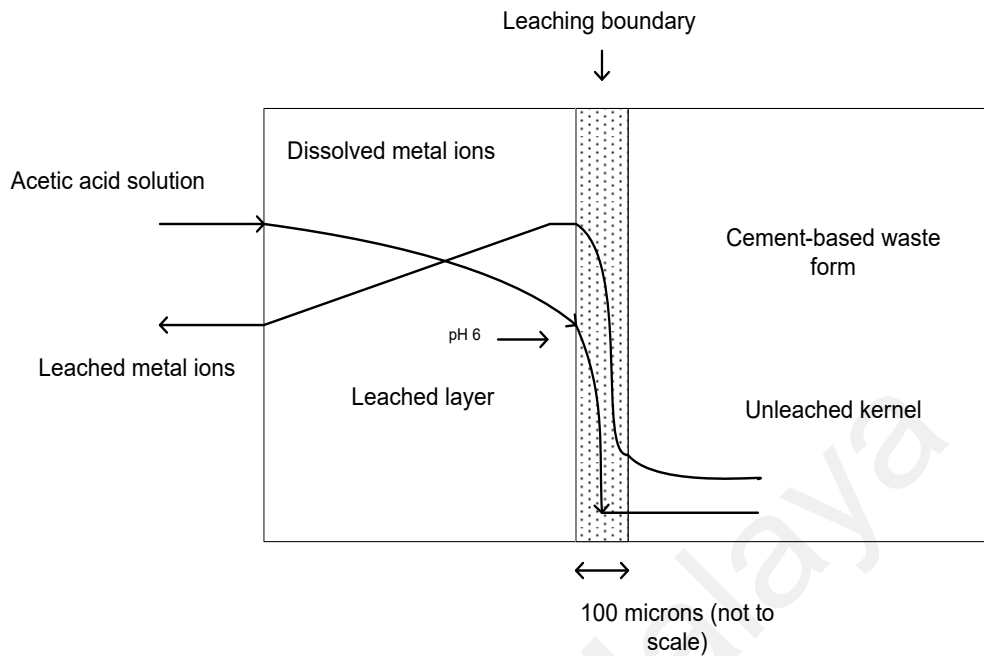


Figure 2.7: Conceptual leached model of cement based waste form (Cheng, 1991)

Environmental attack by H^+ , CO_2 , O_2 , Cl^- and SO_4^{2-} will release Ca^{2+} , OH^- , soluble salt, trace elements and dissolved organic carbon. Test method factors also contribute to the leaching rate such as surface area, agitation and time of contact but most of the factors are not considered due to the applicable standard used for leaching test.

Leaching of metal is pH dependent. Normally high pH is desirable because metal hydroxides have minimum solubility in the pH range of 7.5 to 11 (Barth et al., 1990). Some metal shows amphoteric behaviour with high solubility in both acidic and alkaline solution. Examples of amphoteric metals compound including Zn, Cr and Pb (Bone et al., 2004). The compromise of controlling suitable pH to minimize leaching is subject to the specific metal's elimination in leachant solution.

Leaching test measure the potential of a stabilized waste to release contaminants to the environment. Various tests were developed to assess the leaching potential to the

receiving medium. The agitated extraction test includes toxicity characteristic leaching procedure (TCLP) by USEPA made by crushed sample into uniform size, extraction procedure toxicity test (EP-Tox) formerly used by USEPA regulatory body, which superseded by TCLP, synthetic precipitation leaching procedure (SPLP) for disposal of waste outside of municipal landfill as an alternative to TCLP. Comparison of three extraction methods based on Japan, USEPA or UK TCLP is tabulated in Table 2.10.

Other leaching evaluations made based on the dynamic test in form of serial batch test includes USEPA multiple extraction test, ANSI/ANS-16/1 2003 the whole block leaching of monolith in simulated leachant to imitate the groundwater environment, and flow around test (NEN 7345) or flow through test (ASTM column extraction) to induce force for diffusion by continuously or intermittent renewed or flowed leachants.

Table 2.10: Extraction procedure for Crushed Block Leaching (CBL)

| <i>Test method</i> | <i>Size fraction (mm)</i> | <i>Leachant</i> | <i>Extraction period</i> | <i>Weight of solid (g)</i> | <i>Solid/Liquid ratio</i> |
|--------------------|---------------------------|---|--------------------------|----------------------------|------------------------------|
| Japan | > 0.5 and < 5.0 | Deionized water pH 5.8-6.3 | 6h | 50 | 50 g/500 mL |
| UK | < 2.00 | deionized water | 1h | 50 | 50 g/500 mL |
| USEPA | < 2.00 < 9.5 | 0.5 M HA deionized water (buffered with 0.5 M HA to pH 4.93 or 2.88) | 1 h 18 ± 2h | 50 100 | 50 g/500 mL 100 g/2000 mL |

Whole block leaching (WBL) try to imitate intact leaching pattern once the solidified waste was buried in a landfill. While crushed block leaching (CBL) measure the

intensive long term behaviour of the leaching by crushed the block into small pieces. CBL extraction is made by specific time agitation of crushed solidified sample. Where at the end of the extraction period leaching is assume to reach equilibrium state.

The semi dynamic leach test imitates by the WBL is made based on American Nuclear Society Leach test ANSI/ANS/16.1. It is used to establish a diffusion coefficient for comparison of S/S treated waste. The test is conducted over a period of 90 days to simulate the contaminant release rate in distilled water. The leaching result is collected for each time interval and recorded in cumulative fraction relative to the mass of waste sample.

2.7.4.2 Leaching mechanism

Solidified waste constitutes of porous matrix and has void portion. The leaching can occur through dissolution of exposed surface matrix of the solidified by the solution. For the case of ground water, the leaching rate is controlled by the molecular diffusion, while for acidic condition the supply of H⁺ limit the leaching rate but after hydrogen ion depleted, the molecular diffusion are controlling the leaching rate. Molecular diffusion is driven by the concentration gradient of constituent in solution and solid.

The flux of constituent location is described by first Fick's Law. Cote (1986) derived the law and modified the diffusion model to counter for a porous matrix as given by Equation 2-6. A widely accepted model for leaching of S/S waste was proposed by Goodbee and Joy (Cote and Isabel, 1984) as described in Equation 2-7 which is applicable to semi-infinite medium.

$$\frac{dC}{dt} = Ds \frac{d^2C}{dz^2} \quad \text{Eq. (2-6)}$$

where

C = concentration

t = time

Z = distance

D_s = molecular coefficient of diffusion

$$\frac{\sum a_n}{A_0} \left[\frac{V}{S} \right] = \left[2 \frac{D_e}{\pi} \right]^{0.5} t_n^{0.5} \quad \text{Eq. (2-7)}$$

where

a_n = contaminant loss during leaching period n , mg

A_0 = initial amount of a contaminant present in the specimen, mg

S = surface area of the specimen, cm^2

V = volume of the specimen, cm^3

t_n = time to the end of the leaching period p , s

D_e = effective diffusion coefficient, cm^2/s

Based on Equation 2-7, D_e is calculated from a slope of $\sum a_n/A_0$ versus $t_n^{1/2}$ as represented by Equation 2-8. The linear line of $\sum a_n/A_0$ plotted against $t_n^{1/2}$ passes through the origin indicated the leachability is controlled by diffusion. Leaching rate, l is calculated using Equation 2-9. The ANS leaching test based on series of seven sequential batch leaching test used to find the leachability index as in Equation 2-10.

$$D_e = \pi \left[\frac{a_n/A_0}{\Delta t_n} \right] \left[\frac{V}{S} \right] \left[\frac{1}{2} (t_n^{1/2} + t_n^{1/2}) \right]^{1/2} \quad \text{Eq. (2-8)}$$

$$l = \frac{a_n}{A_0} \frac{V}{S t_n} \quad \text{Eq. (2-9)}$$

$$Li = \frac{1}{n} \sum \left[\log \left(\frac{\beta}{D_i} \right) \right]_n \quad \text{Eq. (2-10)}$$

where

Li = leachability index

β = constant, $1 \text{ cm}^2/\text{s}$

n = number of leaching periods

D_i = effective diffusivity of metal i

Li is used to predict the S/S viability in landfill by a given yardstick scale. Li of higher than 8 allows S/S waste to be used in segregated or sanitary landfill but if the value is lower than 8, S/S waste is not appropriate for disposal (Moon and Dermatas, 2006).

The effective diffusion coefficient of non adsorbed leached metal ions is governed by porosity, ε and tortuosity factor, δ as defined in Equation 2-11.

$$D_e = \frac{\varepsilon D}{\delta} \quad \text{Eq. (2-11)}$$

where

D_e = effective diffusion coefficient

ε = porosity

δ = tortuosity factor (4 for non adsorbed ions)

D = diffusion coefficient

2.7.4.3 Strength and porosity

Strength test indicates how well a material will hold up under mechanical stress caused by overburden or earth-moving equipment. It is assumed that better strength

provides a better physical barrier for containment of contaminants. Unconfined compressive strength (UCS) test is measured according to ASTM C 109-92 method. U.S. EPA considers a stabilized material as satisfactory if it has a compressive strength of at least 50 psi. Porosity indicates the void space that may or may not contain liquids. The method to measure porosity is by liquid displacement techniques for measuring total porosity of cementitious systems based on the ASTM Method for Specific Gravity, Absorption, and Voids in Hardened Concrete, C 642 (Hearn et al., 2006). Strength has inverse relationship with porosity as described by Equation 2-12 for homogenous solid material (Mehta and Monteiro, 2006).

$$S = S_0 e^{-k\varepsilon} \quad \text{Eq. (2-12)}$$

where

S = strength of material with a given porosity ε

S_0 = intrinsic strength at zero porosity, 234 MPa for 28-day cement mortar

k = constant.

ε = porosity

Porosity decreases with time as cement hydration continues with the availability of water. Percentage of porosity depends on the water to cementitious ratio and degree of hydration. Continuous pore developed in hardened cement due to lacks of water in the mixture or micro crack in hardened cement, which affected by the curing process or environmental exposure.

The durability of solidified sludge was affected by the porosity and pore size distribution. The movement of fluid into the pore volume influence leachability of

contaminants in solidified waste. Solidified cement has low permeability normally in range of 10^{-5} to 10^{-9} cms^{-1} with fine pore size contributed to the increase in strength. Pore size, pore volume and surface area were measured by Brunauer, Emmett and Teller (BET) using nitrogen gas based on Langmuir multiple layer adsorptions. The linearized BET equation provides details of derived information from adsorption isotherm as in Equation 2-13.

$$\frac{1}{V[(P_0/P)-1]} = \frac{1}{V_m C} + \frac{C-1}{V_m C} \left(\frac{P}{P_0} \right) \quad \text{Eq. (2-13)}$$

where

P/P_0 = relative pressure, P_0 is saturated vapor pressure

V = volume of nitrogen gas adsorbed at pressure P in cm^3/g at STP

V_m = monolayer capacity

C = BET constant

Permeability can be calculated using Equation 2-14 which is applicable to 27 °C (Hearn et al., 2006). At specimen porosity of 26 %, the capillary porosity, P can be found by Equation 2-15. The permeability in terms of capillary porosity is computed by Equation 2-16.

$$\log 10^{12} K \frac{C}{(1-C)^2} = 4.2 - 2.097 \left(\frac{C}{1-C} \right) \quad \text{Eq. (2-14)}$$

$$P = (1 - C) - 0.26 \quad \text{Eq. (2-15)}$$

$$K = 10^{\exp \left[4.2 - 2.097 \left(0.74 - \frac{0.74-P}{0.26+P} \right) - \log \left(\frac{0.74-P}{0.26+P^2} \right) \right] - 12} \quad \text{Eq. (2-16)}$$

where

K = coefficient of permeability in cm/s

P = capillary porosity

C = particle concentration, volume of solids per unit volume of specimen

2.8 Regulatory Requirement of S/S

Acceptable limit of USEPA TCLP or UK NRA leaching test for constituent concentration prior to sanitary landfill disposal was quantified based on a multiplier of drinking water standards of commonly 100 (Al-Tabba and Perera, 2003).

The TCLP EPA SW-846 Method 1311 is used with the purpose to compare toxicity data with the regulatory level. The USEPA regulatory TCLP is listed in Table 2.11.

Table 2.11: U.S. EPA maximum TCLP extract and drinking water standard (adopted from Merrit, 1996)

| <i>Metals</i> | <i>Toxicity characteristic (mg/L)</i> | <i>Drinking water (mg/L)</i> |
|---------------|---------------------------------------|------------------------------|
| Arsenic | 5.0 | 0.05 |
| Barium | 100.0 | 1.0 |
| Cadmium | 1.0 | 0.01 |
| Chromium | 5.0 | 0.05 |
| Lead | 5.0 | 0.05 |
| Mercury | 0.2 | 0.002 |
| Nickel | NA | NA |
| Selenium | 1.0 | 0.01 |
| Silver | 5.0 | 0.05 |

Table 2.12 shows the secure landfill criteria for scheduled waste at Malaysian facility. The TCLP data can also be compared to drinking water standard. Since the

drinking water standard is the final safeguarding limit for potable household water that have the safe contaminant level.

Table 2.12: Landfill criteria of Malaysian scheduled wastes (adopted from Kualiti Alam S.B., 2003

| <i>Parameters</i> | <i>Limit</i> |
|-------------------|--------------|
| Total solid | > 20 % |
| pH | 5.5-12 |
| Cyanide | 0.5 mg/kg |
| Oil and grease | 1000 mg/kg |
| Chloride | 2 % |
| Arsenic | 5 mg/L* |
| Barium | 100 mg/L* |
| Boron | 400 mg/L |
| Cadmium | 1 mg/L* |
| Chromium | 5 mg/L* |
| Copper | 100 mg/L |
| Lead | 5 mg/L * |
| Mercury | 0.2 mg/L* |
| Nickel | 100 mg/L |
| Selenium | 1 mg/L* |
| Silver | 5 mg/L* |
| Tin | 100 mg/L |
| Zinc | 100 mg/L |

*Similar to U.S.EPA TCLP maximum concentration limit

2.9 Safety and Health Aspects

Sludge containing numerous toxic compounds, some of it has been classified as hazardous and required special treatment for the concentration above the hazard level. The dosage of hazard level is classified as lethal dose 50 % (LD₅₀) for solid or lethal concentration 50 % (LC₅₀) for air or liquid. The LD₅₀ was found based specified dosage administered to tested animal, normally rat that can kill 50 % of the tested specimen and measured in mg per kilogram of specimen body weight. Similarly, LC₅₀ was used for the

concentration of toxic compound that can kill 50 % population of tested animal in the specified period of 1 to 4 hours, expressed as part per million of material exposed per kilogram of the tested specimens. The LD₅₀ of most toxic substances in the petroleum refineries and sludge are listed in Table 2.13.

Table 2.13: Lethal dose 50 % of volatile organics (adopted from IChemE, 2005)

| <i>Substances</i> | <i>LD₅₀ (mg/kg)</i> |
|---------------------|--------------------------------|
| Toulene | 636 |
| Benzene | 930 |
| Xylene | 4,300 |
| Ammonia | 350 |
| Ethylene oxide | 72 |
| Ethanol | 10,000 |
| Tetrachloroethylene | 8,850 |

The toxicity rating of 1 to 6 was given to the specified range of LD₅₀ or LC₅₀ values based on the impact of toxic substances to the receiver as shown in Table 2.14. The route of entry of toxic substance to the receivers practically through any following passage:

1. Absorption through exposed skin or eyes which normally caused dermatitis or irritation.
2. Ingestion or drinking of contaminated food or water may cause acute poisoning effect for large dosage.
3. Inhalation through breathing of contaminated air normally contributed to asphyxiation or dizziness.

Extremely toxic contaminant received in small dosage may contribute to the immediate impact to human health due to its low LD₅₀ or LC₅₀ value. Repeated exposure to highly toxic contaminant may cause cancer or disturbance to specific internal organs that accumulate the toxic substances.

Table 2.14: Toxicity rating of hazard levels (adopted from Martin et al., 2000)

| Toxicity classes | | | |
|------------------|-----------------------|--------------------------|------------------------|
| Toxicity rating | Toxic impact | LD ₅₀ (mg/kg) | LC ₅₀ (ppm) |
| 1 | Extremely toxic | 1 or less | < 10 |
| 2 | Highly toxic | 1 – 50 | 10 – 100 |
| 3 | Moderately toxic | 50 – 500 | 100 – 1,000 |
| 4 | Slightly toxic | 500 – 5,000 | 1,000 – 10,000 |
| 5 | Practically non-toxic | 5,000 -15,000 | 10,000 – 100,000 |
| 6 | Relatively harmless | 15,000 or more | > 100,000 |

The excessive dosage of toxic substances at manufacturing site or workplace should be monitored within high risk working area. Personal protective equipment (PPE) must be worn to reduce or prevent the toxic from enter the human body. The PPE commonly used in the industrial site included coveralls, safety goggles, hard hat, boot, respirator and resistant gloves. At the same the engineering and administrative controls must be adopted as the main safety control measured to reduce the toxic substances level.

2.10 Long Term Durability of Solidified Waste

The solidified hazardous waste performance for an extended period can be monitored to find its long term integrity. The U.S. EPA RREL is sponsoring a laboratory work on synthetic and real wastes to develop a protocol for accelerated weathering testing

of cementitious waste forms (Means et al., 1995). Durability testing focused on the use of elevated temperature and acidic medium to accelerate the degradation process like the use of modified semi dynamic leaching ANS/16.1.

Another way to analyze long-term performance is by field project conducted to develop sampling and analysis method for assessment of waste form durability after various periods of exposure to field conditions. The durability performance of solidified waste buried in landfill can be made by monitoring the leachate from weathered sample and bulk sample. Many demonstration projects were developed by U.S.EPA under Superfund budget used real organic wastes such as Chemfix technologies, Geo-Con, Solidtech and Hazcon as described in Chapter 2.

2.11 Critical Review

The integrity of waste in the monolith is subjected to the interference of organic and inorganic content in the waste materials. As the organic may interfere the setting time or retard the cementation process (Jones, 1992), similarly the metal or metal salts may retard setting or alter final products of the solidified waste (Jones, 1992; Stegemann, 2005). The organic and inorganic mixes may have neutralization or compound effect based on the chemical reactions in the S/S system or binders interaction in cement hydration. Important properties of solidified waste include porosity as it has inverse relationship with strength (Mehta and Monteiro, 2005) and diffusion coefficient which controlled leaching rate of contaminants released to the environment. Solidified waste performance criteria subjected to the local requirement must be achieved prior to utilization or land disposal.

CHAPTER 3.0 MATERIALS AND METHODS

3.1 Introduction

The sludge and binder material were collected from the wastewater treatment plant and manufacturer's site. The materials were characterized for its physical and chemical properties. Mix design and curing were conducted to determine the optimum design parameters. Selected performance tests of solidified waste as shown in Figure 3.1 were performed to the cured samples and compared against appropriate standard. S/S experimental flowchart is illustrated in Figure 3.2.

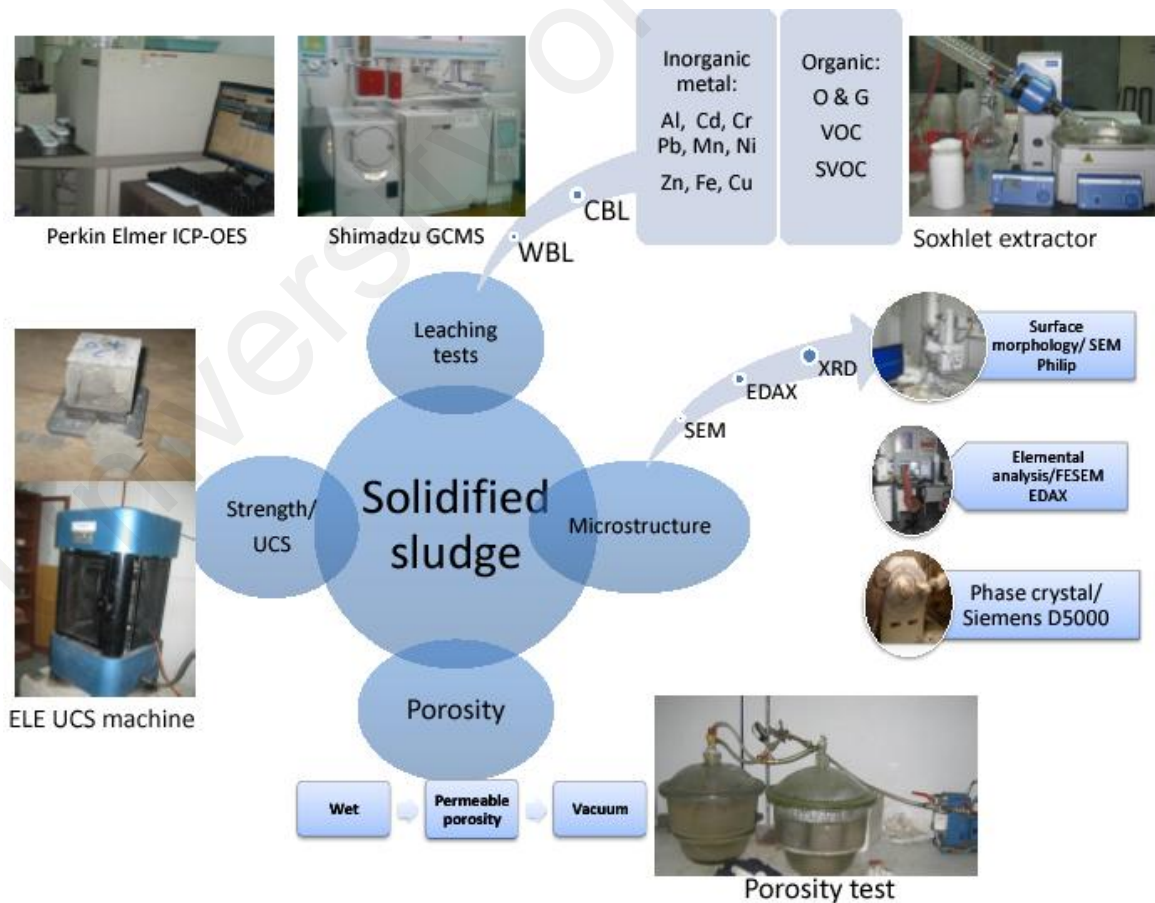


Figure 3.1: Performance tests for solidified waste

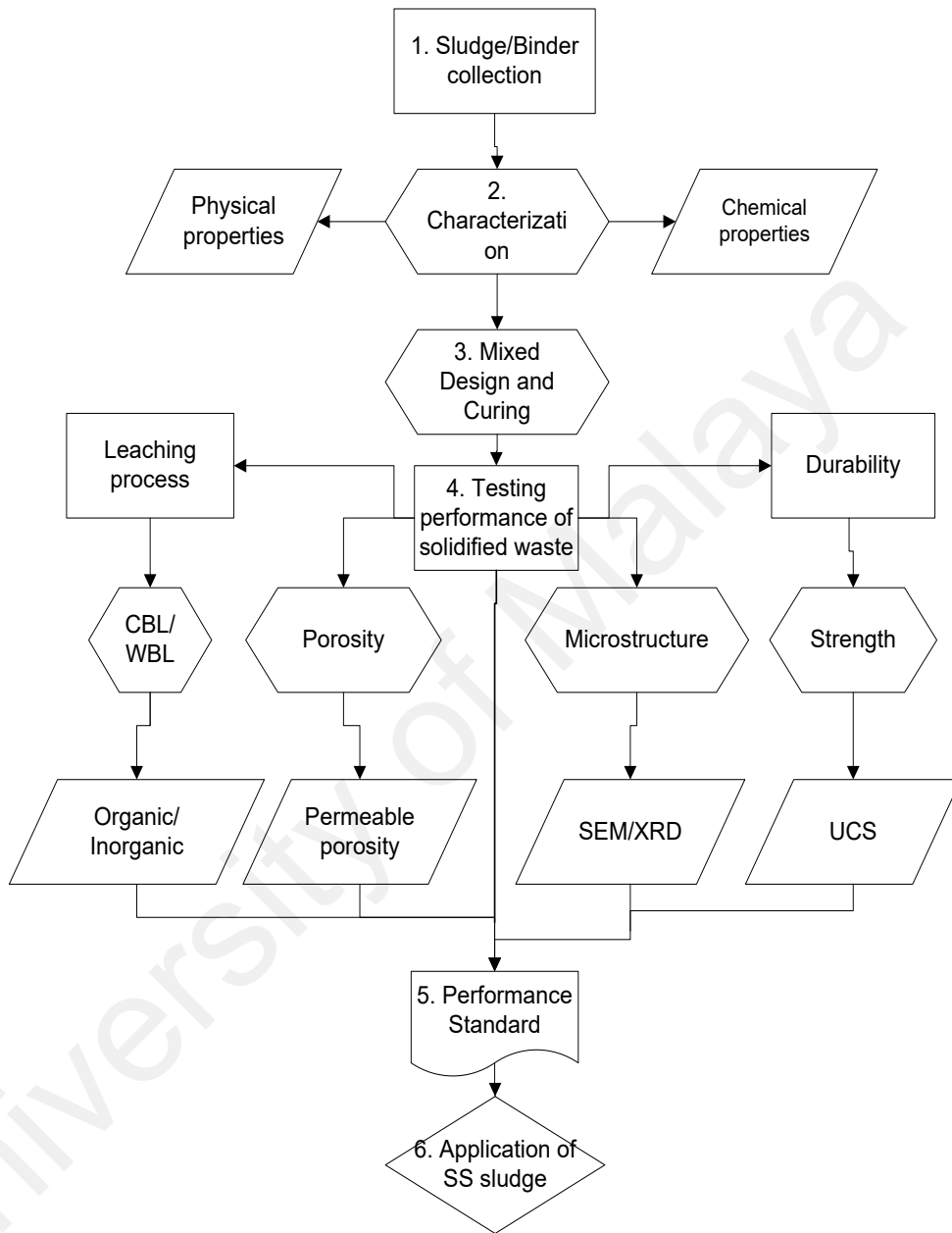


Figure 3.2: Experimental flowchart of stabilization and solidification

3.1 Materials

3.1.1 Waste

Sludge was obtained from local refinery wastewater treatment facility. Sludge was collected from decanter unit after the oil recovery and moisture removal process is completed. The sample was labeled and stored in a cool room at temperature of 4 °C.

3.1.2 Binders

3.1.2.1 Ordinary Portland cement

Main binder used in S/S process is OPC Type I supplied by Lafarge Cement. OPC used is complied with MS 522 Part 1 2003 standard. The OPC was stored in air tight drum with steel drum's liner to protect from moisture. Portland cement was prepared by firing of crushed calcareous material such as limestone and argillaceous material like clay or alumino silicate in a heated kiln at about 1500 °C.

3.1.2.2 Rice husk ash

RHA is originated from rice husk, residue of paddy field, one of the national agricultural activities. RHA was prepared by slow burned of rice husk in ferrocement furnace, and the ash was ground to the average size of less than 45 µm. Combustion temperature below 500 °C for a prolongs period or up to 900 °C for one hour were used to form amorphous silica RHA. Crystalline silica RHA requires higher temperature of 1000 °C but at shorter combustion time of greater than 5 minutes.

3.1.2.3 Metakaolin

Metakaolin was prepared from Merck kaolin lab grade by calcinated the kaolin in the muffle furnace at 750 °C for three hours. The calcinations of kaolin will cause dehydroxylyzation which resulted in the amorphous state of kaolinite particle which highly pozzolanic.

3.1.2.4 Activated carbon

Activated carbon powder derived from the coconut shell from Laju Carbon Group. The coconut shell is activated by steam at the high temperatures of 900 to 1100 °C in the rotary kiln. The steam reaction at the internal surface creates more sites for adsorption process. The activated carbon is ground to a powder formed with surface area from 900 to 1500 m²/g.

3.1.2.5 Fly ash

Fly ash used in the work is based on the pulverized coal fired fuel from TNB power plant with combustion temperature of 1200 to 1800 °C. The FA is classified as class F with high silica and calcium content. The FA is the residue from the plant chimney and normally used as cement replacement material. FA has pozzolanic properties with some advantages for cement hydration. FA has a fineness of < 45 µm (40 %).

3.1.2.6 Condensed silica fume

Condensed silica fume used in the research was source from BASF Sdn. Bhd. The CSF is the byproduct of smelting process in silicon metal and ferrosilicon alloy industry. Silica fume condenses from the gases escaped from electric arc furnace producing very fine silica and has highly reactive pozzolan properties. The advantage of CSF is due to its high surface area $20,000 \text{ m}^2/\text{kg}$, which provides large response surface and as filler to cement hydration process.

3.1.3 Chemicals

Chemicals involve in S/S experimental work are Merck glacial 100 % purity acetic acid was used to prepare leachant for leaching test, nitric acid 65 % purity for the metal digestion, rinsing, and washing of sample bottles and moulds. Decont90 was used for cleaning bottles, glassware and containers to remove organic impurities.

3.1.4 Water

Double deionize water was used for preparation of acid solution and leachability test while deionize water was used in mixing of waste cement. Distilled water was used for rinsing of glassware and tool.

3.1.5 Mould

Perspex mould used for casting unconfined compressive strength (UCS) block is 50 x 50 x 50 mm (ASTM International, 2005a). The stainless steel cylinder of 100 mm height and 50 mm diameter was used to cast for permeable porosity sample. Whole block leaching

sample is cast in Perspex mould of 24.3 x 24.3 x 24.3 mm. Crushed block leaching sample was cast in 1-litre cylinder polyethylene bottles. All mould must be cleaned from any contaminant by washing with Decon90 to remove any organic residue and followed by 5 % nitric acid solution and deionize water.

3.2 Methods

3.2.1 Characterization of sludge

The petroleum sludge wastes typically are water-in-oil emulsions stabilized by fine solids. The sources of waste will determine the behavior and properties of waste. The characterization study involves chemical and physical properties of waste.

3.2.1.1 Chemical properties

The pH was measured using pH meter of HANNA instruments 8417. The oil and grease were extracted by soxhlet extractor using Merck n-hexane 99 % purity and Merck tert-butyl methyl ether solvent. Organic contaminants was determined using gas chromatography based on USEPA 3570, 8270C (USEPA, 1996) for polyaromatic hydrocarbon (PAH) and polychlorinated biphenyls (PCB), while benzene, toluene, xylene and ethyl benzene (BTEX) was determined by USEPA 5030B, 8260B (USEPA, 1996). The organics are also measured in collective groups of total petroleum hydrocarbon (TPH). The elemental analysis to determine metal was conducted by Optima 3000 Perkin Elmer Inductively Couple Plasma Atomic Electronic Spectrophotometer (ICP-OES).

3.2.1.2 Physical properties

Physical property tests conducted for the waste are specific gravity, moisture content, total solid, volatile solid and fixed solid. The method used in the physical properties determination is based on APHA standard method (APHA, AWWA, & WEF, 1990).

3.2.1.3 Microstructure analysis

Surface structure of dried sludge was captured by PHENOM Scanning Electron Microscopy (SEM). Photomicrograph of the sludge specimens was made based on-field sample.

3.2.2 Characterization of Portland cement and binders

The binder's surface morphology was captured by Philip SEM on gold-coated sample. Metal content in the OPC was prepared using Merck nitric acid digestion and determined by ICP-OES. The leached metal from OPC was performed by Merck acetic acid 100 % purity and determined by ICP-OES. The Portland cement oxide analysis was performed by PANanalytical MiniPAL 4 XRF unit using 1 g of sample fusion in sodium metaborate glass bead at temperature of 1200 °C. Elemental analysis in OPC was determined by EDAX XL30 FESEM. Functional groups of the binders were analyzed by Nicolet iS10 Thermo Scientific Fourier Transform Infrared. While the thermal weight loss was determined by TA Instrument Q500. The pore size and surface area were measured by BET of Quantachrome Autosorb. Particle size and zeta potential was determined by Zetasizer Nano, Malvern Instruments Ltd., U.K. on 20 mg of sample in deionize water.

3.2.3 Synthetic metals

Metal was added to observe the effect of binder's strength to the stabilized/solidified sludge. Selected metal used to simulate the presence of metal in S/S system are copper, chromium, lead and zinc. The metals' concentrations of 5000 ppm were selected to represent the maximum boundary of metal as part of the waste that can be stabilized and solidified in the OPC.

3.2.4 Mix design of solidified OPC and Waste

Well mixed waste and cement are weighted according to the modified Sherbrook mix design proportion and blended in a 25-liter stainless steel Hobart mixer. Water was added to the mixture of cement and waste. Mixing was performed for 3 minutes based on BS 4550: Part 3 (BSI, 1978). K-Slump test was conducted to determine the workability of cement paste. The cement paste was casted into the mould and vibrated to remove air voids. Triplicate samples were prepared for each of the selected parameters. Casted cement was demoulded after 24 hours. The sample was placed in Perspex cabinet under air dry curing at temperature of 25 °C and relative humidity of 90 %. The humidity was measured by Brannan Thermometers.

3.2.5 Leachability of solidified waste

Leachability tests conducted for aggressive leaching potential and gradual leaching simulation as in the landfill by semi-dynamic leaching. Both tests used the same sample but by two different methods.

3.2.5.1 Toxicity leaching characteristic procedure

Aggressive leaching by crushed block leaching was made according to Toxicity Characteristic Leaching Procedure (TCLP) U.S.EPA SW-846 method 1311 (USEPA, 1996). The cement paste was solidified into 1-liter plastic container and cured to a specific period before it was crushed, and ground to the size of less than 9.52 mm. Crushed sample was mixed with extractant fluid. The extractant liquid was prepared using glacial CH_3COOH with reagent water (ASTM Type II standard). The expected pH would be 2.88 ± 0.05 of extractant fluid no. 2 of TCLP. Discard the fluid if impurities were found or pH is not within the specification and replace with new one. A minimum of 100 g of waste (in solid form) for TCLP 1311 and its extraction fluid can be calculated as in Equation 3-1.

$$\text{Weight of extraction fluid} = (20 \times \% \text{ solid} \times \text{weight of waste filtered})/100 \quad \text{Eq. (3-1)}$$

If the sample is 100 % solid, extraction fluid (acetic acid pH 2.88 ± 0.05 and deionize water) is 2 liters. Extraction fluid is added to a zero head space extractor at a liquid to the solid ratio of 20:1, and the sample was agitated by a rotary agitator for 18 ± 2 hrs at rotation speed of 30 ± 2 rpm. Once the extraction was completed, the solid and fluid component was separated by filtering through a 0.6 to 0.8 μm glass fiber filter under pressure of 50 psi. Filter should be acid washed if mobility of metal is evaluated. pH of the TCLP extract must be recorded. Immediately measured the aliquot and preserved for analysis or stored in the freezer at 4 °C. If analysis of undigested extracts shows the level of regulated metal concentration exceeds the specified standard; the sludge is considered hazardous. The extracted sample was tested for metal and organic using ICP-OES and GCMS.

3.2.5.2 Semi-dynamic leaching

Semi-dynamic leaching was simulated by whole block leaching to determine the diffusivity of the waste in landfill by preparing a sequential semi dynamic leach test. The test was adopted based on ANS 16.1 (ANS, 2003). Selected static leaching interval was used after the leaching medium is expected to saturate with leach metals and organic from waste monolith. A new extractant medium was replaced to continue the leaching process. Accumulated extractant was recorded to find the leached materials at the end of sequential leaching test.

The monolith sample was exposed to the deionize waste and extractant fluid no. 2 to imitate the neutral water and mild acidic water of acetic acid accordingly. The two conditions are expected to occur in the natural landfill sites. A one-inch cube was tied by nylon string in 100 ml of extractant and covered by Teflon tape to prevent from outside contamination. At the day 1, 3, 7, 15, 31, 63 and 127, pH was recorded and filtered for measuring the leached metals in the extractant. A new extractant must be replaced after each of the selected time intervals complete. Cumulative fraction release is computed from all consecutive extractant. Leached metals in extractants were determined by Perkin Elmer Inductively Couple Plasma optical emission spectrometer (ICP-OES).

3.2.6 Strength of solidified waste.

The matured solidified/stabilized sample cube with a dimension of 50 x 50 x 50 mm was tested for UCS using ELE compression machine, which complied with British Standard 1881: Part 116 (BSI, 1983). The sample was deformed until failure occurred based on the crack to the cube using the applied maximum load. The unconfined

compressive strength was computed based on the surface area and the final load of the sample according to ASTM C109-91 (ASTM, 2005a).

3.2.7 Porosity of solidified waste

The porosity of the sample was measured based the ASTM C 642 (ASTM International, 2005b). The sample was dried at 100 to 110 °C in the oven for 24 hours before measuring the permeable porosity. The permeable porosity was conducted for wet, boil and vacuum method (Safiuddin and Hearn, 2005). The permeable porosity measurement was made to the sample volume of more than 350 cm³. Adsorption capacity of solidified sample was determined by Autosorb Quanta Chrome 6S using nitrogen gas adsorbate to determine the pore size of the sample porosity.

3.2.8 Microstructure of solidified waste.

Solidified waste surface morphology was captured by Philip EDAX XL30 using the gold-coated dry sample. Elemental analysis was made by Zeiss FESEM EDAX on gold-coated fractured samples using secondary electron beam. Solidified samples mineralization was analyzed using X-Ray Diffractometer of Siemens D-5000 using powder method. The sample used was 1 to 2 g of sample powder placed on 1.0- inch Perspex slider. The spectrum was captured using copper detector based on Bragg's law, χ of $2d \sin \theta$ with the theta in range of 10 to 70 degrees. The XRD scans were performed with steps of 0.10 ° with three-second counting time. Solidified sample was prepared by pulverized sample with agate mortar.

Thermal decomposition of solidified sludge was measured by TA Instrument Q500 and analyzed by TA Universal Analysis 2000 software. Dry sample was used to measure the mass change as a function of temperature. Weight loss as a result of thermal change was associated with sample decomposition, sublimation, reduction, desorption, absorption and vaporization for certain temperature range. The pore size and surface area were measured by BET nitrogen adsorption using Quantachrome Autosorb about 1 to 2 g of dry sample.

3.2.9 Organic analysis of solidified sludge

Organic compound was determined by Shimadzu QP2010 GCMS based on the U.S.EPA 8260B and 8270C for volatiles and semivolatiles. The sample preparation used for each method are 5030B for aqueous and microscale solvent extraction, method 3570 for extraction of volatile, semivolatile and nonvolatile compound from solids such as soil, sludges and waste. The external standards for target organic constituents are Supelco analytical benzene, toluene, ethyl benzene, xylenes, naphthalene and phenanthrene solution in 200 µg/mL. The concentration of the targeted constituents can be found based on linear external standard calibration curve (Wang, 2001). Supelco analytical EPA 8260 and semivolatile internal standard mix of 2000 µg/ml were used in the organic determination. Internal standard coefficient of response for the detector used must be in the same order of magnitude as one of the products to be determined (Vial and Jardy, 2001). Five or minimum of three calibration points were prepared at the selected range for each of the standards. The surrogate standard used in the determination was Dr Ehrenstorfer 5-Alpha Androstane for aliphatic and O-Terphenyl for aromatic.

The solid sample was extracted into methylene chloride solvent based on the solid to the liquid ratio of 0.2083 and agitated by end-to-end rotation for four hours using rotary agitator. The solvent containing organics compound was separated from solid by glass fiber filter. The solvent was preconcentrated using a 25 mL Kuderna Danish concentrator by water bath heating at temperature below 100 °C until the final volume of 1 to 2 ml remains in the receiving vessel. The heating must be conducted in the fume hood to prevent any spillage of solvent to the face or on the floor.

Solid phase microextraction (SPME) was used to extract the volatiles and semivolatiles from leachate of solidified sludge. SPME principles based on the extraction of volatiles and semivolatiles by fiber layer coated on the surface of a fused silica needle. The SPME optimization can be made by controlling few factors such as contact time, agitation and temperature of extraction. Suitable fiber for targeted analyte was used for the extraction of nonpolar hydrocarbon. PDMS fiber with thickness of 100 μm was used.

3.2.10 Experimental design

Mix design was carried out to find the best proportion based on the composition of cement to sludge (C/Sd). Cement and sludge were mixed at the different ratio in consistent moisture and temperature. Cement without waste was used as the control sample. Experimental design is as shown in Figure 3.3. Optimum CRMs was determined based on the optimum W/C and C/Sd.

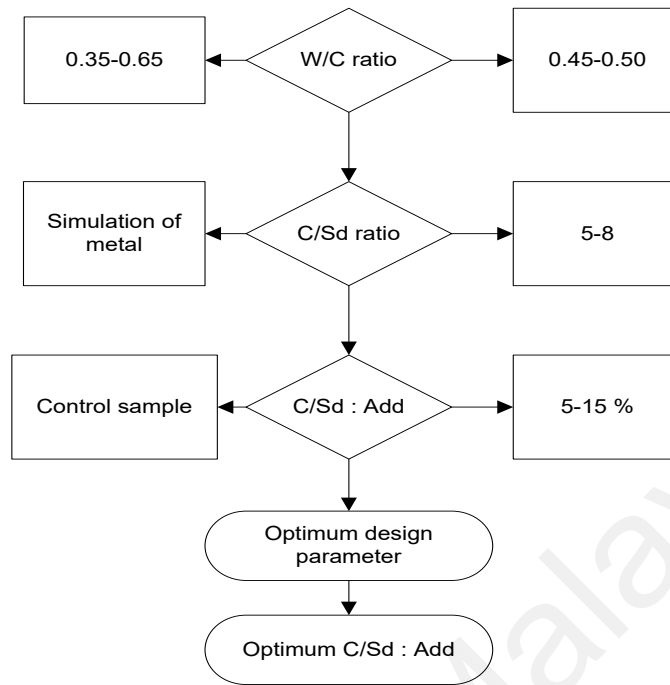


Figure 3.3: Experimental design of S/S

The benchmark used for the outcome of S/S product is the requirement by the UK waste disposal authority as in Table 3.1.

Table 3.1: UK solidified waste performance characteristics (adopted from Sollars and Perry, 1989)

| <i>Characteristics</i> | <i>Requirement</i> |
|------------------------|--|
| Permeability | $< 1 \times 10^{-7}$ m/s |
| Compressive strength | > 0.34 N/mm ² |
| Leachate quality | pH 8 - 11 |
| | COD < 280 g/m ³ |
| | Total CN < 1 g/m ³ |
| | Total Sulphide < 5 g/m ³ |
| | Total Phenol < 5 g/m ³ |
| | NH ₃ < 40 g/m ³ |
| | Toxic heavy metals: |
| | Zn < 10 g/m ³ , Hg < 0.5 g/m ³ |
| | Others (Cd, Cr, Cu, Ni, Pb, V, Ba, Co, Mb, Sn, As, Se, Sb): < 5 g/m ³ total |
| | Pesticides < 0.1 g/m ³ |

3.2.11 Statistical analysis

Minitab 14 (MINITAB Inc., Pennsylvania, USA) was used to analyze statistical values such as correlation, regression and ANOVA for tested parameter, such as C/Sd, CRMs percentage and W/C ratio. Graphical relationships between parameters were plotted and analyzed by Microsoft Office Excel 2007, Surfer 10, version 10.2.601 and Grapher 9 version 9.0.444 (Golden Software, Inc. Colorado, USA).

University of Malaya

CHAPTER 4.0 RESULTS AND DISCUSSION

4.1 Waste Characterization

Characterization of the sludge was conducted to investigate physical, chemical and microstructure properties of the waste sludge that may influence the solidified product's performance. The characterization study provides the insight values of the physical nature such as pH, moisture content, specific gravity and total solid, which will be used in mix design of cement, water and sludge proportions. The sludge chemical properties influence the chemical reaction to occur in the hydration of cement and final products quality in such a way that it will also affect the contaminant released in leaching, and strength developed of solidified sludge. Microstructure properties revealed the morphology of sludge molecular surface.

4.1.1 Physical properties of raw sludge

Sludge physical properties and its values were described as followed:

1. The average pH value for petroleum waste measured by pH meter is almost neutral, 7.06 at room temperature of 26.0 °C.
2. Specific gravity and density of the waste are 0.9596, and the waste density is 959.60 kg/m³, accordingly.
3. Moisture content of the waste measured by water bath drying method is 53.81 %.

4. Total solid content of the waste was measured using APHA method 2540G. The average total solid, volatile solid and fixed solid of the petroleum waste are 46.19 %, 92.08 % and 7.91 % accordingly.
5. The petroleum waste collected is dark brownish in color due to the crude oil residue, which formed oily sludge emulsion. The sludge has gasoline odor representing the volatiles component of hydrocarbon.

Details of data and calculation for the physical properties of petroleum sludge are attached in Appendix A (Table A4-1 to Table A4-4).

4.1.2 Chemical properties

The organic and inorganic content of the sludge were determined to find its interference to stabilize and solidified of sludge.

1. Inorganic constituents were measured by ICP-OES in form of a total metal concentration present in the sludge. Since every single metal may influence the final product of solidified waste, it is very critical to identify the metal to predict potential reactions occurred during hydration and setting of cement paste, which later will affect the strength and leachability of the solidified sludge. Nitric acid digestion method APHA 3030E was employed as sample preparation for metal detection. Petroleum sludge has the significant amount of aluminum, 0.283 mg/g and iron, 0.344 mg/g. The summaries of physical and chemical properties of the sludge are tabulated in Table 4.1.

Table 4.1: Sludge physical and chemical properties

| <i>Properties</i> | <i>Value</i> | <i>APHA method</i> |
|-------------------|--------------|--------------------|
| pH | 7.03 | Photometric |
| Specific gravity | 0.9614 | 2710F |
| Moisture content | 53.80 % | 2540G |
| Oil & grease | 156.60 mg/L | 5520E |
| Total solid | 46.92 % | 2540G |
| Volatile solid | 92.08 % | 2540G |
| Fixed solid | 7.91 % | 2540G |
| Fe | 0.344 mg/g | 3030E |
| Al | 0.283 mg/g | 3030E |

2. Organic content measurements in petroleum sludge are the main focus as the waste contains oil & grease, and volatiles compounds. Organic compound has been acknowledged to interfere with Portland cement hydration (Conner, 1990; Cullinane and Bricka, 1992). The main organic contaminants measured for the petroleum sludge are as follows:
 - a. The average oil & grease concentration in the sludge is 156.60 mg/L or 39.23 %. Details of data and calculation are given in Appendix B Table A4-5 to Table A4-6.
 - b. Volatiles organic of BTEX and PAH concentration are illustrated in Figure 4.1(a).
 - c. Total petroleum hydrocarbon (TPH) concentration as shown in Figure 4.1(b). C₁₀ - C₁₄ and C₁₅ - C₂₈ is the dominance groups. In crude distillation, C₁₀ - C₂₀ is known as middle distillate and C₂₀ - C₄₀ forms vacuum gas oil, whereas light fraction hydrocarbons C₆ - C₉ formed naphtha (Barker, et al.,

2007). Hydrocarbon residues of C₂₉ - C₃₆ consists of gas oil, heavy heating oil, lubricating and greases.

Volatile organic compound in the waste was measured based on U.S.EPA standard. The sample was frozen dry for 72 hours to remove moisture while maintaining the volatiles contaminants in the waste. The volatile organics found in the sludge are naphthalene, xylene, phenanthrene, toluene, benzene and ethyl benzene. Some of the properties of selected volatile organics and its OSHA permissible exposure limits (PEL) are tabulated in Table 4.2. The PCB was found below the detectable limits.

Benzene and toluene are single ring aromatic alkenes. Solid waste containing 0.5 mg/L benzene must be treated according to RCRA regulations, and it was considered as one of the human carcinogen (Griesbaum et al., 2007). Similarly, toluene resembles benzene toxicological properties but devoid its chronic effect by oxidized to benzoic acid in the human system. Xylenes are homologues of benzene, which includes o-xylene, m-xylene, p-xylene and ethyl benzene. Long-term exposure to xylene isomers caused chronic effects to central nervous system. Naphthalene is a bicyclic aromatic while phenanthrene is a polycyclic or polynuclear aromatic hydrocarbon. Both of naphthalene and phenanthrene had been categorized as non carcinogen. However, all the above mentioned organics must be handled with care since the substances are toxic and may create a hazard in the laboratory work. The structures of detected alkenes are illustrated in Figure 4.2.

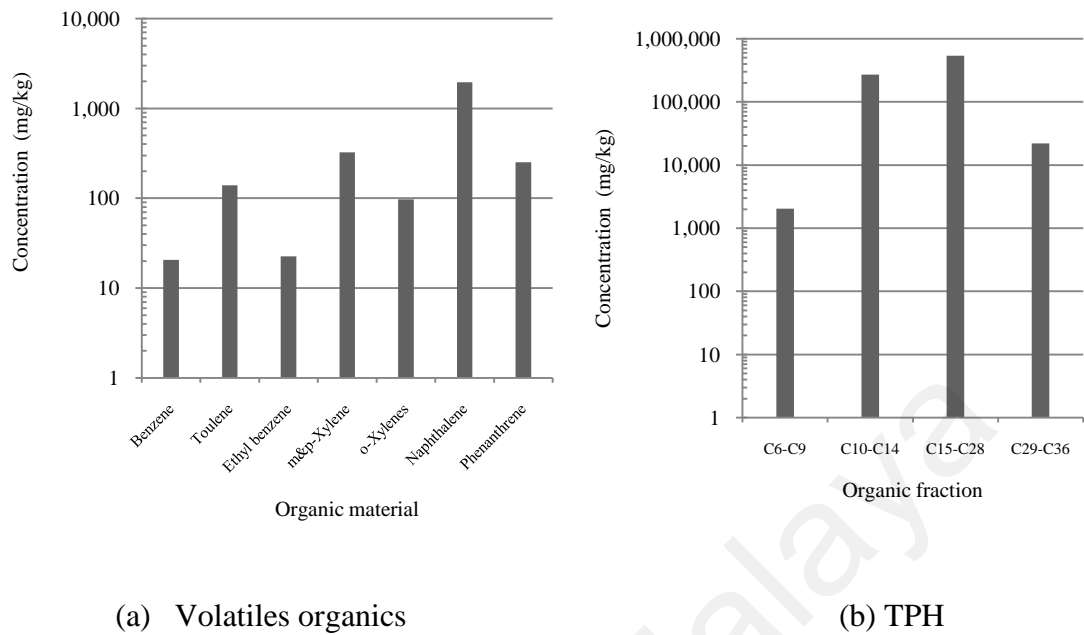


Figure 4.1(a): Volatile organic material and (b) TPH organic fraction in the sludge

Table 4.2: Properties of detected volatiles contaminant in the sludge (adopted from Griesbaum et al., 2007)

| <i>Volatile organics</i> | <i>Molecular structure</i> | <i>Molecular weight (g/mol)</i> | <i>Boiling point (°C)</i> | <i>PEL (OSHA) (ppm)</i> |
|--------------------------|---------------------------------|---------------------------------|---------------------------|-------------------------|
| Benzene | C ₆ H ₆ | 78.11 | 80.09 | 1 |
| Toluene | C ₇ H ₈ | 92.14 | 110.6 | 200 |
| Ethyl benzene | C ₈ H ₁₀ | 106.16 | 136.2 | 100 (ACGIH) |
| Xylene: m-xylene | C ₈ H ₁₀ | 106.16 | 139.1 | 100 (for all |
| p-xylene | | 106.16 | 138.4 | xylene isomer) |
| o-xylene | | 106.16 | 144.4 | |
| Naphthalene | C ₁₀ H ₈ | 128.18 | 217.95 | Not a carcinogenic |
| Phenanthrene | C ₁₄ H ₁₀ | 178.23 | 336.0 | Not a carcinogenic |

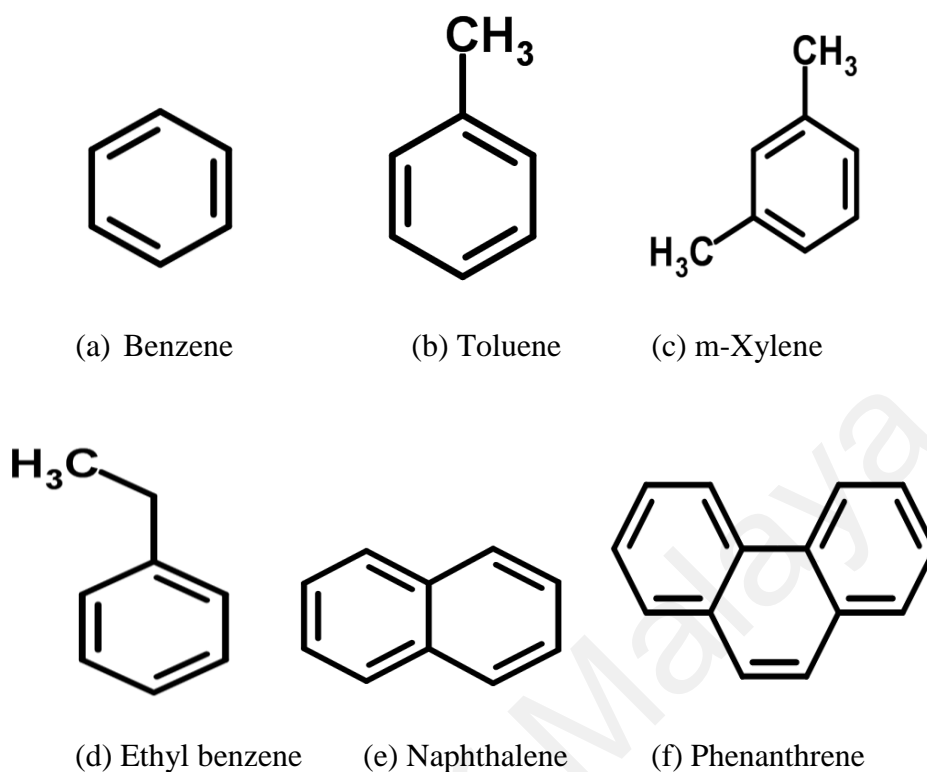
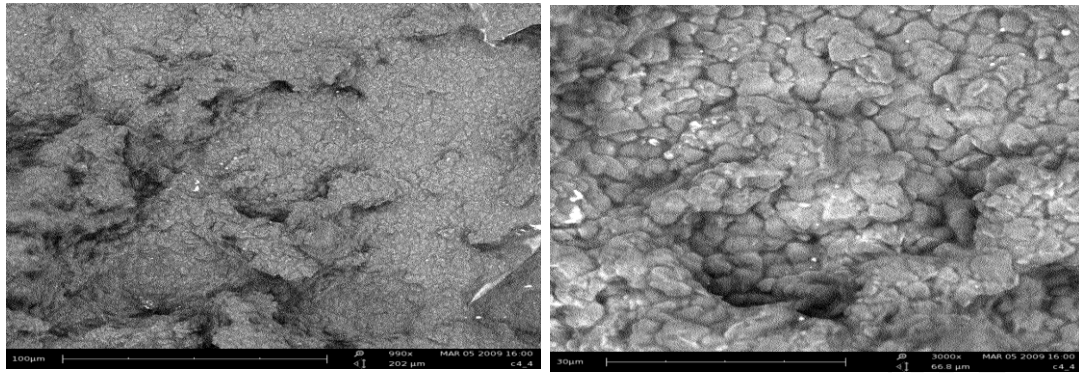


Figure 4.2: Structure of aromatic alkenes (Royal Society of Chemistry, 2011)

4.1.3 Microstructure of petroleum sludge

The petroleum waste microstructure was formed by granules of the oil molecules bonded with solids in the moisture sludge. The oven-dried oily sludge forming agglomerated sludge layers was viewed by high-resolution scanning electron microscope (SEM). Photomicrographs of the sludge using PHENOM SEM is illustrated in Figure 4.3 captured on a moisture-free basis sample at 1024 resolutions.

The sludge image showed interconnected oily globules forming the bulk of the sludge, which can be clearly observed in Figure 4.3(b) at 3000 magnifications. The oily globules with an estimated size of less than 10 μm formed thick sludge layers. The sludge was initially in liquid form with a high moisture content of 53.80 %.



1. 990x

(b) 3000x

Figure 4.3: Photomicrographs of dried petroleum sludge at (a) 990x and (b) 3000x

4.1.4 Conclusions of waste characterization

The salient points sought from waste characterization were summarized as follows:

1. The sludge can be categorized as hazardous waste since it contains a significant amount of benzene, one of the carcinogenic substances plus other volatiles organics.
2. The sludge has a neutral pH of 7.03 with a high total solid of 46.91 %.
3. The sludge has high volatiles solid and moisture content of 92 % and 53.80 % accordingly.
4. Significant amount of oil and grease concentration, 156.6 mg/L was found in the sludge.
5. The sludge microstructure resembles oily globules formed by interconnected globules' layers in moisture free conditioned.

4.2 Binders Characterization

Binder's characterization was important in the research since reaction mechanism is governed by the quantified element forming the selected binders. It controlled the finished products, interaction with the incorporated sludge and forming acceptable monolith. Some of the physical properties like BET and surface charge may give a direct effect to the solidified OPC-sludge properties.

4.2.1 Physical properties

Binder's properties are important for designing the mixing proportion. The property has the significant effect to the cement paste setting and strength. The smaller the size of material, the better the strength of solidified forms. Similarly the larger surface area of binder materials the higher the water requirement. Summary of binder's physical properties are given in Table 4.3. The raw binder materials in powder form are depicted in Figure 4.4.

Table 4.3: Physical properties of selected binders

| <i>Physical properties</i> | <i>OPC</i> | <i>FA</i> | <i>CSF</i> | <i>RHA</i> | <i>AC</i> | <i>MK</i> |
|--------------------------------------|------------|-----------|------------|------------|-----------|-----------|
| BET surface area (m ² /g) | 3.89 | 2.54 | 15.9 | 14.6 | 923 | 14.3 |
| Specific gravity | 2.87 | 2.37 | 0.65 | 2.01 | 0.44 | 2.22 |
| Size (nm) | 4992.33 | 2025.00 | 265.86 | 699.83 | 449.63 | 3588.00 |
| Density, (kg/m ³) | 2870 | 2370 | 650 | 2010 | 440 | 2222 |
| LOI (%) | 5.95 | < 0.50 | 0.85 | 2.69 | 73.34 | < 0.50 |

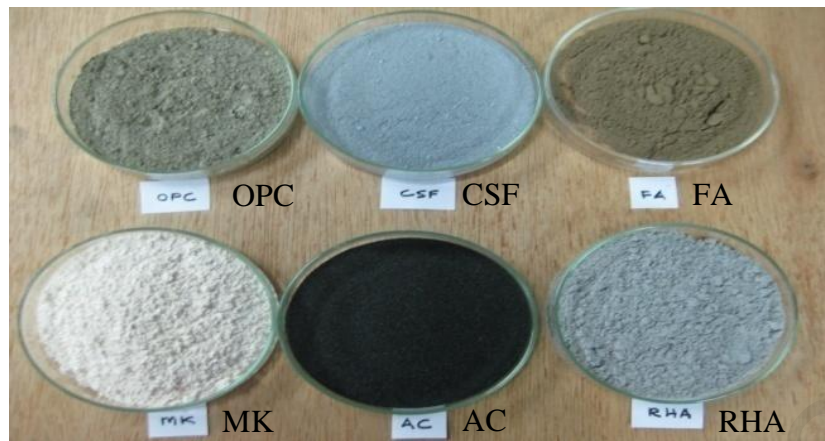


Figure 4.4: Binder materials in powder form

4.2.2 Chemical properties

Raw binder leaching was conducted to investigate the metal leached from individual binder based on the component present in the binder's matrix. Figure 4.5 depicted the metal concentration in raw binder leachate. The figure shows that aluminum is the main leached metal from all raw binders. MK recorded significantly high concentration of aluminum, 44.53 mg/L since the aluminum is one of the main elements in MK. The binder's elemental analysis was captured by Zeiss FESEM EDAX to gold-coated fractured sample as tabulated in Table 4.4. OPC and FA constituted by numerous elements while CSF and AC mainly consist of silica oxide and carbon accordingly.

RHA and MK are also rich in silica oxide. Al^{3+} , Fe^{3+} and Cr^{3+} are hard metal ions that can easily chelate a molecule with oxygen atoms. In soil, Al^{3+} induced toxicity as it can increase acidity by releasing H^+ by reaction with OH^- with its three charges and preventing other cations exchange to occur. In general, Al's ions were found as a dominant metal in the leachate. Cd^{2+} and Cu^+ are soft metal ions that easily form complexes with ligands containing sulfur.

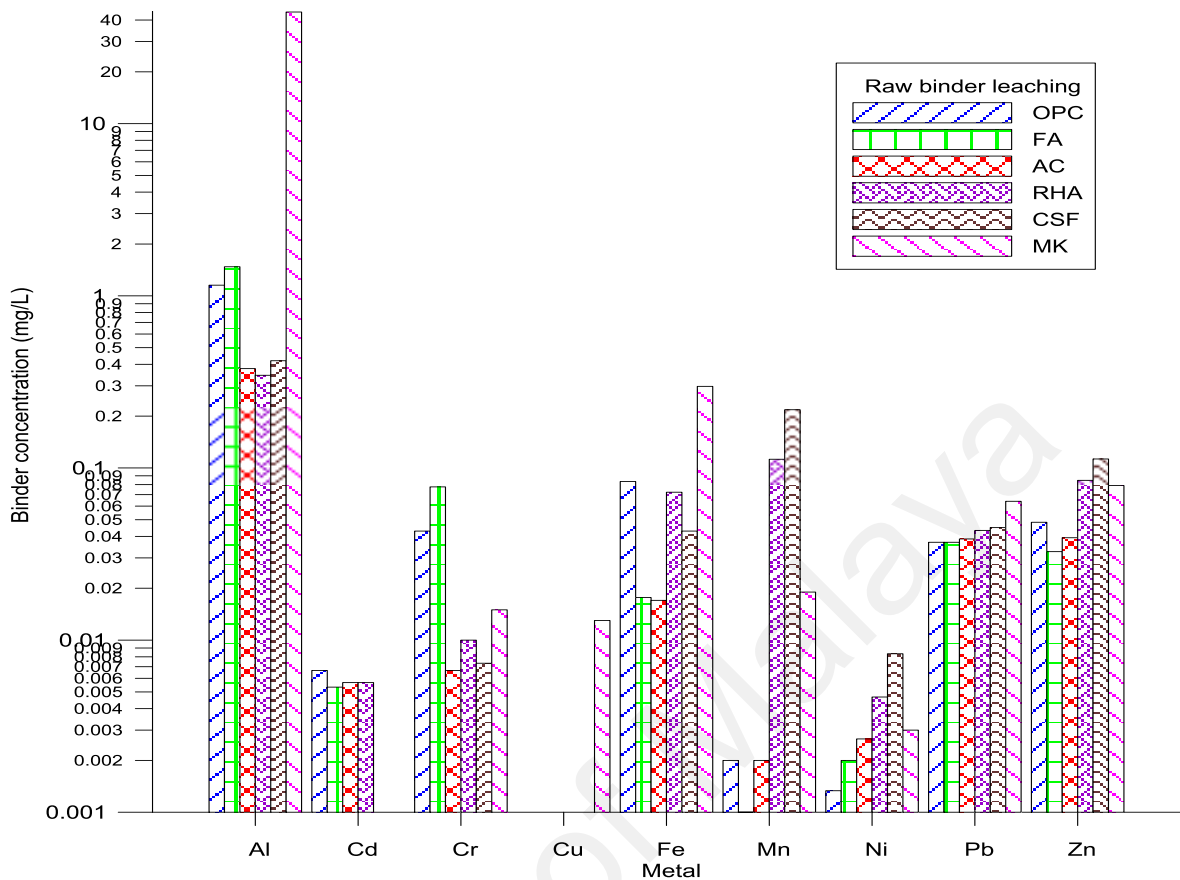


Figure 4.5: Metal concentration in raw binder leachate

Table 4.4: Composition of binders by EDAX analysis

| <i>Element</i> | <i>OPC</i> | <i>FA</i> | <i>CSF</i> | <i>RHA</i> | <i>AC</i> | <i>MK</i> |
|----------------|------------|-----------|------------|------------|-----------|-----------|
| Carbon | 7.04 | 56.48 | - | 7.31 | 100 | 8.97 |
| Oxygen | 35.02 | 23.78 | 43.55 | 43.13 | - | 34.68 |
| Magnesium | - | 0.55 | - | - | - | - |
| Aluminum | 2.55 | 3.32 | - | - | - | 25.81 |
| Silicon | 8.74 | 11.62 | 50.79 | 46.14 | - | 30.53 |
| Sulfur | 1.56 | - | - | - | - | - |
| Potassium | 0.82 | 0.51 | - | 3.43 | - | - |
| Calcium | 44.27 | 1.49 | - | - | - | - |
| Iron | - | 2.26 | - | - | - | - |
| Indium | - | - | 5.66 | - | - | - |

Properties of cement are governed by the compound composition. The potential cement composition can be calculated using Bogue equation shown by Equation 4-1 to Equation 4-4. The Bogue equation is applicable to the value of Al_2O_3/Fe_2O_3 or A/F of \geq

0.6 (Gani, 1997). The oxide compounds in weight percent determined by PAN analytical Minipal 4 ED-XRF analysis, and its abbreviation symbols are tabulated in Table 4.5 are used for calculating the cement composition by Bogue estimation. The potential percentage of cement composition is represented in Table 4.6. C_3S is the main composition of the cement with 52.22 weight percent. The C_3S contribute to the early strength and has a fast rate of reaction with water (Mehta and Monteiro, 2006).

$$C_3S = 4.07(C) - 7.6(S) - 6.72(A) - 1.43(F) - 2.85(S) \quad \text{Eq. (4-1)}$$

$$C_2S = 2.87(S) - 0.75(C_3S) \quad \text{Eq. (4-2)}$$

$$C_3A = 2.65(A) - 1.69(F) \quad \text{Eq. (4-3)}$$

$$C_4AF = 3.04(F) \quad \text{Eq. (4-4)}$$

Table 4.5: Oxide of cement in percent weight and its abbreviation symbol

| Oxide compound | Abbreviation | Weight percent (%) |
|--------------------------------|--------------|--------------------|
| CaO | C | 64.53 |
| SiO | S | 22.25 |
| Al ₂ O ₃ | A | 4.52 |
| Fe ₂ O ₃ | F | 3.13 |
| MgO | M | 3.22 |
| SO ₃ | S | 2.27 |

Table 4.6: Potential cement composition

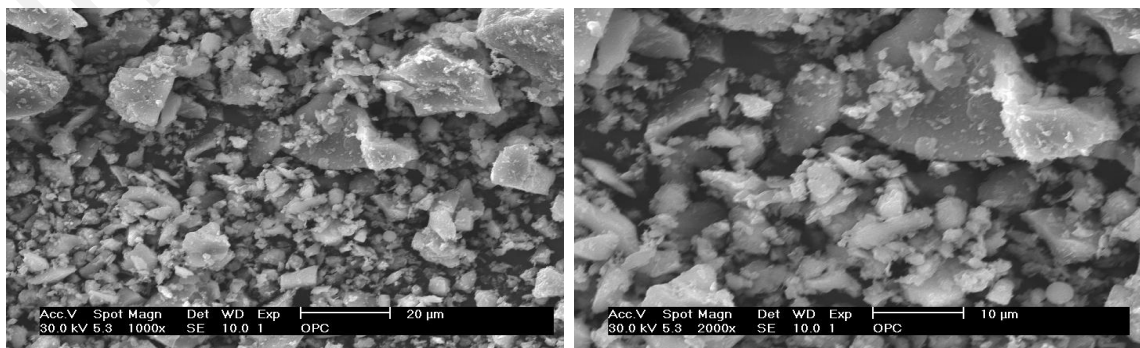
| Cement composition | Percentage |
|--------------------|------------|
| C_3S | 52.22 |
| C_2S | 24.69 |
| C_3A | 6.69 |
| C_4AF | 9.51 |

Bogue calculation did not account for MgO and alkalis, which formed the remaining weight percent in the cement mixture of 6.89 %. Since MgO formed 3.22 % of the total oxide as in Table 4.5, the remaining alkalis formed were 0.08 %. The alkalis are derived from clay were in form of N_2O and K_2O .

4.2.3 Microstructure

4.2.3.1 Ordinary Portland cement

The OPC particles resemble angular shapes of cement clinker as shown by SEM photomicrographs of OPC in Figure 4.6. The SEM image was captured using accelerated voltage of 30 kV using secondary electron for surface morphology at working distance of about 27 mm. Fractured sample was sputtered gold-coated prior to the imaging to reduce charging effect. The average size of cement is 5531.66 nm with the surface charge or zeta potential of -1.06 mV. The cement particle has micropore surface area $3.54 \text{ m}^2/\text{g}$ slightly less than its BET value $3.89 \text{ m}^2/\text{g}$. The cement particles have adsorption energy of 5.21 kJ/mol. The cement minerals mainly constituted by alite, C_3S and belite, C_2S as shown in OPC diffractogram as predicted by Bogue calculation.



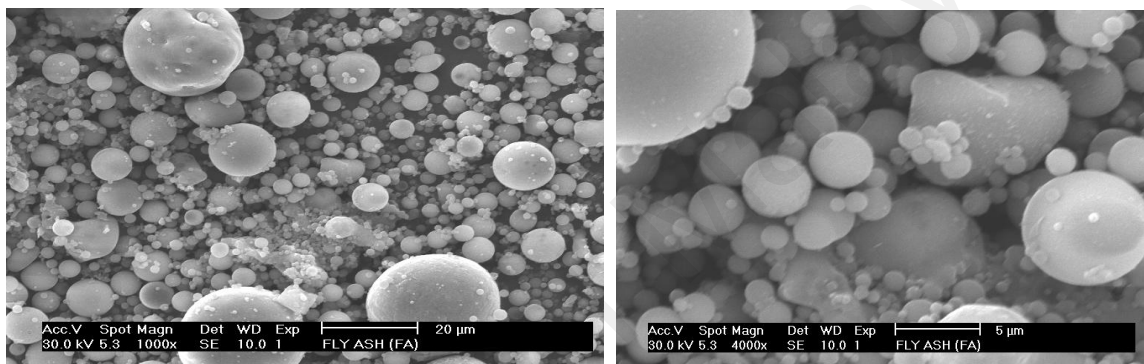
(a) 1000x

(b) 2000x

Figure 4.6: Photomicrographs of OPC at (a) 1000x and (b) 2000x

4.2.3.2 Fly ash

Fly ash (FA) has the spherical shape in nature as shown in Figure 4.7. FA has finer average size of 483.23 nm with high reducing zeta potential of -62.27 mV. Its micropore surface area $2.06 \text{ m}^2/\text{g}$ is lower than OPC. FA has 5.58 kJ/mol of adsorption energy. FA mineral composed of gypsum, quartz, C_3A and C_4AF as shown in the Diffractogram. The FA has low calcium content as measured by EDAX analysis.



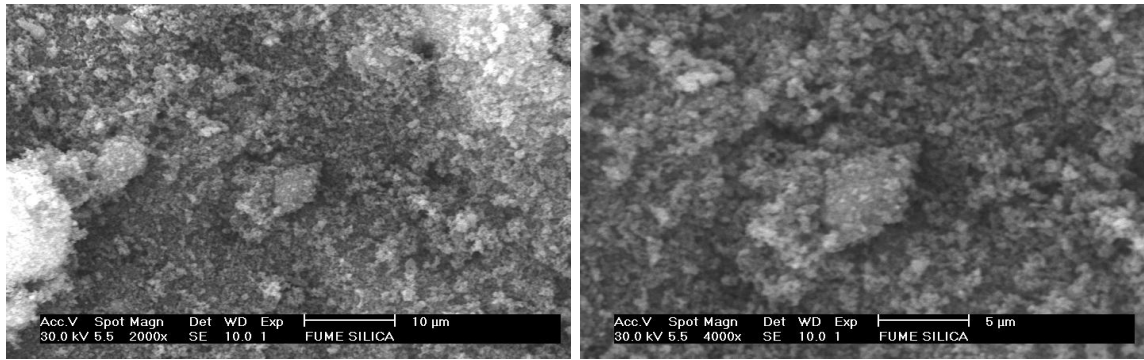
(a) 1000x

(b) 4000x

Figure 4.7: Photomicrographs of fly ash at (a) 1000x and (b) 4000x

4.2.3.3 Condensed silica fume

Condensed silica fume (CSF) has sphere's shapes and one of the reactive additives pozzolan due to its smaller size and higher surface area (Figure 4.8). CSF has particle size of 315.23 nm and reducing zeta potential of -76.23 mV. It has higher micropore surface area of $16.6 \text{ m}^2/\text{g}$. CSF has high adsorption energy of 6.39 kJ/mol, which attributed by the silica oxide compound as measured by EDAX analysis. Amorphous diffractogram of CSF as in Figure 4.12 showed noncrystalline phase of disordered Si-O structure, which is the products of condensation material (Malhotra and Mehta, 1996).



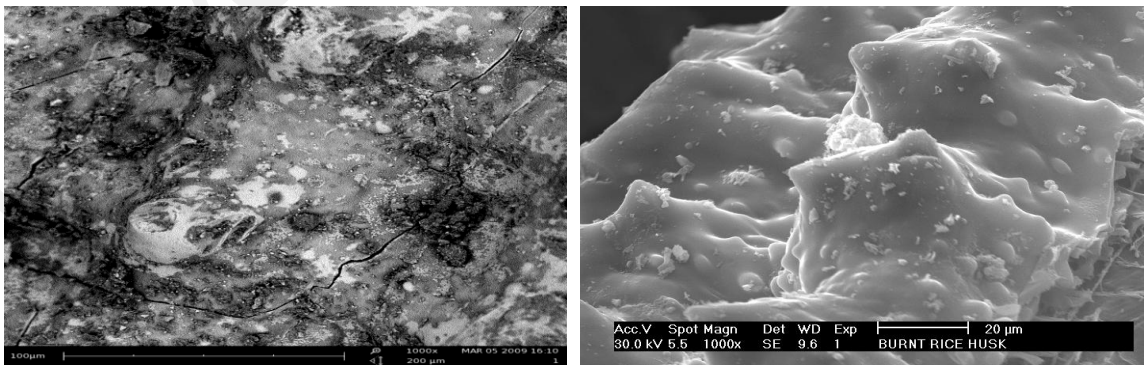
(a) 2000x

(b) 4000x

Figure 4.8: Photomicrographs of silica fume at (a) 2000x and (b) 4000x

4.2.3.4 Rice husk ash

Rice husk ash (RHA) is attributed by its cellular surface structure (Figure 4.9) was a reactive pozzolan with high specific surface area. The average particle size of RHA is 1325.10 nm and zeta potential of -54.11 mV. Its micropore surface area is 13.3 m²/g with higher adsorption energy of 7.7 kJ/mol compared to other binders. RHA contained high silica oxide and potassium oxide. XRD diffractogram of RHA exhibit an amorphous spectrum of Si-O.



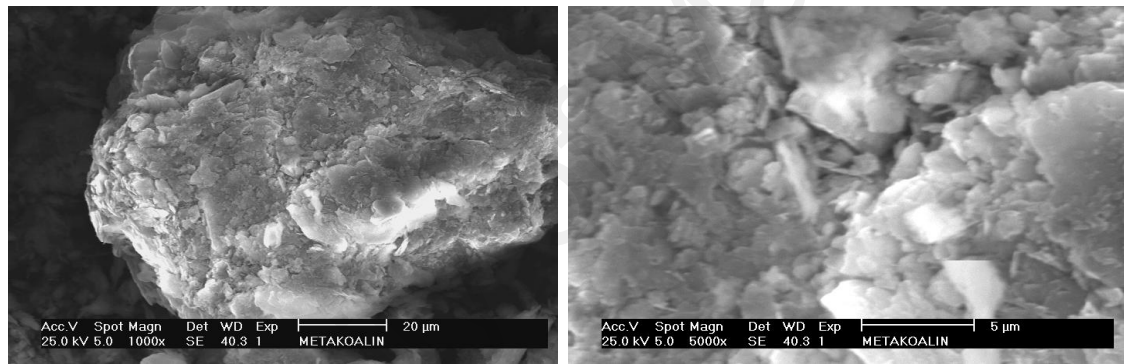
(a) raw at 1000x

(b) calcined at 1000x

Figure 4.9: Photomicrographs of rice husk (a) raw at 1000x and (b) calcined at 1000x

4.2.3.5 Metakaolin

Metakaolin (MK) particles consist of thin platy layer overlay irregularly into spherical shape as depicted in Figure 4.10. The average particle size of MK is 4711.66 nm with zeta potential of -67.89 mV. Its micropore surface area is 13.5 m²/g with the adsorption energy of 5.81 kJ/mol. Kaolin mineral which formed by hydrated aluminum disilicate will be dehydroxylized forming two-dimensional order crystal structure when calcined at temperature of 500-800 °C (Siddique, 2008). Major MK minerals are SiO₂ and Al₂O₃ with XRD diffractogram showed an amorphous spectrum.



(a) 1000x

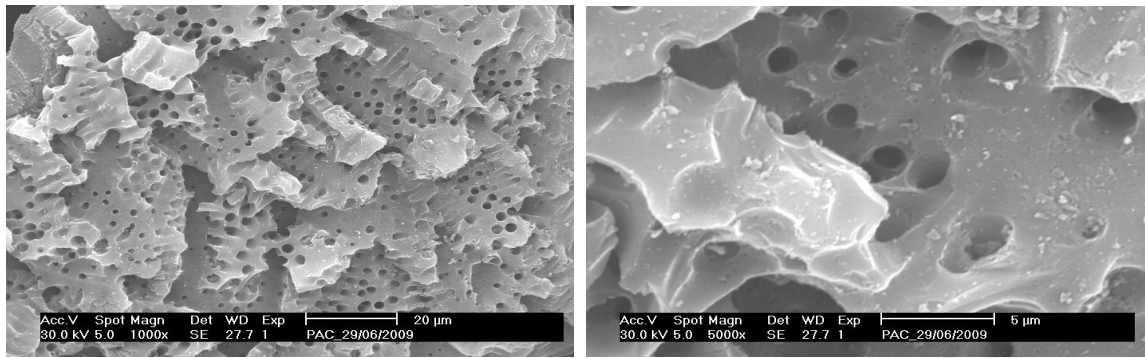
(b) 5000x

Figure 4.10: Photomicrographs of metakaolin at (a) 1000x and (b) 5000x

4.2.3.6 Activated carbon

The activated carbon (AC) has macro and micro porous surface as illustrated in Figure 4.11. The size and surface charge of AC is 291.73 nm and -61.81 mV accordingly. The AC micropore and BET surface area of activated carbon are 12700 m²/g and 923 m²/g accordingly. The adsorption energy of AC is 2.37 kJ/mol.

The summary of binder's properties as measured by the Zetasizer Nano and BET nitrogen adsorption were tabulated in Table 4.7.



(a) 1000x

(b) 5000x

Figure 4.11: Photomicrographs of powder activated carbon at (a) 1000x and (b) 5000x

Table 4.7: Microstructure properties of binders

| <i>Binders</i> | <i>OPC</i> | <i>FA</i> | <i>CSF</i> | <i>RHA</i> | <i>MK</i> | <i>AC</i> |
|--|------------|-----------|------------|------------|-----------|-----------|
| <i>microstructure</i> | | | | | | |
| Particle size (nm) | 5531.66 | 483.23 | 315.23 | 1325.10 | 4711.66 | 291.73 |
| Surface charge (mV) | -1.06 | -62.27 | -76.23 | -54.11 | -67.89 | -61.81 |
| Conductivity (mS/cm) | 0.1546 | 0.1272 | 0.026 | 0.0386 | 0.0178 | 0.0234 |
| Polydispersity Index (PDI) | 0.6987 | 0.599 | 0.2527 | 0.7210 | 0.8153 | 0.479 |
| Mobility ($\mu\text{mcm/Vs}$) | -1.5840 | -1.9953 | -2.2570 | -2.6257 | -2.3237 | -2.9557 |
| Micropore surface area (m^2/g) | 3.54 | 2.06 | 16.60 | 13.30 | 13.50 | 12700.00 |
| BET surface area (m^2/g) | 3.89 | 2.54 | 15.90 | 14.60 | 14.30 | 923.00 |
| Average pore size (\AA) | 105.0 | 55.5 | 69.9 | 91.4 | 139.0 | 18.1 |
| Total pore volume (cc/g) | 0.0102 | 0.00353 | 0.0277 | 0.0334 | 0.0498 | 0.418 |
| Adsorption energy (kJ/mol) | 5.21 | 5.58 | 6.39 | 7.70 | 5.81 | 2.37 |

4.2.3.7 Conclusions

OPC has the highest particle size of 5531.66 nm compared to other binders. Binder's particle charges were all in reducing state and OPC pore fluid as reported in the literature review were in oxidizing state but the raw particle was found in an almost neutral state -1.06 mV whereby the reducing state can help to immobilize waste by reducing polyvalent ions.

The reducing redox potential of OPC should be enhanced further by blending with other binders as shown in Table 4.7 since all binders were in reducing state. AC showed significant physical property compared to other binders in terms of its smallest particle size and yet largest micropore surface area or BET, which provides adsorption sites to the contaminant in waste, especially for organic adsorption. Even though it has the lowest adsorption energy since it was the most inert particles formed by long carbon ring while RHA has the highest adsorption energy 7.70 kJ/mol, which form a good binder property toward waste adsorption.

OPC as the main binder has the conductivity and average pore size larger than the other binder with 0.1546 mS/cm and 105 Å accordingly. MK has highest polydispersity index of 0.8153 compared to other binders. OPC particle has the highest mobility of -1.584 $\mu\text{mcm/Vs}$ while AC particle was the least mobile.

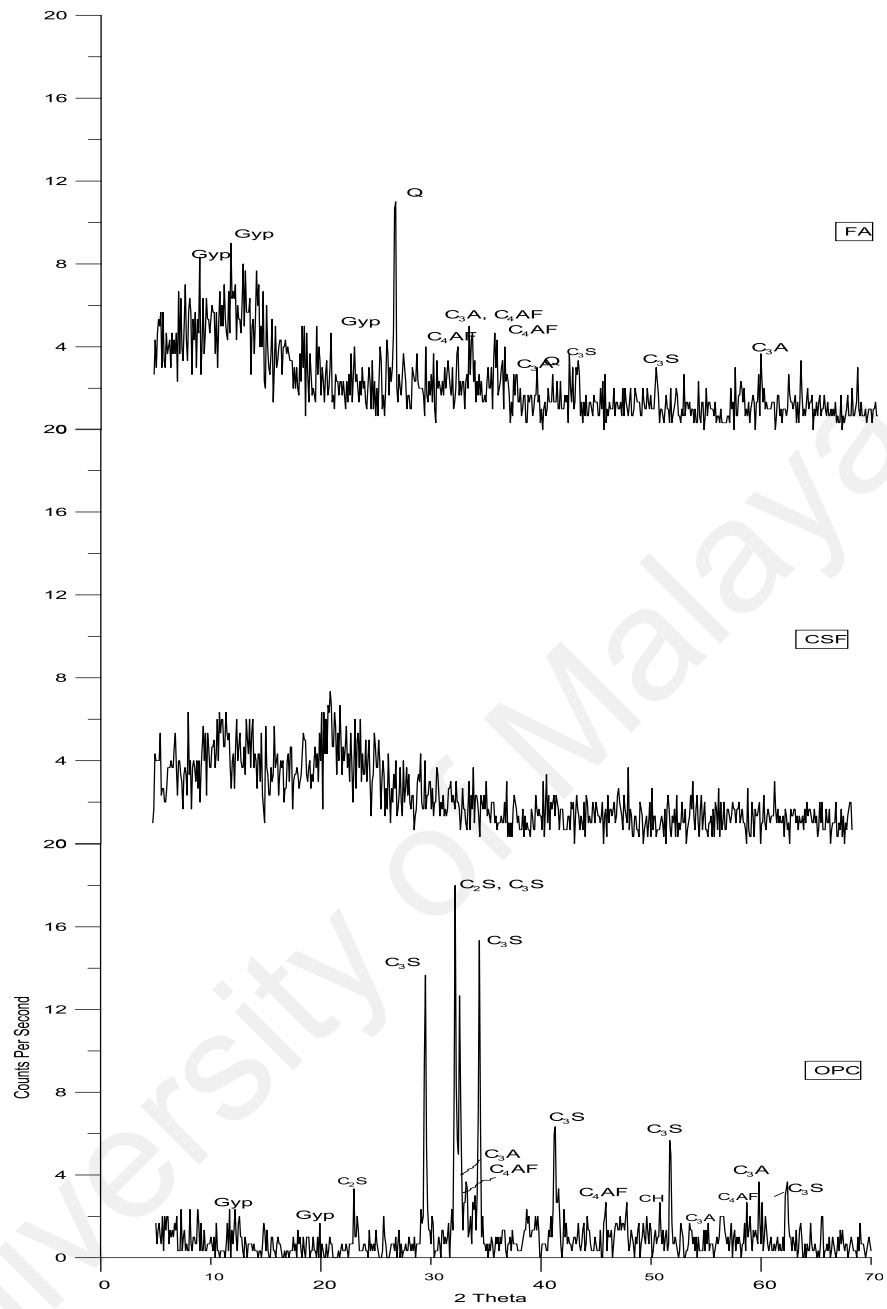
4.2.4 Binders crystallization

Binder X-ray diffraction (XRD) analysis performed by using a Siemens D-5000 spectrometer are illustrated in Figure 4.12 for OPC, CSF and FA and Figure 4.13 for AC, RHA and MK. The mineral crystallization indicated by spectrum peaks was identified by

matching of the spectrum with built in equipment's library. The main OPC mineral consists of alite, belite, portlandite and calcium silicate. Minor mineral found in the OPC are gypsum, calcium aluminum iron oxide and calcium aluminum sulfate oxide.

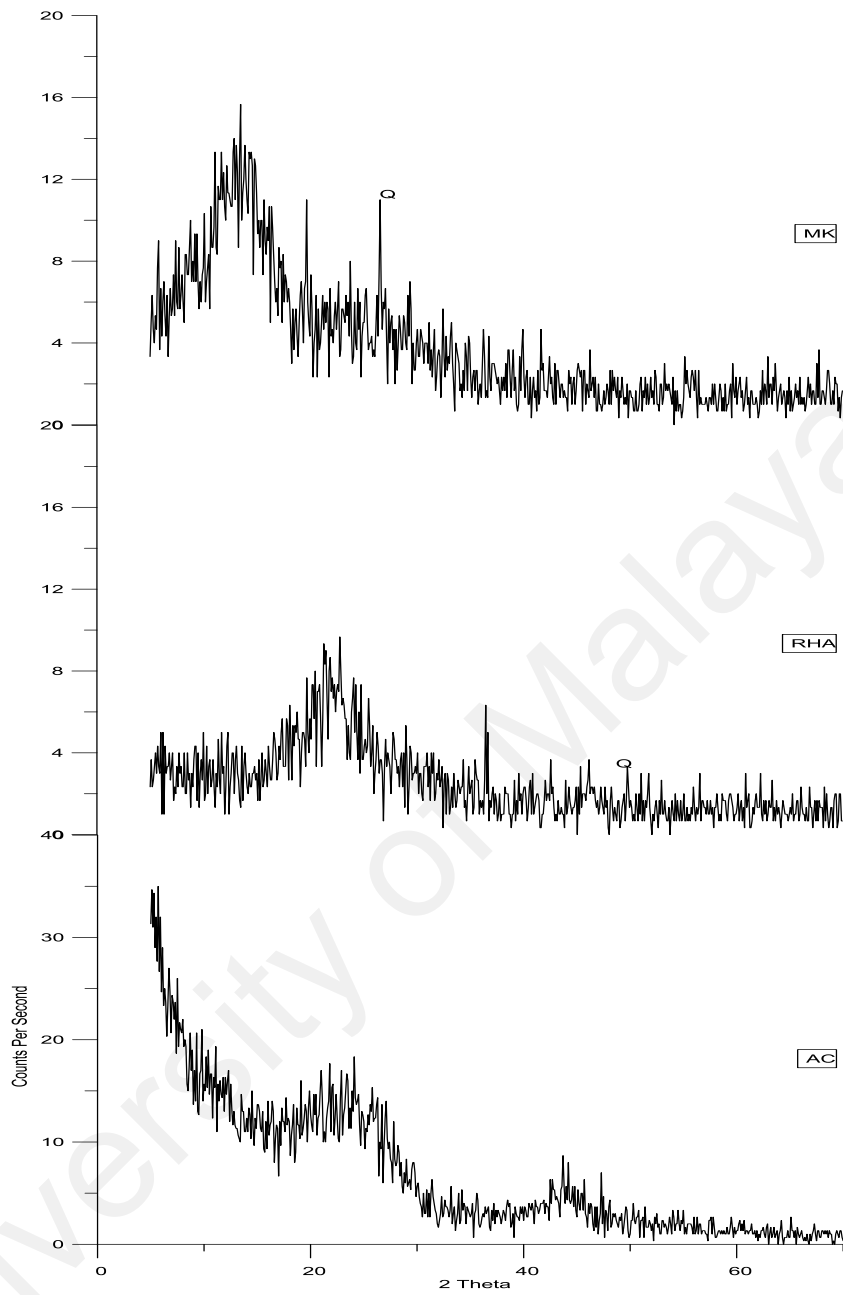
Alite, the most abundance mineral in cement was detected at 2θ of 23.0° , 29.5° , 32.6° , 34.4° , 41.3° and 51.8° . The alite mineral was found in monoclinic and triclinic shape. Belite mineral in monoclinic shape was found at 32.2° , 34.4° and 41.3° . Cubic calcium aluminum oxide, C_3A can be found at 33.3° , 37.9° and 59.5° while monoclinic at 32.2° . Calcium aluminum iron oxide, C_4AF was found at 34.2° and 53.0° . Gypsum in the monoclinic form was found at 12.0° and 21.0° . The present of $Ca(OH)_2$ or portlandite is normally associated with pozzolanic activity, which was determined at 18.2° , 34.3° , and 47.3° and 50.8° .

Calcium aluminum sulfate oxide, C_4AF was found in FA at 2θ of 43.1° and 51.9° . Quartz mineral, SiO_2 was found in FA and MK at 26.6° . Amorphous diffractograms exhibited by AC, CSF and RHA due to non crystalline surface of carbon and silica.



Note: Gyp-gypsum, C₃S-tricalcium silicate, CH-Ca(OH)₂, C₂S-calcium silicate oxide, Q-quartz, C₃A-calcium aluminum oxide, C₄AF- calcium aluminum iron oxide

Figure 4.12: Diffractograms of raw binder's spectrum for OPC, CSF and FA



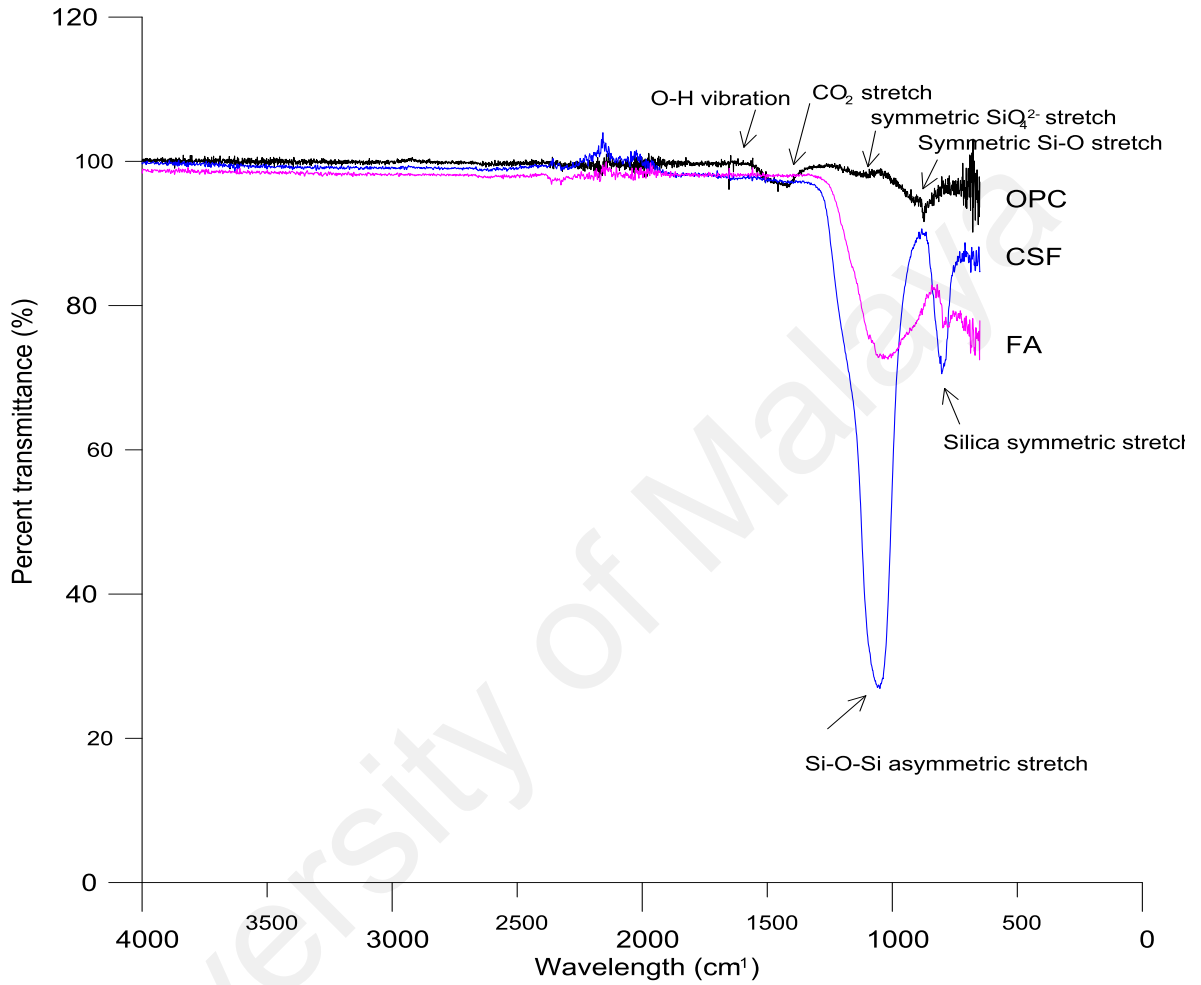
Note: Gyp- gypsum, C₃S-tricalcium silicate, CH-Ca(OH)₂, C₂S-calcium silicate oxide, Q-quartz, C₃A-calcium aluminum oxide, C₄AF- calcium aluminum iron oxide

Figure 4.13: Diffractograms of raw binder's spectrum for AC, RHA and MK

4.2.5 Fourier Transforms Infrared analysis

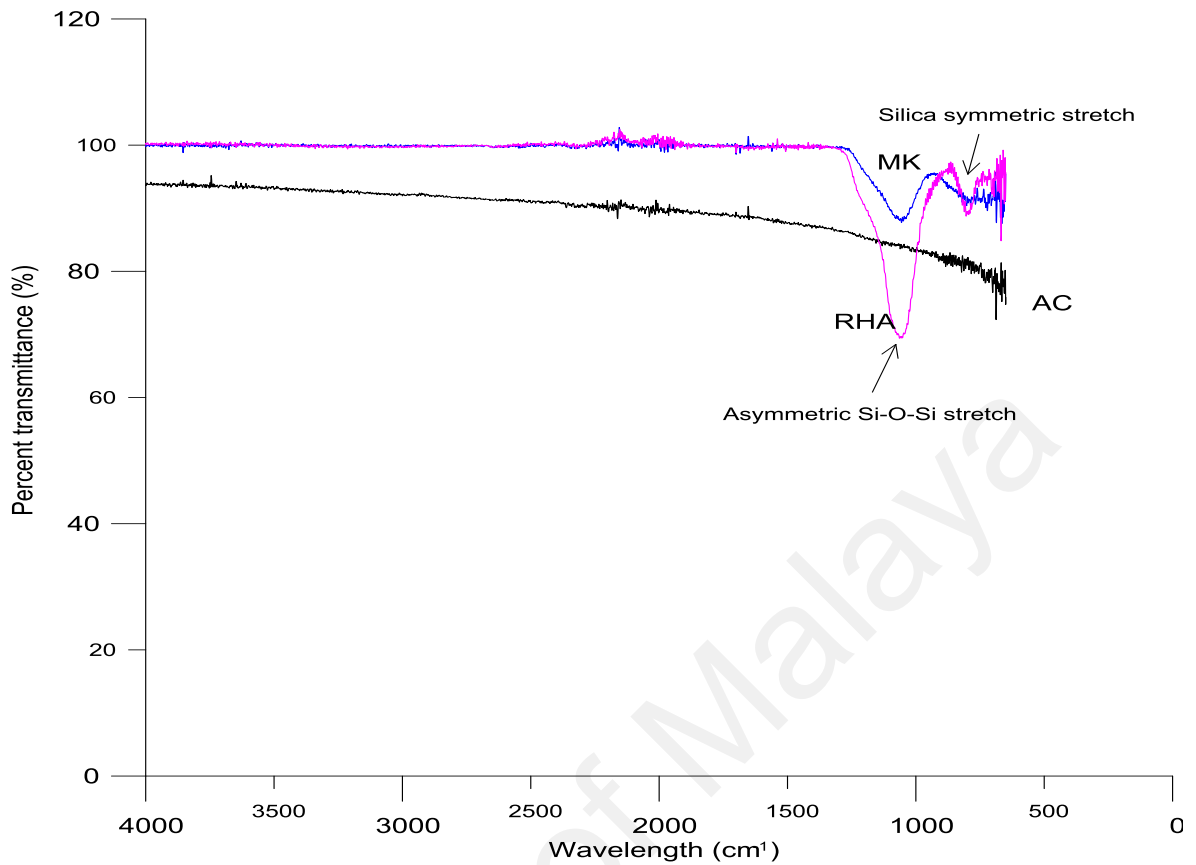
The binder functional group was determined by the Nicolet iS10 Thermo Scientific Fourier transforms infrared (FTIR) based on the wavelength of 500 – 4000 cm⁻¹. The

binders infrared spectra are illustrated in Figure 4.14 (a) for OPC, CSF and FA and Figure 4.14 (b) for AC, MK and RHA used in cement mixture.



(a) OPC, CSF and FA

Figure 4.14: Infrared spectra of binders (a) OPC, CSF and FA (b) AC, MK and RHA



(b) AC, MK and RHA

Figure 4.14: Infrared spectra of binders (a) OPC, CSF and FA (b) AC, MK and RHA

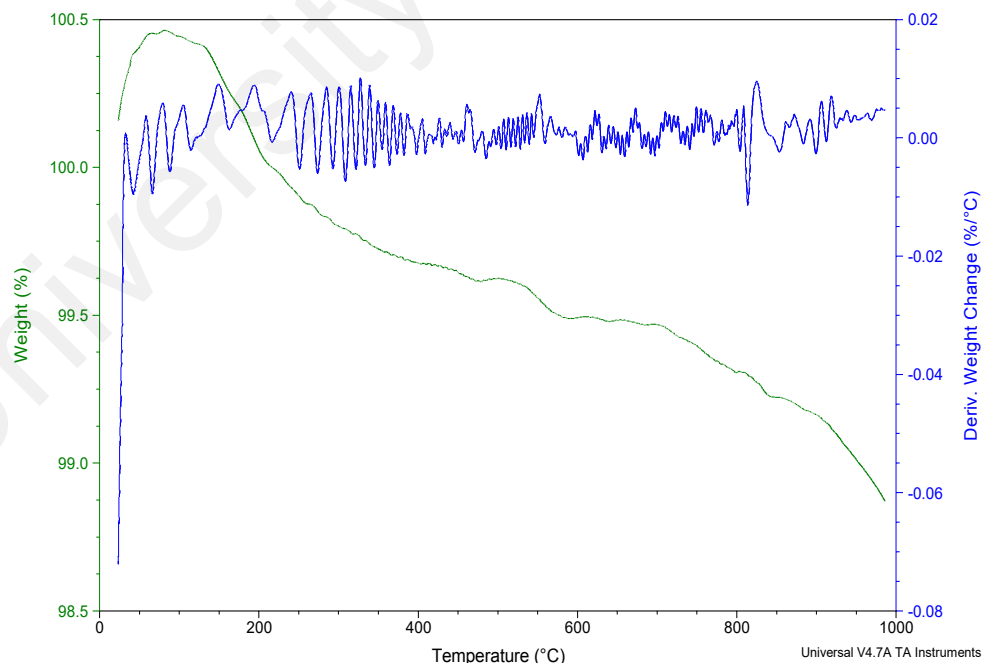
(continued)

Binder's infrared spectrum shows the presence of silica oxide, SiO_4^{4-} tetrahedral forming long chain of Si-O-Si exist as crystalline formed as quartz (Smith, 1999). The silica vibration symmetric stretch can be found at wavelength of 805 cm^{-2} . Silanol, Si-O stretch was located at 940 cm^{-1} . Asymmetric stretch of Si-O-Si was observed at $1200 - 1000 \text{ cm}^{-1}$. CSF and RHA dominantly constituted of asymmetric Si-O-Si stretch with minor symmetric Si-O stretch. OPC spectrum indicates symmetric SiO_4^{2-} at 1083 cm^{-1} and CO_2 stretch at $1450 - 1360 \text{ cm}^{-1}$. MK and FA also showed the asymmetric Si-O-Si stretch at 1083 and 1024 cm^{-1} accordingly. In contrast to other binders, AC spectrum shows no

silica or CO₂ vibration due to its structure consist of mainly inert carbon atoms bounded one to another. The absorbed water is vibrated as O-H bond at 1653 cm⁻¹ in OPC.

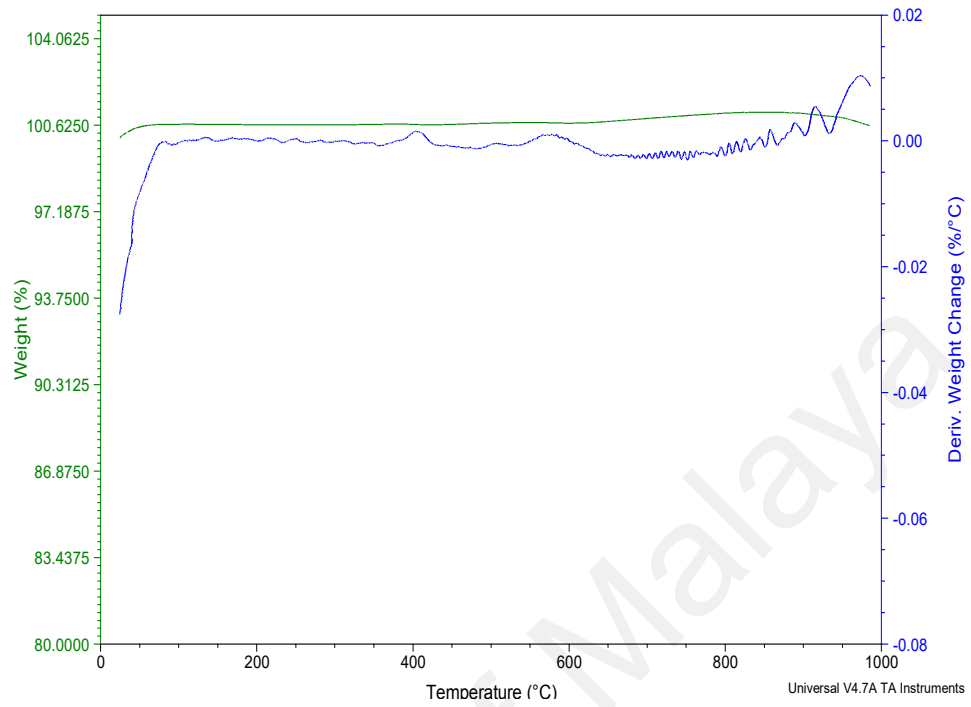
4.2.6 Thermogravimetry analysis of binders

Thermogravimetry analysis provides the weight loss of material based on degradation of material subjected to high-temperature combustion of up to 1000 °C. The binder thermograms were illustrated in Figure 4-15 (a) to (e). Most of the binders such as FA, MK composed of very inert compounds with insignificant weight loss, LOI of < 0.50 %, CSF of 0.85 % and RHA of 2.69 %. On the contrary, to pozzolan binder, AC structure that consists of organic molecule structure has significantly large mass decomposition with 73.34 % found at temperature of 500 to 700 °C.

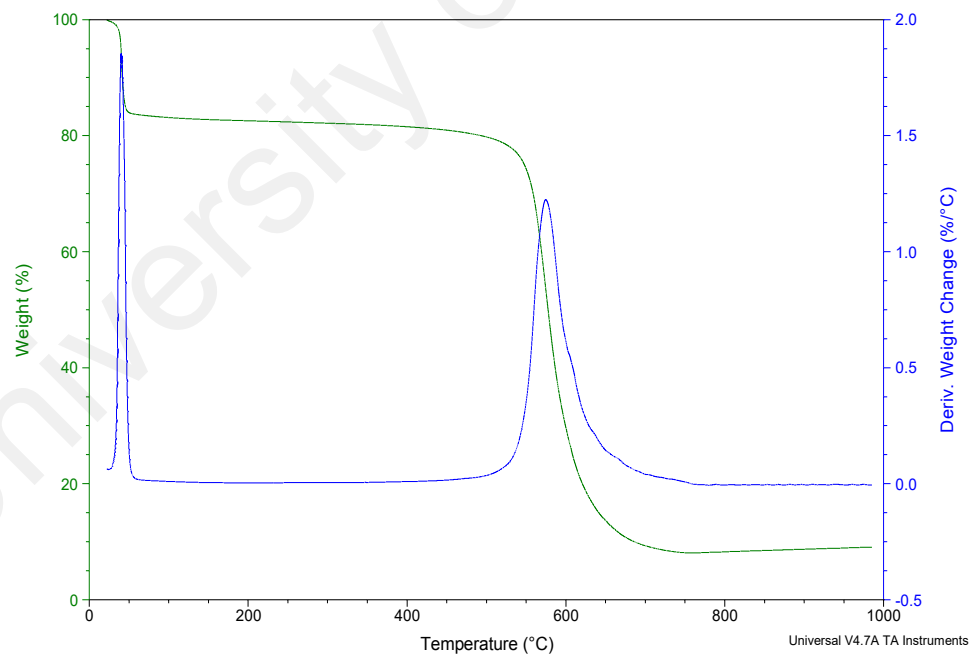


(a) CSF

Figure 4.15: Thermograms of binders (a) CSF (b) FA (c) AC (d) MK and (e) RHA



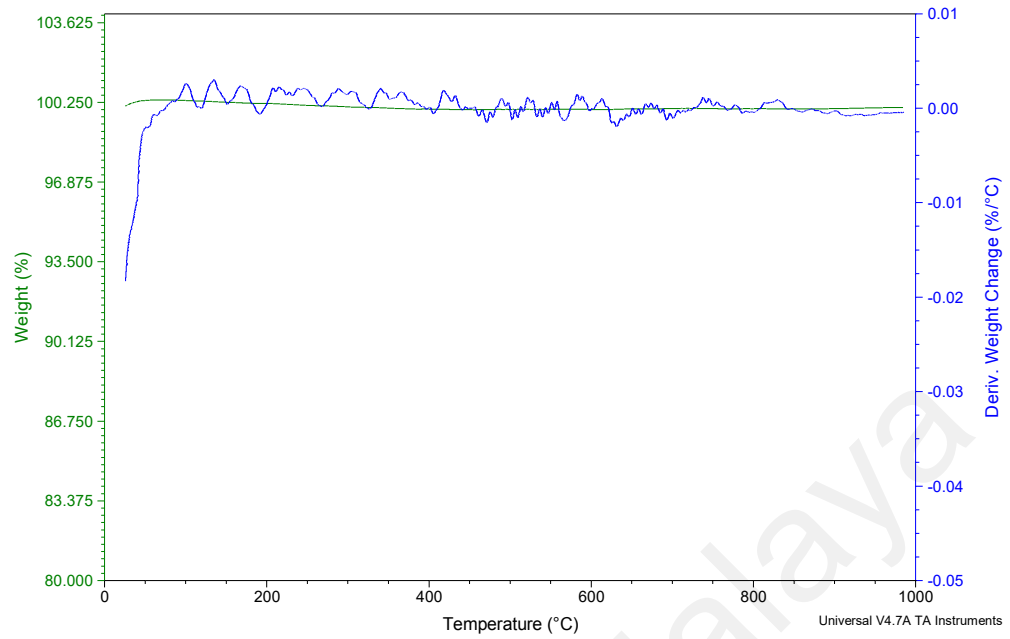
(b) FA



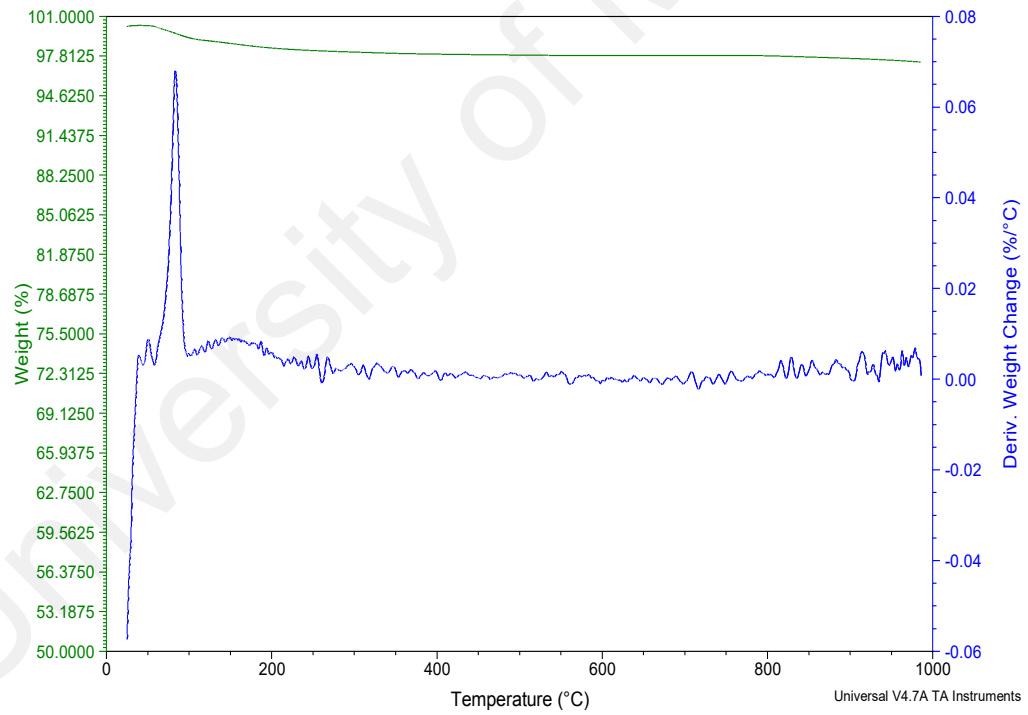
(c) AC

Figure 4.15: Thermograms of binders (a) CSF (b) FA (c) AC (d) MK and (e) RHA

(continued)



(d) MK



(e) RHA

Figure 4.15: Thermograms of binders (a) CSF (b) FA (c) AC (d) MK and (e) RHA

(continued)

4.2.7 Conclusions of binder characterization

Based on binders characterization conducted few salient points were found as follows:

1. Main component of OPC by Bogue analysis showed that main components are tricalcium silicate and dicalcium silicate with 52.22 % and 24.69 % accordingly.
2. Metals in the binder material can leached out through leaching process.
3. The binders have reducing zeta potential, which induces the precipitation of metal hydroxide in cement hydration.
4. AC has largest micropore surface area, which provides adsorption site for contaminant.
5. Highest adsorption energy, 7.70 kJ/mol of RHA formed an attractive CRM property for enhancement of contaminant adsorption.
6. Mineral crystallizations were found in OPC and FA whereas other binders showed amorphous diffractogram.
7. IR spectra of binder materials showed the presence of asymmetric stretch of Si-O-Si at 1000-1200 cm^{-1} superseded the symmetric Si-O-Si at 800-900 cm^{-1} , as an important functional group especially in CSF and RHA.
8. Generally all binders have minimum LOI except AC with 73.34 %, which was significantly high due to decomposition of organic structure.

4.3 Cement Paste Properties

Once cement reacted with water, a dynamic process occurs as hydration of major cement clinker take place. The cement phase is transformed from wet paste to solid during

the active hydration period by set of the main product of cements such as ettringite, portlandite and C-S-H gel. Setting time was measured to ensure the appropriated mixture of cement has been used. The ease of cement application for expected forms will depend on its workability values measured by slump test.

4.3.1 Setting time

Setting time for the water to cement, cement to sludge and CRMs addition was measured by ASTM C 191 - 04b standard test methods for time of setting of hydraulic cement by Vicat Needle (ASTM, 2005). The initial setting time was determined as the elapsed time required to achieve a penetration of 25 mm and the final time of setting as the total time elapsed until the needle does not leave a complete circular impression in the paste surface. The reaction of water with cement involving C_3S forming crystalline $Ca(OH)_2$ and C-S-H gel spearhead the setting of cement hydration. The calcium hydroxide produced by the reaction made the cement alkaline with pH of about 12.5 (Gani, 1997).

4.3.1.1 Effect of water to cement ratio

The setting time was conducted for the selected water to cement ratio in the experimental work was illustrated in Figure 4.16. The initial setting time (minute) was determined at 25 mm depth of penetration as tabulated in Table 4.8. The increased in water to cement ratio (W/C) was found to increase the setting time by 44 % and 16 % for 0.4 to 0.45 and 0.45 to 0.5 accordingly. Bleed water can be seen on the surface of cement paste masses for W/C of 0.5, and it was the initial bleeding W/C ratio as reported by other researchers (Conner, 1990). Since OPC has high C_3S , 55.22 % and C_3A , 6.69 % content whereby both minerals contribute to early strength. Setting of cement is balanced by the

aluminate and sulfate content. Normal setting occurs in 1-2 hours for high reactivity of aluminate and high sulfate content, but the set is delayed to 2-4 hours if both minerals are in low reactivity or availability.

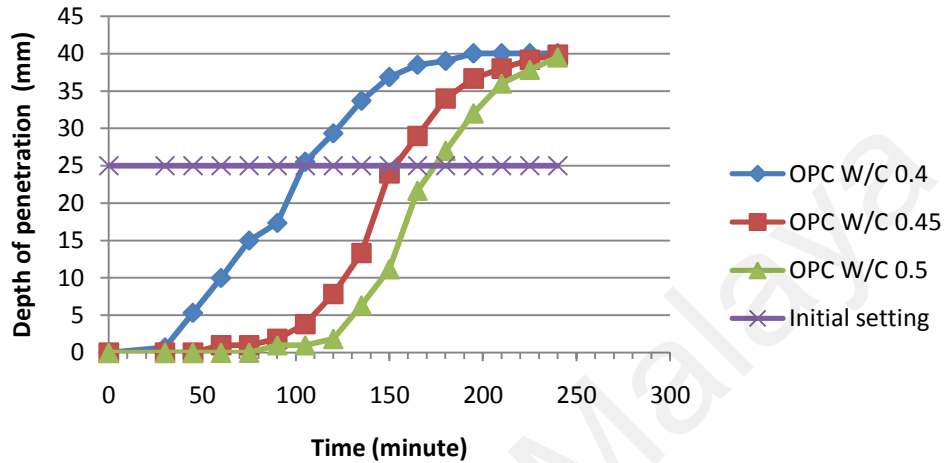


Figure 4.16: OPC depth of penetration versus time

Table 4.8: Initial setting time for OPC

| <i>Water to cement ratio</i> | <i>Initial setting time (minute)</i> |
|------------------------------|--------------------------------------|
| 0.40 | 104.08 |
| 0.45 | 150.00 |
| 0.50 | 174.37 |

Two models were developed to represent cement setting, the osmotic and crystalline model (Conner, 1990). In crystalline model, initial hydration proceeds by nucleation and growth of hexagonal calcium hydroxide crystal that fill up the space between cement grain leaving rich silicate layer on the surface of the grains, which reduced the movement of water to cement surface and release of calcium and silicate ions from cement. The calcium silicate hydrate grows outward of cement grain and form of the needle. The needle growth intertwined with other needles and formed tobermorite crystal. Similarly osmotic model explained by the formation of C-S-H gel around the cement

particle surface. The gel allows inward flow of water and outflow of Ca^{2+} and OH^- ions, which cause in excess of $\text{Ca}(\text{OH})_2$ on the outside of gel resulting in precipitation of portlandite (Cocke and Mollah, 1992). While silicate ion builds up on cement grain inside the gel layer producing osmotic pressure differential on the gel. The pressure ruptures the gel membrane periodically and reform by extruding concentrated silicate solution. The gel membrane formation was associated with the retardation of setting in the present of heavy metal. Hydration of typical Portland cement involving the setting time of major products are illustrated in Figure 4.17.

Carbonation of cement has been followed by vibrational spectroscopy. Cement carbonation occurs due to complex process that may depends on parameters like porosity, water to cement ratio and CO_2 partial pressure. Carbonation of C-S-H converts OH^- and Ca^{2+} to calcium carbonate which resulted in the apparent formation of a highly polymerized silica gel which is acid stable and maintains the same morphology as the original hydrate.

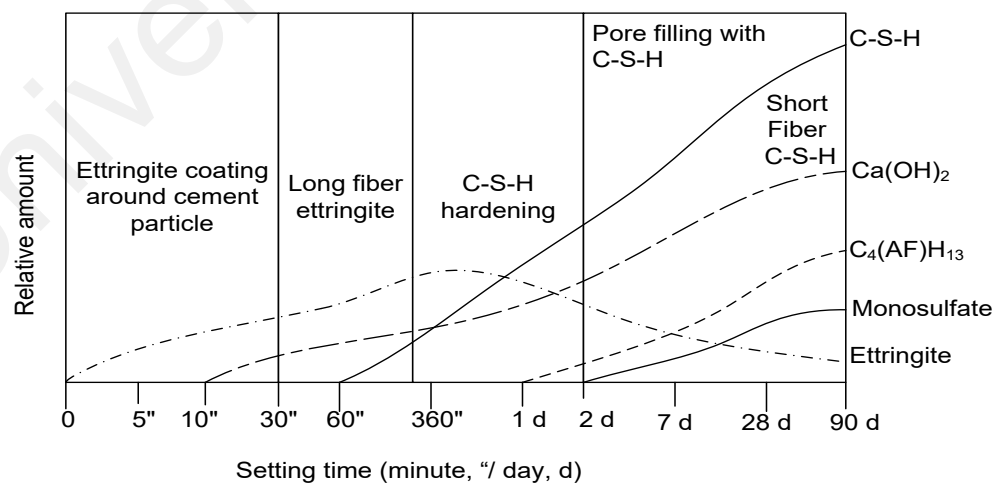


Figure 4.17: Hydration of Portland cement (adopted from Cocke and Mollah, 1992; Mehta and Monteiro, 2006)

4.3.1.2 Effect of cement to sludge ratio

The incorporations of sludge into cement pastes were conducted at the W/C of 0.45. Generally, the increase in cement to the sludge ratio slightly decreases the initial setting time as given in Table 4.9 but the depth of penetration versus time curve has a closely similar pattern to each other (Figure 4.18). Incorporation of sludge into cement has delayed the set of cement by the increased of 12 to 20 percent in initial setting time from the control cement. The increased in setting time of aliphatic and aromatic hydrocarbon waste cement was observed by CIRIA (1995). Organic compound has the hydrophobic group like methyl, ethyl, butyl and octyl with positive surface charge that interfere with cement hydration reaction. However, the organics will be attracted to the negative charge ion such as OH⁻ and neutralized for ettringite bridging to occur. The volatiles organics are also subjected to volatilization during S/S processing with the average of 0.11 % of the feed into the process was emitted to the air (Ponder and Schmitt, 1991).

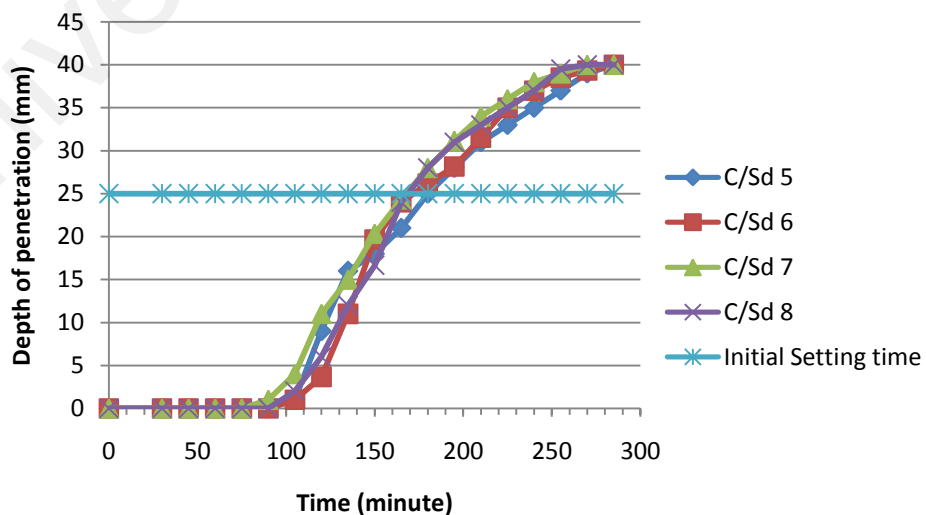


Figure 4.18: OPC and sludge depth of penetration versus time

Table 4.9: Initial setting time for the cement to sludge ratio

| <i>Cement to sludge ratio</i> | <i>Initial setting time (minute)</i> |
|-------------------------------|--------------------------------------|
| 5 | 180.00 |
| 6 | 171.91 |
| 7 | 167.74 |
| 8 | 168.75 |

4.3.1.3 Effect of CRMs to solidified sludge

The CRMs incorporation in the solidified sludge has changed the setting time in two different ways either increased or decreased the initial set. CSF, FA and AC were found to increase the setting but MK and RHA decreased the set time compared to the control OPC-Sd. Both MK and RHA have about the same BET values, high adsorption energy, with almost identical FTIR spectrum with Si-O-Si asymmetric stretch found in range of 1000 to 1200 cm^{-1} . The CRMs in OPC-sludge depth of penetration behaviors were represented in Figure 4.19. The initial setting times are tabulated in Table 4.10.

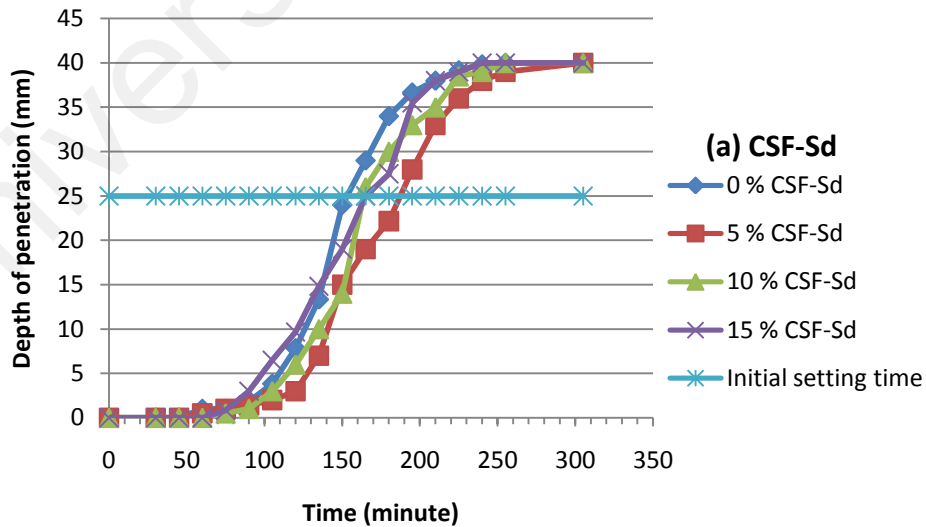


Figure 4.19: CRMs sludge depth of penetration versus time (a) CSF-Sd (b) FA-Sd (c) AC-Sd (d) MK-Sd and (e) RHA-Sd

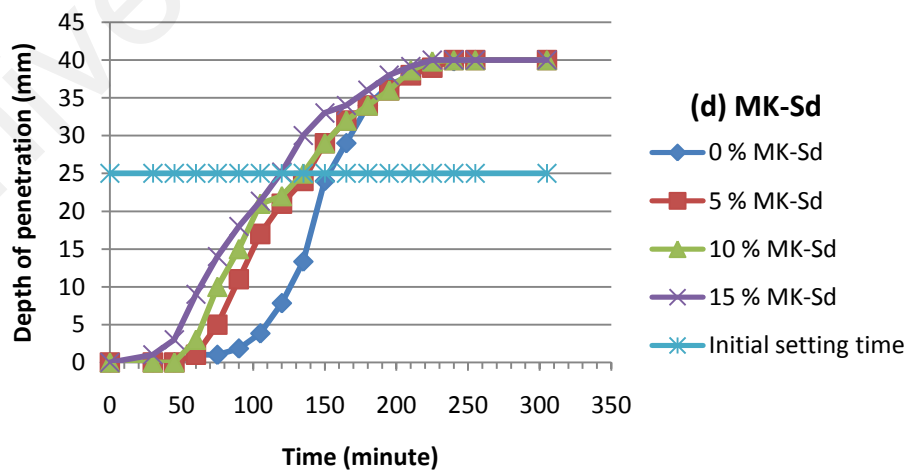
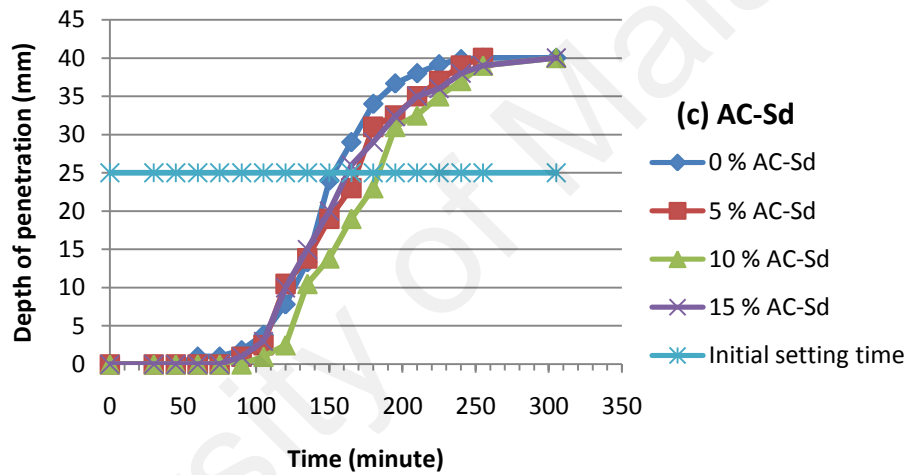
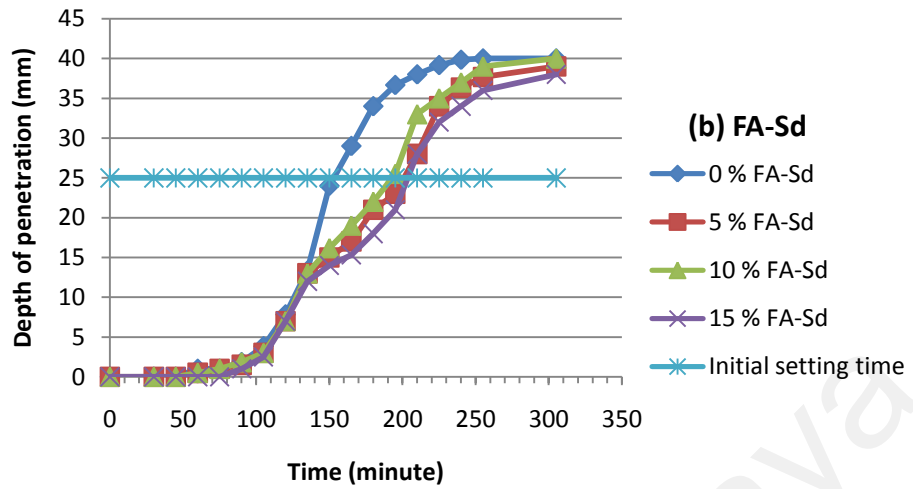


Figure 4.19: CRMs sludge depth of penetration versus time (a) CSF-Sd (b) FA-Sd (c) AC-Sd (d) MK-Sd and (e) RHA-Sd (continued)

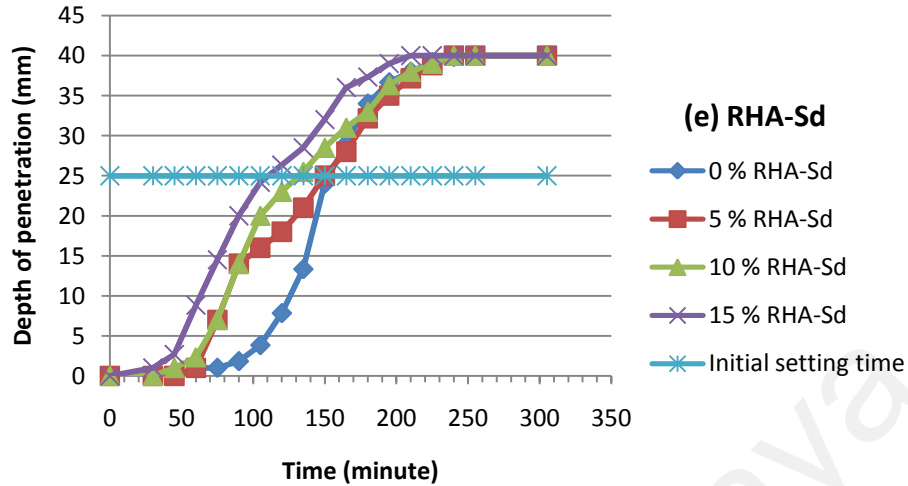


Figure 4.19: CRMs sludge depth of penetration versus time (a) CSF-Sd (b) FA-Sd (c) AC-Sd (d) MK-Sd and (e) RHA-Sd (continued)

The initial setting time for the CRMs-sludge tabulated in Table 4.10 can be correlated to the behavior of the CRMs as being described to contribute to different effect in the solidified sludge. Increasing the dosage of MK and RHA accelerated the set time to a shorter initial setting time. Both have moderately high silicon content. MK paste recorded the shortest setting time with the dosage of 5 % compared to other CRMs at the same dosage. MK recorded highest PDI value of 0.8153 which facilitate setting of cement. Further increasing of the CRMs dosage in the cement mixture has led to decrease in setting time of both MK and RHA. Incorporation of CSF has retardation effect on setting due to excessive silicon content than required for cement reaction. The similar retardation effects were observed for FA and AC. FA contains higher carbon content and small amount magnesium and iron, which delay the setting of cement longer than other CRMs since the magnesium compound, may change the final product property and iron compound may retard the setting as indicated in Table 2.10.

Table 4.10: CRMs-sludge initial setting time in minute

| <i>Percent of CRMs</i> | <i>CSF-Sd</i> | <i>FA-Sd</i> | <i>AC-Sd</i> | <i>MK-Sd</i> | <i>RHA-Sd</i> |
|------------------------|---------------|--------------|--------------|--------------|---------------|
| 0 | 153.00 | 153.00 | 153.00 | 153.00 | 153.00 |
| 5 | 187.28 | 201.00 | 173.57 | 138.00 | 150.00 |
| 10 | 163.75 | 192.86 | 183.75 | 135.00 | 132.00 |
| 15 | 165.00 | 203.57 | 162.50 | 119.33 | 110.76 |

4.3.2 Workability

The workability of cement is measured by the K-slump tester. The slump test was carried out by plunging K-slump 25 times into the cement paste in a cylinder shape container with at least 125 mm diameter x 200 mm heights before letting the K-slump rod move freely into the cement. The workable ranges of the cement paste slump are 2.54 cm to 5.08 cm for mass concrete as recommended by ACI 211.1-7 (ACI, 1998). The slump value may increase with addition of water reducing admixture or decrease with increasing temperature. The measurement made by K-slump recorded depth of penetration in range of 17.5 to 21.5 cm to ensure the ease of cement handling. The larger range of slump value was due to the two contrast factors, CRMs properties such as sorbent material that absorb moisture and the oily waste that contribute to the lubricant effect.

4.3.3 Conclusions of cement paste properties

Cement paste contains sludge and CRMs have the following behaviors:

1. The increase in water to cement ratio has increased the initial setting time by 44 % from W/C of 0.4 to 0.45.

2. The incorporation of more sludge in the cement mix has retarded the cement hydration by delayed the initial setting time. The sludge incorporation gives retardation effect with the increased of up to 20 % of initial setting time.
3. Incorporation of CRMs may give the acceleration or retardation effect. The CSF, FA and AC retard the setting of cement whereas MK and RHA accelerate the cement hydration. The CRMs with pozzolanic character showed delayed in the setting of cement.
4. MK and RHA have sorbent property of high PDI values that quickly absorbed moisture for cement hydration, which leads to acceleration effect.

4.4 Solidified Waste in OPC

4.4.1 Compressive strength

Hydraulic cement set and hardens with significant compressive strength development subjected to reaction with available water for hydration. Compressive strength is a common test to indicate its capacity to resist loads in structural application. The compressive strength load was measured by UCS machine until the deformed of the solidified sludge sample was observed. The UCS was measured based on load applied per deformed surface area.

4.4.1.1 Baseline compressive strength

A baseline study of solidified waste in OPC shows that W/C of 0.4 has highest UCS value of solidified petroleum sludge with 25.47 N/mm^2 at 28-day as represented in Figure 4.20. Relationship of UCS associated with curing period and W/C ratio was illustrated in

Figure 4.21 was plotted by Surfer 10 using point kriging method, it can be seen that the UCS increased with decreasing W/C ratio. The UCS values of baseline study increases with the increasing of cement to the sludge ratio, especially at 28-day curing period (Figure 4.22).

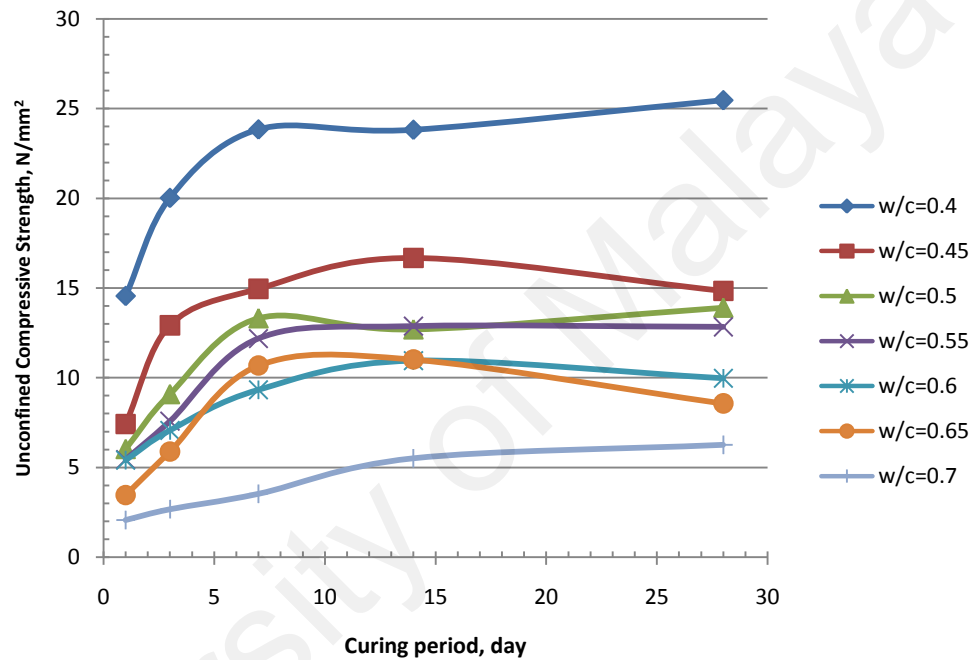


Figure 4.20: UCS of solidified petroleum sludge at different W/C ratio

Based on the isostrength of both diagrams in Figures 4.21 and 4.22, the high-strength area was contributed by the low W/C ratio and high C/Sd ratio, i.e. at 0.4 and 8 accordingly. Curing period was an insignificant parameter toward the strength values as shown by both planar regression's equations in the Figures 4.21 and 4.22.

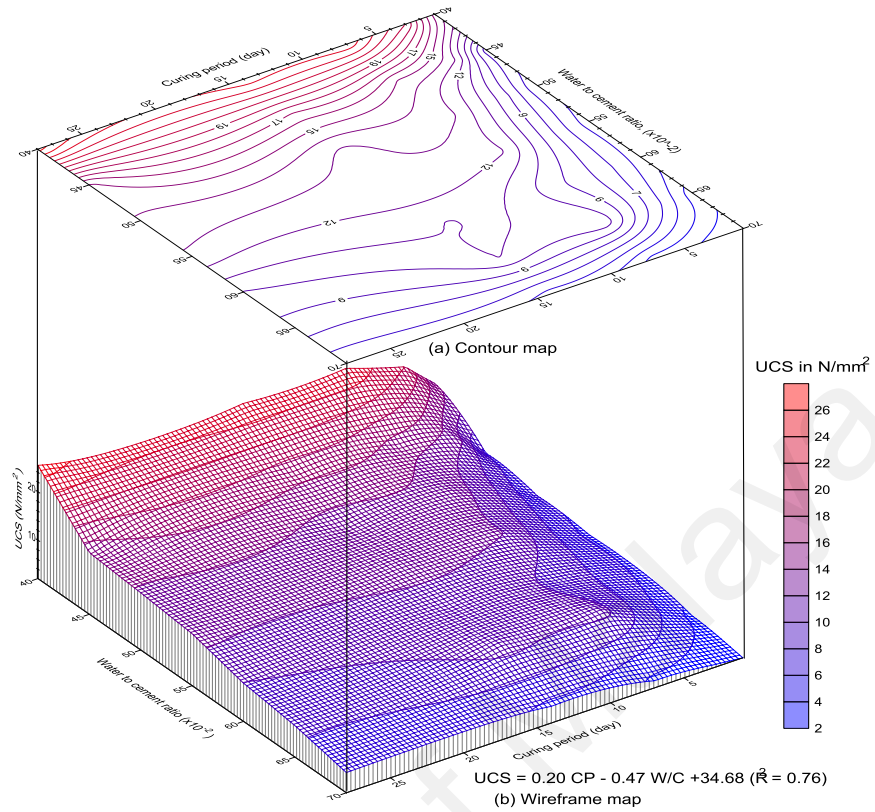


Figure 4.21: Contour and wireframe maps showing relationship of UCS with curing period and W/C ratio

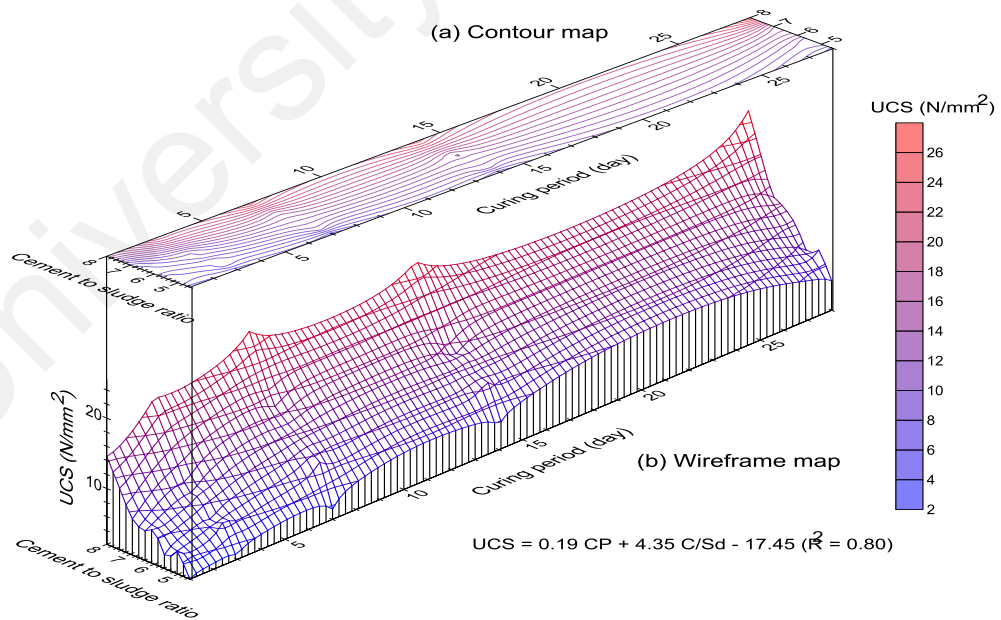


Figure 4.22: Contour and wireframe maps showing UCS of solidified petroleum sludge based on curing period and cement to sludge ratio

4.4.1.2 Compressive strength of OPC-sludge at different W/C

The UCS of solidified sludge was measured based on W/C of 0.4, 0.45 and 0.5. Real application of concrete W/C is fall in the range of 0.4 to 0.5 (Beall and Jaffe, 2003) for different exposure condition as given in Table 4.11. The strength development of solidified materials are reflected by Figure 4.23 for W/C of (a) 0.4 (b) 0.45 and (c) 0.5.

The UCS of 0.45 W/C at C/Sd of 8 follow closely the control OPC as reflected by Figure 4.23(b) compared to other curves. The 180-day UCS is 38.16 N/mm² slightly below the solidified OPC of 40.42 N/mm². Thus, the design parameters are used as base parameters for the cement replacement material study. It may be desirable to maximize the ratio of W/C if the waste is wet or in solution and for the economic reasons (Glasser, 1997).

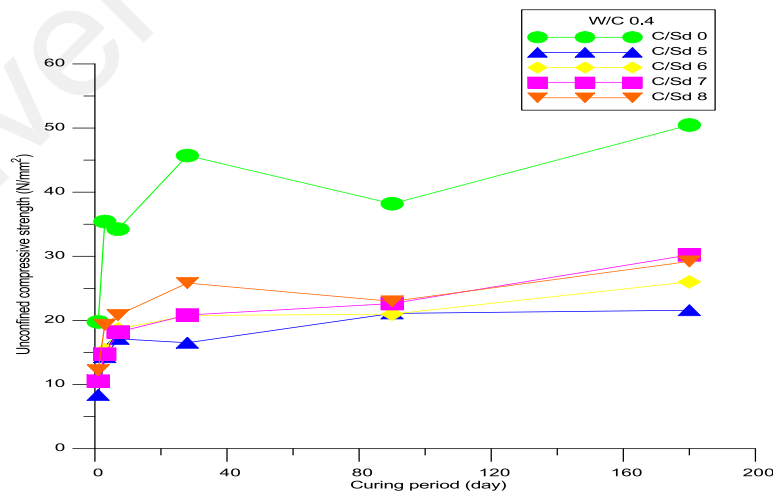
Table 4.11: Maximum W/C ratio for various conditions (adopted from Beall and Jaffe, 2003)

| <i>Exposure condition</i> | <i>Medium/Purpose</i> | <i>Maximum W/C (w/w)</i> |
|--|---|------------------------------|
| Water tight | Freshwater | 0.5 |
| | Brackish water or seawater | 0.45 |
| Freeze and thaw in a moisture | Curbs, gutter, guardrails or thin section | 0.45 |
| | Other elements | 0.45 |
| | In presence of deicing chemical | |
| Corrosion protection for reinforced concrete | Salt, brackish and seawater | 0.4 |

Organic materials can be difficult to stabilize with inorganic binder and interfere with setting reaction (Means, et al., 1995). Organic interfere with the cement hydration due to the adsorption of contaminants on the cement surface that blocks normal hydration

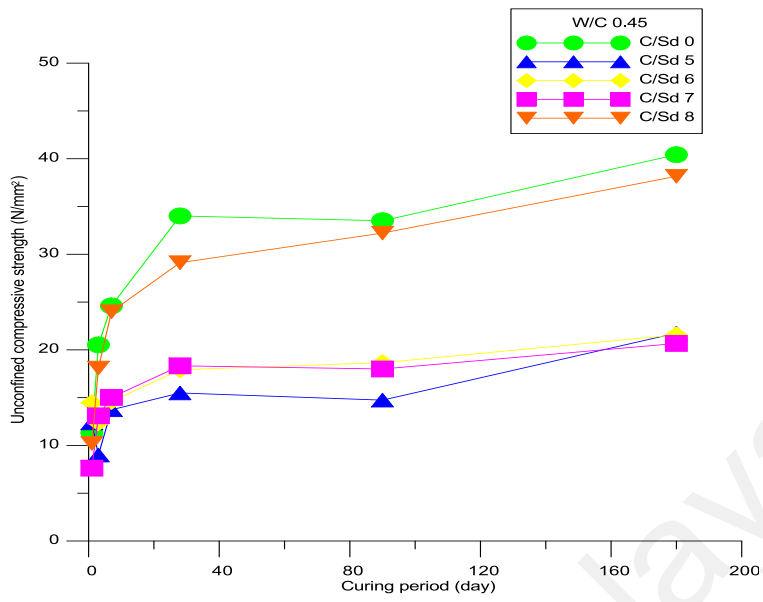
process. Other interference mechanisms include complexation of aluminate, ferrite and silicate delay the formation of hydration products. Nucleation inhibition can occur by organic as well as soluble silica or precipitating products of phosphates, borates and oxalates. Substituted aromatic undergo free radical oxidation (Conner, 1990).

Higher SO_3 content can cause the formation of ettringite at later ages, and this can result in cracking in solidified waste, which degrades mechanical properties and leaching behavior of waste forms (Caijun and Roger, 2004). Sodium hydroxide increased the rate of setting but reduce the strength at the 28-day strength of Portland cement. The presence of sodium hydroxide in solidified OPC-sludge was reflected by rapid increased in strength at early hydration period and follow by a sharp bending of UCS exactly at 28-day before lightly reduce to form almost the plateau strength line as shown in Figure 4.23. At higher W/C of 0.5, the strength was slightly reduced at day 180 but in higher W/C of 0.4 and 0.45 it strength still continues to increase. Sodium hydroxide act as pH adjuster may solubilized silica for quicker reaction (Conner, 1990).

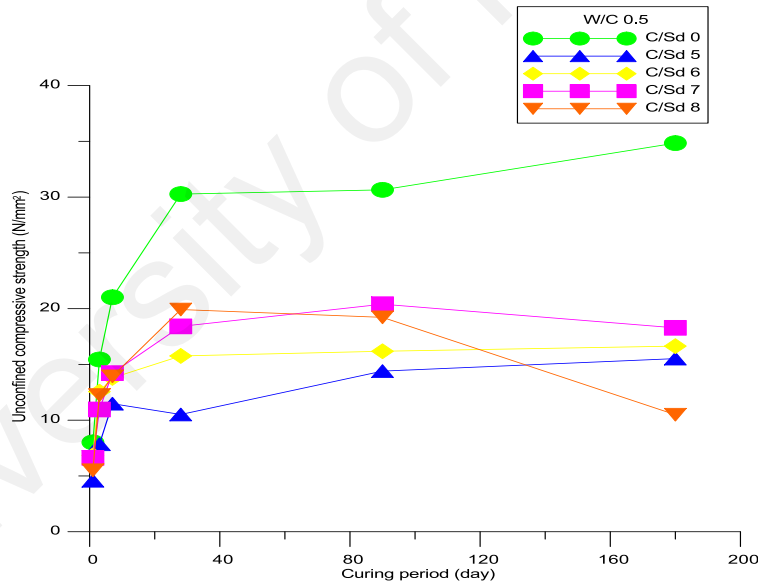


(a) 0.4

Figure 4.23: UCS evolution for three batches of OPC-sludge at W/C (a) 0.4, (b) 0.45 and (c) 0.5.



(b) 0.45



(c) 0.5

Figure 4.23: UCS evolution for three batches of OPC-sludge at W/C (a) 0.4, (b) 0.45 and (c) 0.5 (continued)

The correlation analysis was executed by MINITAB 14 (MINITAB Inc., Pennsylvania, USA) for UCS values with curing period (CP) and C/Sd. UCS has significant correlation with CP. Correlation was determined by Pearson's correlation. Fitted line was plotted using quadratic regression for two variables of UCS as response and logeCP as the predictor based on Power model (De Veaux et al., 2005). The relationships between two variables are represented by Equation 4-5, 4-6 and 4-7 for three batches of W/C. The correlation and its P value, standard deviation (S), multiple determination coefficient (R^2) and adjusted R^2 for the three batches of OPC mixed is tabulated in Table 4.12.

$$\text{W/C0.4: LogUCS} = 1.03 + 0.13 \text{ LogCP} - 0.01 \text{ LogCP}^2 \quad \text{Eq. (4-5)}$$

$$\text{W/C0.45: LogUCS} = 1.03 + 0.21 \text{ LogCP} - 0.03 \text{ LogCP}^2 \quad \text{Eq. (4-6)}$$

$$\text{W/C0.5: LogUCS} = 0.78 + 0.21 \text{ LogCP} - 0.02 \text{ LogCP}^2 \quad \text{Eq. (4-7)}$$

Table 4.12: Statistical analysis of OPC-sludge

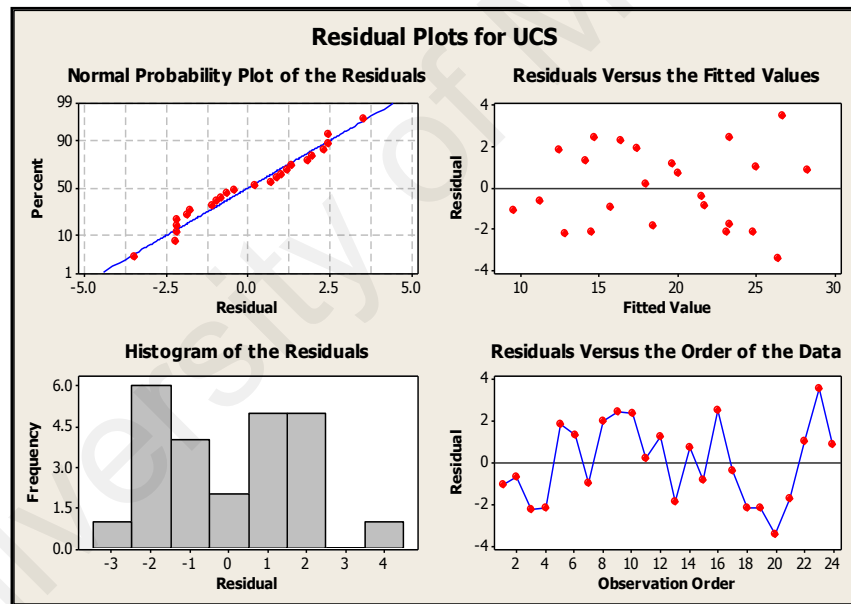
| <i>Observation</i> | <i>Statistical parameter</i> | | |
|--|------------------------------|--|---------------|
| | <i>W/C</i> | <i>Value</i> | <i>Method</i> |
| Correlation | 0.4 | UCS:CP 0.76 (0.00) UCS:C/Sd 0.33 (0.11) | Pearson |
| | 0.45 | UCS:CP 0.59 (0.00) UCS:C/Sd 0.49 (0.01) | Correlation |
| | 0.5 | UCS:CP 0.64 (0.01) UCS:C/Sd 0.34 (0.10) | (P value) |
| Fitted line UCS and LogeCP | | S, R^2 (%), Adj. R^2 (%) | Logarithmic |
| | 0.4 | 2.75, 78.7, 76.7 | |
| | 0.45 | 5.62, 45.1, 39.9 | |
| Regression of UCS with LogeCP and C/Sd | | S, R^2 (%), Adj. R^2 (%) | Multiple |
| | 0.4 | 2.00, 88.7, 87.6 | |
| | 0.45 | 4.19, 69.3, 66.4 | Regression |
| | 0.5 | 1.91, 85.3, 83.9 | |

The multiple regression equations for three parameters of UCS, LogeCP and C/Sd for the three batches of W/C are given by the Equation 4-8, 4-9 and 4-10. Empirical model was developed for selected parameters with linear relationship of UCS as a response to CP and C/Sd (Navidi, 2010). Residual plots of the regressions are depicted by Figure 4.24.

$$\text{W/C 0.4: UCS} = 1.21 + 2.67 \text{ LogeCP} + 1.65 \text{ C/Sd} \quad \text{Eq. (4-8)}$$

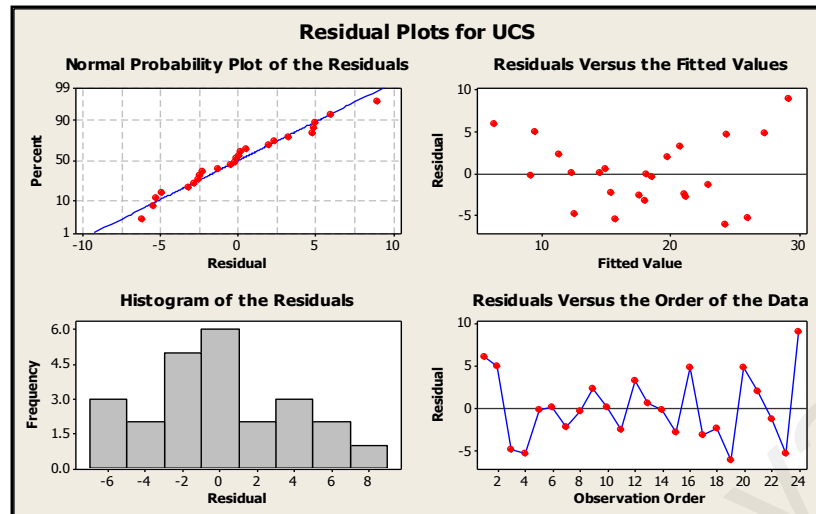
$$\text{W/C 0.45: UCS} = -9.28 + 2.59 \text{ LogeCP} + 3.12 \text{ C/Sd} \quad \text{Eq. (4-9)}$$

$$\text{W/C 0.5: UCS} = -1.50 + 2.18 \text{ LogeCP} + 1.42 \text{ C/Sd} \quad \text{Eq. (4-10)}$$

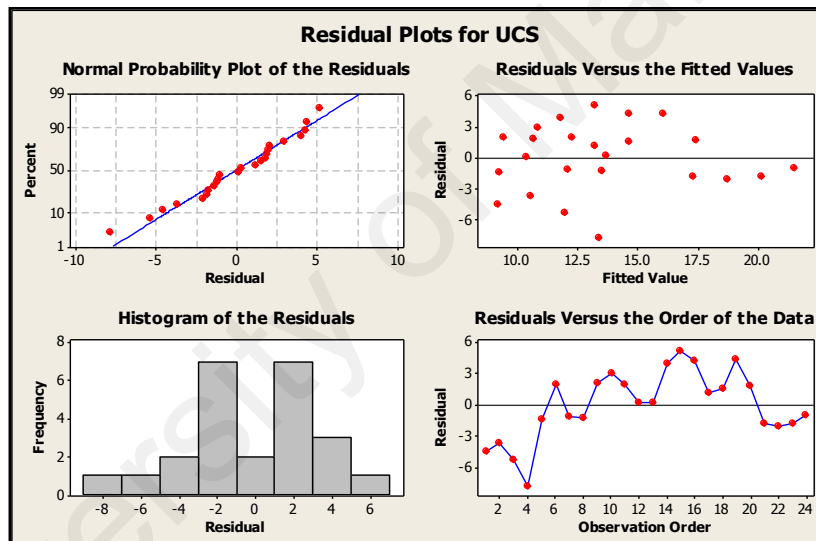


(a) 0.4

Figure 4.24: Residual plots of OPC-sludge mixed of W/C (a) 0.4 (b) 0.45 and (c) 0.5



(b) 0.45



(c) 0.5

Figure 4.24: Residual plots of OPC-sludge mixed of W/C (a) 0.4 (b) 0.45 and (c) 0.5

(continued)

4.4.1.3 Strength of solidified OPC-sludge simulated metal and RHA

Baseline study shows that, the optimum strength was reflected by cement mixture with simulated metals, but without RHA based on the highest strength of 20 N/mm^2 at the

C/Sd ratio of 7.0 and W/C ratio of 0.45 shown in Figure 4.25. Cement mixture with 15 % RHA shows better UCS than 25 % RHA at 28-day curing period.

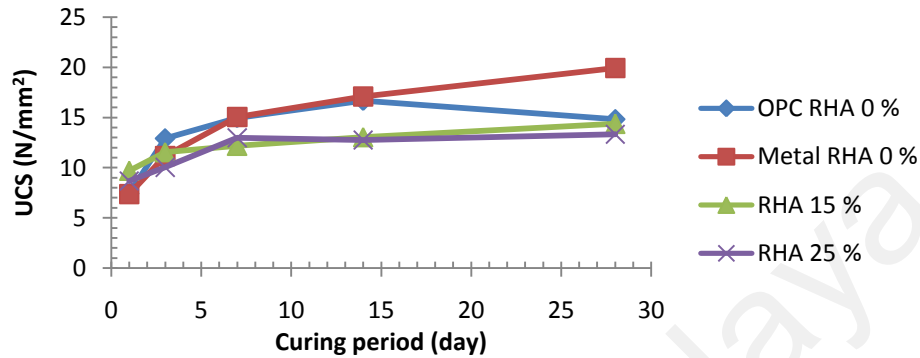


Figure 4.25: Compressive strength of solidified sludge with RHA

Response surface regression of UCS at 15 % RHA as a predictor with the independent variables of W/C, CP and C/Sd shows that all parameters have significant second order interaction with the R^2 of 97 % and S of 0.53. Strength relationship with the three variables was defined by the Equation 4-11. The 15 % RHA was considered as a higher boundary for the next step mixing of CRMs used to solidify the waste.

$$UCS_{rha15} = 5.28 - 3.38 CP - 0.01 CP^2 + 3.99 W/C \bullet CP + 0.28 CP \bullet C/Sd \quad \text{Eq. (4-11)}$$

4.4.1.4 Strength of solidified OPC-sludge with CRMs

The effect of cement replacement materials (CRMs) to UCS of solidified sludge are illustrated in Figure 4.26 (a) to (e). The CRMs used as part of the cementitious proportions are 5, 10 and 15 % weight in OPC. Addition of RHA showed a positive effect to the strength values compared to the control value until age 90-day (Figure 4.26). Thereafter, the control solidified sludge UCS performed better at 180-day. RHA as a reactive

pozzolanic additive provides soluble silicate to cement hydration process may causes a lower setting time to cement hydration as it may act as filler. Similar trend was observed for all CRMs. The usage of CRMs were effective at 5 % weight based on the strength of RHA, 28.34 N/mm² at 180-day. At higher percentage, RHA can modify the solidified sludge to a porous structure by inhibiting cement hydration and cause reduction in strength of monolith. The effect was also due to the high silica content in RHA, which forms soluble silicate and retards the tricalcium silicate hydration by nucleation mechanisms. However, the solidified sludge showed a sharp rise in the strength value after 90-day, which was notable high at 180-day. The U.S. EPA considers a stabilized material is satisfactory if it has UCS of 0.34 N/mm².

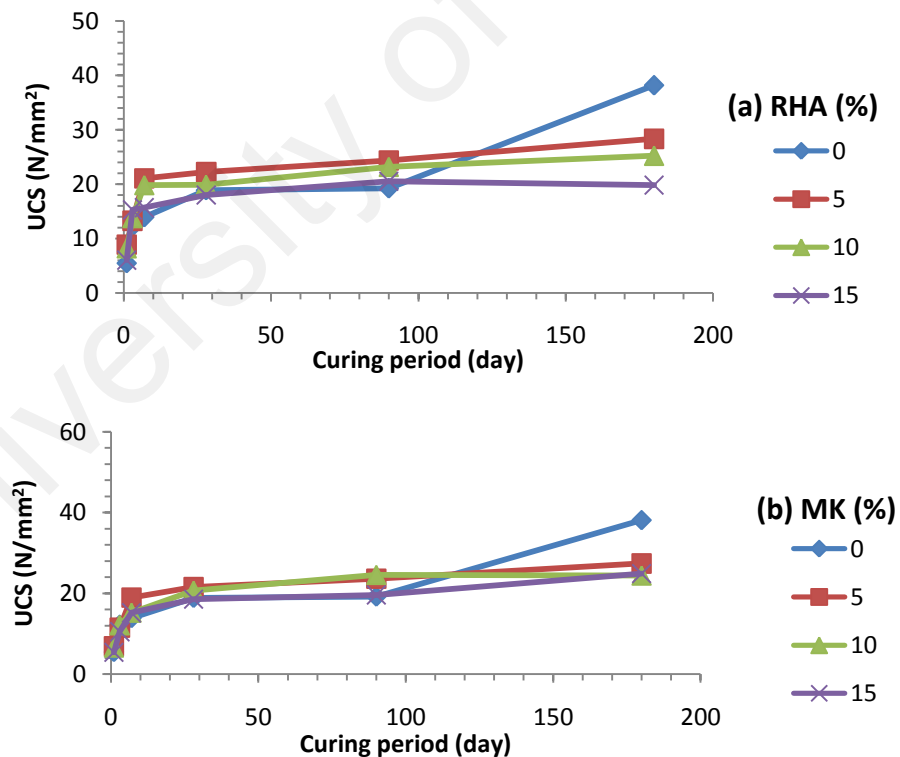


Figure 4.26: UCS evolution of 5, 10 and 15 % OPC-sludge with CRMs (a) RHA (b) MK
(c) AC (d) FA and (e) CSF

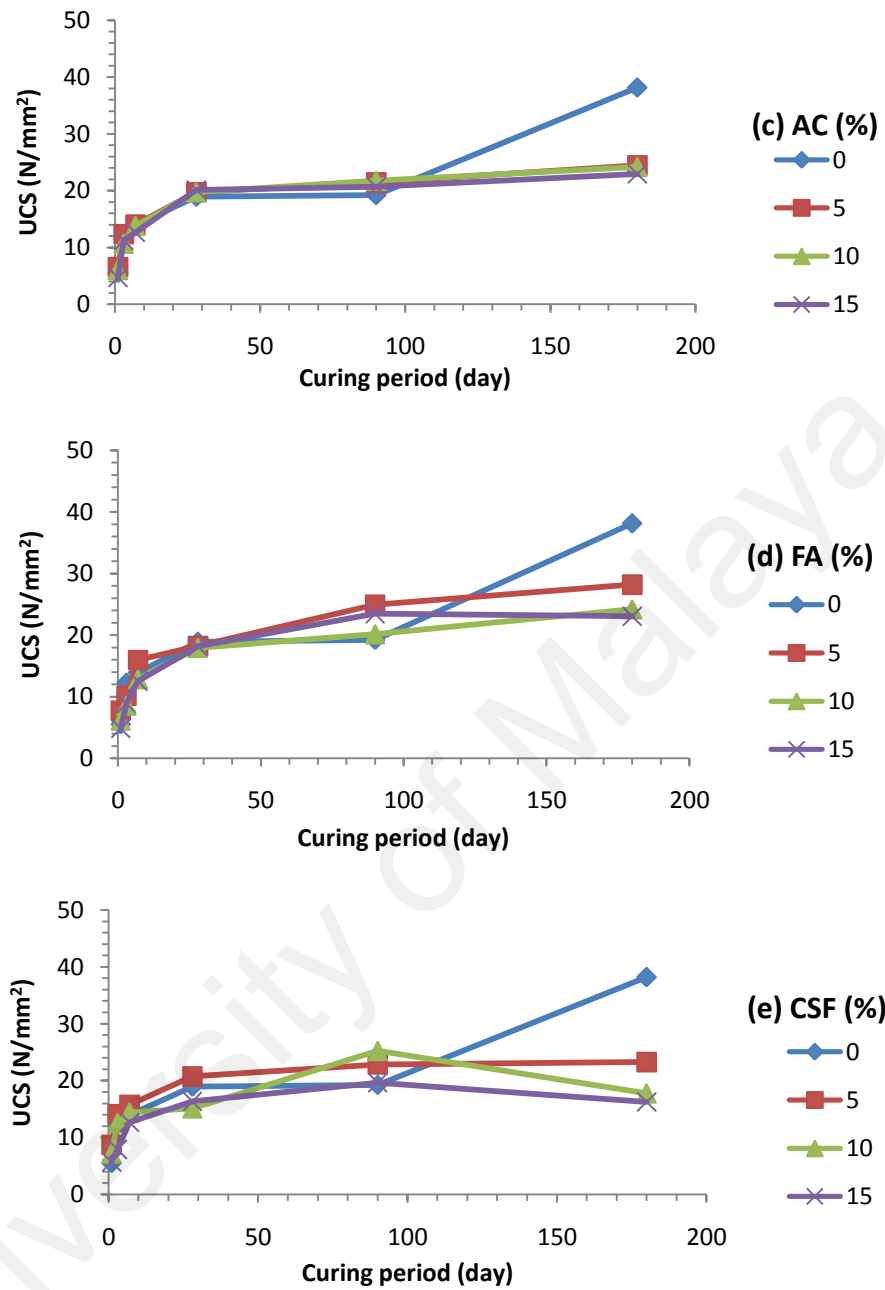


Figure 4.26: UCS evolution of 5, 10 and 15 % OPC-sludge with CRMs (a) RHA (b) MK
(c) AC (d) FA and (e) CSF (continued)

4.4.1.5 Conclusions of UCS

Based on the series of UCS performed on solidified OPC and OPC sludge, the salient points gathered from the strength analysis were summarized as follows:

1. Based on the strength of baseline OPC, low W/C ratio of 0.4 performed better than the higher ratio with the UCS of 25.47 N/mm² at the 28-day period.
2. C/Sd increases with the increased of UCS whereby the higher-end ratio of 8 shows a prominent peak strength. The curing period was an insignificant parameter in determining the strength.
3. The combination of W/C of 0.45 and C/Sd of 8 has resulted in the optimum UCS of solidified sludge which recorded 38.16 N/mm² slightly below the control sample 40.42 N/mm² at 180-day.
4. The incorporation of spiked metals in the solidified sludge produced monolith with better UCS value compared to the incorporation of RHA or without RHA, which indicates high metal content blended in the organic waste can enhance the UCS value at 28-day.
5. The inclusion of 5 % weight of CRMs exhibit optimum strength than the higher percentage of CRMs at 180-day. However, the UCS of solidified sludge performance was better compared to CRMs incorporation.

4.4.2 Porosity

Smallest void in C-S-H is 0.50 to 2.50 nm which account for 27 % of porosity, but give little effect to strength. While the capillary void in well hydrated low W/C is 10 to 50 nm and 3000 to 5000 nm in the high mixed ratio. Capillary void of < 50 nm are detrimental to strength (Mehta and Monteiro, 2006). Total volume of capillary voids was measured as porosity. Air void is in range 0.05 to 0.20 mm. Air void normally introduced to increase freeze-thaw resistance damage of monolith. Hydrated cement exposed to CO₂ will produce calcite and silica gel, which can incorporate metals. Carbonation can decrease porosity and

shrinkage cause cracking to monolith (Garrabrants and Kosson, 2004). The carbonation may change the microstructure which includes cracking and increased permeability but in contrast, the CaCO_3 precipitation in pore space may also lead to increase in strength (Perera, et al., 2003).

4.4.2.1 Porosity of OPC-sludge

The porosity increases with the increased of cement in the mixture as shown by Figure 4.27. The organic contaminant has occupied the cement pore voids, and this has results in lower percentage of permeable pore in the solidified OPC-sludge. Bulk density of the solidified sludge was found from 1.23 to 1.47 kg/m^3 based on the water content and the cement to the sludge ratio. The higher water content in the mixture resulted in lower bulk density whereas increasing cement to the sludge ratio increased the bulk density.

It can be concluded that higher permeable porosity of 27.48 % was found in the solidified sludge with W/C 0.45 and C/Sd 8. This permeable porosity provides surface adsorption toward sludge incorporated in the cement. The W/C and porosity are important factors that determine the strength of solidified waste. The porosity increases with the increased of W/C ratio of the solidified sample.

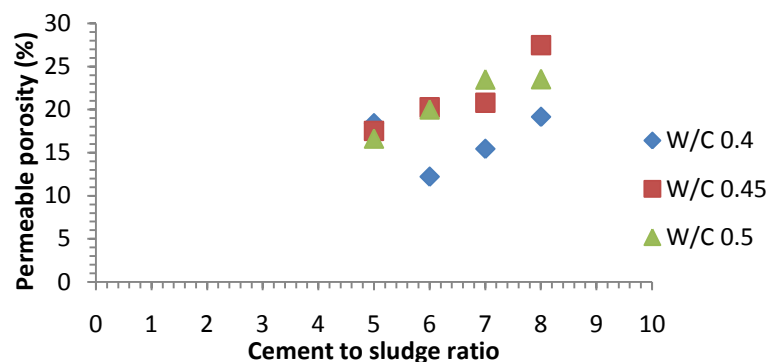


Figure 4.27: Porosity of solidified OPC-sludge

4.4.2.2 Porosity of OPC-sludge with CRMs

Addition of RHA percentage has a positive effect of increasing the permeable porosity in solidified OPC-sludge due to its high silica content that creates nucleation similar like organic, which inhibit cement hydration as seen in Figure 4.28(a). The increase in porosity has reversal effect in density value. RHA and CSF exhibited closely similar permeable porosity and vacuum porosity. MK showed linear vacuum porosity in contrast to permeable porosity and wet porosity which diverging into upward and downward direction as in Figure 4.28(b). In general, insignificant changes of porosity values with increasing CRMs percentage were observed in AC, FA and CSF as depicted by Figure 4.28(c), (d), and (e). Even though insignificant porosity changes, density of AC, FA and CSF were reduced with the increasing CRMs percentage. It was noted that RHA OPC-sludge was found to have surface cracked after the porosity test. Solidified RHA cement is prone to swelling once subjected under thermal change and water absorption that lead to crack on the surface.

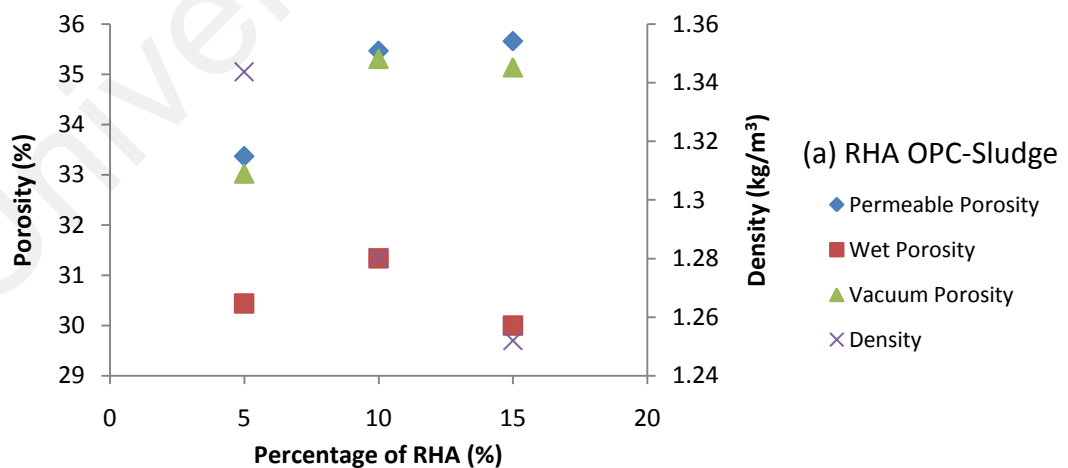


Figure 4.28: Porosity of solidified (a) RHA OPC-Sludge (b) MK OPC-Sludge (c) AC OPC-Sludge (d) FA OPC-Sludge and (e) CSF OPC-Sludge

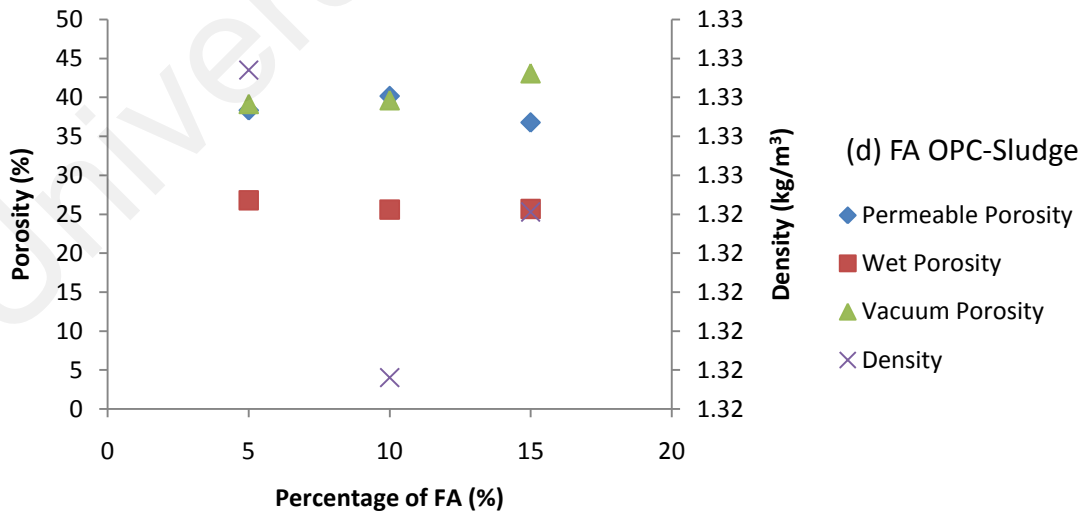
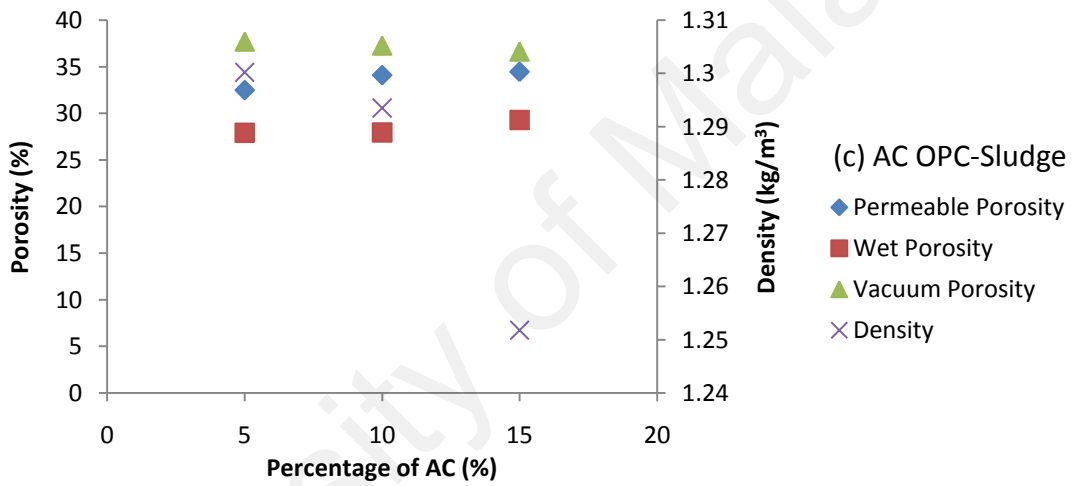
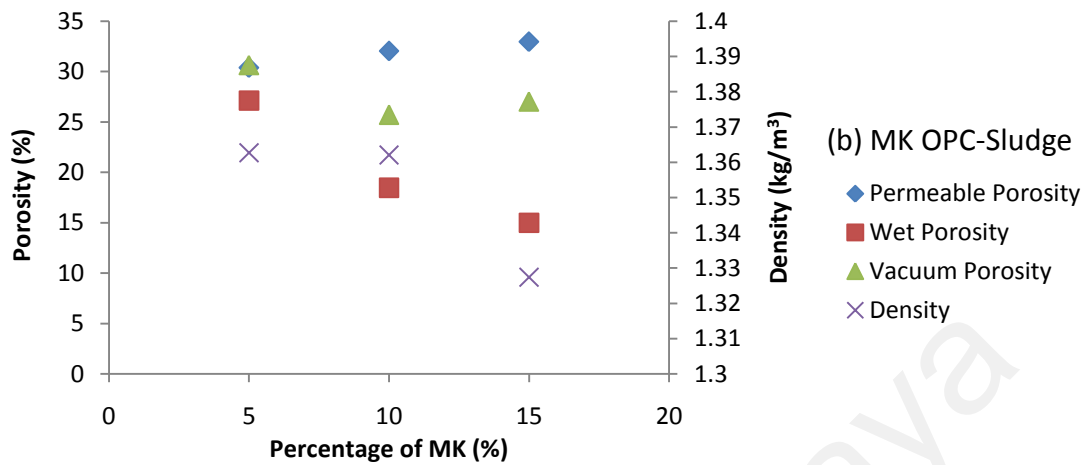


Figure 4.28: Porosity of solidified (a) RHA OPC-Sludge (b) MK OPC-Sludge (c) AC OPC-Sludge (d) FA OPC-Sludge and (e) CSF OPC-Sludge (continued)

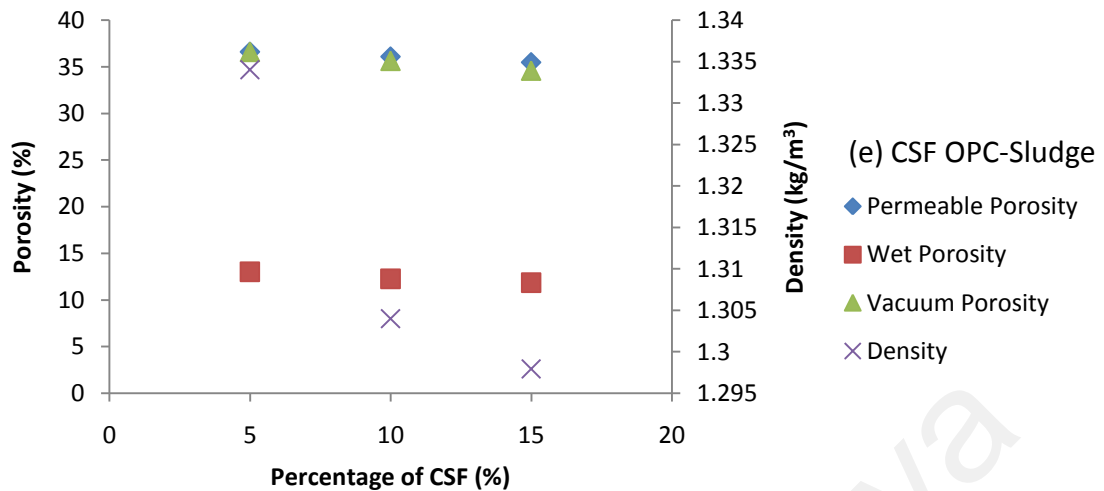


Figure 4.28: Porosity of solidified (a) RHA OPC-Sludge (b) MK OPC-Sludge (c) AC OPC-Sludge (d) FA OPC-Sludge and (e) CSF OPC-Sludge (continued)

In conclusion, the addition of more CRMs in the OPC-sludge has contributed to lower density in general. Addition of AC, FA and CSF did not significantly alter the permeable porosity but RHA, and MK incorporation has slightly increased the permeable pore found in solidified sludge. The changes in permeable pore may be contributed by the irregular cellular structure of RHA particles and the octahedral layers of aluminum silica oxide in clays, which have trapped the air volume during the mixing of cement pastes even though part of the lattice structure was ruptured during calcination and formed amorphous surface.

4.4.2.3 Isostrength of solidified sludge with porosity and C/Sd

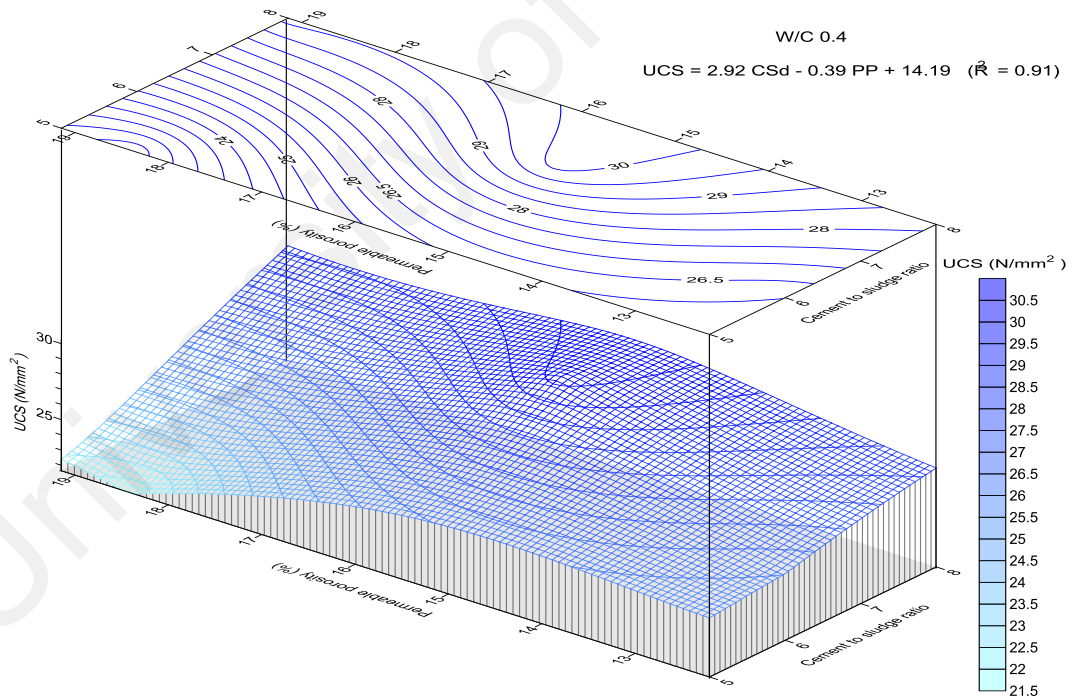
The isostrength of solidified sludge plotted against the changes in permeable porosity and cement to the sludge ratio were depicted by Figure 4.29 (a) W/C = 0.4 (b) W/C = 0.45 and (c) W/C = 0.5. Based on the relationship of the three parameters, the increases in cement to the sludge ratio has contributed to the increased in strength for W/C

of 0.4 and 0.5. Permeable porosity was found to affect differently in W/C of 0.4 with maximum strength was found at 15 to 16 % compared to W/C of 0.45. Solidified sludge with W/C of 0.45 has a higher porosity concurrent with a gradual increase in strength. The ideal relationship of strength and permeable porosity shown by the W/C of 0.45 can be explained by water in smaller capillary pore space has been utilized for hydration process leaving discontinuous pores formed in between ettringite, portlandite and C-S-H crystal similar to W/C of 0.4, albeit smaller pore size belongs to W/C of 0.4 which cause faster discontinuous pore in shorter time but with a lower degree of hydration (Hearn, et al., 2006). In contrast to the W/C of 0.45, even though additional water in the mixture of W/C of 0.5 give strong connection between porosity and strength by R^2 of 99 %, but the strength is weaker due to the existence of free water in combination of hydrophobic organic. Bleed water caused the continuous pore path in the cement paste and permit intrusion of organic layer on water, which affected the growth of crystallization products thus inhibit the hydration of cement, as observed in Figure 4.29 (c). Free water occupies capillary pore of >50 nm do not change volume, but the water removal from smaller capillary pores can cause shrinkage to cement structure (Mehta and Monteiro, 2006). The planar regression equations for the three W/C isostrength plots are as shown in the Figure 4.28.

Based on the relationship of porosity with strength and cement to the sludge ratio, it can be concluded that the organic acts differently from normal solidified cement without organic waste. In normal solidified cement, porosity was found to decrease with the increased of strength but for solidified organic sludge, the increase in porosity has led to the increased of strength applied to W/C of 0.45 and 0.5. Strength was affected by water to cement ratio and cement to the sludge ratio in the design mix. Whereby at W/C of 0.4, increasing porosity value has an adverse impact to the strength but concurrent increased in

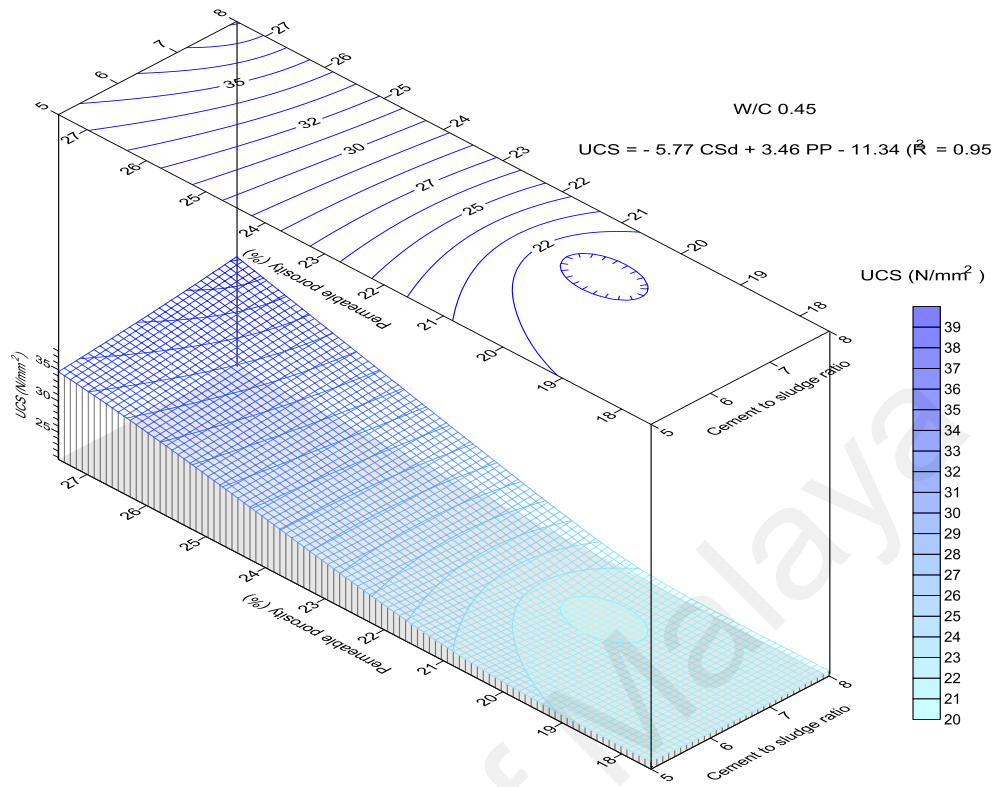
the C/Sd ratio has remarked positive effect to the strength. Anyway, the optimum isostrength peak (30 MPa) was found at the porosity of 15 to 16 % and C/Sd of 7 to 8. Different scenario was observed in W/C of 0.45. The increases in porosity of up to 27 % have shown a better isostrength peak of more than 35 MPa, and C/Sd has less influence to the strength value with the ascending movement of the optimum peak strength align toward increasing porosity values. The performance of W/C ratio of 0.5 showed a weaker strength value of 18 MPa at porosity of 23 % with minor contribution of the C/Sd factor.

As a conclusion the W/C ratio of 0.45 outperformed better strength compared to other W/C ratios with other advantages of less influence given by the C/Sd which permit for the used of more sludge in the cement mixture without compromise to strength value.

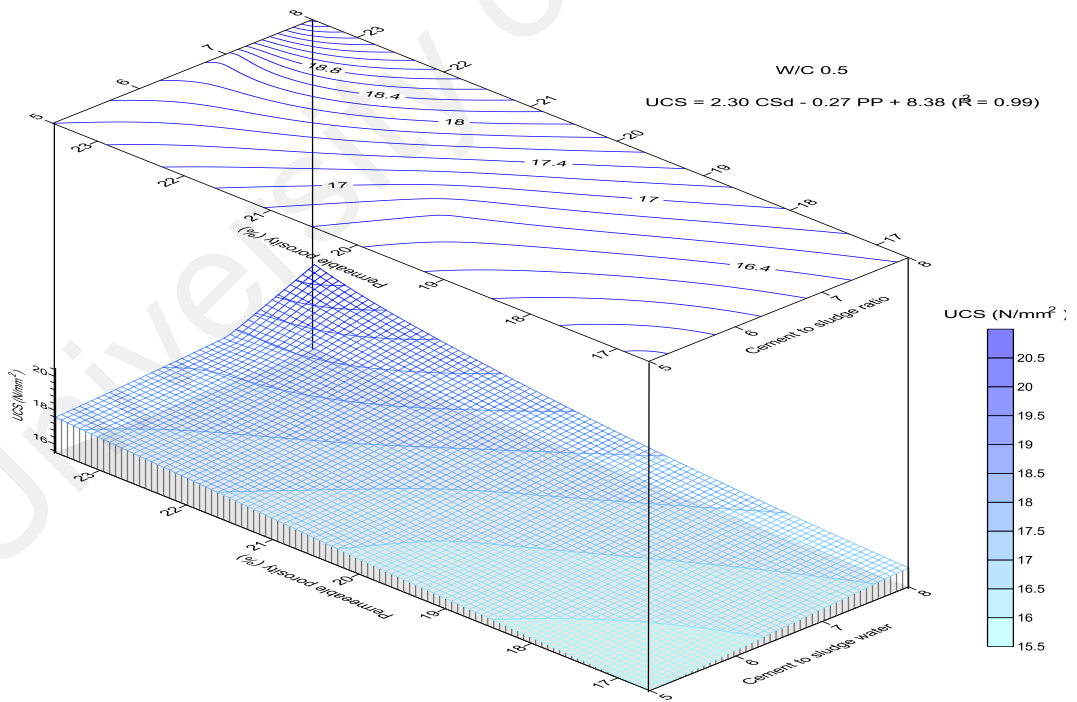


(a) W/C=0.4

Figure 4.29: Isostrength and its relationship with permeable porosity and cement to the sludge ratio (a) W/C 0.4 (b) W/C 0.45 and (c) W/C 0.5



(b) W/C=0.45

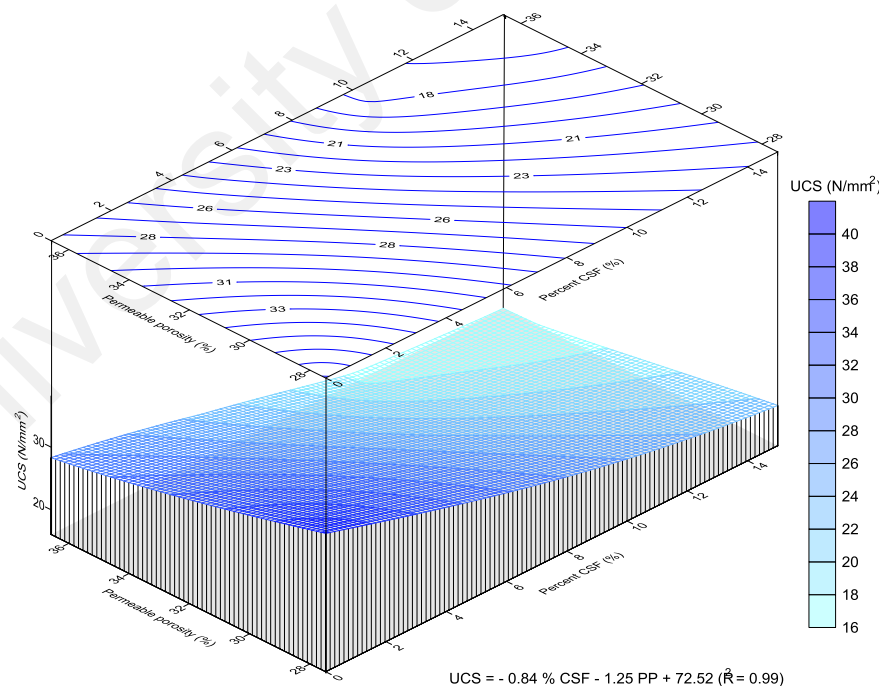


(c) W/C=0.5

Figure 4.29: Isostrength and its relationship with the permeable porosity and cement to sludge ratio at (a) W/C=0.4 (b) W/C=0.45 and (c) W/C=0.5 (continued)

4.4.2.4 Isostrength of solidified sludge CRMs with porosity and CRMs

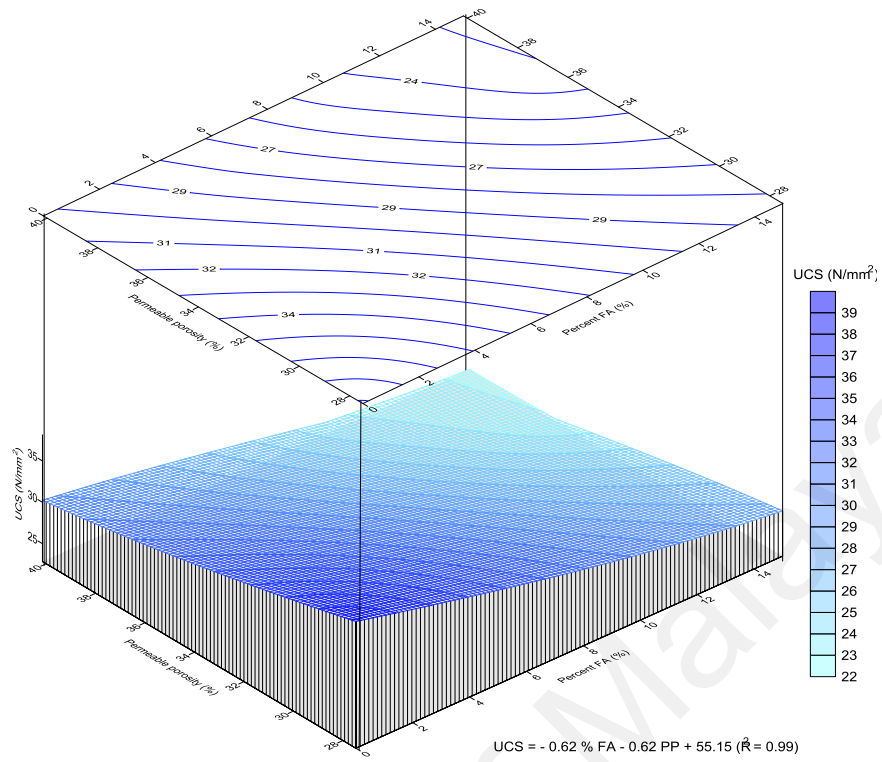
In general, the incorporation of more CRMs lowers the strength gained, as illustrated by the isostrength relationship with percentage of CRMs and permeable porosity contour map Figure 4.30. The wireframe and contour maps in Figure 4.30 interpolate the isostrength plotted by point kriging method using Surfer 10 indicate that the keen area of interest with optimum strength was always found at lower porosity and lower percentage of CRMs. Due to the similarity in the isostrength relationship with the other parameters for all CRMs, it can be concluded that smaller amount of CRMs should be used for the inclusion in the cement mixture. In the study, the lowest percentage used was 5 %. The planar regression equations of the CRMs isostrength plots depicted in Figure 4.30 indicate R^2 value of 0.99 to 0.98.



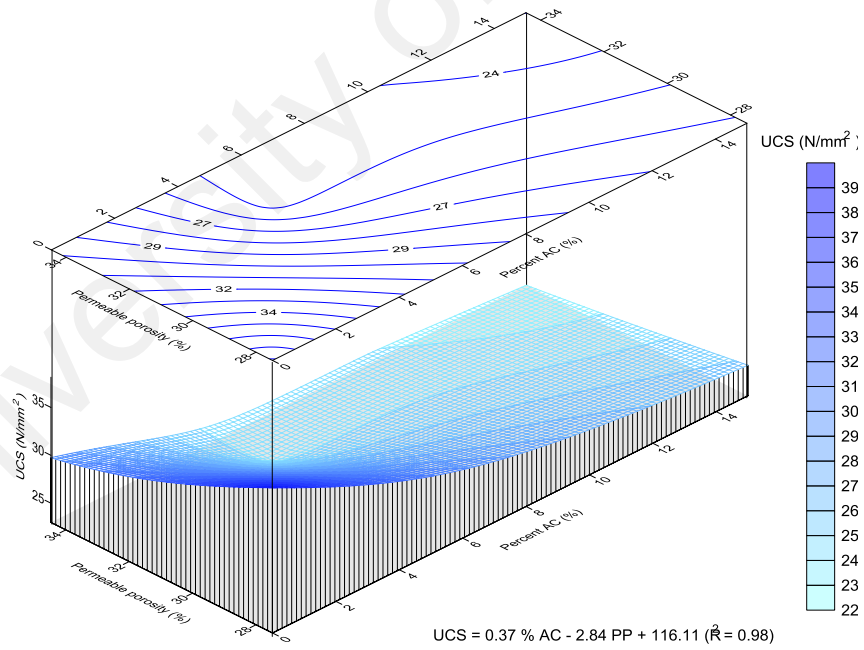
(a) CSF

Figure 4.30: Isostrength and its relationship with percent CRMs and permeable porosity

(a) CSF (b) FA (c) AC (d) MK and (e) RHA



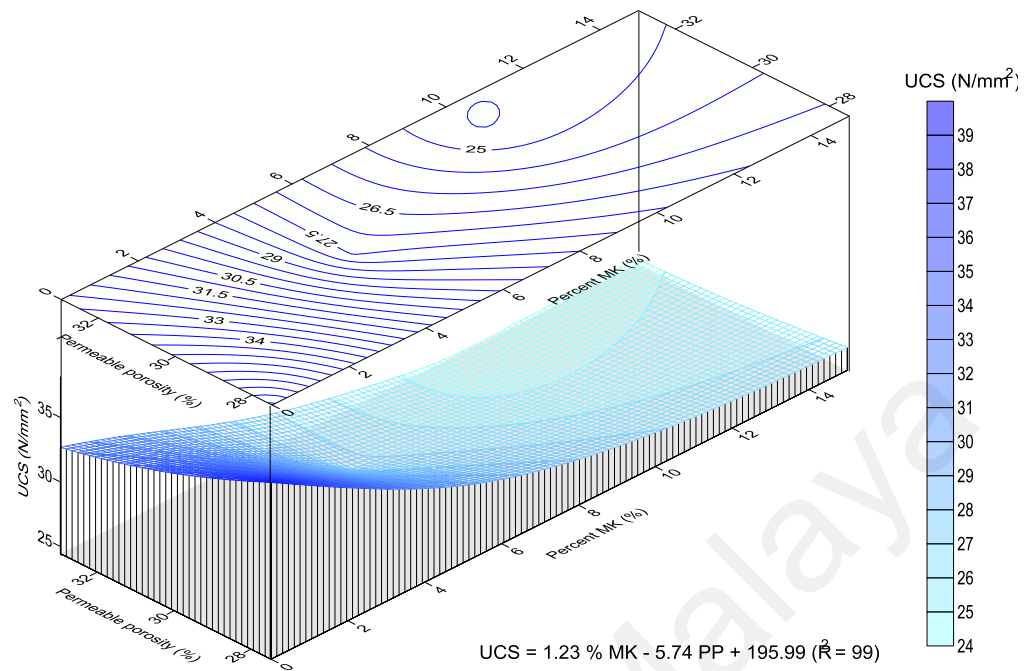
(b) FA



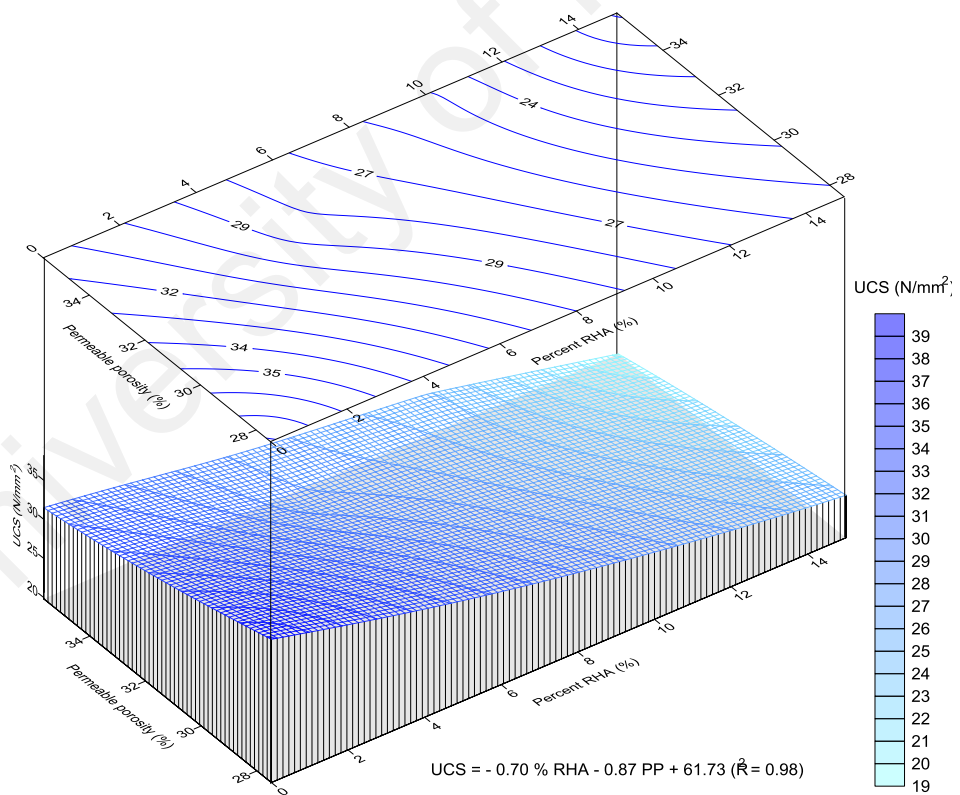
(c) AC

Figure 4.30: Isostrength and its relationship with percent CRMs and permeable porosity (a)

CSF (b) FA (c) AC (d) MK and (e) RHA (continued)



(d) MK



(e) RHA

Figure 4.30: Isostrength and its relationship percent CRMs and permeable porosity (a) CSF

(b) FA (c) AC (d) MK (e) RHA (continued)

4.4.2.5 Pore size distribution of solidified waste

Pore size distribution was measured by the BET using nitrogen adsorption. For the Langmuir isotherm at equilibrium, adsorption was equal to desorption. Pressure rise was recorded as relative pressure as the nitrogen adsorption increased to the maximum, and desorption continued with the decreasing of pressure forming a cycle of an adsorption-desorption isotherms. The pore size can be categorized as micropore, mesopore and macropore with diameter of $< 20 \text{ \AA}$, $20 \text{ to } 500 \text{ \AA}$ and $> 500 \text{ \AA}$ accordingly.

The isotherm plot of solidified sludge is represented in Figure 4.31. The isotherm of the solidified sludge types IV with hysteresis type C tapered/wedge whereby the hysteresis indicates the presence of mesopores in the solid material.

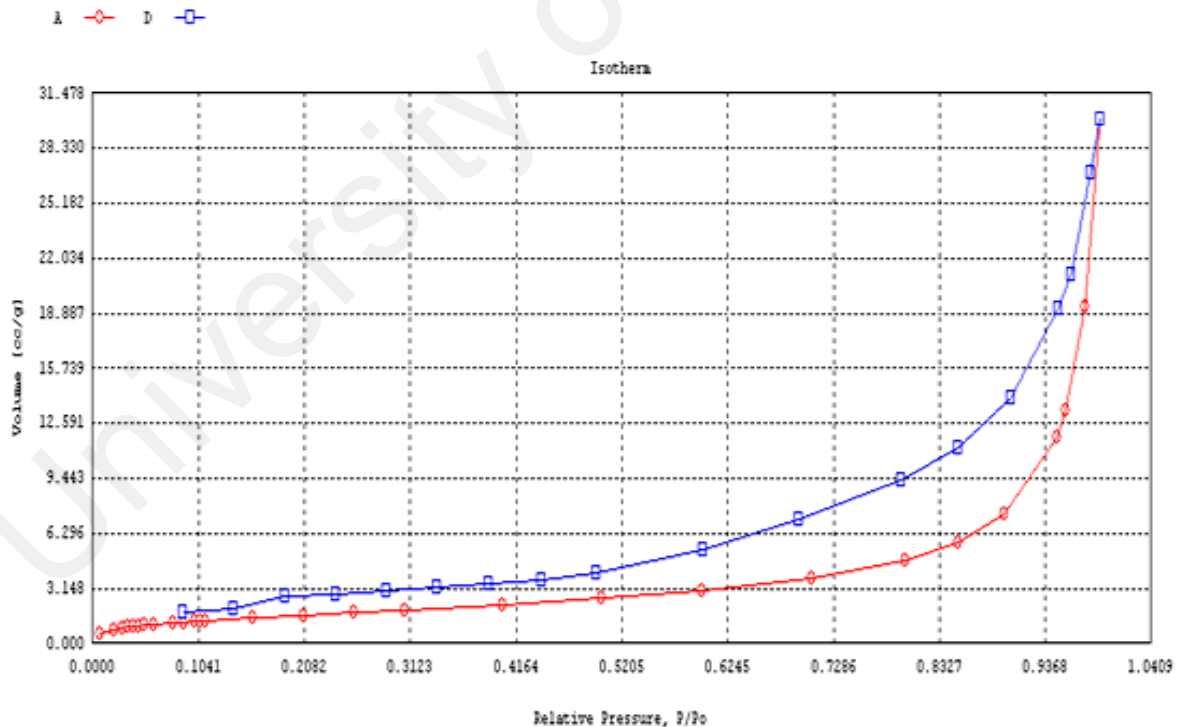
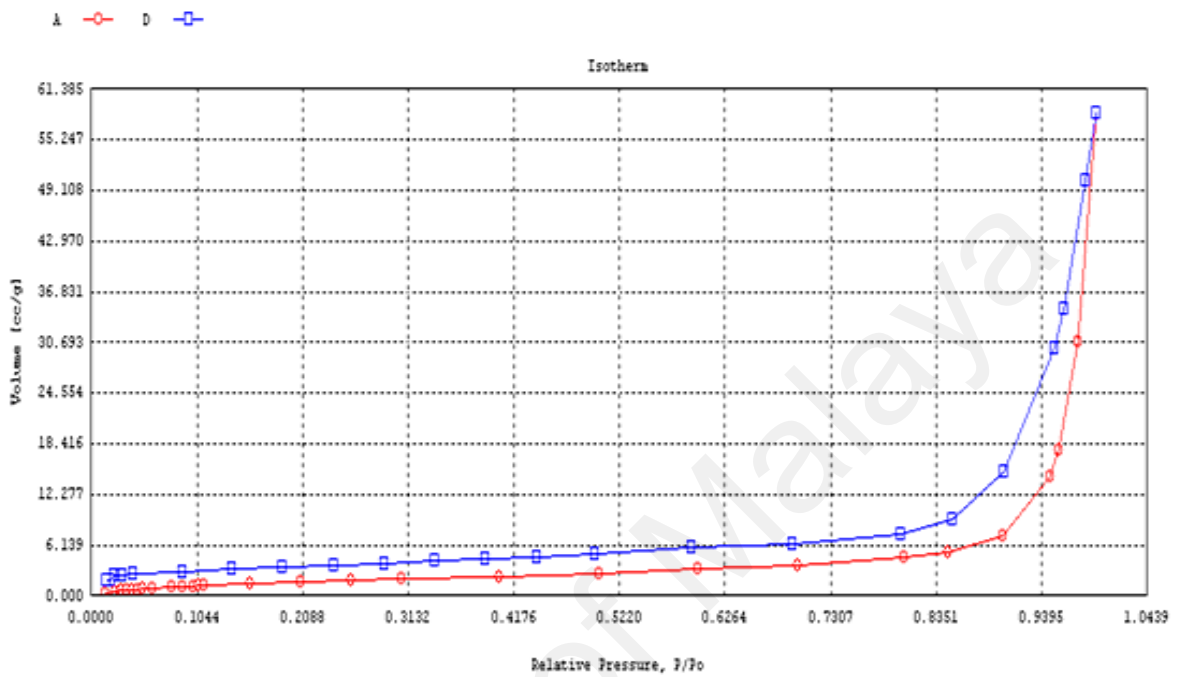
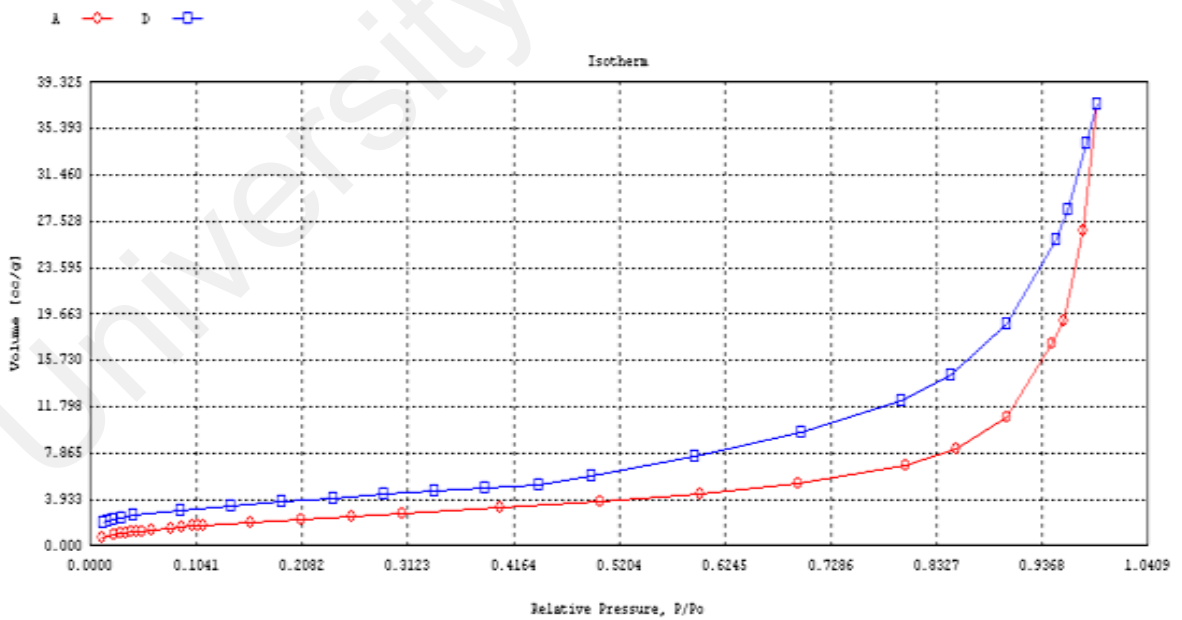


Figure 4.31: Isotherm plot of solidified sludge

The solidified sludge with CRMs isotherms plots based on the volume in cm^3/g versus relative pressure are depicted by Figure 4.32 (a) to (e).

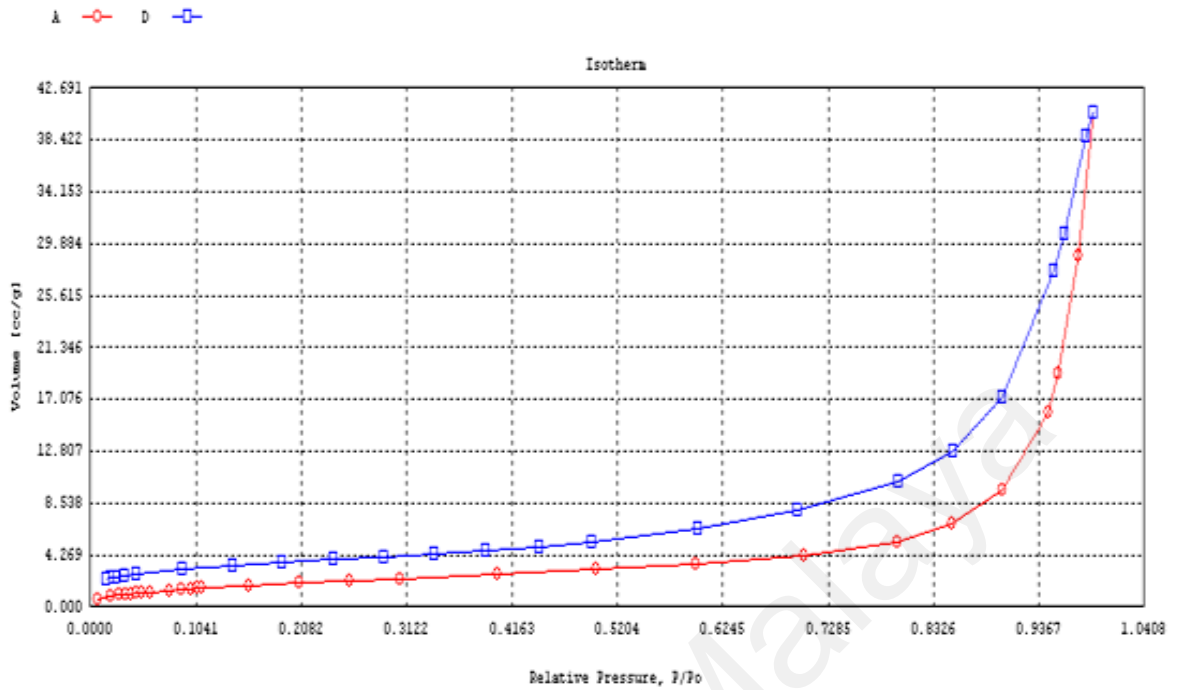


(a) CSF

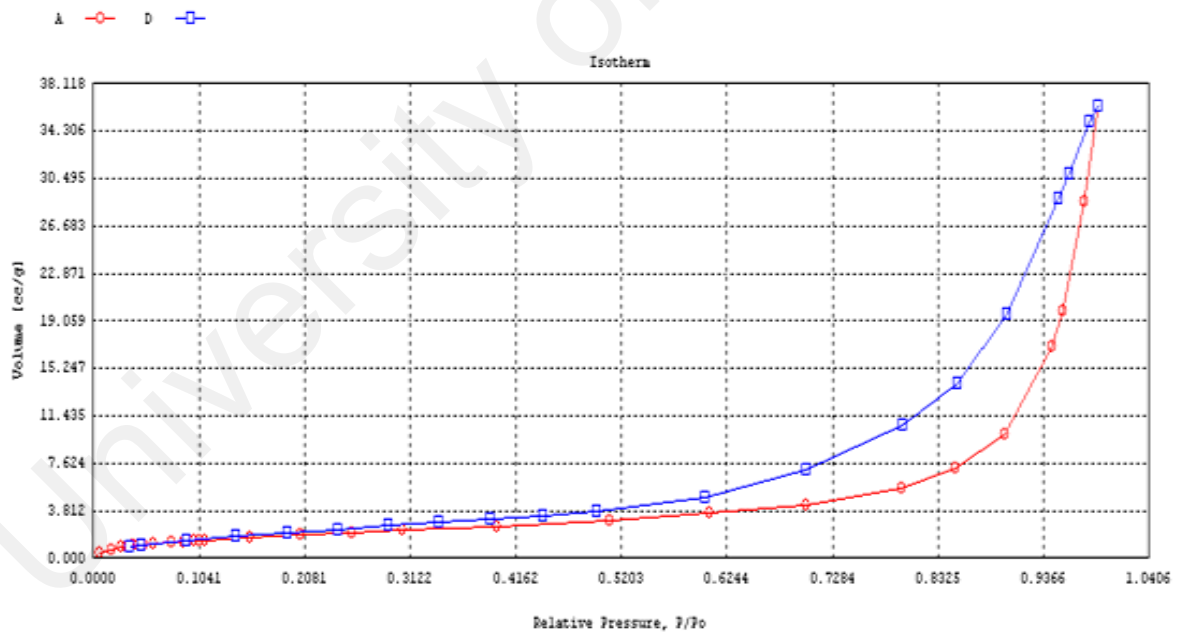


(b) FA

Figure 4.32: Isotherm plots of solidified sludge with 5 % weight CRMs (a) CSF (b) FA (c) AC (d) MK and (e) RHA

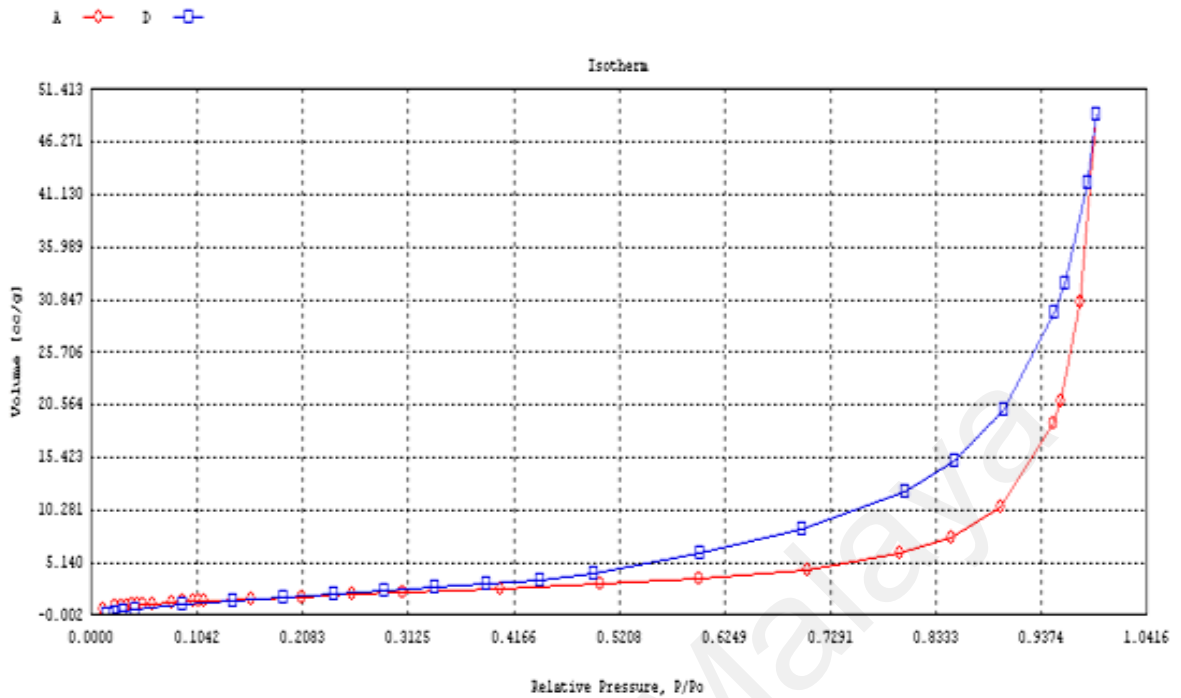


(c) AC



(d) MK

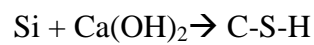
Figure 4.32: Isotherm plots of solidified sludge with 5 % weight CRMs (a) CSF (b) FA (c) AC (d) MK and (e) RHA (continued)



(e) RHA

Figure 4.32: Isotherm plots of solidified sludge with 5 % weight CRMs (a) CSF (b) FA (c) AC (d) MK and (e) RHA (continued)

The solidified sludge with CSF showed less mesopores distribution compared to other CRMs as shown by narrower hysteresis loop. This pore refinement was due to abundant silica in CSF binder, which contributed to high pozzolanic activity that reduced pore size in the cement matrix. Pozzolanic reaction shown in Equation 4-12 is secondary cement reaction forming C-S-H gel and simultaneously reduced coarse CH crystal. The similar type IV isotherm and hysteresis were depicted by the 5 % weight CRMs incorporation in the solidified sludge. Pore size distribution normally counted by desorption branch.



Eq. (4-12)

The Barrett-Joyner-Halenda (BJH) method was used to plot the cumulative adsorption pore volume of solidified sludge. Figure 4.33 shows the adsorption pore volume of solidified sludge, which composed of mesopore and macropore volume.

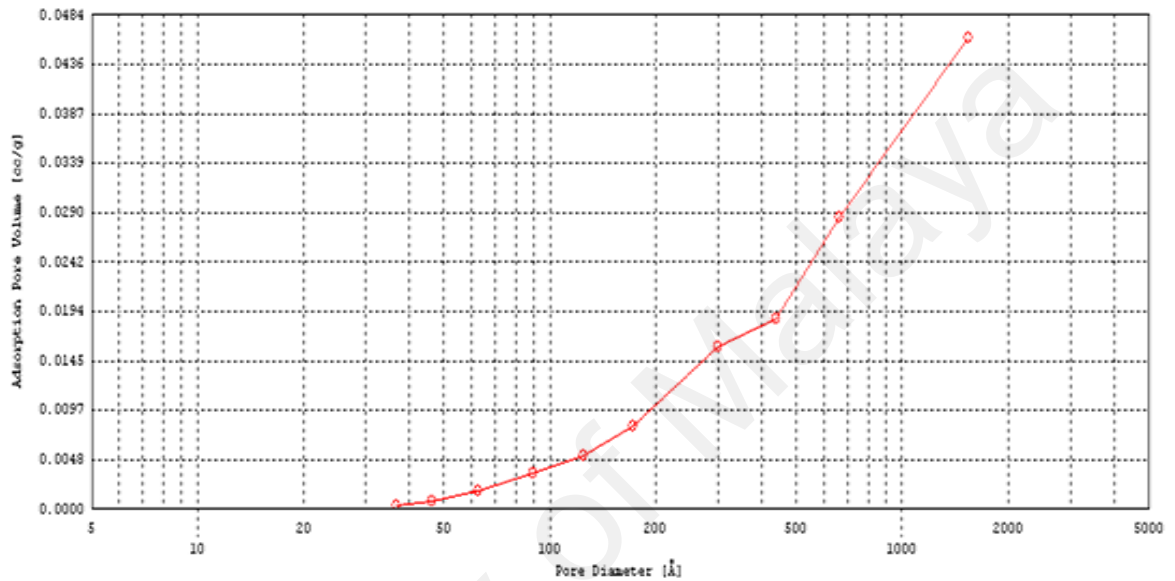
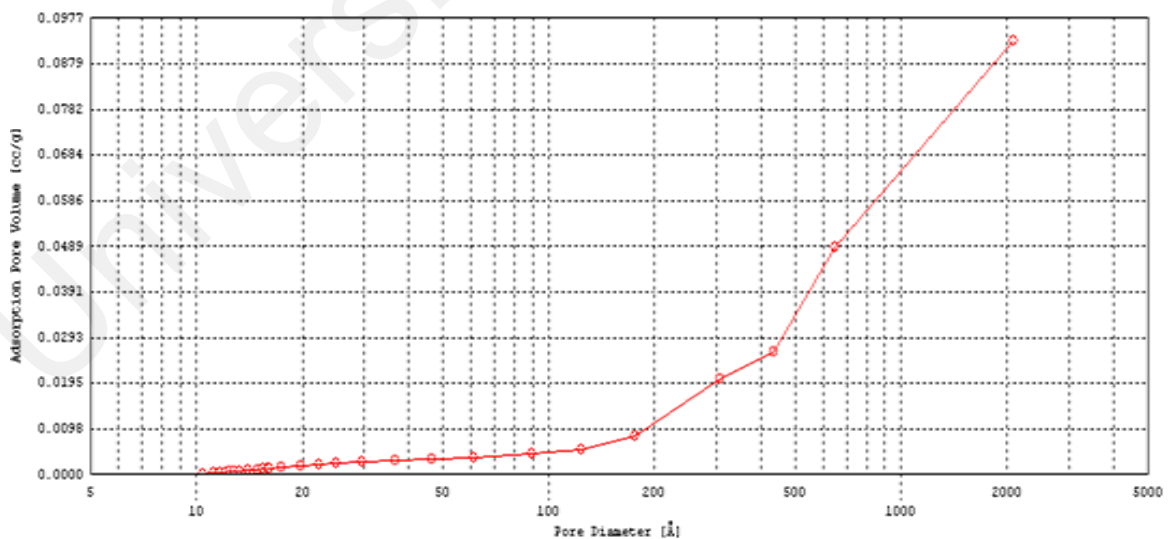
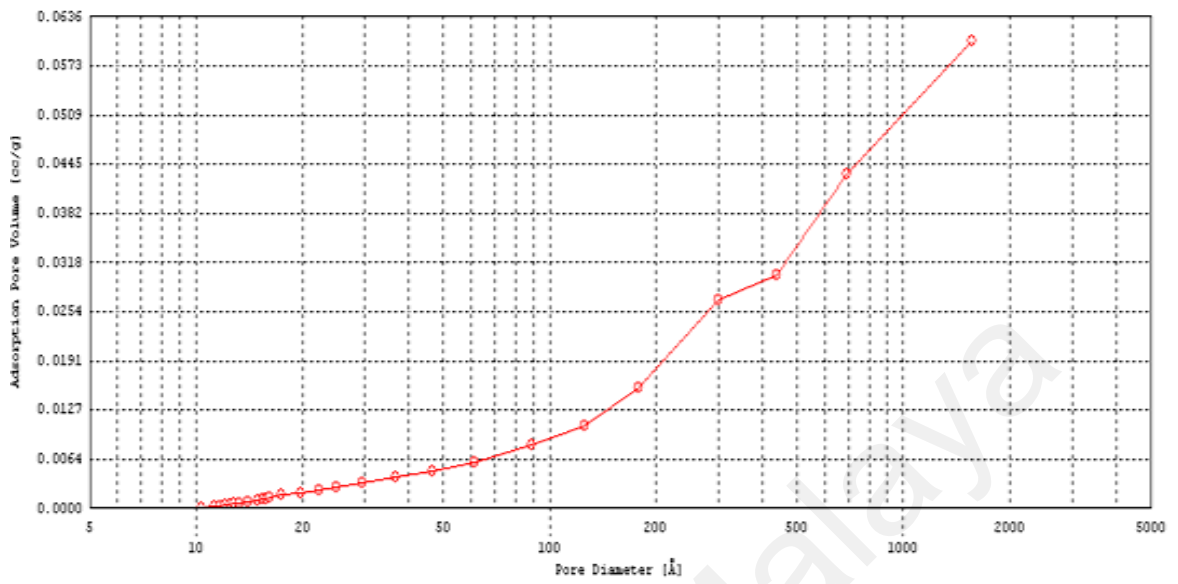


Figure 4.33: BJH cumulative adsorption pore volume of solidified sludge

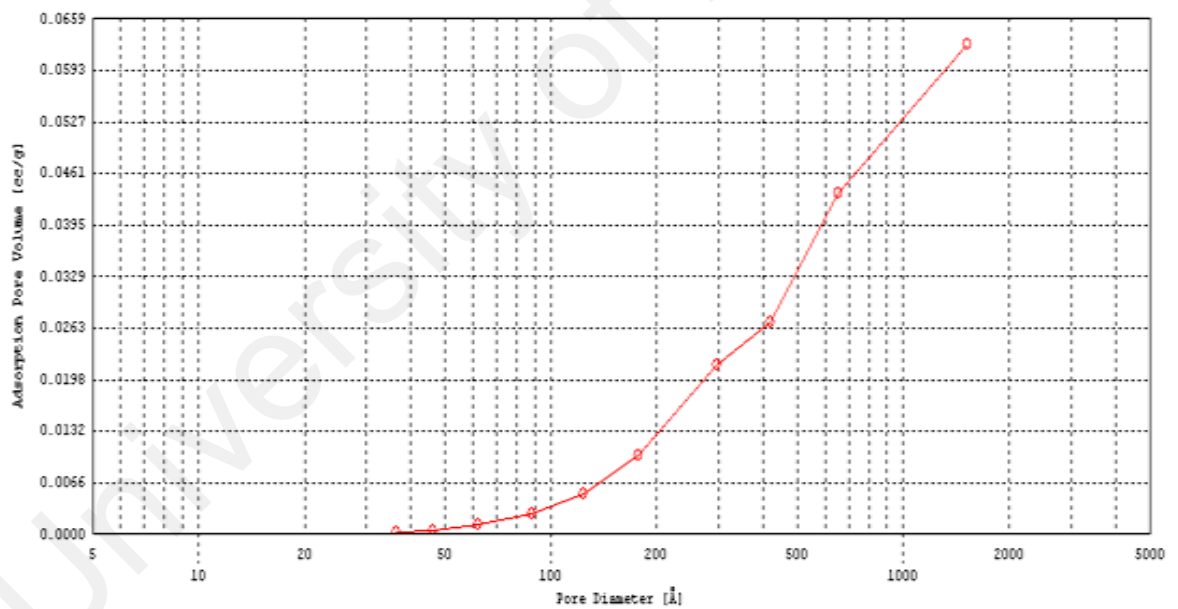


(a) CSF

Figure 4.34: BJH cumulative adsorption pore volume of solidified sludge with 5 % weight CRMs (a) CSF (b) FA (c) AC (d) MK and (e) RHA

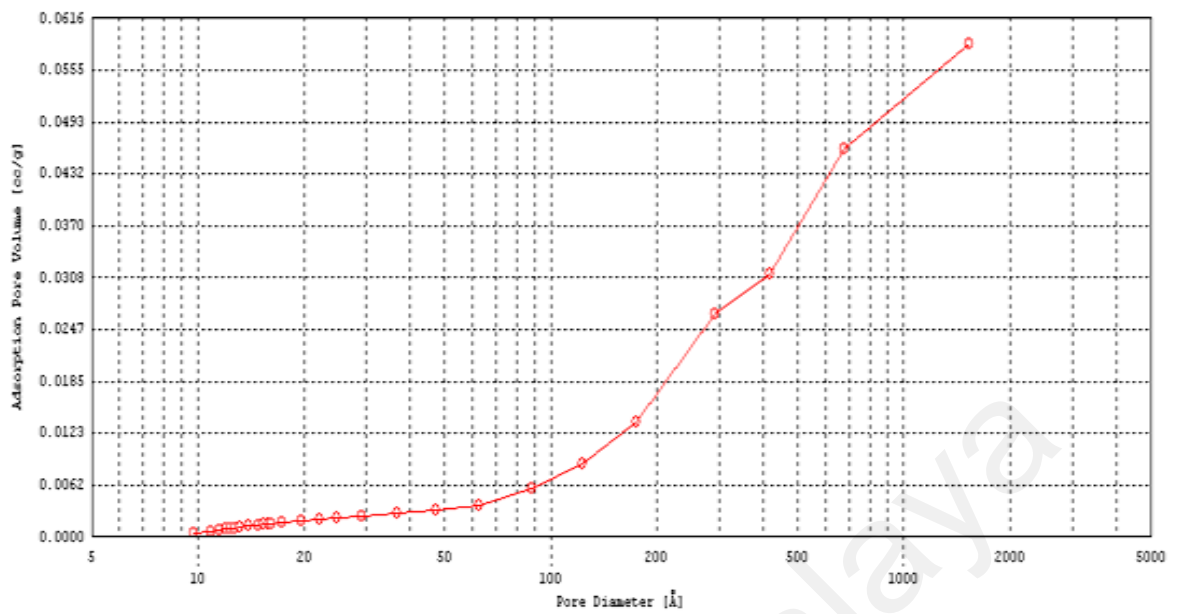


(b) FA

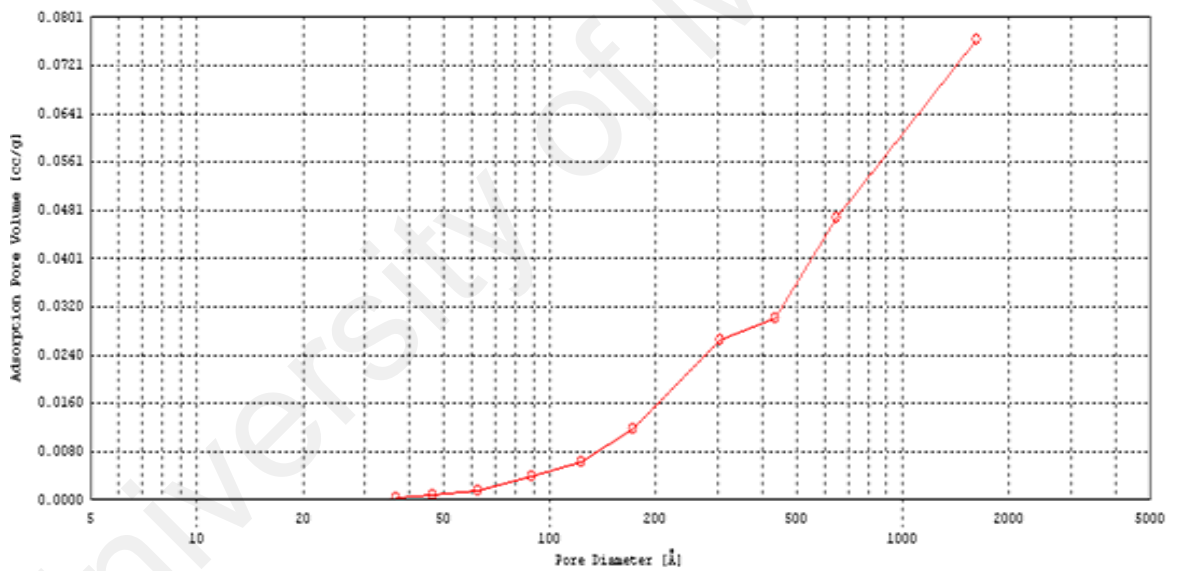


(c) AC

Figure 4.34: BJH cumulative adsorption pore volume of solidified sludge with 5 % weight CRMs (a) CSF (b) FA (c) AC (d) MK and (e) RHA (continued)



(d) MK



(e) RHA

Figure 4.34: BJH cumulative adsorption pore volume of solidified sludge with 5 % weight CRMs (a) CSF (b) FA (c) AC (d) MK and (e) RHA

(continued)

The BJH cumulative adsorption pore volume for solidified sludge with 5 % weight CRMs showed that the incorporation of CSF, FA and MK has increased the micropore in the cement matrix with the diameter of 10 to 20 Å. The cumulative pore volume and average pore diameter of solidified waste form are tabulated in Table 4.13. Generally, addition of 5 % weight CRMs exhibit the increases in average pore diameter except FA as the effect of it smaller pore size. Accumulated pore volume also increase with MK and RHA by 1.0 and 1.25 higher, respectively.

Table 4.13: Accumulated pore volume and average pore diameter

| <i>Sample</i> | <i>Accumulated pore volume (cm³/g)</i> | <i>Average pore diameter (Å)</i> |
|---------------|---|--------------------------------------|
| 8045 | 2.07 x 10 ⁻² | 140 |
| CSF5 | 2.73 x 10 ⁻² | 163 |
| FA5 | 2.95 x 10 ⁻² | 135 |
| AC5 | 2.98 x 10 ⁻² | 162 |
| MK5 | 3.07 x 10 ⁻² | 174 |
| RHA5 | 3.25 x 10 ⁻² | 194 |

4.4.2.6 Conclusions of porosity

1. Bulk density of solidified sample was recorded in the range of 1.23 to 1.47 kg/m³.
2. Permeable porosity increases with the increased in C/Sd ratio. However, lower W/C ratio indicates less permeable pore.
3. Inclusion of CRMs exhibit reduction in density value.
4. The increased in RHA and MK percentage in solidified sludge showed the effect of slight increment in the permeable pore but insignificant changes were observed in the AC, FA and CSF incorporation.
5. The strength has antagonism effect with porosity in solidified OPC and solidified sludge. Porosity was found to decrease with strength in solidified OPC but with

sludge inclusion, the reverse trend was observed. Based on the isostrength relationship with porosity and C/Sd, porosity increases with the increased of strength in W/C 0.45 and 0.5 samples. But at low W/C of 0.4, increasing porosity severely affected the strength.

6. Strength development was less affected by the C/Sd at W/C of 0.45.
7. The isostrength relationships with permeable pore and percentage of CRMs showed that at minimum 5 % CRMs incorporation and low porosity depict the maximum strength peak for all CRMs.
8. Adsorption isotherm of the solidified sludge types IV with hysteresis type C tapered/wedge indicates the presence of mesoporous monolith.
9. Pore size of solidified sludge was dominated by the mesopores in the size range of 20 to 500 Å.
10. BJH cumulative adsorption pore volumes in the 5 % inclusion of CSF, FA and MK have exhibited the increase in micropore volume of the cement matrix with the diameter of 10 to 20 Å.
11. Average pore diameter was increased by the incorporation of 5 % weight CRMs except FA.
12. Accumulated pore volume of the solidified sludge with 5 % weight of MK and RHA rise by 1.0 and 1.25 units higher compared to the solidified sludge.

4.4.3 Leachability of solidified sludge

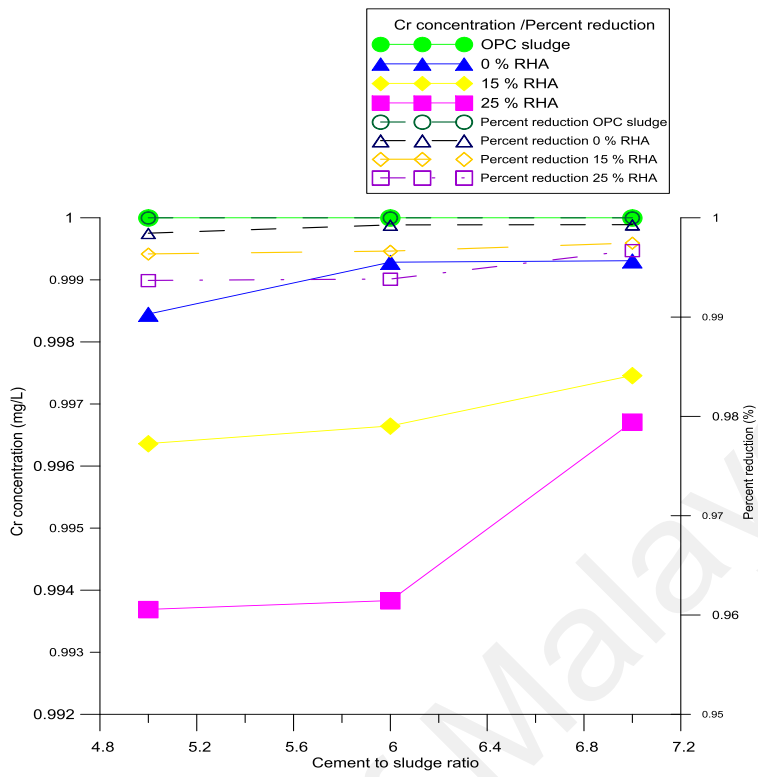
Metal leachability is controlled by pH of the solution. The solution used in the leaching was 0.5 M acetic acid. The weak acetic acid dissociated as the conjugate base of

H^3COO^- at pH of 9.26 (25 °C). Acetic acid is a polar solvent capable of dissolved ionic compounds by free hydrogen ions, H^+ and acetate ions that diffused into the leached layer. Free hydrogen ions can attacked the cement boundary at the pH of 4.75, which resulted in the leaching of metals at the surface boundary. The diffusion coefficient of H^+ was $9.33 \times 10^{-5} \text{ cm}^2/\text{s}$ in water at 25 °C (Cheng, 1991) but the value is reduced once it moved into porous media.

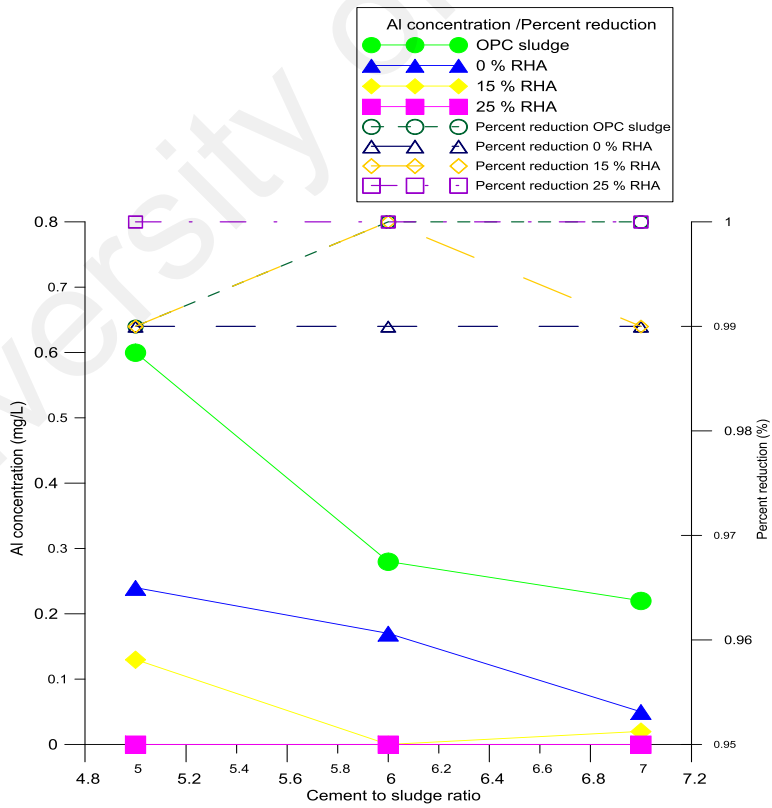
4.4.3.1 Leachability of simulated metals

Leachability potential of spike metals in solidified sludge was conducted with the blend of RHA incorporation. Out of the four spike metals (Cr, Cu, Pb and Zn) only Cr was leached out from the solidified waste forms as depicted by Figure 4.35(a). Cr leachability increased with the increasing RHA percentage with reduction rate of more than 99 %. Chromate compound normally reduced to trivalent state and precipitated in bases medium as $\text{Cr}(\text{OH})_3$ in most of the cement hydration system and chromium hydroxide has lower solubility compared to other metals (Conner, 1990). Inherent Al in the sludge was significantly immobilized by the additions of 15 % RHA as shown in Figure 4.35(b).

Oil and grease were significantly immobilized by OPC S/S with reduction of 98.55 % (Figure 4.36). Higher C/Sd ratio performed better immobilization for Al, Cr, oil and grease in solidified sludge. In higher C/Sd ratio more cement clinker is available to bind with the contaminants while reduced the interference effect of the sludge.



(a) Cr



(b) Al

Figure 4.35: Leached metal in solidified sludge and RHA for (a) Cr and (b) Al

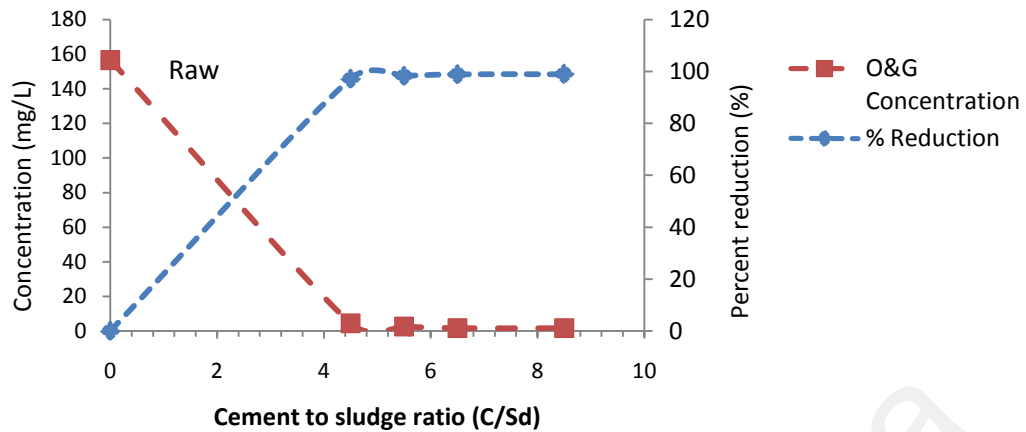


Figure 4.36: Oil and grease concentration leached from OPC-sludge

4.4.3.2 Metal in TCLP of solidified OPC-sludge

TCLP was found to be aggressive leaching due to the extract leachate is higher than EPT from 40 to 80 percent for contaminant like arsenic, barium, cadmium and lead (Conner, 1990). Crushed block leaching conducted to the solidified waste by the TCLP indicates the presence of leached metal as tabulated in Table 4.14. The basic mixed of S/S waste TCLP for nine metals are depicted by Figure 4.37, 4.38 and 4.39 for W/C of 0.4, 0.45 and 0.5 accordingly. Higher W/C of 0.5 able to retain most metals in the solidified matrix whereby fewer metals were leached from cement into the solution. Al was found as one of the highest leached metals in mostly all W/C ratios. Since Al is amphoteric metal, the pH change in the aqueous from acid to alkaline will cause the changes of Al compound in the solution as represented in Equation 4-13 (Glasser, 1993). Cu was not found in the TCLP leachate in all W/C ratios. The alkaline pH of solidified sludge leachate was in the narrowed range of 11.22 to 12.25 due to the exposed of leachant to OPC hydration product's particles as in Figure 4.40.

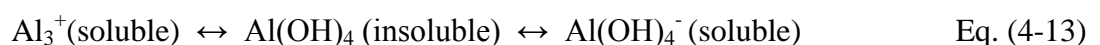


Table 4.14: Average metals concentration leached in TCLP leachate of solidified OPC-sludge in mg/L

| W/C | 0.4 | | | | | 0.45 | | | | | 0.5 | | | | |
|------|------|------|------|------|------|------|------|------|------|------|------|------|------|------|------|
| C/Sd | 0 | 5 | 6 | 7 | 8 | 0 | 5 | 6 | 7 | 8 | 0 | 5 | 6 | 7 | 8 |
| Al | 0.20 | 0.12 | 0.12 | 0.04 | 0.00 | 0.00 | 0.08 | 0.00 | 0.25 | 0.00 | 0.00 | 0.00 | 0.42 | 0.00 | 0.33 |
| Cd | 0.00 | 0.00 | 0.00 | 0.04 | 0.05 | 0.00 | 0.07 | 0.09 | 0.06 | 0.00 | 0.10 | 0.01 | 0.07 | 0.10 | 0.01 |
| Cr | 0.02 | 0.03 | 0.04 | 0.04 | 0.00 | 0.05 | 0.00 | 0.00 | 0.06 | 0.03 | 0.00 | 0.00 | 0.00 | 0.00 | 0.00 |
| Cu | 0.00 | 0.00 | 0.00 | 0.00 | 0.00 | 0.00 | 0.00 | 0.00 | 0.00 | 0.00 | 0.00 | 0.00 | 0.00 | 0.00 | 0.00 |
| Fe | 0.25 | 0.07 | 0.05 | 0.05 | 0.03 | 0.08 | 0.01 | 0.06 | 0.00 | 0.03 | 0.00 | 0.00 | 0.00 | 0.02 | 0.00 |
| Mn | 0.00 | 0.01 | 0.01 | 0.01 | 0.00 | 0.00 | 0.01 | 0.01 | 0.00 | 0.00 | 0.00 | 0.00 | 0.00 | 0.00 | 0.01 |
| Ni | 0.03 | 0.01 | 0.03 | 0.05 | 0.05 | 0.00 | 0.08 | 0.06 | 0.00 | 0.08 | 0.00 | 0.00 | 0.02 | 0.02 | 0.07 |
| Pb | 0.11 | 0.07 | 0.00 | 0.00 | 0.05 | 0.00 | 0.06 | 0.05 | 0.00 | 0.00 | 0.00 | 0.40 | 0.00 | 0.09 | 0.00 |
| Zn | 0.10 | 0.03 | 0.03 | 0.04 | 0.00 | 0.04 | 0.00 | 0.00 | 0.01 | 0.00 | 0.00 | 0.00 | 0.00 | 0.00 | 0.00 |

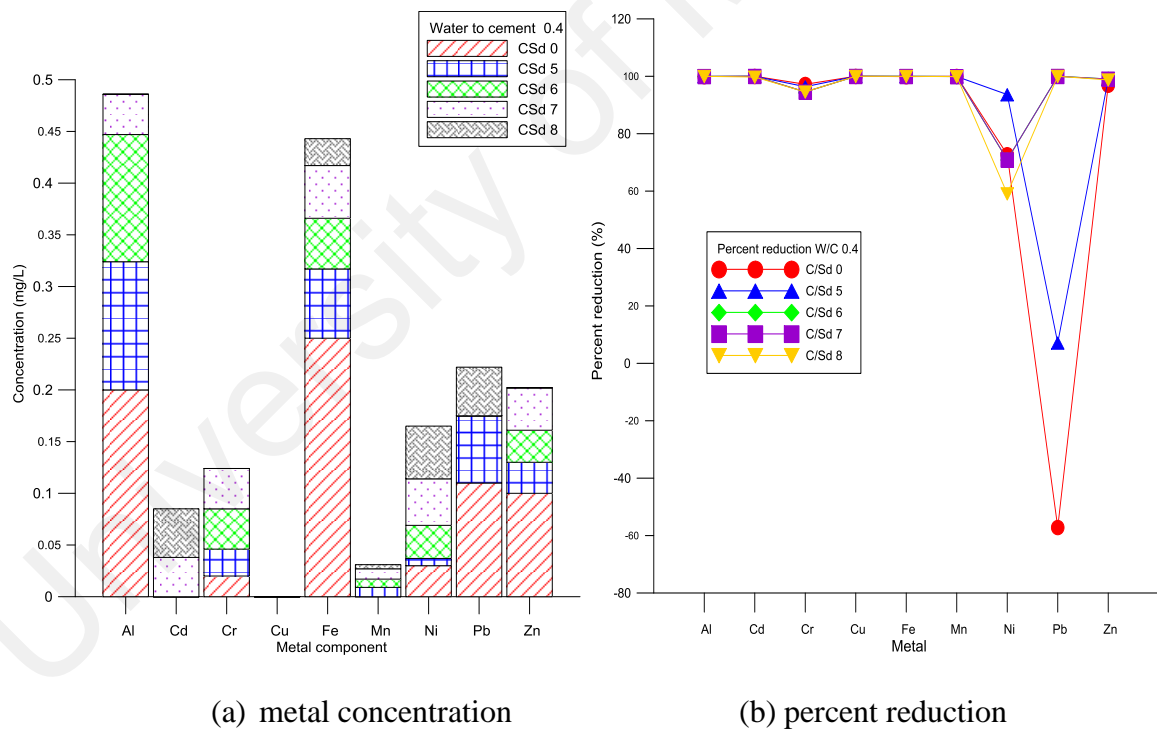


Figure 4.37: TCLP leachate of W/C 0.4 (a) metal concentration and (b) percent reduction

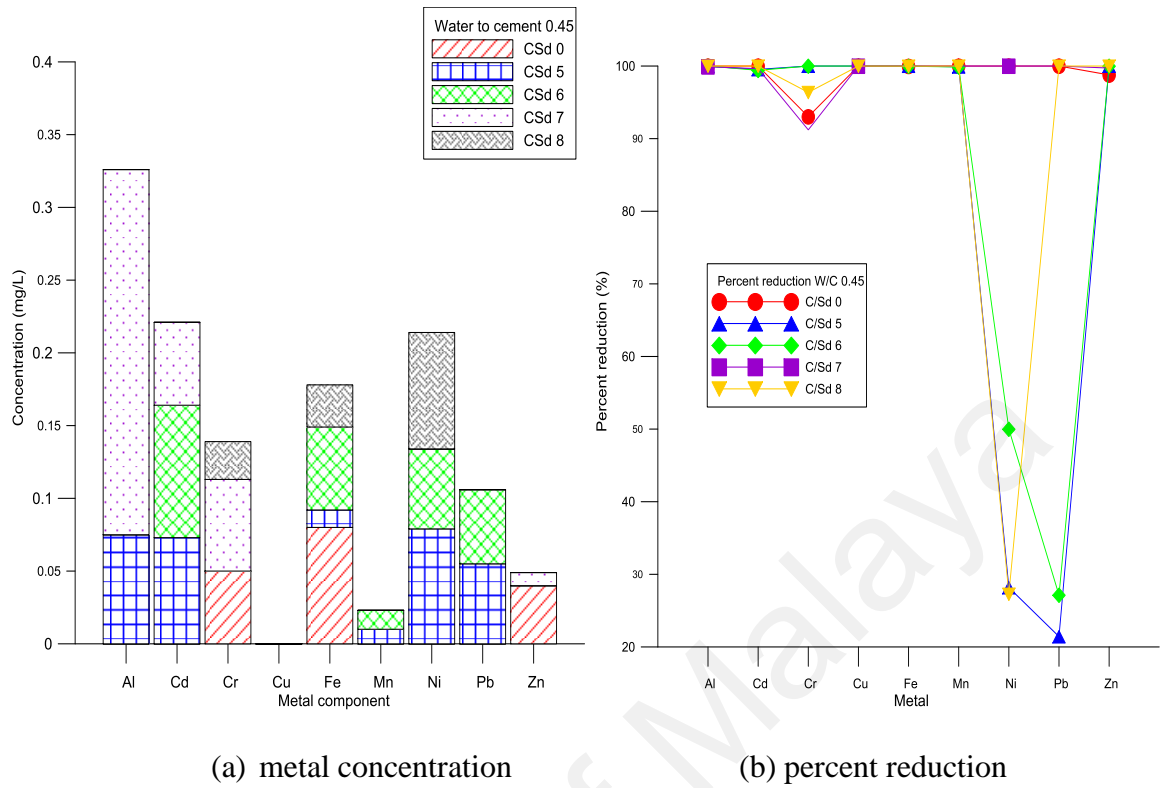


Figure 4.38: TCLP leachate of W/C 0.45 (a) metal concentration (b) percent reduction

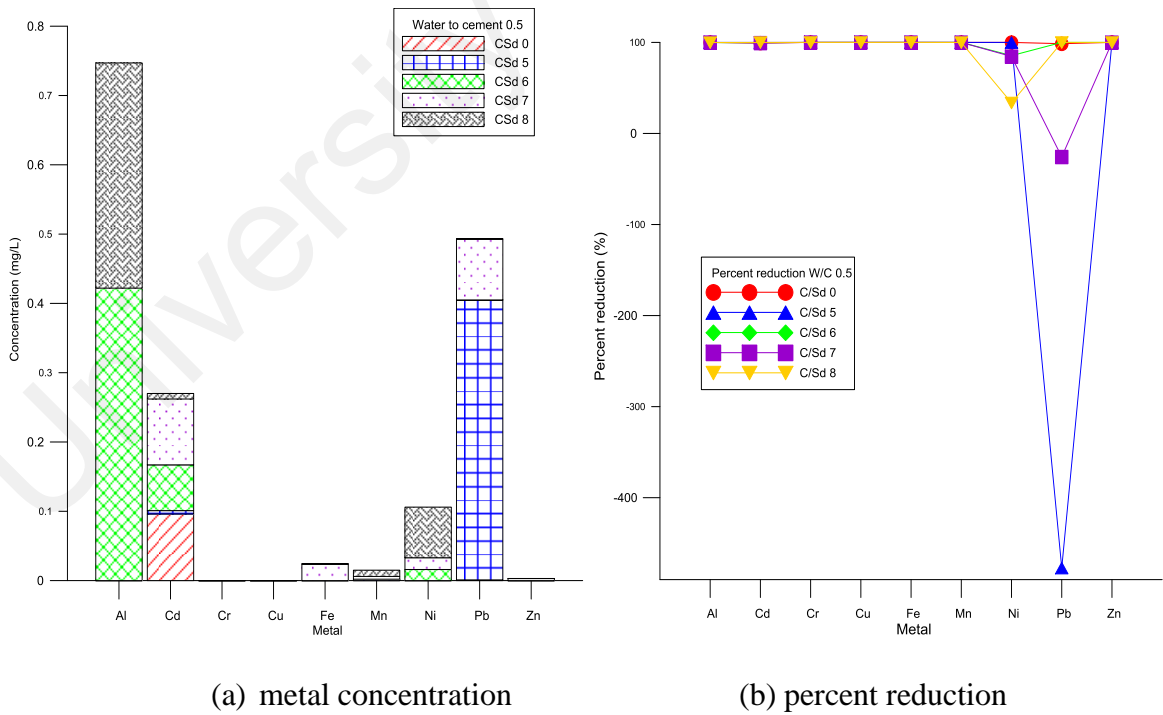


Figure 4.39: TCLP leachate of W/C 0.5 (a) metal concentration (b) percent reduction

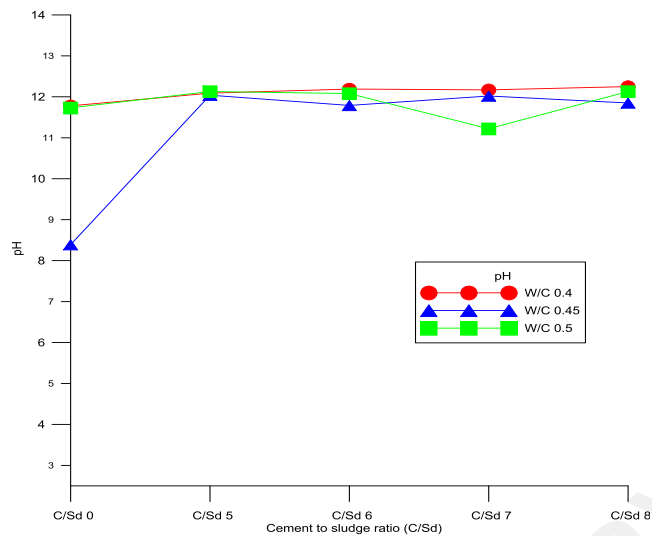


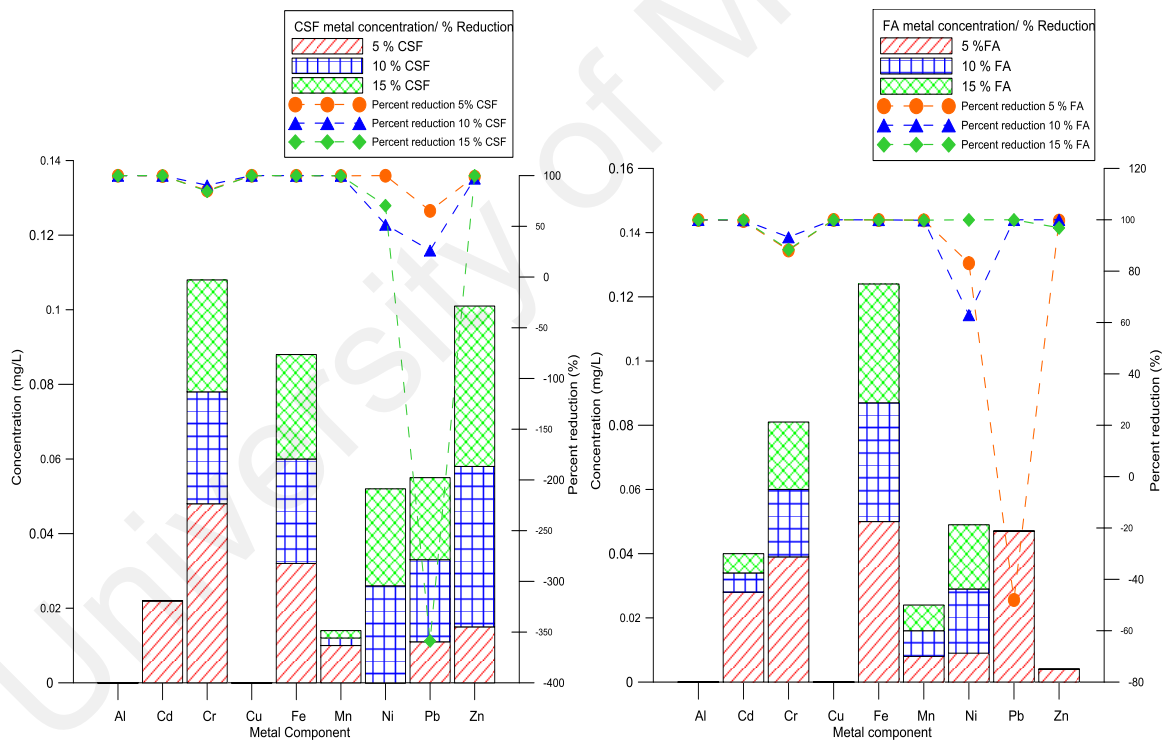
Figure 4.40: pH of solidified sludge

4.4.3.3 Metals in TCLP of solidified OPC-sludge with CRMs

Metal's concentration in TCLP extracts of solidified OPC-sludge with CRMs incorporation at 5, 10 and 15 percent are tabulated in Table 4.15. The individual plot of binders incorporated in OPC-sludge namely CSF, FA, AC, RHA and MK for nine metals are represented in Figure 4.41 (a) to (e). CSF, FA and AC have no Al and Cu in leachate at all percentage. MK also shows no Cu in the solidified matrix and minimum concentration for other metals. In contrast to Cu, Al was the highest metal found in the leachate as it was the main element in MK composition ($Al_2Si_2O_7$). Most metals have lowest solubility in alkaline range and Cu has lowest solubility at pH of nine. The leachate extracted from all solidified waste with CRMs has alkaline pH of 12.06 to 12.46. In general, the incorporation of CRMs has increased pH, whereby CSF and FA have 0.25 units higher than solidified sludge 8045 while other binders rise by 0.50 units. All measured metals in TCLP leachate were found below the Environmental Quality Act 2009 standard as shown by radar plots in Appendix C.

Table 4.15: Average leached metals concentration of solidified OPC-sludge CRMs in mg/L

| CRMs | CSF | | | FA | | | AC | | | RHA | | | MK | | |
|--------|------|------|------|------|------|------|------|------|------|------|------|------|------|------|------|
| | 5.0 | 10.0 | 15.0 | 5.0 | 10.0 | 15.0 | 5.0 | 10.0 | 15.0 | 5.0 | 10.0 | 15.0 | 5.0 | 10.0 | 15.0 |
| % CRMs | 5.0 | 10.0 | 15.0 | 5.0 | 10.0 | 15.0 | 5.0 | 10.0 | 15.0 | 5.0 | 10.0 | 15.0 | 5.0 | 10.0 | 15.0 |
| Al | 0.00 | 0.00 | 0.00 | 0.00 | 0.00 | 0.00 | 0.00 | 0.00 | 0.00 | 0.00 | 0.05 | 0.00 | 0.01 | 0.14 | 0.44 |
| Cd | 0.02 | 0.00 | 0.00 | 0.03 | 0.01 | 0.00 | 0.00 | 0.00 | 0.01 | 0.02 | 0.00 | 0.05 | 0.01 | 0.04 | 0.05 |
| Cr | 0.05 | 0.03 | 0.05 | 0.04 | 0.02 | 0.03 | 0.03 | 0.05 | 0.03 | 0.04 | 0.04 | 0.07 | 0.02 | 0.02 | 0.03 |
| Cu | 0.00 | 0.00 | 0.00 | 0.00 | 0.00 | 0.00 | 0.00 | 0.00 | 0.00 | 0.00 | 0.01 | 0.00 | 0.00 | 0.00 | 0.00 |
| Fe | 0.03 | 0.03 | 0.06 | 0.05 | 0.04 | 0.03 | 0.05 | 0.03 | 0.01 | 0.05 | 0.04 | 0.06 | 0.03 | 0.05 | 0.06 |
| Mn | 0.01 | 0.00 | 0.01 | 0.01 | 0.01 | 0.01 | 0.01 | 0.01 | 0.01 | 0.00 | 0.01 | 0.01 | 0.01 | 0.01 | 0.01 |
| Ni | 0.00 | 0.03 | 0.02 | 0.01 | 0.02 | 0.00 | 0.00 | 0.03 | 0.03 | 0.01 | 0.05 | 0.03 | 0.02 | 0.02 | 0.00 |
| Pb | 0.01 | 0.02 | 0.13 | 0.05 | 0.00 | 0.00 | 0.04 | 0.02 | 0.29 | 0.14 | 0.00 | 0.08 | 0.01 | 0.00 | 0.00 |
| Zn | 0.02 | 0.04 | 0.00 | 0.00 | 0.00 | 0.04 | 0.05 | 0.04 | 0.04 | 0.01 | 0.03 | 0.03 | 0.00 | 0.03 | 0.00 |

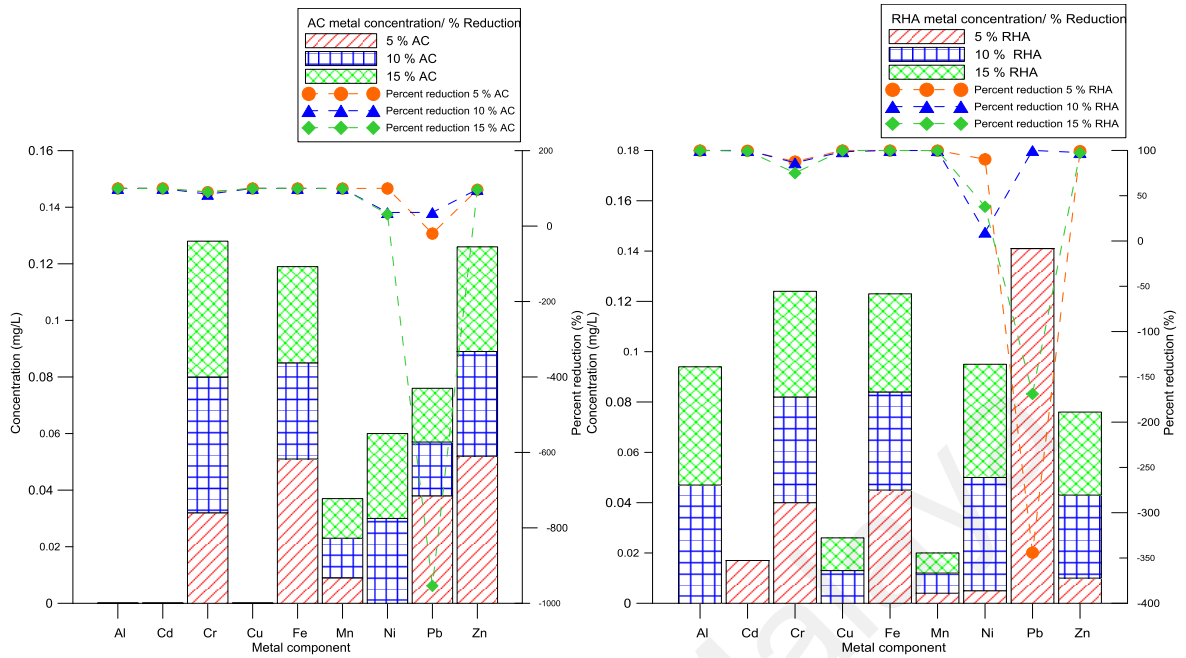


(a) CSF

(b) FA

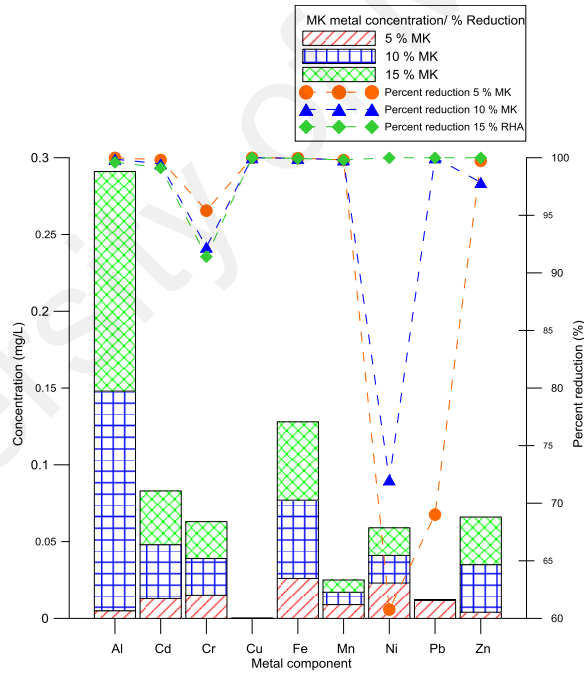
Figure 4.41: OPC-sludge TCLP metals leachate concentration for (a) CSF (b) FA

(c) AC (d) RHA and (e) MK



(c) AC

(d) RHA



(e) MK

Figure 4.41: OPC-sludge TCLP metals leachate concentration for (a) CSF (b) FA (c) AC (d) RHA and (e) MK (continued)

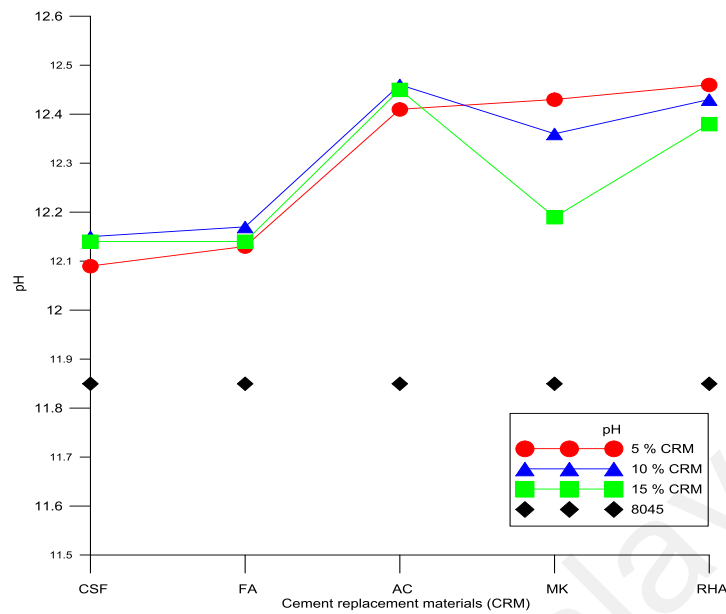


Figure 4.42: pH of solidified sludge with CRMs

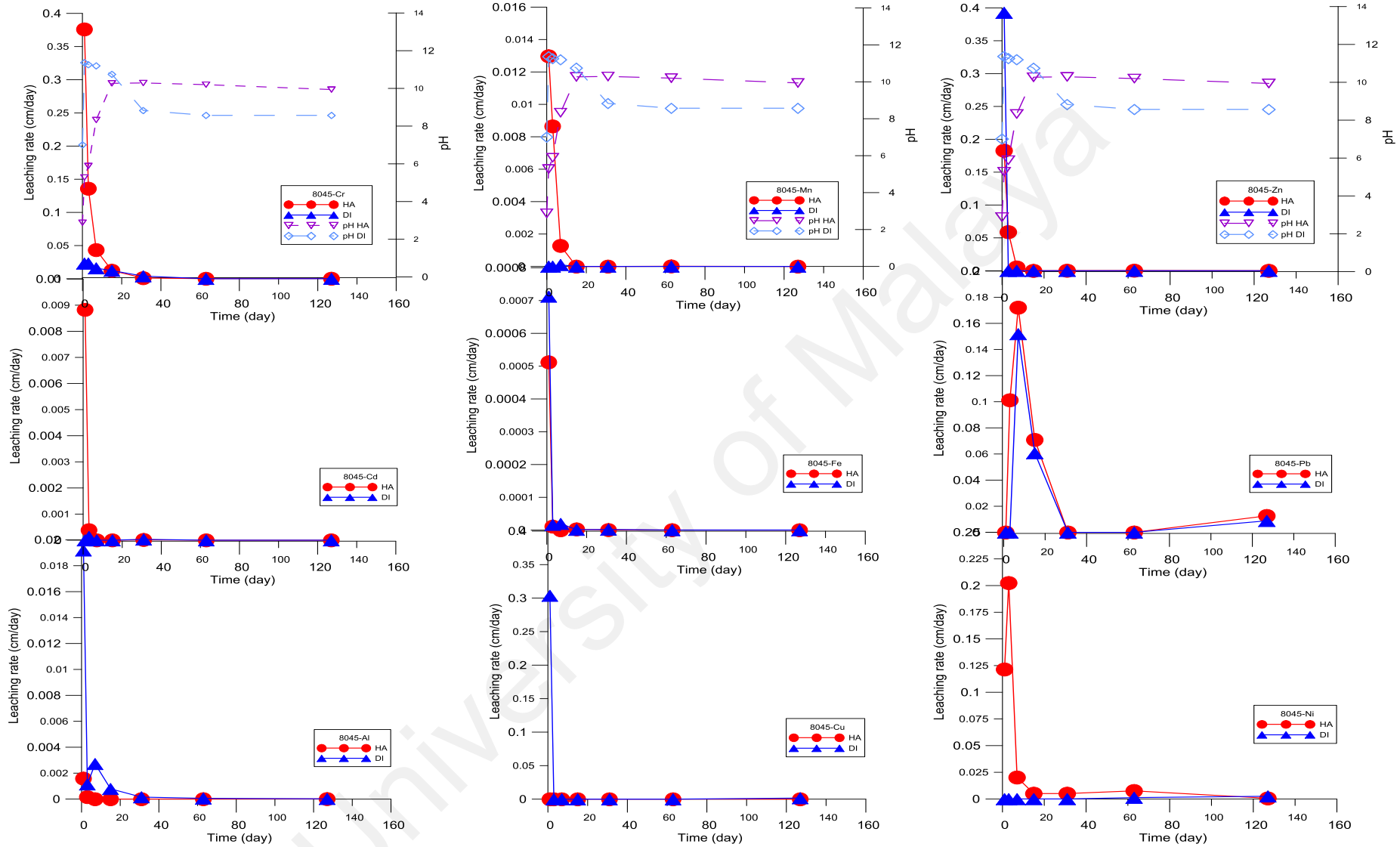
4.4.3.4 Semi-dynamic leaching test

The semi-dynamic leaching test is used to represent progressive leaching in landfill, and the accelerated leaching was imitated by using acidic leaching medium at pH 2.88. The leaching rate was measured based on the initial metal content in the solidification of sludge using modified ANS method in Equation 2-5. The leaching rates of metals from solidified OPC-sludge are represented in Figure 4.43.

Solidified OPC-sludge leaching rate with 5 % weight CRMs are represented in Figures 4.44 to 4.48. Semi-dynamic leaching can be used to predict the long term leaching of the specific contaminants by exposed to the accelerating agent such as acetic acid. Since the acidic can be used to simulate the carbonic acid naturally found in soil. The repeated exposure to the fresh leaching agents will ensure the leached substance has reached to its maximum leaching capability limit before it can be concluded as the real leaching rate has already achieved equilibrium as in the field whereby the contaminants are continuously exposed to new leaching agents.

Metal leaching was controlled by pH as depicted by Figures 4.42 to 4.48. Low pH aggravate the released of metals as the H^+ facilitates the diffusion of metals. Leachability of Ni, Zn and Cu are controlled by chemical equilibrium and surface complexation onto ferrihydrite in solid phase of metal hydroxide as pH function (Karamalidis and Voudrias, 2007). Solid metal hydroxide resolubilized in excess alkalinity for Cr, Cu and Pb as reflected by equilibrium chemistry in Equation 4-14 forming soluble metal ion species of Me^{+z} , and its derivative of $MeOH$, $Me(OH)_2$ and $Me(OH)_n$ (Cote, 1986). Most of the leaching rate plots exhibit diffusion curve as in Figure 2.6 (b).





(a) Al, Cd and Cr

(b) Cu, Fe and Mn

(c) Ni, Pb and Zn

Figure 4.43: Solidified OPC-sludge 8045 leaching rate (a) Al, Cd and Cr (b) Cu, Mn and Fe and (c) Ni, Pb and Zn

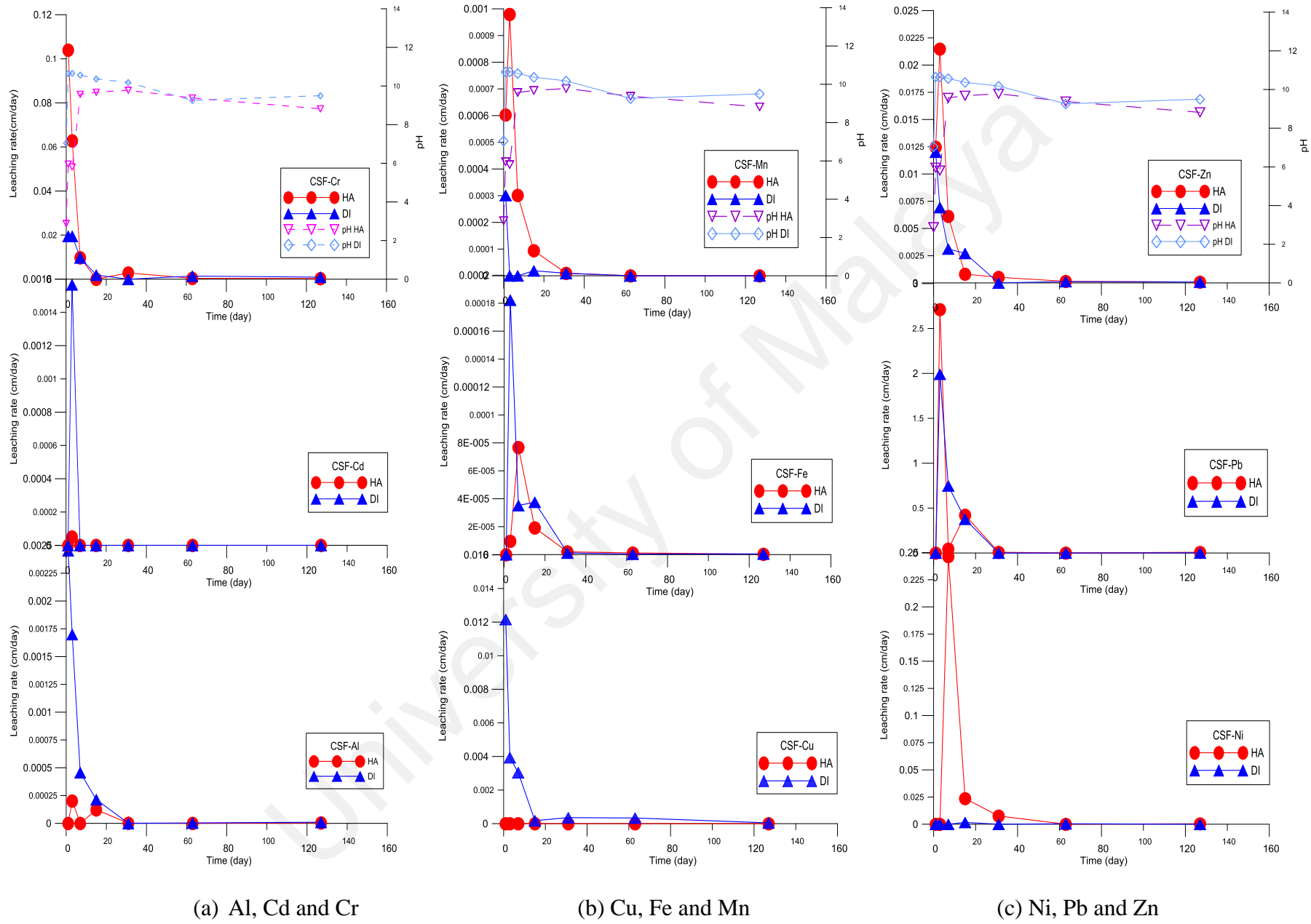


Figure 4.44: Leaching rate of metals from solidified OPC-sludge CSF5 (a) Al, Cd and Cr (b) Cu, Fe and Mn (c) Ni, Pb and Zn

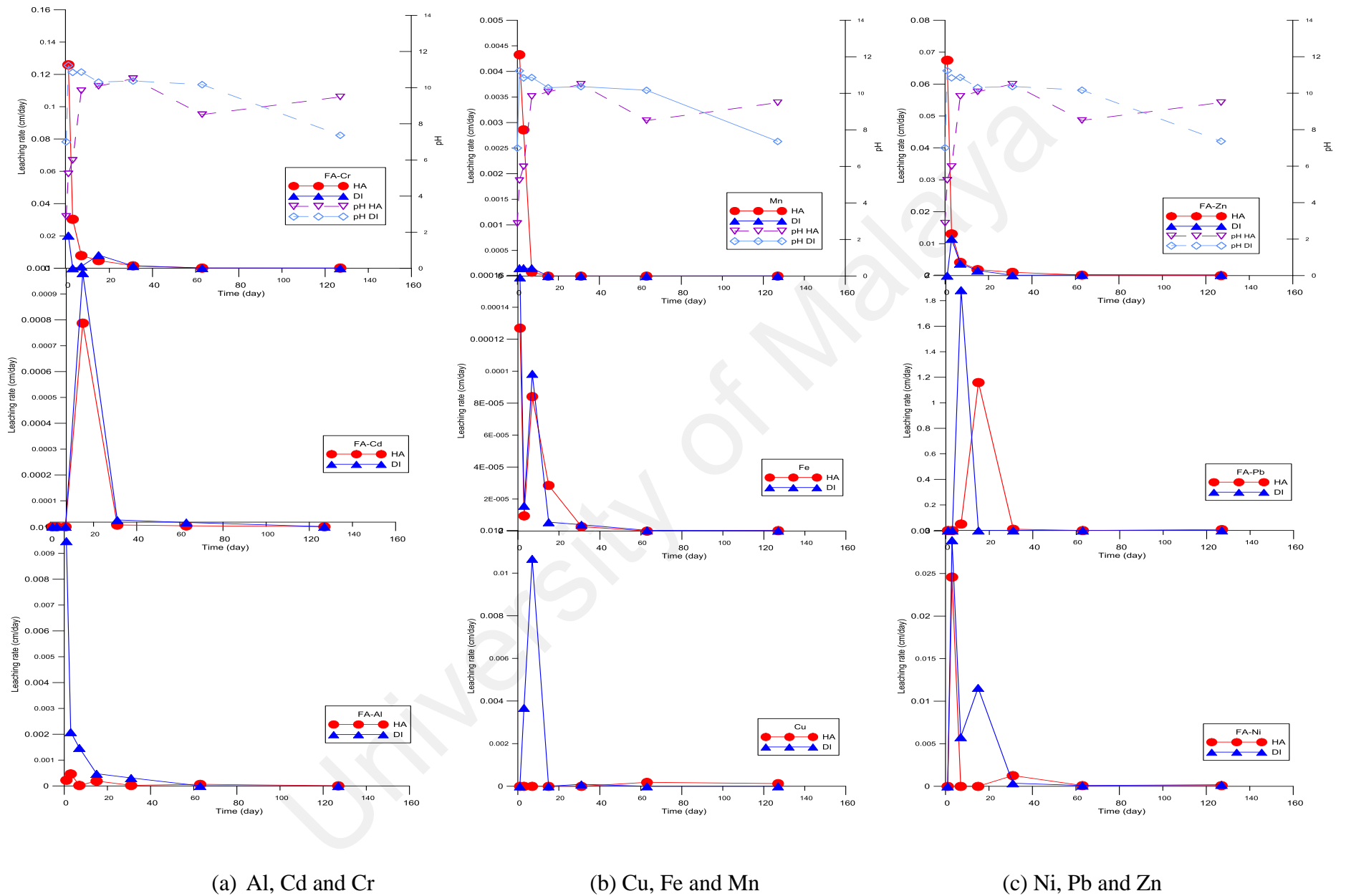
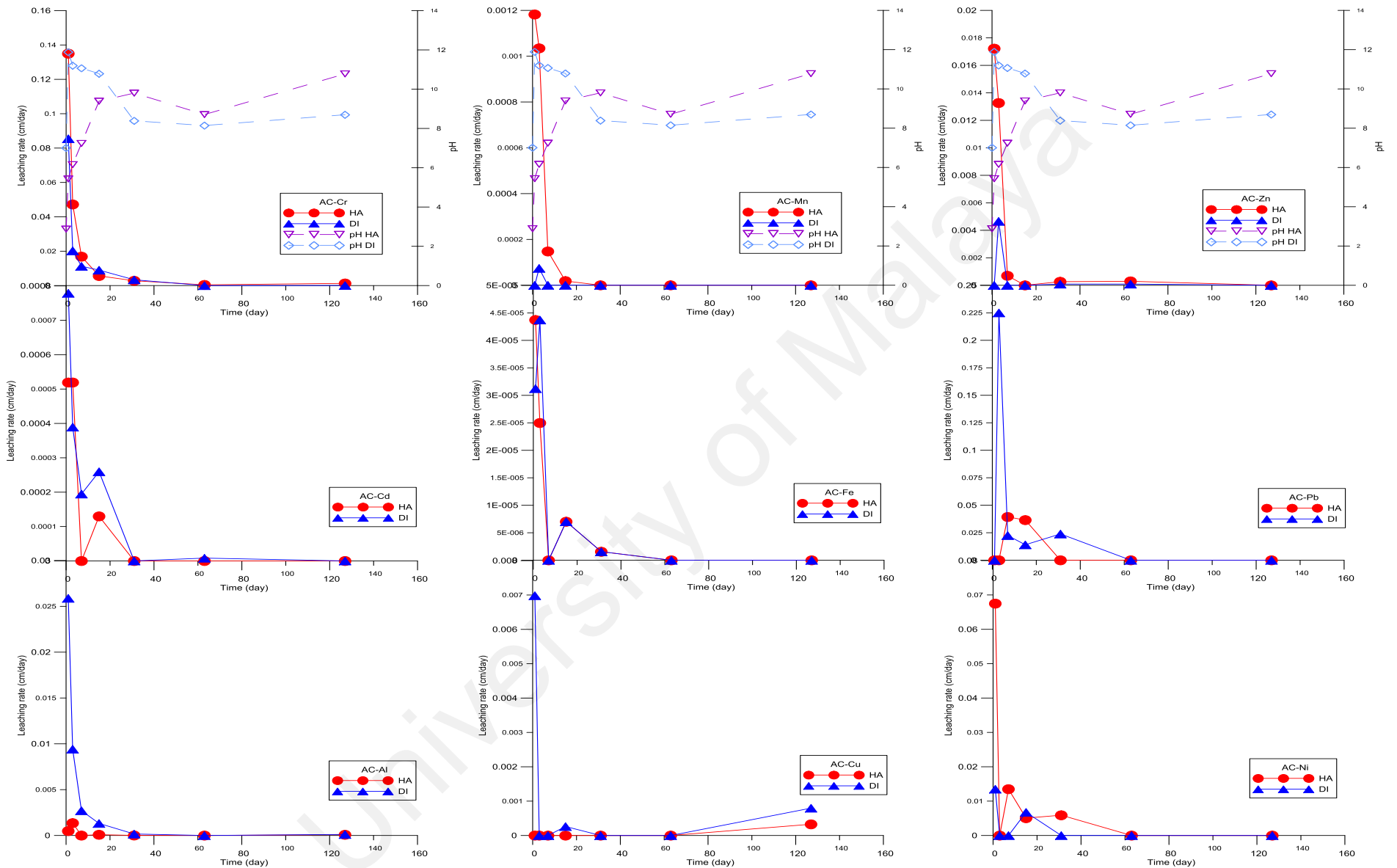


Figure 4.45: Leaching rate of metals from solidified OPC-sludge FA5 (a) Al, Cd and Cr (b) Cu, Fe and Mn (c) Ni, Pb and Zn

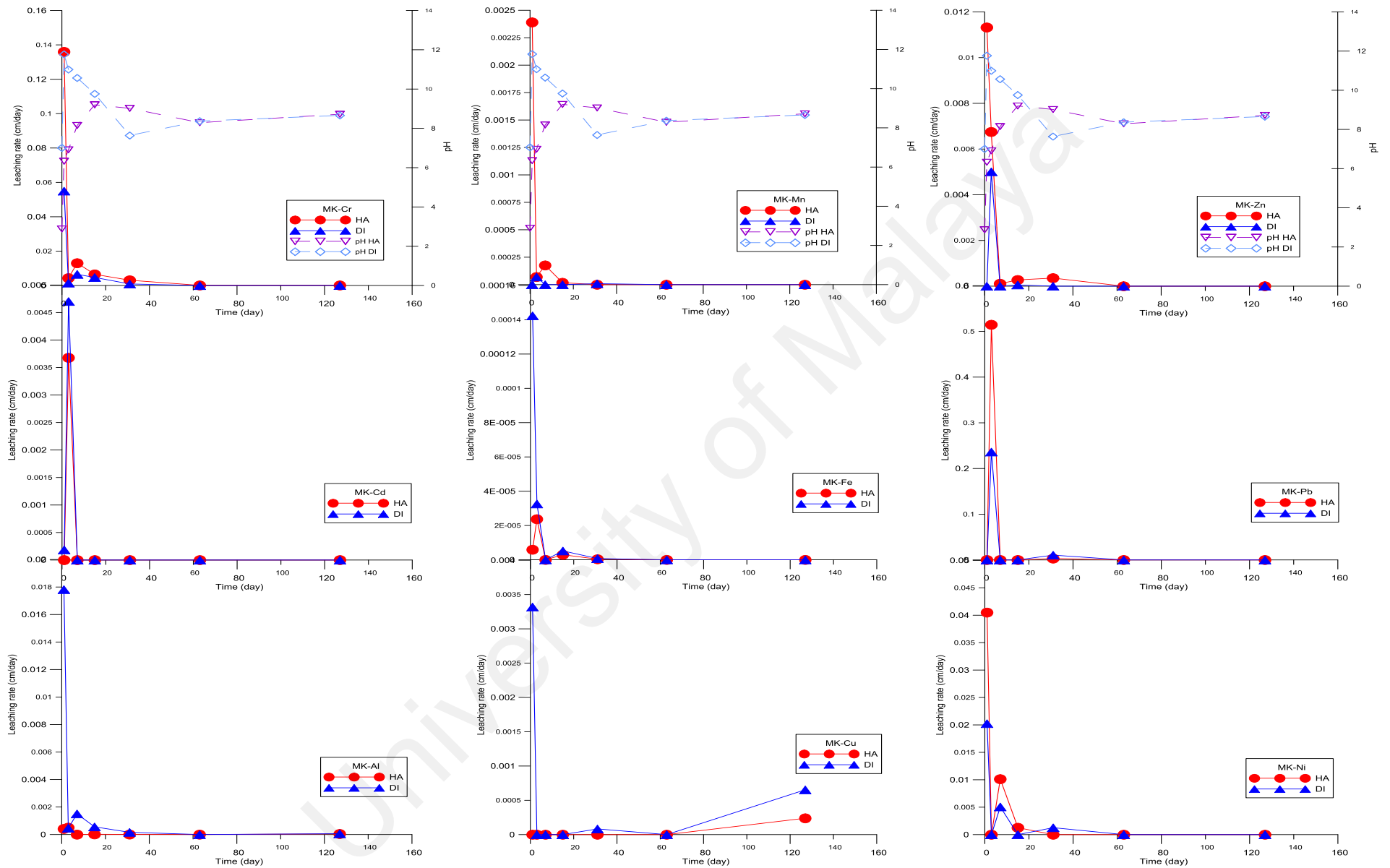


(a) Al, Cd and Cr

(b) Cu, Fe and Mn

(c) Ni, Pb and Zn

Figure 4.46: Leaching rate of metals from solidified OPC-sludge AC5 (a) Al, Cd and Cr (b) Cu, Fe and Mn (c) Ni, Pb and Zn

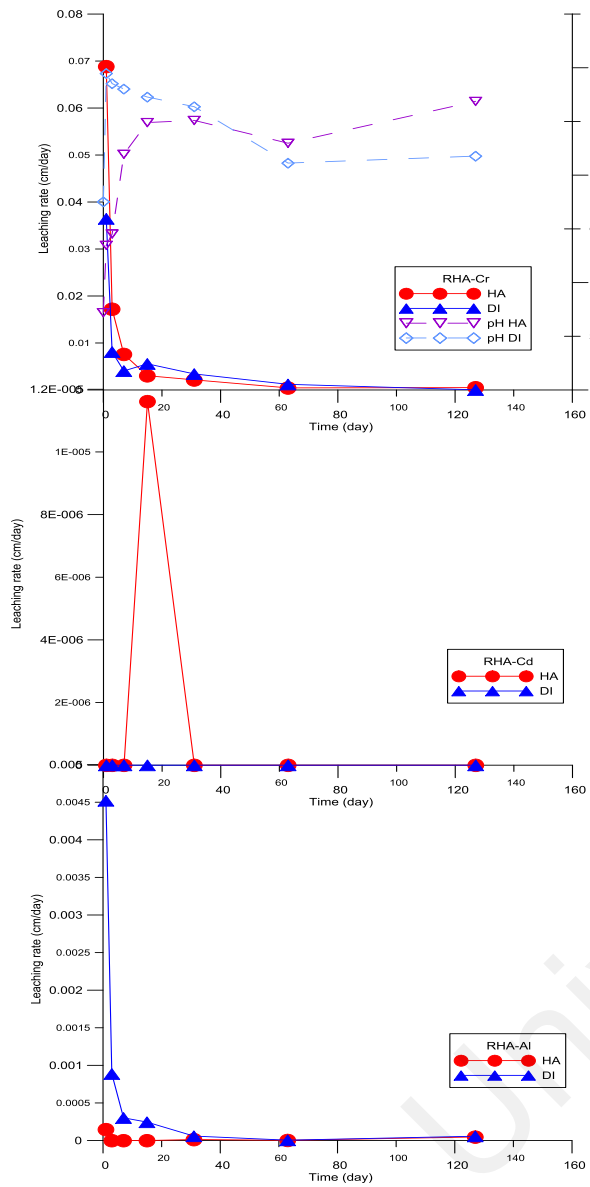


(a) Al, Cd and Cr

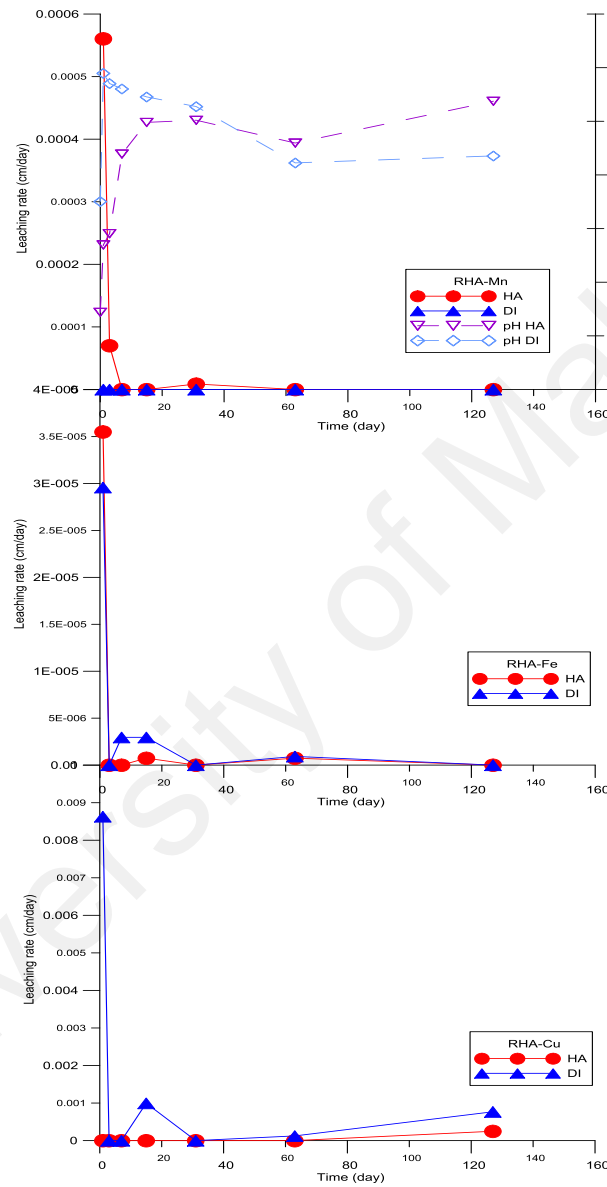
(b) Cu, Fe and Mn

(c) Ni, Pb and Zn

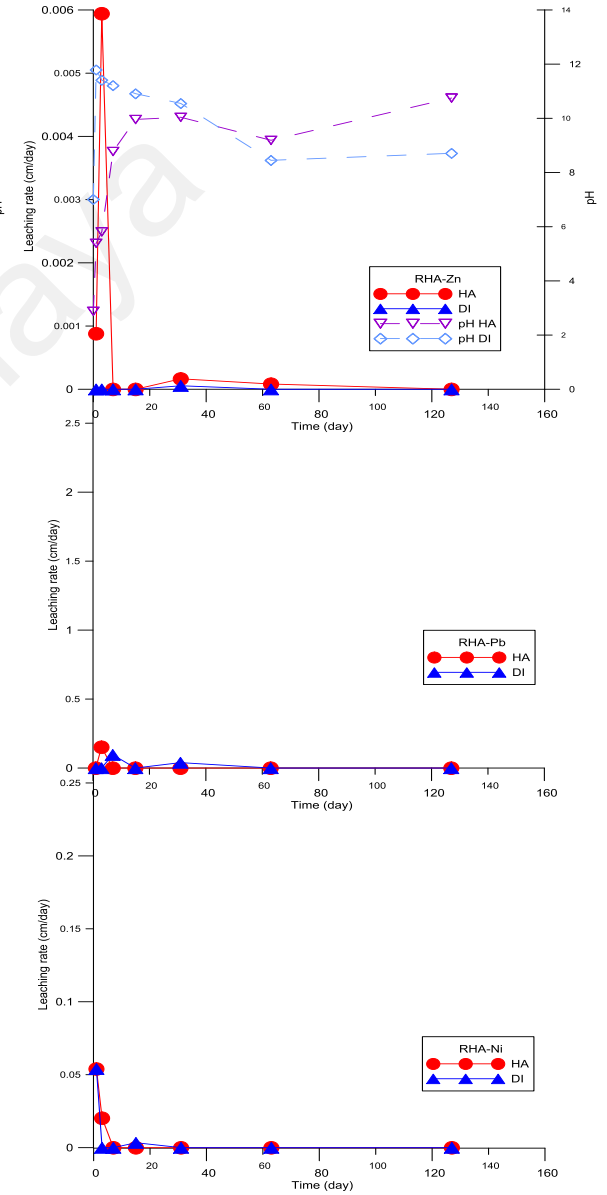
Figure 4.47: Leaching rate of metals from solidified OPC-sludge MK5 (a) Al, Cd and Cr (b) Cu, Fe and Mn (c) Ni, Pb and Zn



(a) Al, Cd and Cr



(b) Cu, Fe and Mn



(c) Ni, Pb and Zn

Figure 4.48: Leaching rate of metals from solidified OPC-sludge RHA5 (a) Al, Cd and Cr (b) Cu, Fe and Mn (c) Ni, Pb and Zn

Most metal leaching reaction reacts immediately for an active period of about 60 days. Thereafter, all metals leaching rate approaching zero for both DI and acidic solution, which mean it achieved equilibrium at pH about 9.5 whereby acetate ions are dominating the solution, and free hydronium ions are depleting. The dissociation constant of acetate ion, k_b is 5.6×10^{-10} (Ying and Yung, 1987) and in the 0.5 M of acetic acid, the CH_3COO^- concentration and pH of solution can be calculated as in Equation 4-15 and 4-16.

$$[\text{CH}_3\text{CHOO}^-] = 5.6 \times 10^{-10} \times 0.5 = 2.8 \times 10^{-10} \quad \text{Eq. (4-15)}$$

$$\text{pH} = \log \frac{1}{2.8 \times 10^{-10}} = 9.55 \quad \text{Eq. (4-16)}$$

Solidified sludge 8045 shown in Figure 4.43 has a stabilized pH at pH 9.94 in acidic leachant. The H^+ ions have facilitated metals to achieve optimum leaching rate for Cd, Cr, Mn, Ni and Pb. In contrast, optimum leached rate for Al, Cu, Fe and Zn were observed in DI leachant. Lower pH in DI leachant of 8.57 in comparison to HA shows that the aggressive H^+ found in HA leachant has contributed to the increase in pH of HA by diffusing more metal ions from the solidified surface by its high diffusion coefficient of $9.33 \times 10^{-5} \text{ cm}^2/\text{s}$ at pH 25 °C (Cheng, 1991).

The pH for OPC-sludge CSF5 exhibited in Figure 4.44(a), shows the leaching rate was facilitated by pH change from acidic to alkaline medium in the first active period of 30 to 40 days before the leachant was stabilized at about pH 8.82 until the day 127 concurrent leaching reaction reached a steady state. In contrast to 8045 terminal pH of DI was found higher than in HA with 9.5. Metal ions are immobilized by the C-S-H large surface area of about 100 to 700 m^2/g , by addition or substitution (Caijun and Roger, 2004). The C-S-H was not stable at pH below 10. Optimum pH to precipitate metal is about 10. Addition of

pozzolanic CSF in solidification of waste containing metal lower the pH of cement solution in an acidic medium which lead to leach of more heavy metals.

Pb has the highest leaching rate compare to other metals with 2.71 cm/day since it is one of the mobile metals. The high solubility of lead hydroxide of 20 mg/L (Grasso, 1993) has contributed to its mobility. Lead in the sample is from OPC binder as lead is ubiquitous in environment. Minimum Pb leaching in S/S leachate was found at pH 8 to 10. Lead is precipitated in solid form forming lead salt such as sulfate, oxide, hydroxide, carbonate and silicate. Pb^{2+} forming soluble nitrate, chlorate, acetate and slightly soluble chloride but Pb^{4+} only present in strong oxidizing condition.

Solidified sludge FA exhibited in Figure 4.45 has upward pH curve with pH 9.49 at the end of leaching period in HA solution while the reverse trend was found in DI solution reaching terminal pH of 7.37. The destabilized pH was due to the leached of rich minerals found in the FA specimen as detected by the EDAX analysis, which would lead to the pH change by the minerals inherited charges.

Similarly, the solidified sludge with AC5 illustrated in Figure 4.46 has an upward pH curve with terminal pH of 10.78 in acidic medium but stabilized pH 8.7 was observed in DI leachant. The H^+ ions have facilitated maximum leached rate of Cr, Mn, Ni and Zn. It was noted that Cu indicates minor leaching occurred on day 127.

The pH curves of solidified sludge with MK5 significantly align to a stabilized pH line in HA and DI leachants with the terminal pH of 8.72 and 8.66 respectively, assemblage at leaching period of 60 days onward. The stabilized pH has brought about the lowest reduction rate for most of the metals found in the specimen.

The leaching rate of solidified sludge with RHA has an upward trend with terminal pH of 10.75 and stabilized pH 8.71 for HA and DI accordingly. Cu was found to show minor leaching in the day 127 similar to solidified sludge with MK5 and AC5 samples. Cu was precipitated as $\text{Cu}(\text{OH})_2$ and lime availability help to precipitate Cu.

The effective diffusion coefficient for metals in both of HA and DI leachants at terminal leaching are tabulated in Table 4.16 based on Equation 2-8. The diffusion coefficients of most metals are smaller than lead, since lead was one of the volatiles metals. Referring to solidified sludge with CSF5, iron has the lowest diffusion coefficient 3.01×10^{-16} in acetic acid solution due to its low hydroxide solubility of 5×10^{-4} mg/L (Grasso, 1993). On the other end, Pb recorded the highest diffusion coefficient 2.19×10^{-07} as its hydroxide solubility was 20 mg/L (Grasso, 1993). The diffusion values are matched with metal hydroxide solubility diagrams of Fe^{3+} and Pb as shown in Figure 2.5.

Cadmium was not diffused at the terminal leaching since the leachate has closely reached minimum cadmium hydroxide solubility pH of 10.00 to 12.00, whereby the cadmium was bound in cement as $\text{Cd}(\text{OH})_2$ or carbonate. In the presence of carbonate ions, cadmium is 99 % speciated as solid carbonate at pH 8 to 11 and after pH 11, hydroxides are primarily formed (Conner, 1990). Cadmium hydroxide precipitates to provide sites for nucleation of hydrated cement products of C-S-H and portlandite (Mattus and Gilliam, 1994).

Table 4.16: Diffusion coefficient of metals leached in solidified OPC-sludge 8045 and OPC-sludge with CRMs in cm²/sec in day 127

| <i>Sample/</i> | | <i>Metals</i> | | | | | | | |
|-----------------|--------------------------|---------------|--------------------------|--------------------------|--------------------------|--------------------------|--------------------------|--------------------------|--------------------------|
| <i>Leachant</i> | <i>Al</i> | <i>Cd</i> | <i>Cr</i> | <i>Cu</i> | <i>Fe</i> | <i>Mn</i> | <i>Ni</i> | <i>Pb</i> | <i>Zn</i> |
| 8045 | | | | | | | | | |
| HA | 7.81 x 10 ⁻¹⁵ | - | - | - | - | 1.2 x 10 ⁻¹⁴ | - | 1.59 x 10 ⁻⁰⁷ | 1.08 x 10 ⁻¹² |
| DI | 3.71 x 10 ⁻¹³ | - | 2.54 x 10 ⁻¹² | - | 5.49 x 10 ⁻¹⁶ | - | - | 1.59 x 10 ⁻⁰⁷ | 1.19 x 10 ⁻¹³ |
| CSF5 | | | | | | | | | |
| HA | 6.77 x 10 ⁻¹⁴ | - | 3.11 x 10 ⁻¹⁰ | - | 3.01 x 10 ⁻¹⁶ | - | 5.96 x 10 ⁻¹⁰ | 2.19 x 10 ⁻⁰⁷ | 2.11 x 10 ⁻¹¹ |
| DI | 3.27 x 10 ⁻¹³ | - | 2.80 x 10 ⁻⁰⁹ | 6.70 x 10 ⁻¹² | 8.37 x 10 ⁻¹⁶ | - | - | 1.49 x 10 ⁻⁰⁸ | 2.51 x 10 ⁻¹¹ |
| FA5 | | | | | | | | | |
| HA | 1.91 x 10 ⁻¹³ | - | 1.04 x 10 ⁻¹⁰ | 5.37 x 10 ⁻¹¹ | 2.97 x 10 ⁻¹⁶ | - | 5.97 x 10 ⁻¹⁰ | 4.83 x 10 ⁻⁰⁸ | 7.79 x 10 ⁻¹³ |
| DI | - | - | 4.14 x 10 ⁻¹² | - | 2.97 x 10 ⁻¹⁶ | 1.97 x 10 ⁻¹⁴ | 2.39 x 10 ⁻⁹ | 3.36 x 10 ⁻¹⁰ | 6.31 x 10 ⁻¹¹ |
| AC5 | | | | | | | | | |
| HA | 8.64 x 10 ⁻¹² | - | 1.20 x 10 ⁻⁰⁹ | 3.59 x 10 ⁻¹⁰ | - | - | - | - | - |
| DI | 1.53 x 10 ⁻¹¹ | - | 3.72 x 10 ⁻¹² | 2.13 x 10 ⁻⁰⁹ | - | - | - | - | - |
| MK5 | | | | | | | | | |
| HA | 7.04 x 10 ⁻¹² | - | 1.34 x 10 ⁻¹¹ | 1.91 x 10 ⁻¹⁰ | - | - | - | - | - |
| DI | 1.18 x 10 ⁻¹¹ | - | 3.36 x 10 ⁻¹² | 1.43 x 10 ⁻⁰⁹ | - | - | - | - | - |
| RHA5 | | | | | | | | | |
| HA | 7.50 x 10 ⁻¹² | - | 8.60 x 10 ⁻¹⁰ | 2.10 x 10 ⁻¹⁰ | - | - | - | - | - |
| DI | 1.10 x 10 ⁻¹¹ | - | 3.40 x 10 ⁻¹² | 2.00 x 10 ⁻⁰⁹ | - | - | - | - | - |

The leachability index (Li) was calculated based on Equations 2-6 and 2-7 as shown in Table 4.17. All metals showed Li values are exceeding 6 as the guidance limit for S/S utilization (Morgan and Bostik, 1992) except for Pb in CSF5 and RHA5. Lead was found in larger quantity than its initial specimen values. The lead found in leachate may source from the solution medium. Based on the metals released in the leachate, solidified sludge has the capability for the final disposal in normal landfill by incorporation of 5 % weight of FA, AC or MK in the cement proportion.

Table 4.17: Leachability index for solidified OPC-sludge

| Specimen | Leachant | Leachability index for metal in solidified OPC-sludge | | | | | | | | |
|----------|----------|---|-------|------|-------|-------|-------|------|------|-------|
| | | Al | Cd | Cr | Cu | Fe | Mn | Ni | Pb | Zn |
| 8045 | HA | 13.17 | 11.74 | 8.59 | - | 15.00 | 10.62 | 8.26 | 6.45 | 9.49 |
| | DI | 10.63 | 12.80 | 8.60 | 9.95 | 14.58 | 12.58 | 9.08 | 6.54 | 10.19 |
| CSF5 | HA | 12.65 | 12.76 | 8.09 | - | 13.94 | 11.41 | 7.04 | 5.55 | 9.27 |
| | DI | 11.21 | 9.77 | 8.28 | 9.77 | 13.69 | 12.69 | 9.24 | 4.91 | 9.30 |
| FA5 | HA | 11.91 | 12.28 | 8.46 | 10.26 | 13.52 | 10.34 | 8.09 | 6.46 | 9.53 |
| | DI | 10.31 | 11.35 | 9.38 | 9.30 | 13.87 | 12.38 | 7.59 | 6.64 | 9.84 |
| AC5 | HA | 11.64 | 12.02 | 8.48 | 9.44 | 13.89 | 11.33 | 7.60 | 6.43 | 9.33 |
| | DI | 9.71 | 12.24 | 8.76 | 9.53 | 13.84 | 12.43 | 8.26 | 6.49 | 10.31 |
| MK5 | HA | 11.65 | 9.04 | 8.96 | 9.72 | 14.83 | 11.73 | 8.26 | 6.41 | 9.93 |
| | DI | 10.00 | 10.66 | 9.30 | 10.03 | 13.80 | 12.83 | 8.55 | 6.23 | 10.35 |
| RHA5 | HA | 11.62 | 13.28 | 8.35 | 9.68 | 14.88 | 12.41 | 7.56 | 5.80 | 10.34 |
| | DI | 11.05 | - | 8.69 | 9.47 | 14.56 | - | 7.97 | 5.84 | 11.61 |

The Li values below 10 indicate rapid diffusion and above 10 for very slow diffusion of the leached metals (Barth, et al., 1990). Pb, Cr and Ni have rapid diffusion in both DI and acidic medium. Al, Fe and Mn showed very slow diffusion with Li values above 10. HA metal's diffusion in decreasing Li values from slowest to the highest diffusion for the solidified samples were arranged as below:

8045: Fe > Al > Cd > Mn > Zn > Cr > Ni > Pb

CSF5: Fe > Cd > Al > Mn > Zn > Cr > Ni > Pb

FA5: Fe > Cd > Al > Mn > Cu > Zn > Cr > Ni > Pb

AC5: Fe > Cd > Al > Mn > Cu > Zn > Cr > Ni > Pb

MK5: Fe > Mn > Al > Zn > Cu > Cd > Cr > Ni > Pb

RHA5: Fe > Cd > Mn > Al > Zn > Cu > Cr > Ni > Pb

Front and tail of the *Li* orders has the same metal for all of the samples, which indicate the consistence diffusion for Fe and Pb.

The metal's cumulative fraction leached against square root of time from solidified sludge is illustrated in Figure 4.49 and solidified sludge with CRMs in Figures 4.50 to 4.54. The linear relationship of the cumulative fraction leached with the square root of times indicates the diffusion control leaching, which is true if at least 20 percent of the initial line remains linear. The control of leaching mechanism was determined by de Groot and van der Sloot model (1992). The control of leaching process was derived from the slope of the logarithm cumulative fraction leached, $\log(B_t)$ versus the logarithm of time, $\log(t)$ whereby if diffusion is considered as a dominant mechanism by following theoretical relationship as shown in Equation 4-17.

$$\text{Log}(B_t) = \frac{1}{2}\log(t) + \log\left[U_{max} \cdot d \cdot \sqrt{\left(\frac{D_e}{\pi}\right)}\right] \quad \text{Eq. (4-17)}$$

where

B_t = cumulative maximum release of contaminant in mg/m^3

D_e = effective diffusion coefficient in cm^2/s

T = contact time in s

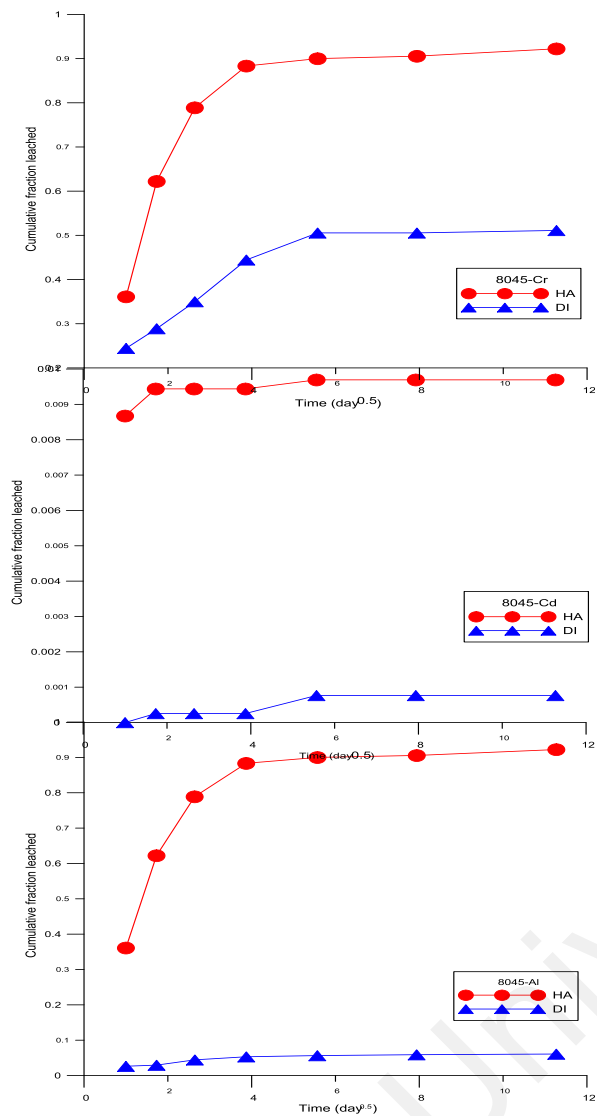
U_{max} = maximum leachable quantity in mg/kg

d = bulk density in kg/m^3

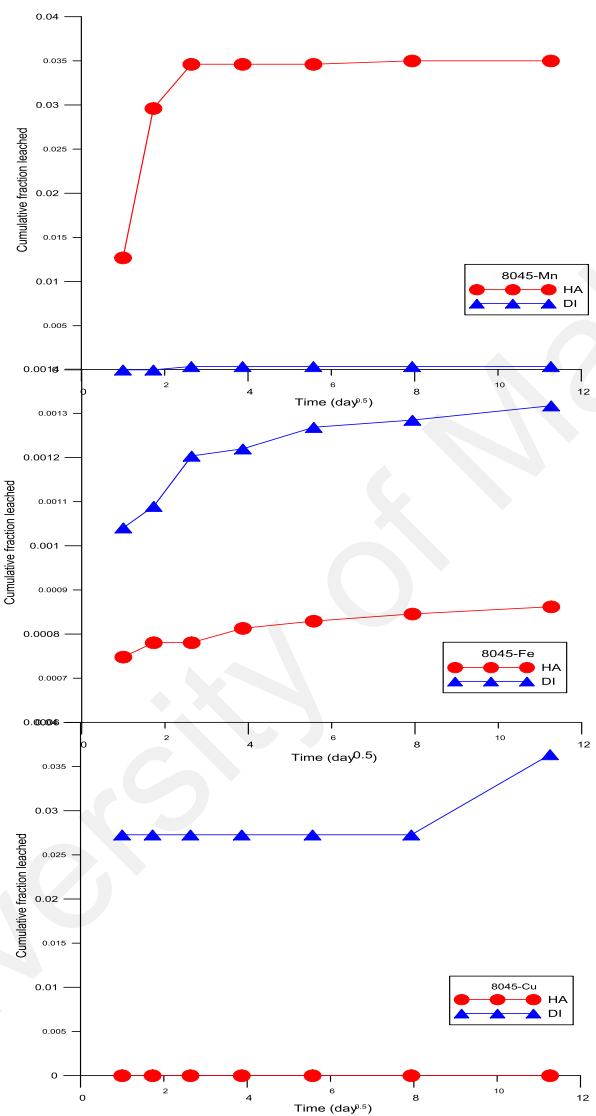
The model predicts that if the slope value is 0.5, the diffusion is controlling the leaching but if the value about 1.0, the contaminant was released by dissolution. Minimum slope approaching 0.0 indicates the surface wash-off are controlling leaching mechanism. The regression analysis of log cumulative fraction leached versus time is tabulated in Table 4.18.

The accumulated metal concentration against time shown in Figures 4.55 to 4.60 were plotted to indicate the saturated leachable metals in the sequential leaching was achieved otherwise increasing trend shows the potential for continuous leaching phenomena.

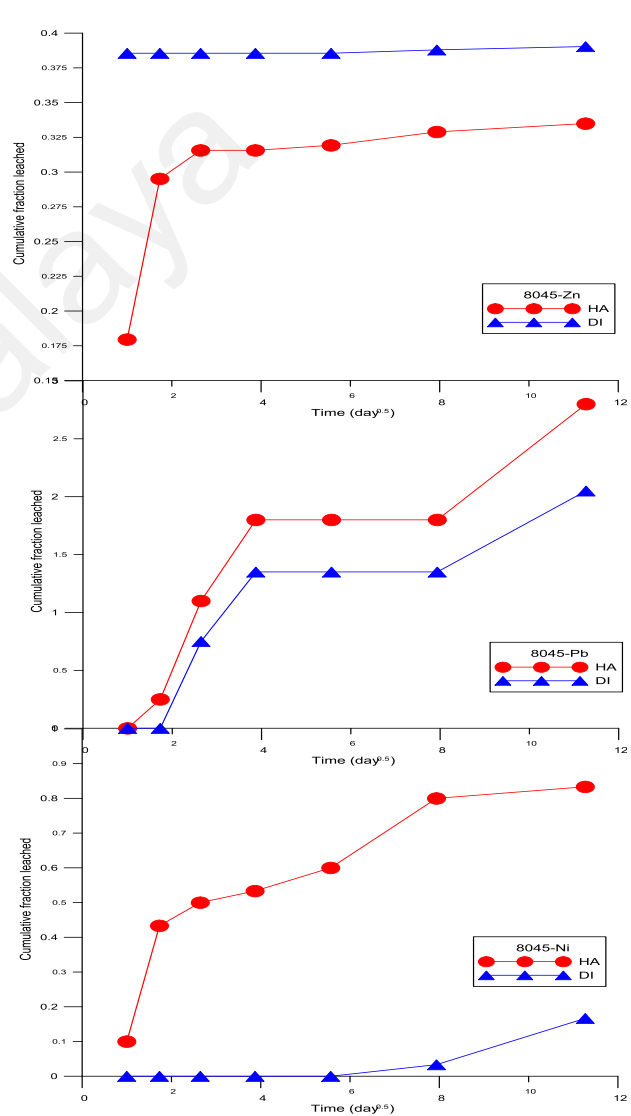
Leached layer containing metals will be dissolved in the leachant and buffer layer was formed at the surface front which coated the inner layer. In most of the leached specimen in HA leachant, the surface was overlaid by soft clear silica gel. The silica product in cement has reacted with oxygen from hydroxyl or acetate ions forming continuous chain of Si-O. Octahedral silica crystal with 54 picometer ionic radii and four positive charges can be covalently bonded to oxygen since oxygen has high electronegativity of 3.5 Pauling scale (Smart, 2002), besides adsorbed to Na, K and Ca as a Lewis base. The bond length of Si-O can be calculated by using additive of single covalent bond between these two elements. Since silica and oxygen single bond, covalent radii were 117 and 73 picometer (Smart, 2002), which formed 190 picometer of Si-O bond length.



(a) Al, Cd and Cr

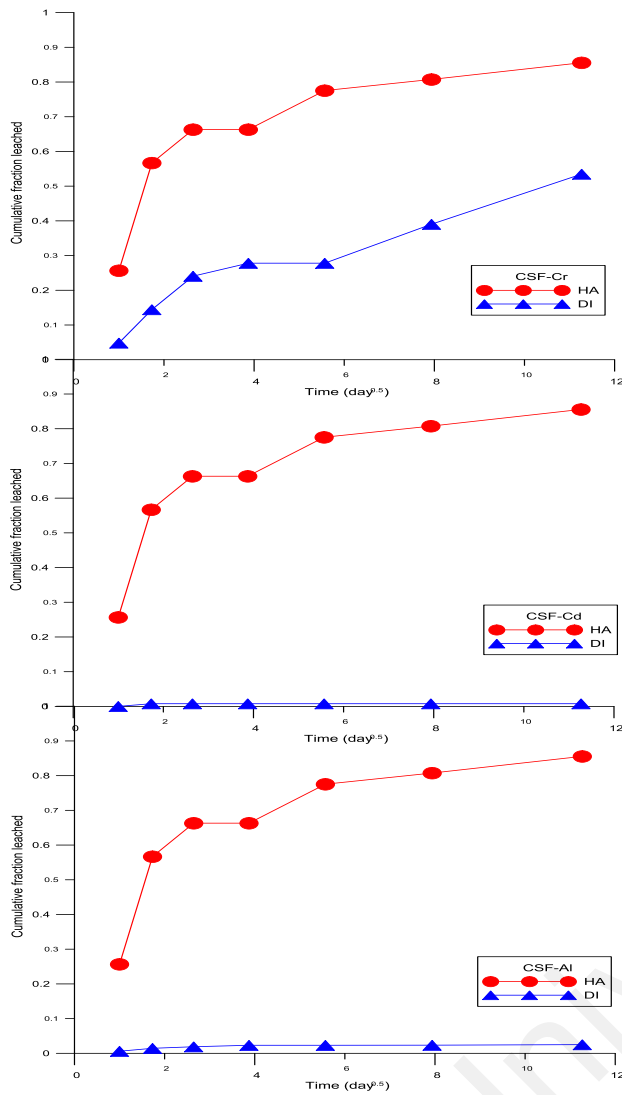


(b) Cu, Fe and Mn

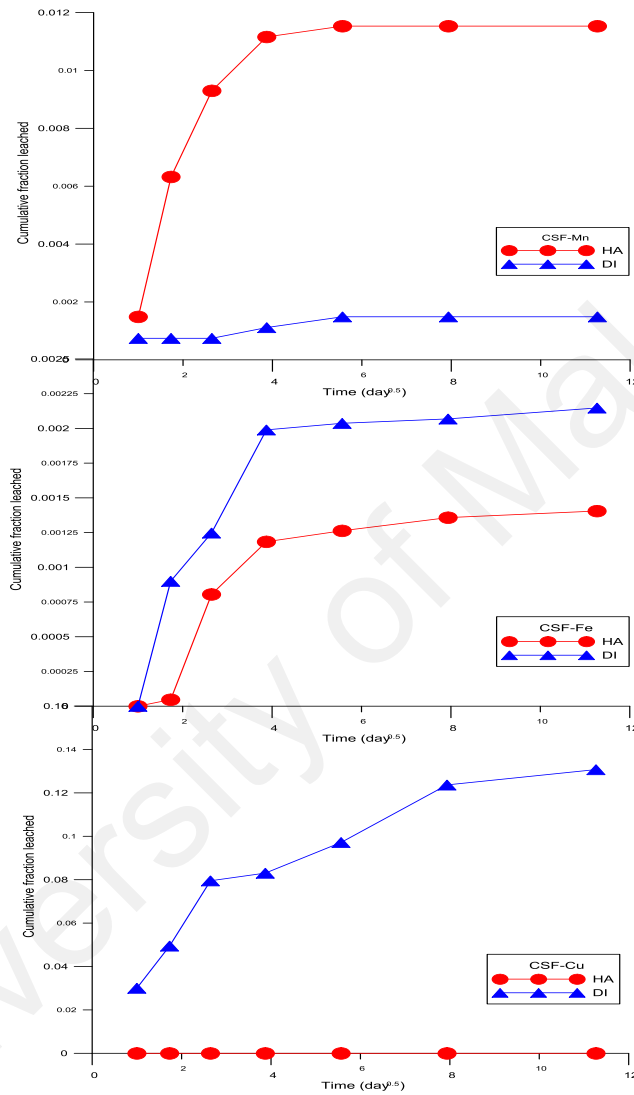


(c) Ni, Pb and Zn

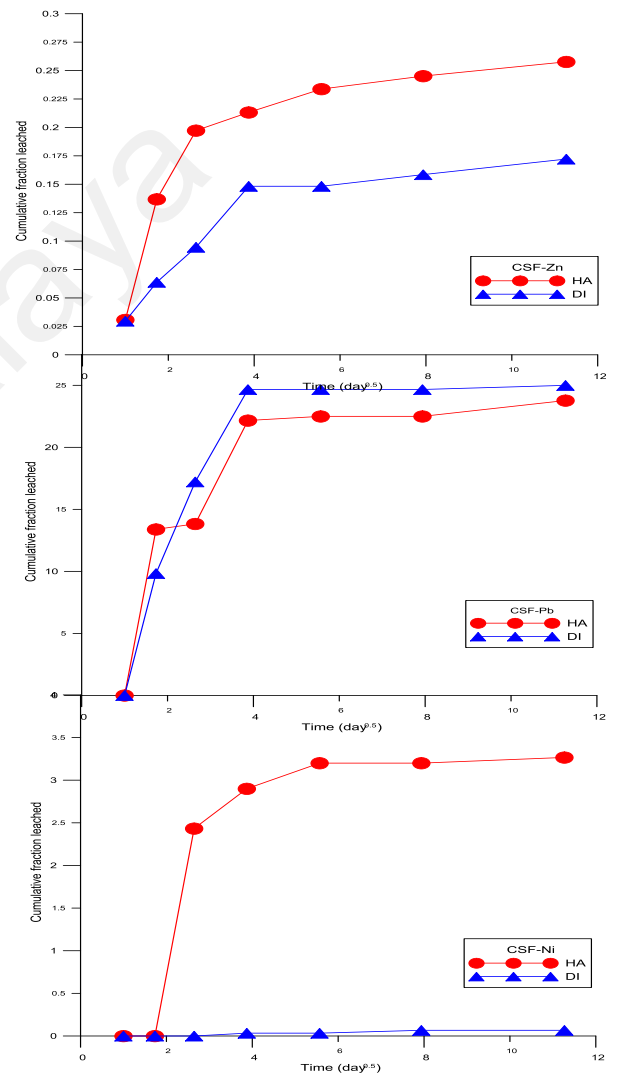
Figure 4.49: Cumulative fraction leached of metals in solidified sludge 8045 (a) Al, Cd and Cr (b) Cu, Fe and Mn (c) Ni, Pb and Zn



(a) Al, Cd and Cr

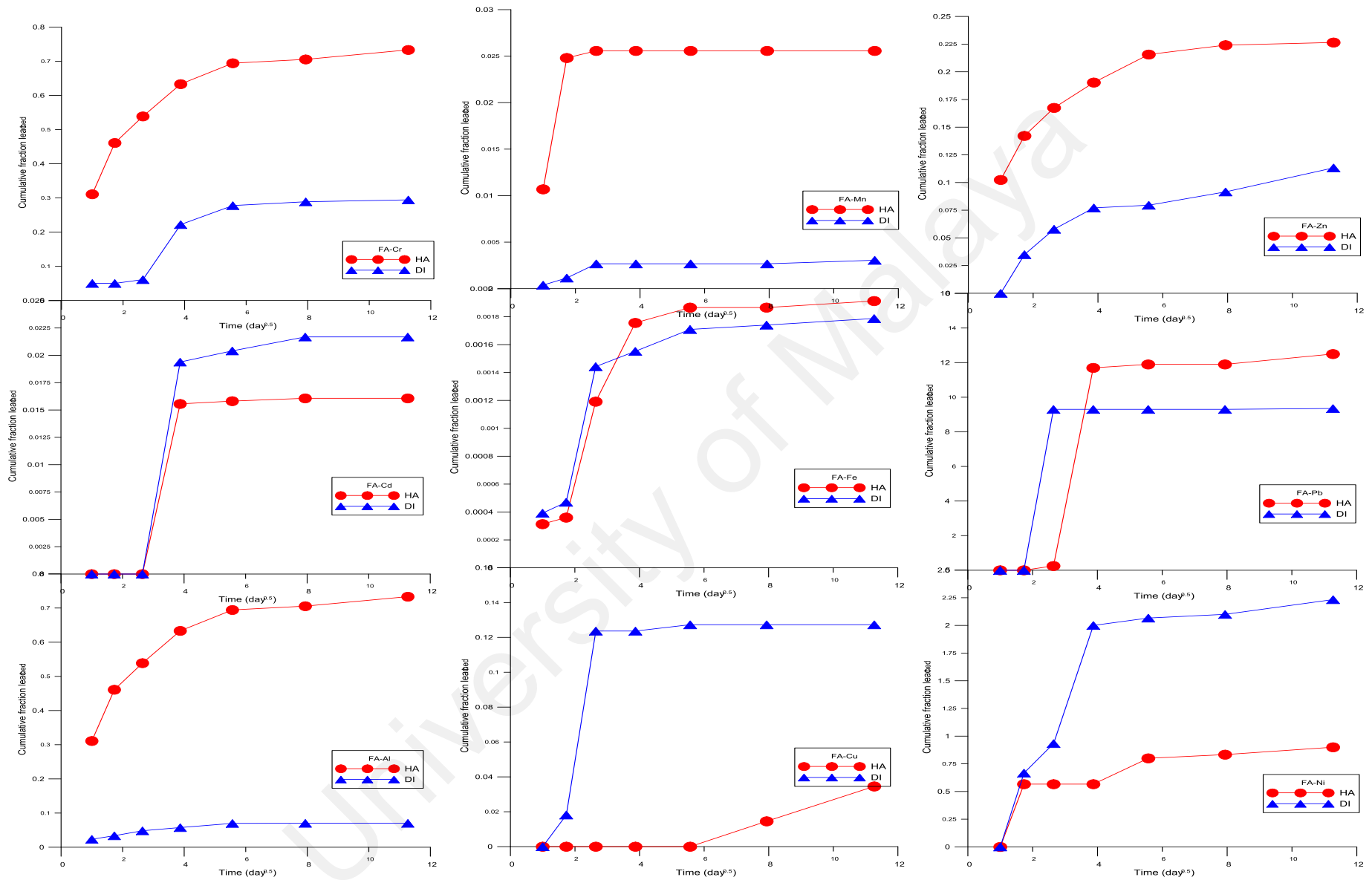


(b) Cu, Fe and Mn



(c) Ni, Pb and Zn

Figure 4.50: Cumulative fraction leached of metals in solidified-sludge CSF5 (a) Al, Cd and Cr (b) Cu, Fe and Mn (c) Ni, Pb and Zn

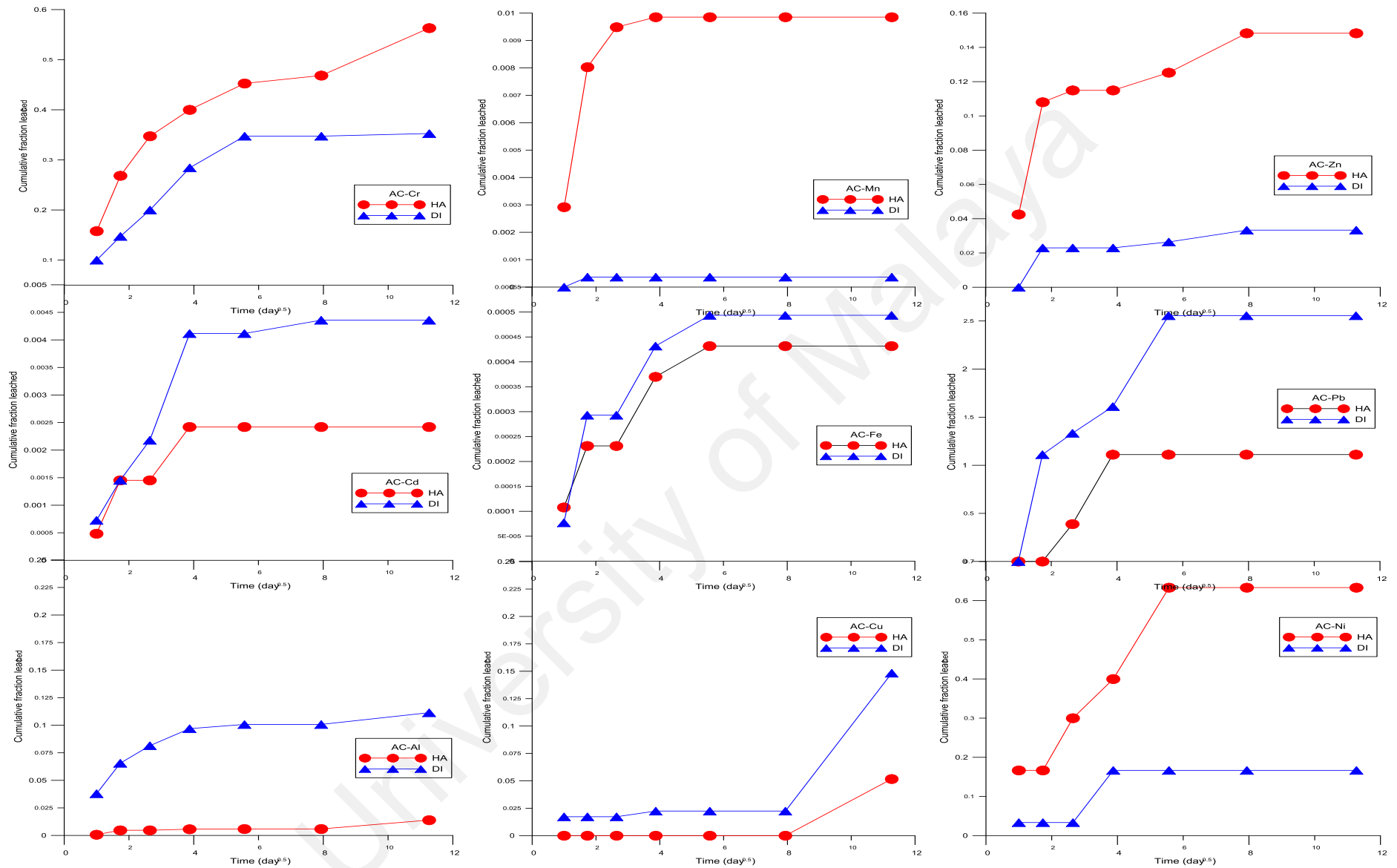


(a) Al, Cd and Cr

(b) Cu, Fe and Mn

(c) Ni, Pb and Zn

Figure 4.51: Cumulative fraction leached of metals in solidified sludge FA5 (a) Al, Cd and Cr (b) Cu, Fe and Mn (c) Ni, Pb and Zn

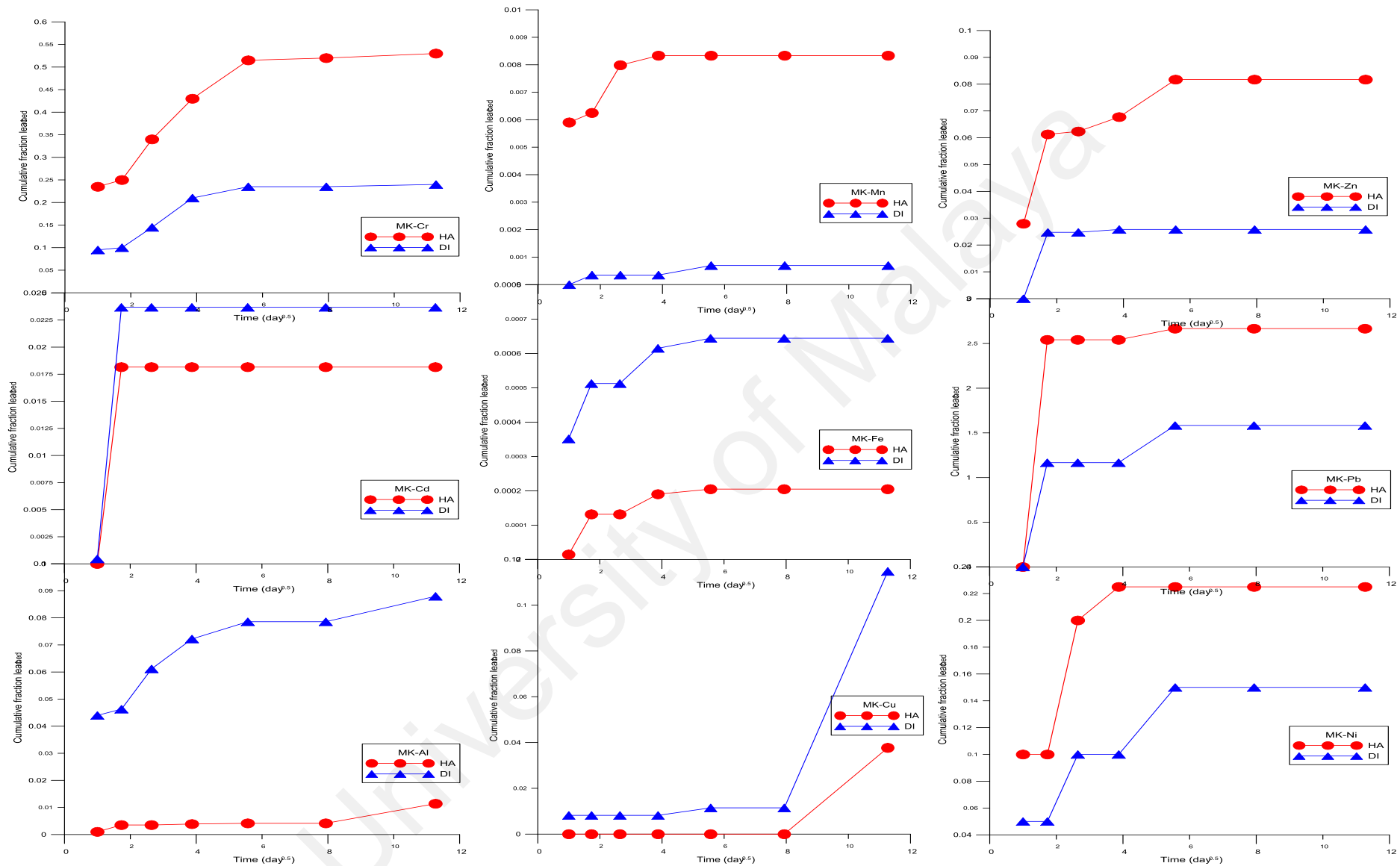


(a) Al, Cd and Cr

(b) Cu, Fe and Mn

(c) Ni, Pb and Zn

Figure 4.52: Cumulative fraction leached of metals in solidified sludge AC5 (a) Al, Cd and Cr (b) Cu, Fe and Mn (c) Ni, Pb and Zn

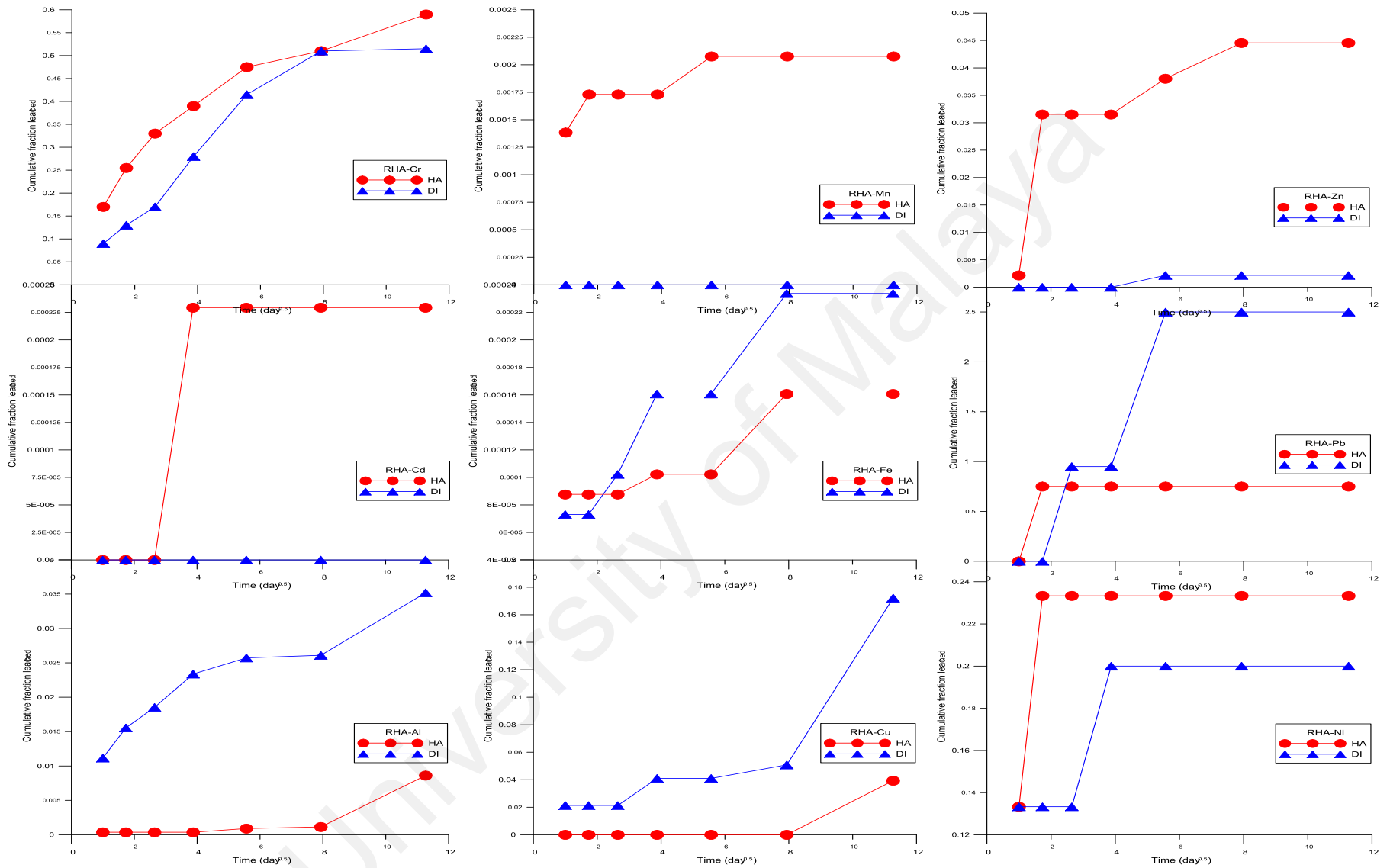


(a) Al, Cd and Cr

(b) Cu, Fe and Mn

(c) Ni, Pb and Zn

Figure 4.53: Cumulative fraction leached of metals in solidified sludge MK5 (a) Al, Cd and Cr (b) Cu, Fe and Mn (c) Ni, Pb and Zn

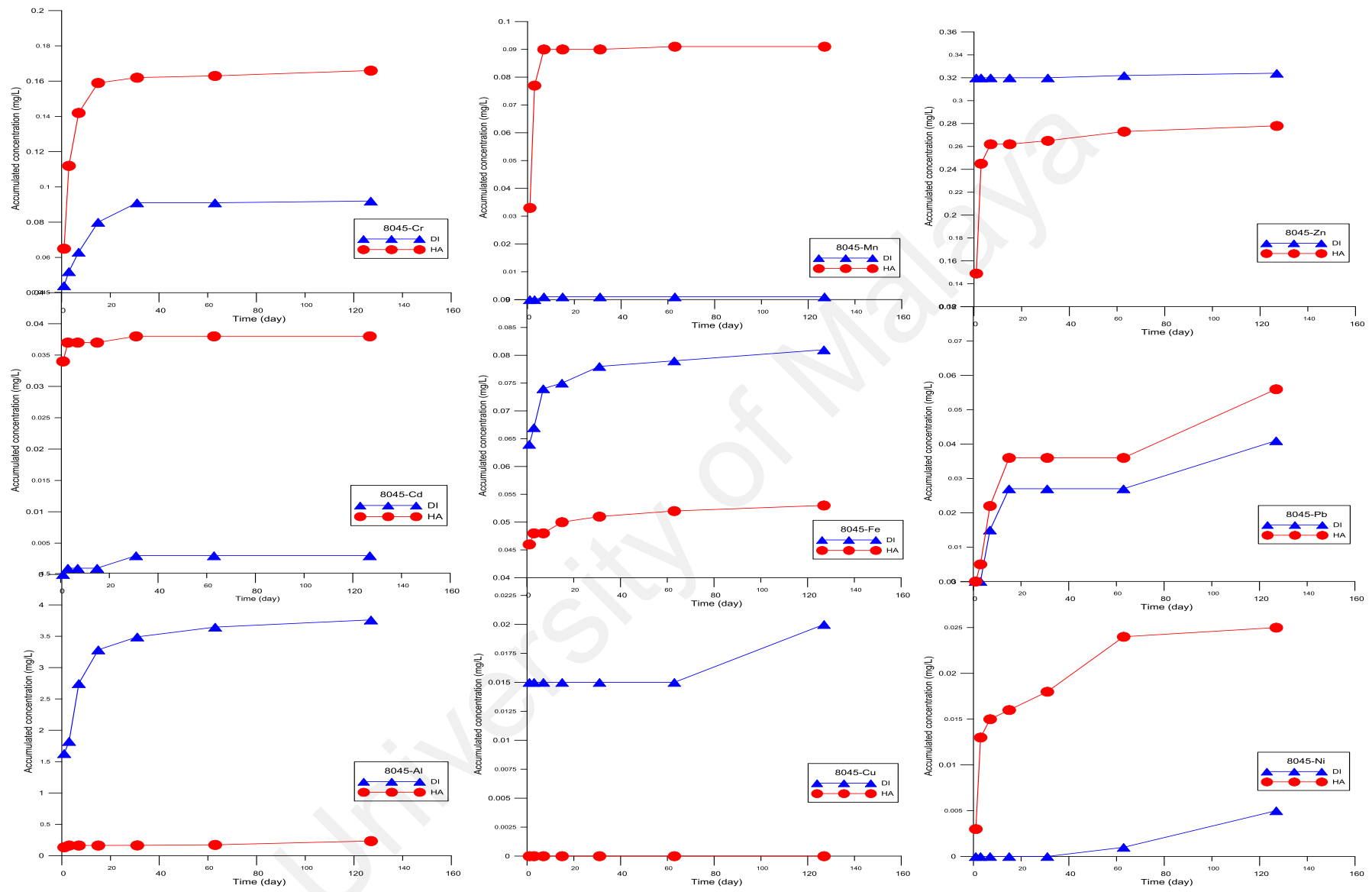


(a) Al, Cd and Cr

(b) Cu, Fe and Mn

(c) Ni, Pb and Zn

Figure 4.54: Cumulative fraction leached of metals in solidified sludge RHA5 (a) Al, Cd and Cr (b) Cu, Fe and Mn (c) Ni, Pb and Zn

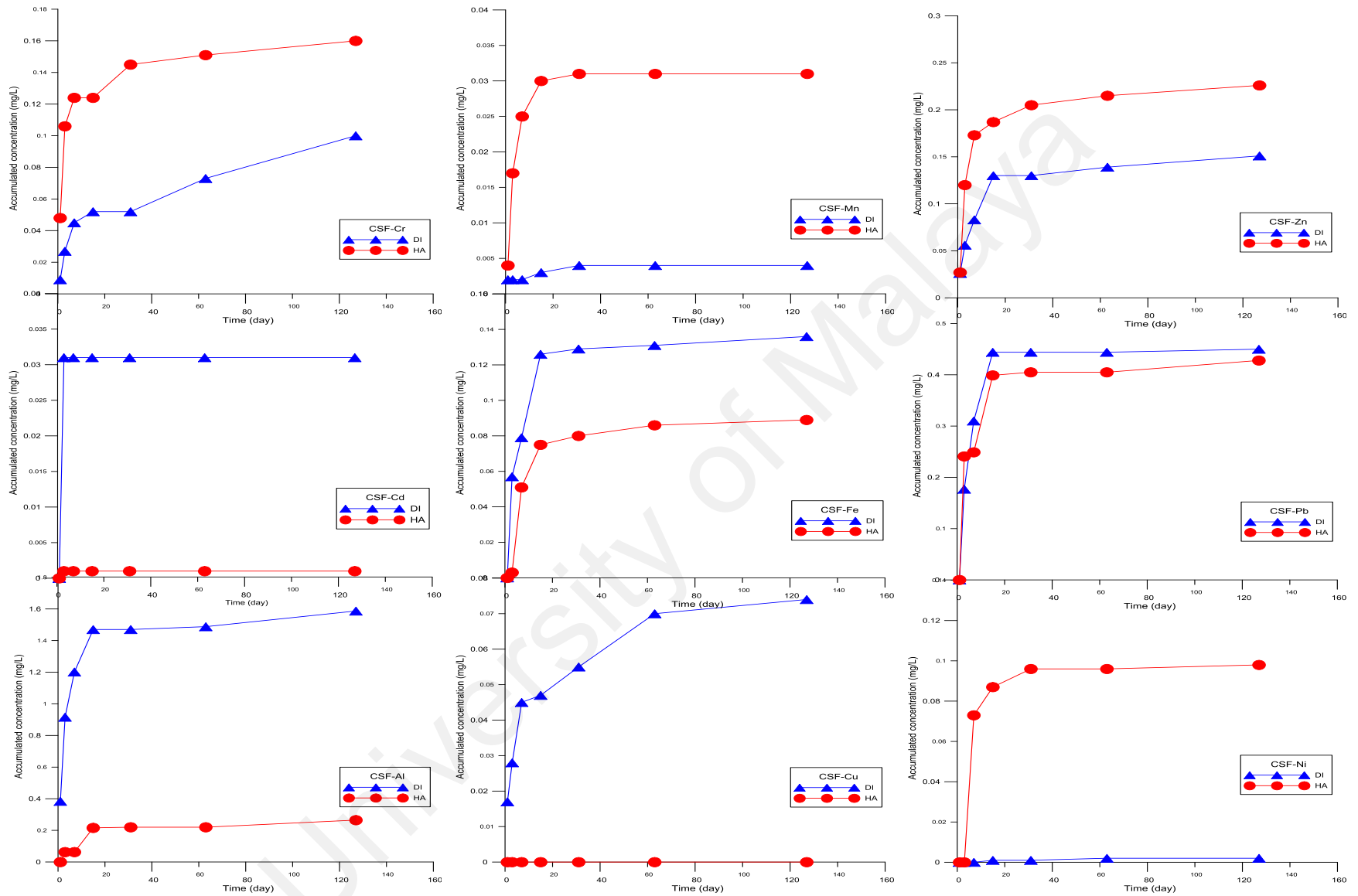


(a) Al, Cd and Cr

(b) Cu, Fe and Mn

(c) Ni, Pb and Zn

Figure 4.55: Accumulated leached metal concentration in solidified sludge 8045 (a) Al, Cd and Cr (b) Cu, Fe and Mn (c) Ni, Pb and Zn

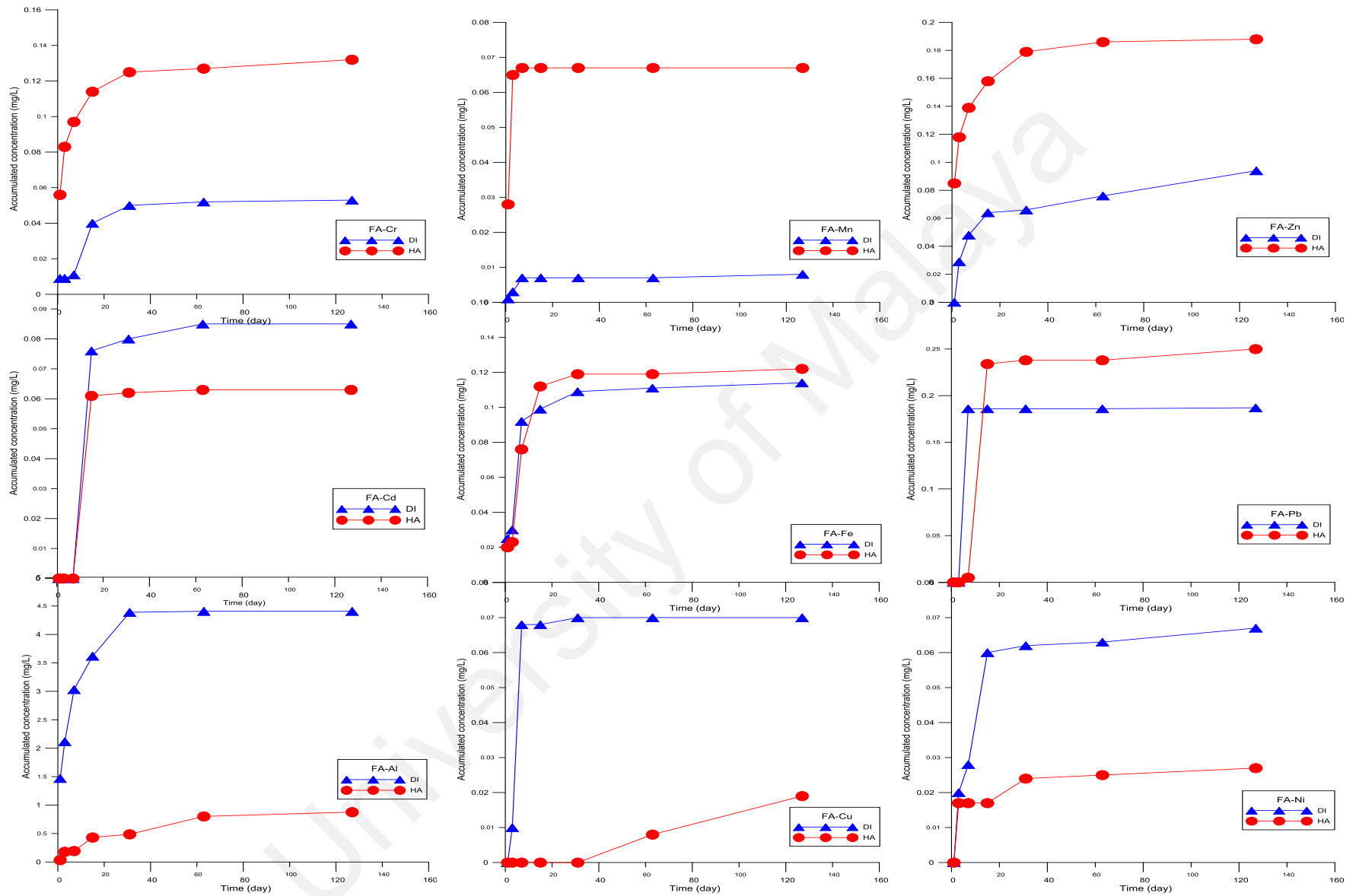


(a) Al, Cd and Cr

(b) Cu, Fe and Mn

(c) Ni, Pb and Zn

Figure 4.56: Accumulated leached metal concentration in solidified sludge CSF5 (a) Al, Cd and Cr (b) Cu, Fe and Mn (c) Ni, Pb and Zn



(a) Al, Cd and Cr

(b) Cu, Fe and Mn

(c) Ni, Pb and Zn

Figure 4.57: Accumulated leached metal concentration in solidified sludge FA5 (a) Al, Cd and Cr (b) Cu, Fe and Mn (c) Ni, Pb and Zn

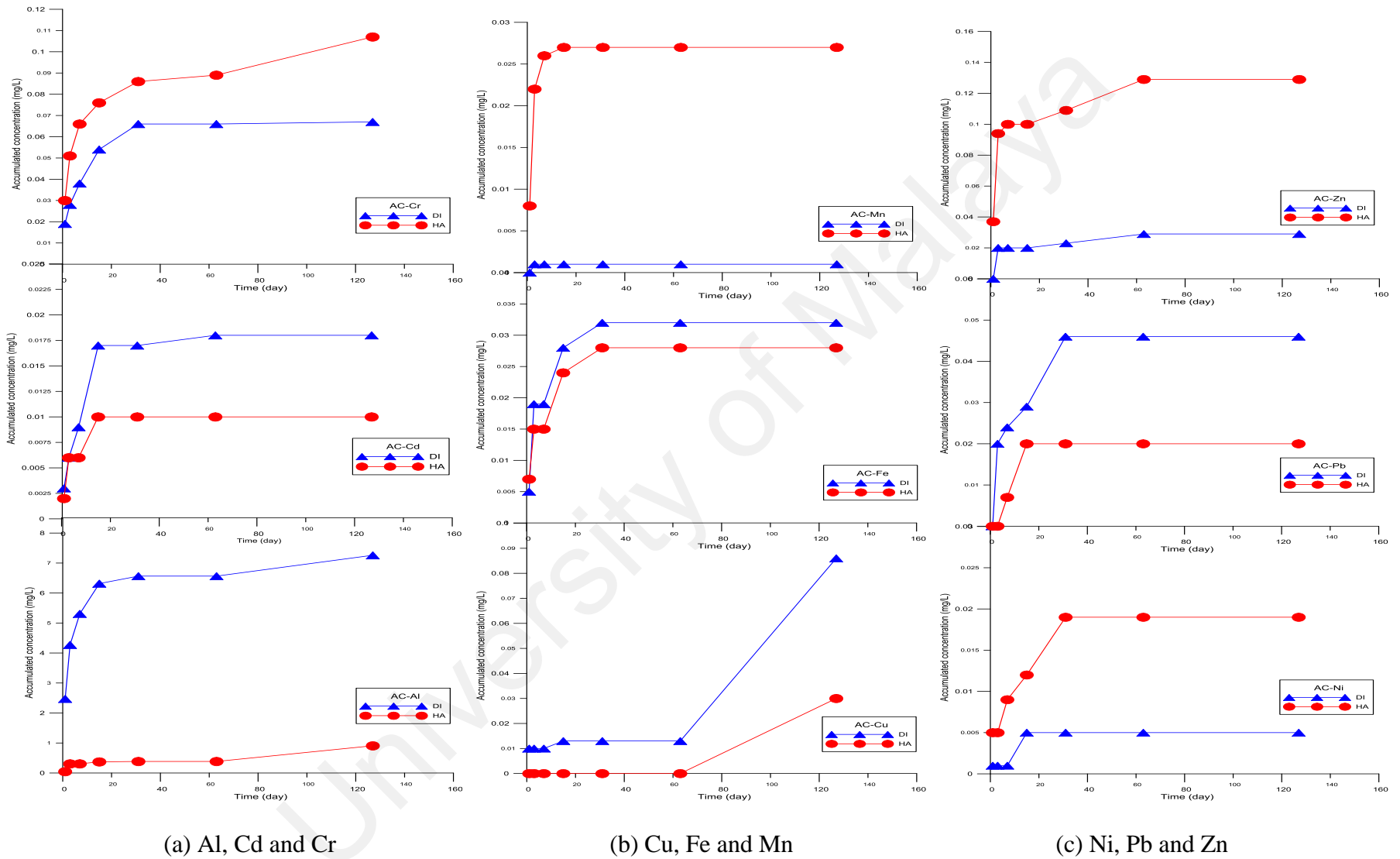
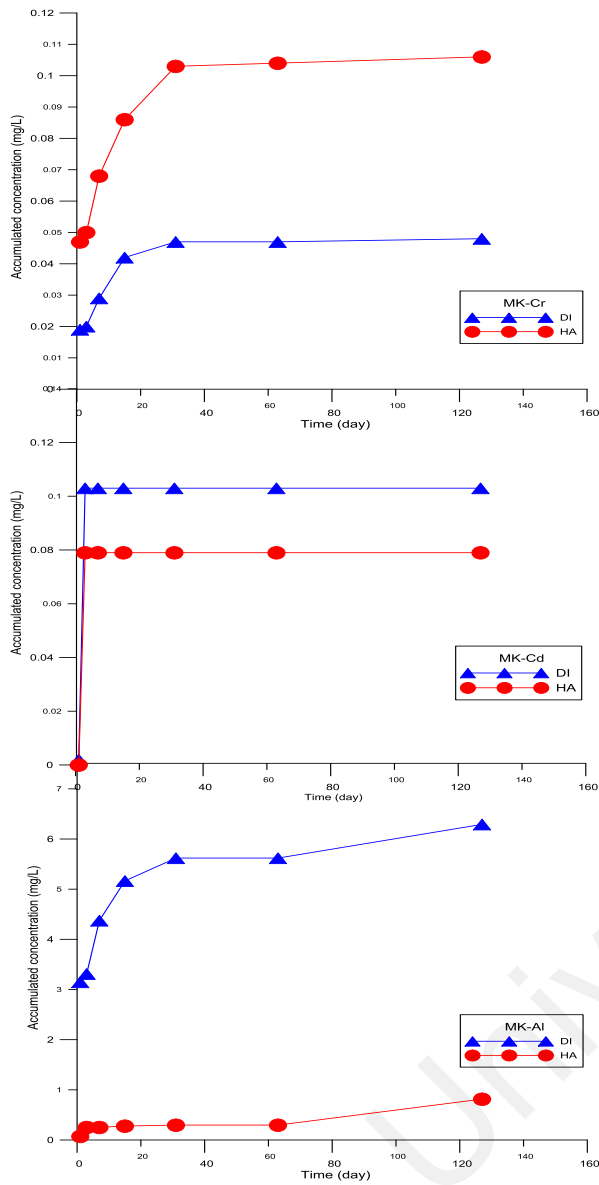
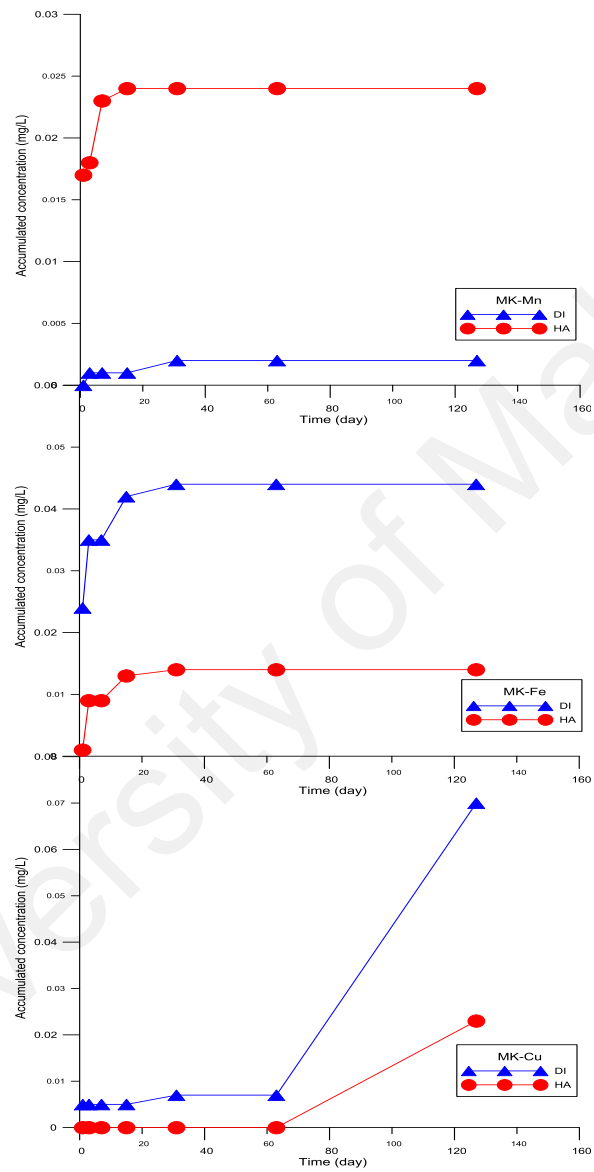


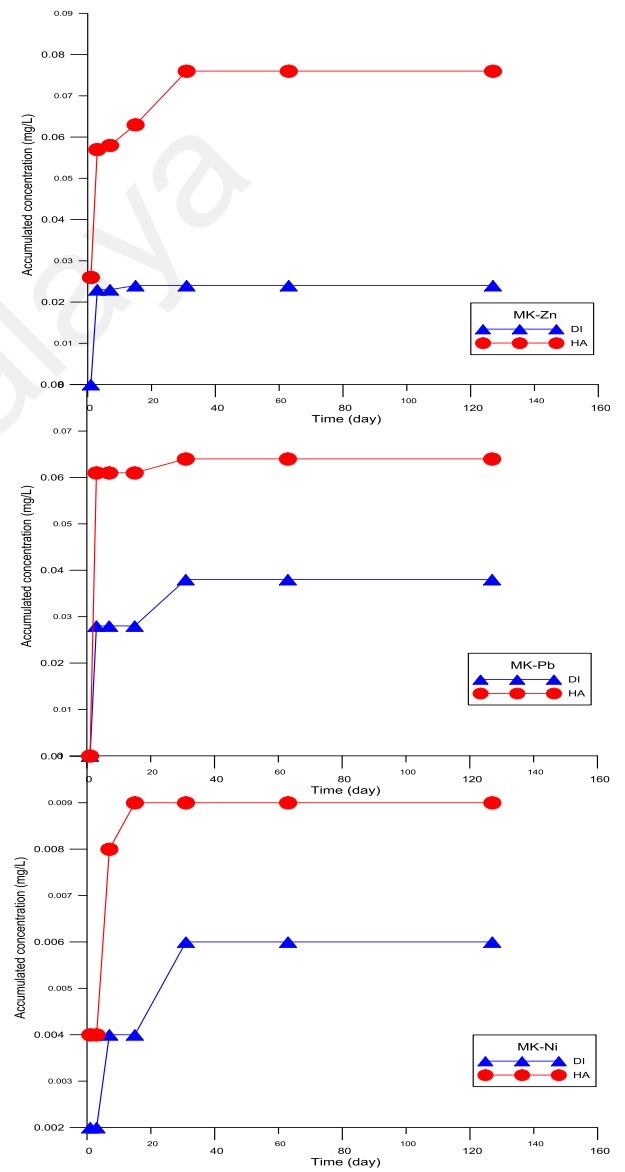
Figure 4.58: Accumulated leached metal concentration in solidified sludge AC5 (a) Al, Cd and Cr (b) Cu, Fe and Mn (c) Ni, Pb and Zn



(a) Al, Cd and Cr



(b) Cu, Fe and Mn



(c) Ni, Pb and Zn

Figure 4.59: Accumulated leached metal concentration in solidified sludge MK5 (a) Al, Cd and Cr (b) Cu, Fe and Mn (c) Ni, Pb and Zn

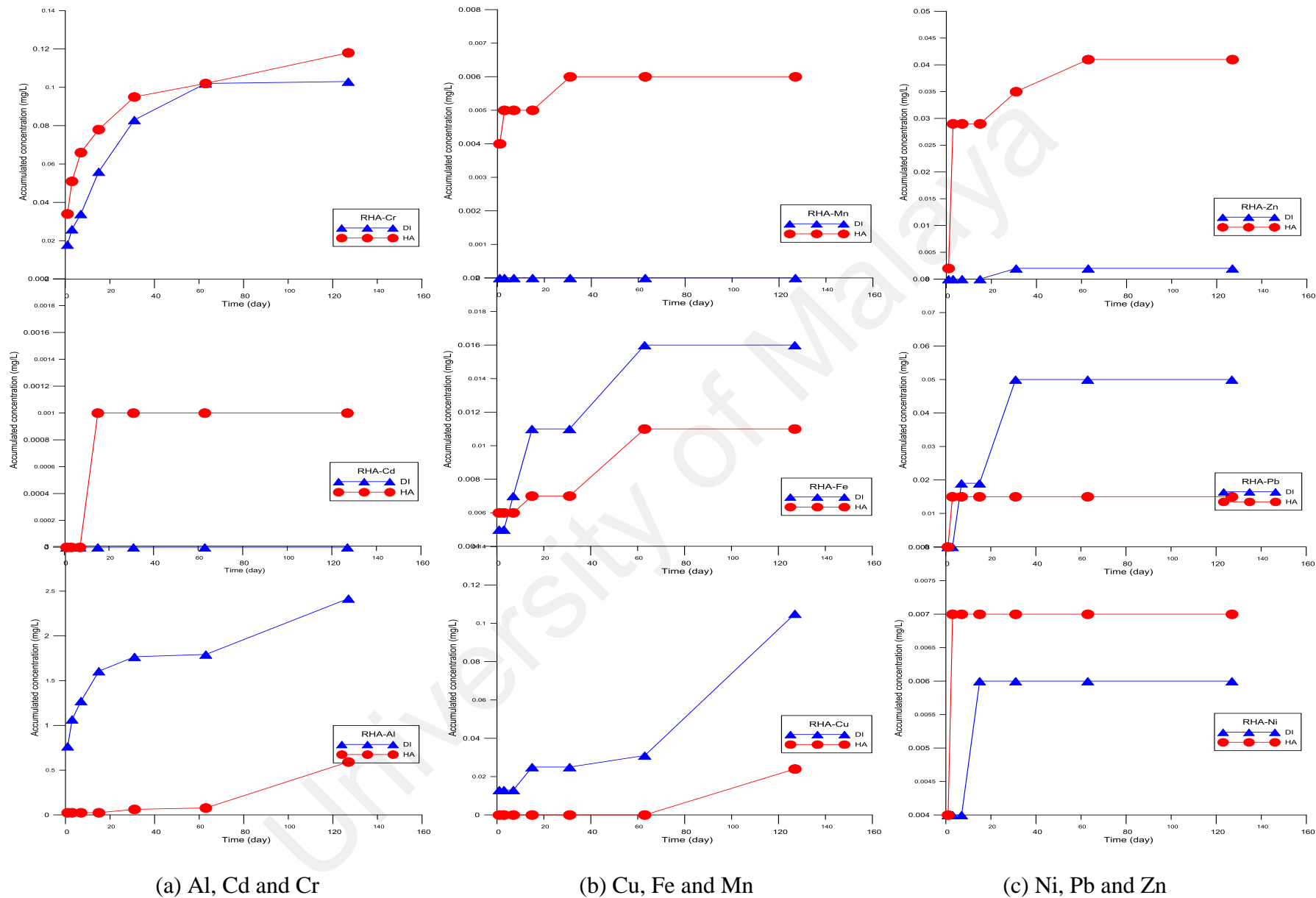


Figure 4.60: Accumulated leached metal concentration in solidified sludge RHA5 (a) Al, Cd and Cr (b) Cu, Fe and Mn (c) Ni, Pb and Zn

Table 4.18: Regression analysis of $\log(B_t)$ versus $\log(t)$ for metals released

| Metal | Leachant | Slope value (R^2) | | | | | |
|-------|----------|-----------------------|-------------|-------------|-------------|-------------|-------------|
| | | 8045 | CSF5 | FA5 | AC5 | MK5 | RHA5 |
| Al | HA | 0.06 (0.68) | 0.41 (0.77) | 0.53 (0.96) | 0.40 (0.82) | 0.31 (0.80) | 0.43 (0.55) |
| | DI | 0.16 (0.90) | 0.23 (0.85) | 0.20 (0.94) | 0.18 (0.92) | 0.13 (0.92) | 0.19 (0.98) |
| Cd | HA | 0.01(0.82) | * | 0.16 (0.89) | 0.27 (0.84) | * | * |
| | DI | 0.26 (0.68) | * | 0.03 (0.94) | 0.33 (0.91) | 0.56 (0.57) | - |
| Cr | HA | 0.15 (0.85) | 0.19 (0.86) | 0.15 (0.95) | 0.21 (0.97) | 0.16 (0.90) | 0.21 (0.99) |
| | DI | 0.14 (0.93) | 0.38 (0.95) | 0.38 (0.79) | 0.24 (0.94) | 0.19 (0.87) | 0.34 (0.95) |
| Cu | HA | - | - | 0.43 (1.00) | * | - | * |
| | DI | 0.02 (0.28) | 0.25 (0.97) | 0.34 (0.66) | 0.25 (0.41) | 0.29 (0.39) | 0.30 (0.69) |
| Fe | HA | 0.02 (0.96) | 0.72 (0.61) | 0.36 (0.82) | 0.24 (0.91) | 0.41 (0.74) | 0.11 (0.67) |
| | DI | 0.04 (0.95) | 0.18 (0.88) | 0.29 (0.81) | 0.30 (0.84) | 0.10 (0.88) | 0.23 (0.88) |
| Mn | HA | 0.15 (0.68) | 0.33 (0.78) | 0.12 (0.60) | 0.18 (0.69) | 0.07 (0.79) | 0.07 (0.89) |
| | DI | - | 0.15 (0.77) | 0.34 (0.80) | * | 0.17 (0.68) | - |
| Ni | HA | 0.32 (0.85) | 0.09 (0.80) | 0.14 (0.83) | 0.28 (0.88) | 0.16 (0.75) | 0.08 (0.57) |
| | DI | 0.80 (1.00) | 0.21 (0.70) | 0.26 (0.86) | 0.36 (0.71) | 0.22 (0.86) | 0.09 (0.71) |
| Pb | HA | 0.51 (0.76) | 0.16 (0.78) | 1.08 (0.54) | 0.29 (0.52) | 0.01 (0.76) | * |
| | DI | 0.19 (0.86) | 0.18 (0.83) | 0.00 (0.35) | 0.19 (0.88) | 0.07 (0.68) | 0.26 (0.73) |
| Zn | HA | 0.09 (0.73) | 0.33 (0.80) | 0.14 (0.97) | 0.19 (0.82) | 0.17 (0.84) | 0.44 (0.69) |
| | DI | - | 0.31 (0.93) | 0.22 (0.98) | 0.81 (0.69) | 0.01 (0.72) | * |

Note: - No leached metal was released
 *Single point leaching, no active leaching
 Mechanism of leaching: 0.0 - Wash-off, 0.5 - Diffusion, 1.0 - Dissolution

Regression analysis of log cumulative fraction leached, $\log(B_t)$ against log time, $\log(t)$ showed that most of the metals were released by surface wash-off and diffusion and rarely by dissolution. The slope value varied greatly in different binders due to the presence of multi minerals in each binder, which affect metal's speciation.

The percent reduction of metals under semi-dynamic leaching is tabulated in Table 4.19 to indicate the effectiveness of inorganic metal immobilization by solidified sludge with selected CRMs. The inclusion of CSF5 and FA5 in solidified sludge has the effect of releasing more lead than its initial concentration which was predicted from lead distribution in the sludge or binder itself. Other binder performances were acceptable and in overall the best inorganic binders was RHA5. Inorganic immobilization of AC5 and MK5 also perform

better than the solidified sludge 8045. In conclusion, the 5 % weight of CRMs for organic waste S/S was optimized by RHA5 in terms of metal immobilization, and next best option was to use AC5 or MK5.

Table 4.19: Percent reduction of solidified sludge with CRMs in semi-dynamic leaching

| <i>Metal</i> | <i>Leachant</i> | <i>Percent reduction (%)</i> | | | | | |
|--------------|-----------------|------------------------------|---------|--------|-------|-------|--------|
| | | 8045 | CSF5 | FA5 | AC5 | MK5 | RHA5 |
| Al | HA | 99.94 | 99.94 | 99.80 | 99.80 | 99.84 | 99.87 |
| | DI | 99.13 | 99.64 | 98.99 | 98.41 | 98.74 | 99.49 |
| Cd | HA | 99.86 | 99.89 | 99.77 | 99.96 | 99.74 | 99.99 |
| | DI | 99.99 | 99.99 | 99.69 | 99.94 | 99.66 | 100.00 |
| Cr | HA | 86.82 | 87.78 | 89.52 | 91.95 | 92.43 | 91.57 |
| | DI | 92.69 | 92.36 | 95.79 | 94.96 | 96.57 | 92.64 |
| Cu | HA | 100.00 | 100.00 | 99.51 | 99.26 | 99.46 | 99.44 |
| | DI | 99.48 | 98.13 | 98.18 | 97.88 | 98.36 | 97.54 |
| Fe | HA | 99.99 | 99.98 | 99.97 | 99.99 | 99.99 | 99.99 |
| | DI | 99.99 | 99.97 | 99.97 | 99.99 | 99.99 | 99.99 |
| Mn | HA | 99.95 | 99.83 | 99.63 | 99.86 | 99.88 | 99.97 |
| | DI | 99.99 | 99.98 | 99.95 | 99.99 | 99.99 | 100.00 |
| Ni | HA | 88.09 | 53.33 | 87.14 | 90.95 | 96.78 | 99.67 |
| | DI | 97.62 | 99.05 | 68.09 | 97.62 | 97.86 | 97.14 |
| Pb | HA | 60.00 | -257.14 | -78.57 | 84.13 | 61.90 | 89.28 |
| | DI | 70.71 | -239.68 | -33.57 | 63.49 | 77.38 | 64.28 |
| Zn | HA | 95.21 | 96.32 | 96.76 | 97.88 | 98.83 | 99.36 |
| | DI | 94.42 | 97.54 | 98.38 | 99.52 | 99.63 | 99.97 |
| Ave | HA | 92.20 | 53.32 | 77.06 | 95.97 | 94.32 | 97.68 |
| | DI | 94.89 | 60.77 | 80.61 | 94.88 | 96.46 | 94.56 |

4.4.3.5 Conclusions of leachability study

The salient points of solidified sludge leachability study can be summarized as follows:

1. Simulated metal in the solidified sludge was successfully immobilized with minimum leaching was found in Cr. Similarly, oil and grease was immobilized with more than 98 % reduction.

2. Solidified sludge showed minimum metals leached in TCLP extract with higher W/C of 0.5 recorded lowest leaching values. No Cu was found in the leachate for all samples of W/C ratios. pH of the leachate was in the range of 11.22 to 12.25.
3. Solidified sludge with CRMs indicates minimum leachability of metals. No Al and Cu were leached out from CSF, FA and AC samples. MK also showed no Cu but highest Al was found in the leachant. CRMs incorporation has increased the pH value 0.25 to 0.5 unit higher than solidified sludge.
4. Semi-dynamic leaching study indicates the leaching rate curve of most metal signifies the diffusion leaching. The leaching dynamic of metal diffusion was under the pH control. Leaching achieved equilibrium at pH about 9.5 where acetate ions were dominating the solution and hydronium ion already depleted in reducing redox potential.
5. Leachability index for most metals in solidified sludge CRMs were found to be above 6 for S/S utilization limit except CSF5 and RHA5.
6. Based on the slope of log cumulative fraction leached versus log time, most metals were leached by wash-off (slope = 0.0) or diffusion mechanisms (slope = 0.5).
7. Fe formed slowest diffusion value, and Pb has highest diffusion value for all solidified sludge CRMs.
8. RHA5 performed the best average metal reduction in an acidic medium with 97.68 % which AC5 or MK5 formed the next-best option for organic sludge S/S.
9. The TCLP and semi-dynamic metals leachate were found below the regulated TCLP standard.

4.4.4 Microstructure of solidified sludge

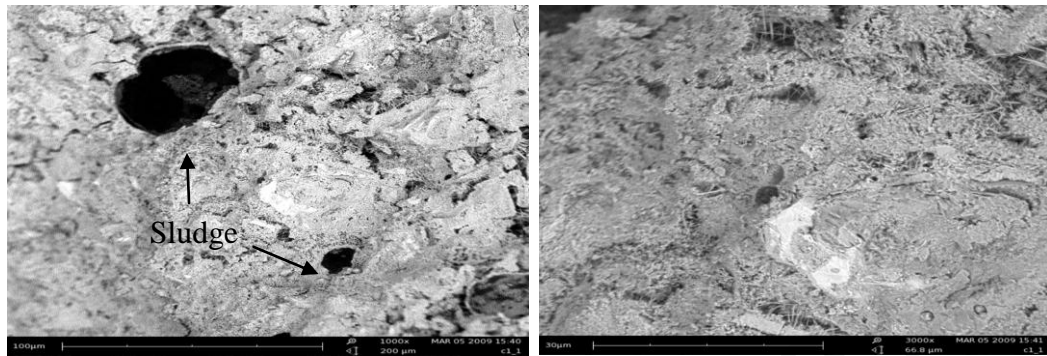
Microstructure details defined the intrinsic characters of solidified sludge in influencing the strength and leachability of solidified waste material. The integrity of stabilized/solidified waste is governed by the microstructure property. Revealing these microscopic views provides underlying factors that effect to the performance and durability of solidified waste.

4.4.4.1 SEM of solidified sludge, metal and RHA

Photomicrographs define surface morphology factors that contribute to performance of the solidified matrix, e.g. hydration products, physical properties like porosity and permeability, which influence its final strength and leachability. Figure 4.61 illustrates the photomicrographs of baseline study of solidified OPC-sludge. The sludge was physically encapsulated and bounded to cement hydration product as represented by intense dark shaded. The UCS of the solidified waste cement is 13.86 N/mm^2 . The images depicted in Figure 4.61, Figure 4.62 and Figure 4.63 were captured by PHENOM SEM based on the field view of moisture dry fractured samples after the maturity period of 28-day.

Higher strength gained in solidified petroleum sludge was due to the more homogenous surface of hydrated cement products of 14.83 N/mm^2 shown in Figure 4.61. Photomicrographs of solidified OPC-sludge containing spiked metals depicted in Figure 4.62 resemble platy layers of metal hydroxide enveloped sludge granule. Pore spaces in between the metal hydroxide are also observed. The UCS of OPC-sludge with metals was slightly higher than OPC-sludge at 19.93 N/mm^2 . Addition of 25 % RHA in the OPC-sludge with metal improves the surface area of the solidified cement since RHA acts as

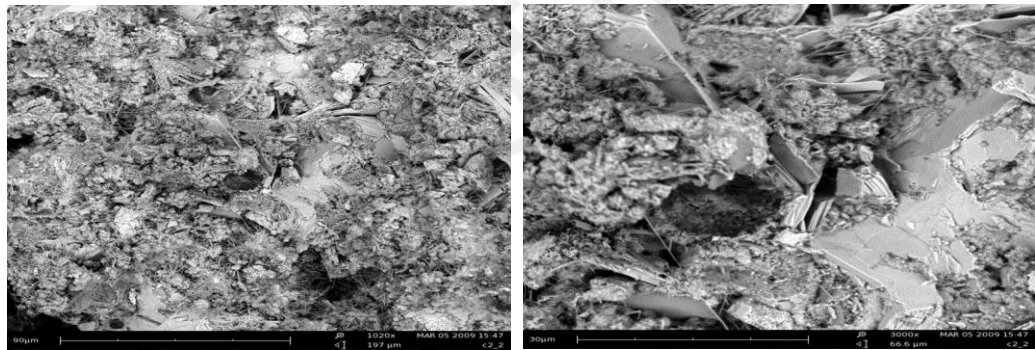
filler as shown by photomicrographs in Figure 4.63 but the strength was slightly reduced compared to solidified sludge as in Figure 4.61 at 13.32 N/mm^2 .



(a) 1000x

(b) 3000x

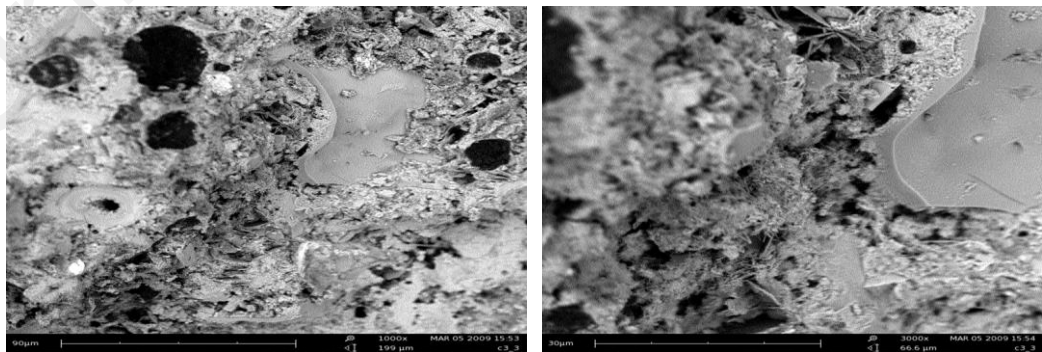
Figure 4.61: Photomicrographs of OPC-sludge at (a) 1000x and (b) 3000x



(a) 1000x

(b) 3000x

Figure 4.62: Photomicrographs of OPC-sludge with metals at (a) 1000x and (b) 3000x

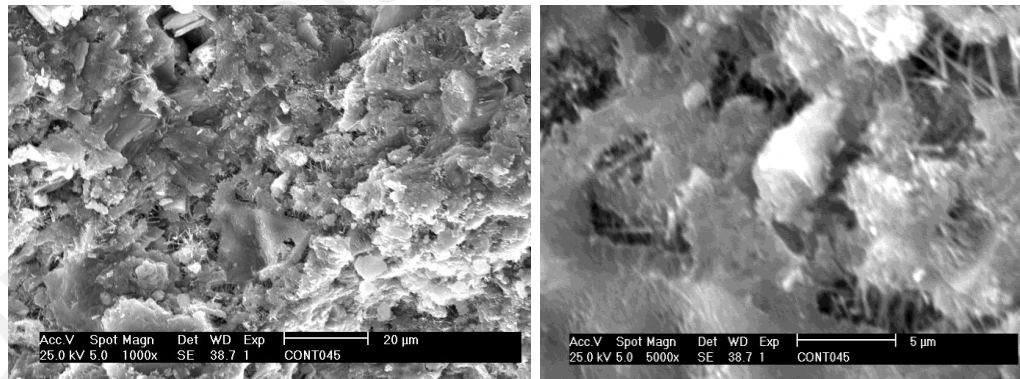


(a) 1000x

(b) 3000x

Figure 4.63: Photomicrographs of OPC-sludge metals and RHA at (a) 1000x and (b) 3000x

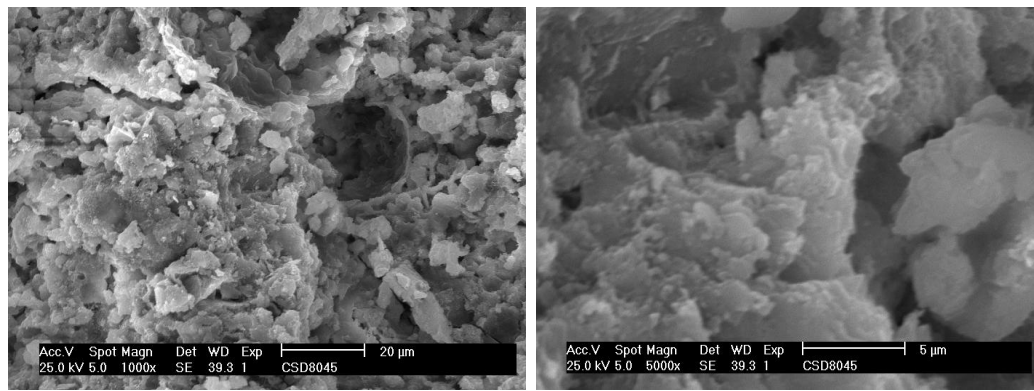
Solidified control OPC at water to cement of 0.45 is depicted by the photomicrograph in Figure 4.64. The close-up view of the solidified OPC photomicrograph in Figure 4.64 (b), ettringite in form of needle shape development was found in the spaces between cement C-S-H gel and cement clinker. OPC-sludge at water to cement of 0.45 and cement to sludge of 8 are depicted by Figure 4.65. The surface solidified OPC-sludge was more compacted, and the sludge has a lubricating effect to the cement particles make it more interconnected with fewer void spaces. The hydrated cement was found in form of C-S-H gel. Obviously, no ettringite was observed in the cement hydration products. The sludge appearance was insignificant since it was well absorbed by the cement C-S-H gel surface as compared to baseline study. Both solidified OPC and OPC-sludge images shown in Figures 4.64 and 4.65 were captured on the gold-coated fractured samples after its maturity period of 28-day.



(a) 1000x

(b) 5000x

Figure 4.64: Photomicrograph of control OPC at W/C of 0.45 (a) 1000x and (b) 5000x



(a) 1000x

(b) 5000x

Figure 4.65: Photomicrograph of solidified OPC-sludge 8045 at (a) 1000x and (b) 5000x

In conclusion, the spike metals in baseline study showed that the metals can enhance the strength of solidified sludge, which permits the mixed of metal with organic waste to be solidified by OPC. Solidified OPC has exhibited the ettringite and C-S-H as the main products of cement hydration. However, sludge inclusion has changed the cement surface with lubricating effect of oily waste to the cement hydration products which formed more interconnected C-S-H with lack of ettringite and fewer voids.

4.4.4.2 FESEM of solidified sludge with CRMs

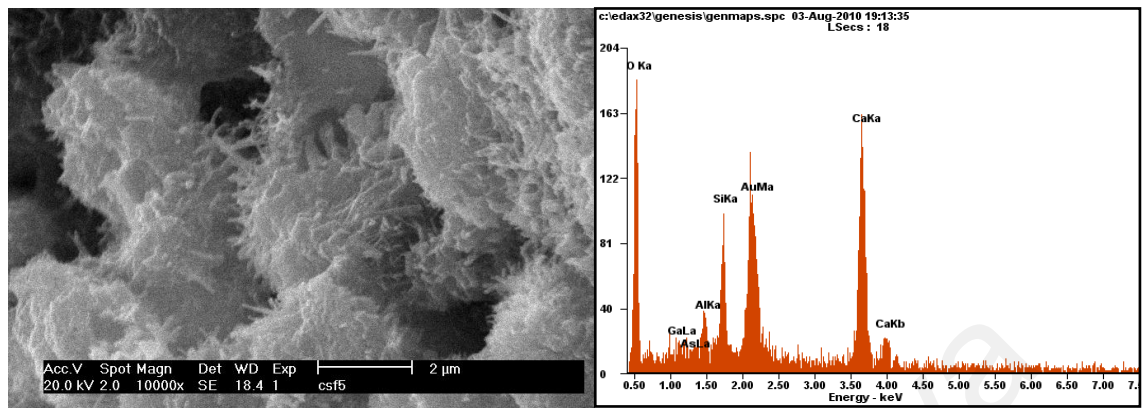
Solidified sludge with 5 % weight each of CSF, FA, RHA, MK, and AC are represented in Figure 4.66(a) to (e). All photomicrographs of OPC-sludge with 5 % CRMs were captured at 10,000 times. The elemental analysis of solidified sludge by FESEM EDAX was tabulated in Table 4.20 including the control sample. The main element in the solidified sludge was calcium distributed in cement product of CH, C-S-H and ettringite. The CRMs incorporation has reduced the calcium concurrently with the increased in carbon, which normally formed calcite. FA constituted the highest carbon content from it

mineral and sludge. Silica content was slightly reduced with the inclusion of waste or CRMs compared to the solidified OPC alone.

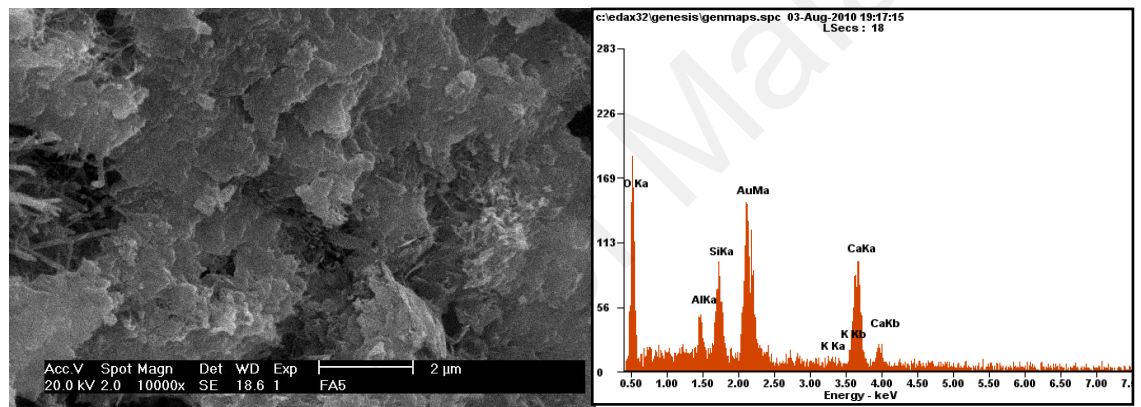
Most of the hydrated products of solidified OPC-sludge have indicated less ettringite distribution except CSF. AC OPC has finer surface and amorphous as organic carbon absorption was magnified by its high surface area. Solidified OPC-sludge containing MK has more voids on the surface compared to other samples. In contrast to other binders, MK contains aluminium that reacts with CH and silicate produced alumina phase and C-S-H. MK addition of up to 30 % acts as accelerating agent that displaced small pores (Ambroise, et al., 1994).

Hydration of MK in cement was measured by the amount of calcium presents by taking into considering the weight loss due to dehydroxylation of Ca(OH)_2 and decomposition of CaCO_3 (Frias and Cabrera, 2000). They found that Ca(OH)_2 increases in the MK cement until age 7 days which due to OPC hydration while the decrease in values after the age is related to the pozzolanic reaction of MK. Grain refinement in MK cement was due to lacks of large portlandite crystal that able to reduce the porosity.

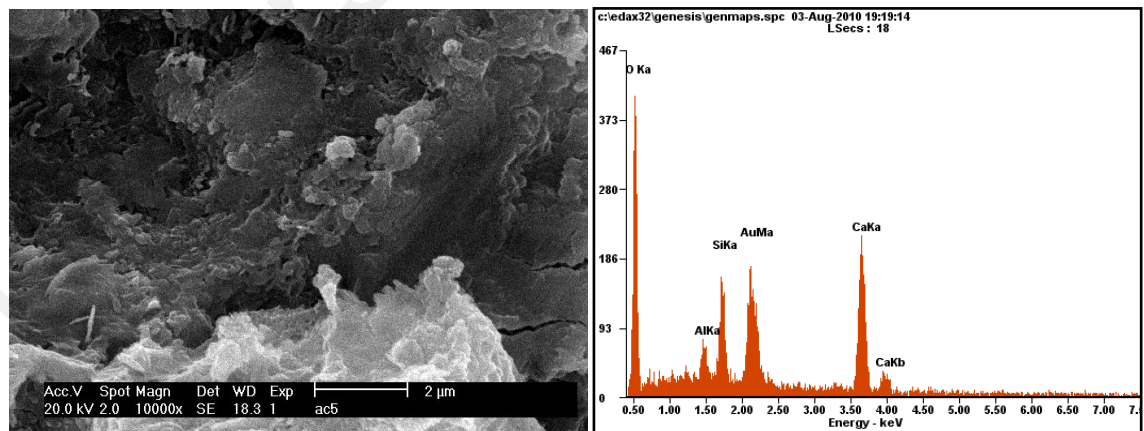
The incorporation of FA has the effect of water reducing capability, and it retards the set of cement hydration whereas CSF can retard the cement hydration due to excessive silica content even though it can increase water requirement similar like RHA. In fact, RHA has high adsorption energy as well as MK to absorb moisture or organics, which accelerate hydration mentioned in section 4.4.3 for fresh cement properties. Adsorption energy in CSF was quite high but the preference in adsorption more toward the CH than organics contaminant. In general, the mineral admixture has advantages of removing CH formation, increase densification and durability, reduce bleeding and increase ultimate strength.



(a) CSF



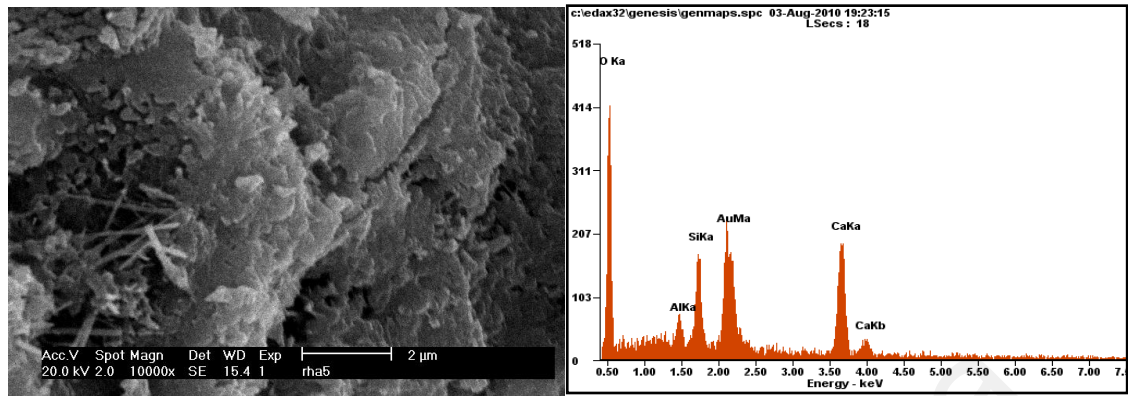
(b) FA



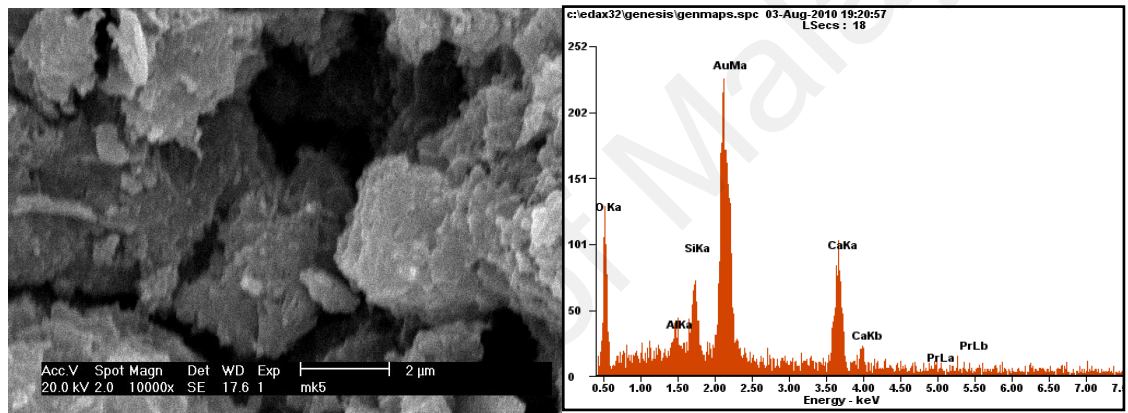
(c) AC

Figure 4.66: Photomicrographs of OPC-sludge with CRMs and EDAX elemental analysis

(a) CSF (b) FA (c) AC (d) RHA and (e) MK



(d) RHA



(e) MK

Figure 4.66: Photomicrographs of OPC-sludge with CRMs and EDAX elemental analysis

(a) CSF (b) FA (c) AC (d) RHA and (e) MK (continued)

Table 4.20: Elemental analysis of solidified sludge with 5 % weight CRMs

| Element | Percent of constituent in solidified sludge with CRMs (%) | | | | | | |
|---------|---|-------|-------|-------|-------|-------|-------|
| | C045 | C8045 | CSF5 | FA5 | AC5 | MK5 | RHA5 |
| C | 9.51 | 10.50 | 16.06 | 36.93 | 13.11 | 18.38 | 19.63 |
| O | 33.26 | 24.37 | 31.63 | 25.78 | 40.59 | 24.25 | 37.95 |
| Ga | 0.50 | 1.03 | 0.93 | 0.00 | 0.00 | 0.00 | 0.00 |
| As | 0.86 | 0.99 | 0.00 | 0.00 | 0.00 | 0.00 | 0.00 |
| Al | 2.52 | 1.59 | 2.00 | 2.30 | 2.54 | 2.57 | 1.62 |
| Si | 10.45 | 8.75 | 7.67 | 7.44 | 8.15 | 7.74 | 8.10 |
| Ca | 42.91 | 52.78 | 41.71 | 25.75 | 35.61 | 29.70 | 32.70 |
| K | 0.00 | 0.00 | 0.00 | 1.79 | 0.00 | 0.00 | 0.00 |
| N | 0.00 | 0.00 | 0.00 | 0.00 | 0.00 | 5.61 | 0.00 |
| Pr | 0.00 | 0.00 | 0.00 | 0.00 | 0.00 | 11.74 | 0.00 |

Based on the FESEM images and the elemental analysis made to the solidified sludge, CRMs incorporation has reduced the calcium concurrent to the rise in carbon content. This was due to the carbonation that occurred with the presence of hydrocarbon in the sludge. Pozzolanic reaction has resulted in consumption of silica that was slightly lower than the solidified OPC. The inclusion of CSF in solidified sludge, provide abundant silica that formed ettringite surface. Finer surface of solidified sludge observed with AC due to large surface areas of AC that enhance waste absorption. MK showed more voids on the surface due to platy MK layer while FA and RHA were dominantly formed by amorphous surface of C-S-H with a little ettringite needle.

4.4.4.3 X-Ray diffraction of solidified sludge

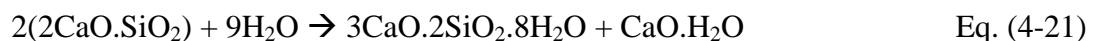
The crystallization in solidified sludge was identified based on the reference library of Siemens D-5000 XRD. The solidified sludge with the CRMs X-ray diffractograms are represented in Figure 4.67(a) Control OPC (b) OPC-sludge (c) OPC-sludge CSF (d) OPC-sludge FA (e) OPC-sludge AC (f) OPC-sludge MK and (g) OPC-sludge RHA. Solidified

samples constituted of amorphous surface of C-S-H and mineral of calcite, portlandite, and calcium silicate hydrate. While ettringite peaks are less pronounced as a dominance peak since, ettringite formation was reduced during hydration progressive as in Figure 4.17. Crystallization of minerals in solidified OPC diffractogram shown in Figure 4.65(a) is almost similar to OPC-sludge diffractogram in Figure 4.65(b) since the sludge mainly contains hydrocarbon and insignificant metal.

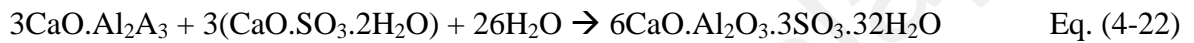
Calcite mineral was well distributed as determined by 2θ at 29.4° , 39.5° , 43.2° , 47.5° and 48.9° in solidified samples in formed of rhombohedron crystal. Calcite crystal was formed by carbonation of C-S-H and Ca(OH)_2 reactions with CO_2 as shown by Equation 4-18 and 4-19 (Cocke and Mollah, 1992). Carbonation is a slow post-hydration process that reduced pH of pore fluid to about 8.3 where all available alkali hydroxides have reacted (Perera, et al., 2003).



Portlandite can be found at 2θ of 18.0° , 34.2° , 47.1° and 50.8° . Portlandite was formed together with amorphous C-S-H based on the following two reactions shown in Equation 4-20 and 4-21. Portlandite and C-S-H distributions were reduced due to the carbonation reaction forming CaCO_3 .

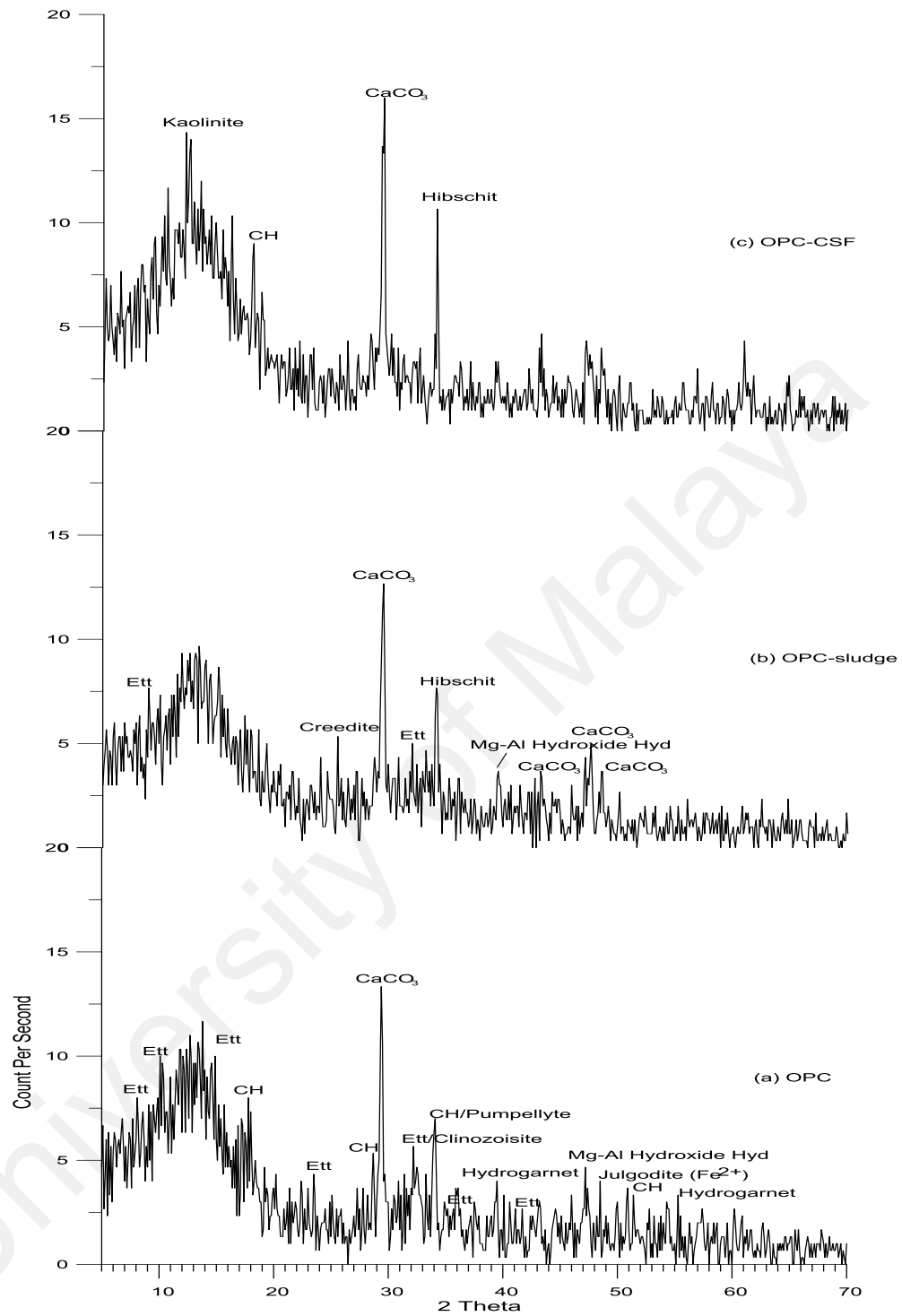


A small peak of ettringite can be found at 9.2°, 11.0°, 23.1°, 32.0° and 32.2°. The reaction of tricalcium aluminate with gypsum formed the ettringite crystal as in Equation 4-22. The ettringite is then reacted with tricalcium aluminate to form calcium mono sulfoaluminate as represented by Equation 4-23, which explained the reduction of ettringite. The hydrogarnet crystal, $\text{Ca}_3\text{Al}_{1.2}\text{Fe}_{0.8}\text{SiO}_{12}\text{H}_8$ was only found in solidified OPC at 40.1° and 55.3°. Kaolinite mineral was observed in MK OPC-sludge and CSF OPC-sludge at 12.5° and 12.7°.



Complex metal minerals such as monoclinic creedite, $\text{Ca}_3\text{Al}_2(\text{OH})_{10}\text{SO}_4(\text{H}_2\text{O})_2$ was observed at 2θ of 12.2° in FA OPC-sludge and 25.5° in OPC-sludge. Other minerals sparingly formed in solidified structure consist of cubic hibschit, $(\text{Ca}_{2.472}\text{Fe}_{528})(\text{Al}_{1.94}\text{FeO}_6)\text{Si}_2.829\text{O}_{11.316}(\text{OH})_{684}$ at 34.1° found in all CRMs OPC-sludge; monoclinic pumpellyte, $\text{Ca}_2\text{FeAl}_2(\text{SiO}_4)(\text{Si}_2\text{O}_7)(\text{OH})_2 \cdot \text{H}_2\text{O}$ at 34.0° in OPC and 36.0° in MK OPC-sludge and RHA OPC-sludge; and monoclinic epidote, $\text{Ca}_2(\text{Al}_2\text{Fe})\text{Si}_2\text{O}_7\text{SiO}_4(\text{OH})$ at 48.7° in FA OPC-sludge.

Monoclinic minerals of clinozoisite, $\text{Ca}_2(\text{Al}_{2.98}\text{Fe} \cdot \text{O}_2)\text{Si}_3\text{O}_{12}(\text{OH})$ and Julgodite, $\text{Ca}_2(\text{FeAl})_3(\text{SiO}_4)(\text{Si}_2\text{O}_7)(\text{OH})_2 \cdot \text{H}_2\text{O}$ found in OPC are observed at 32.2° and 48.5° accordingly. Magnesium aluminium hydroxide hydrates only observed in OPC and OPC-sludge but not present in any CRMs OPC-sludge.



Note: Ett-ettringite, CH-Ca(OH)₂

Figure 4.67: Diffractograms of solidified (a) OPC (b) OPC-sludge (c) OPC-CSF (d) OPC-FA (e) OPC-AC (f) OPC-MK and (g) OPC-RHA

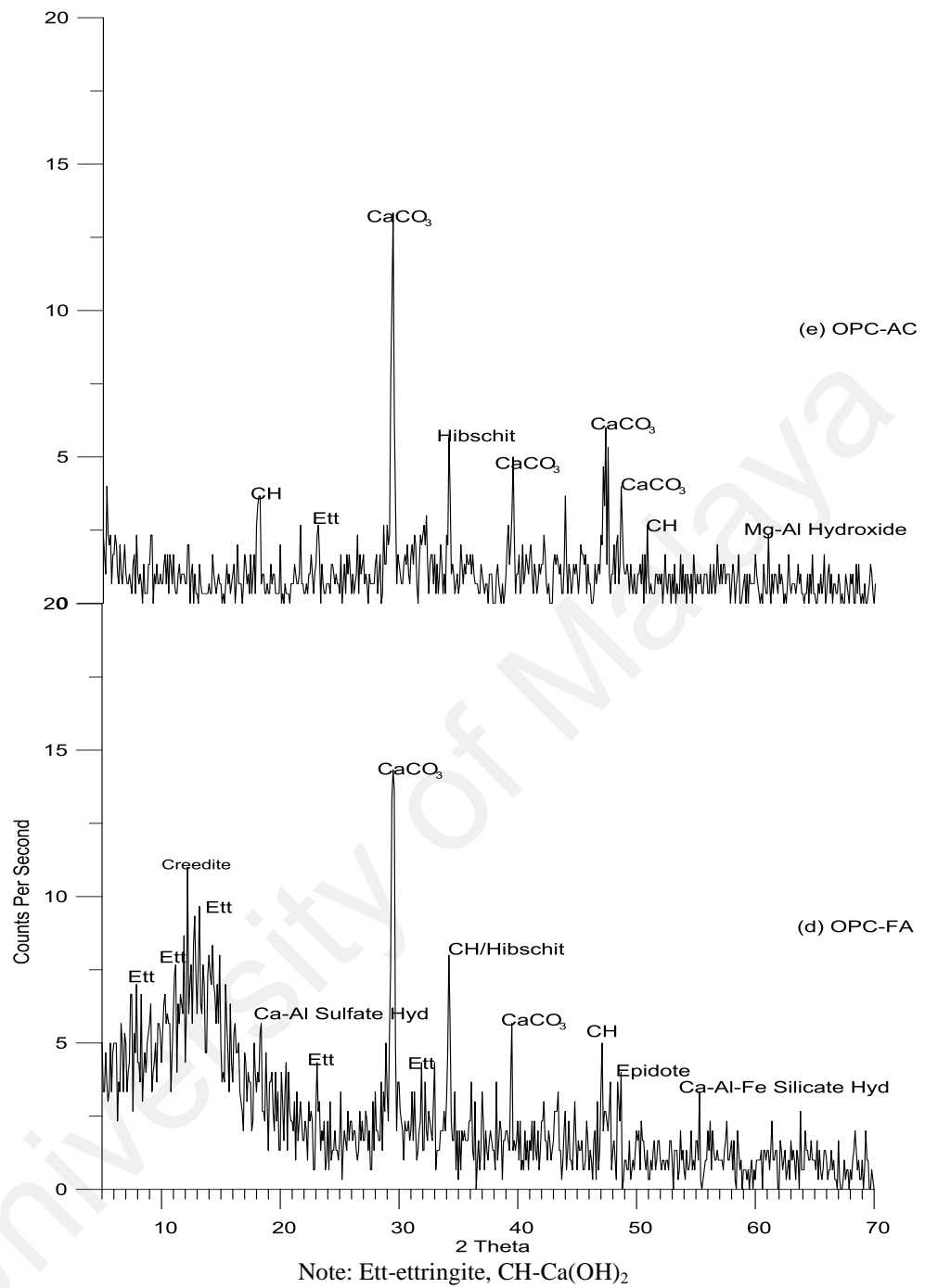
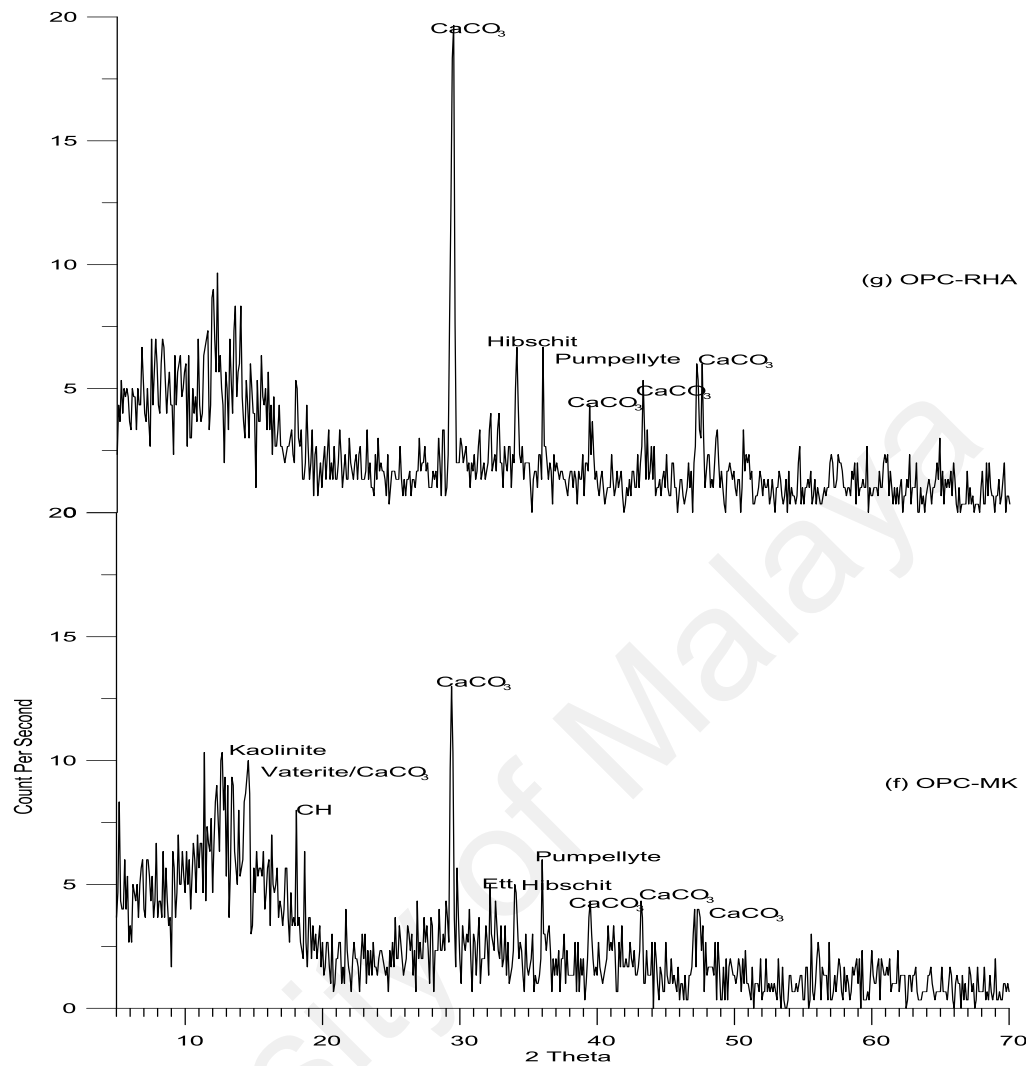


Figure 4.67: Diffractograms of solidified (a) OPC (b) OPC-sludge (c) OPC-CSF (d) OPC-FA (e) OPC-AC (f) OPC-MK and (g) OPC-RHA (continued)



Note: Ett-ettringite, CH-Ca(OH)₂

Figure 4.67: Diffractograms of solidified (a) OPC (b) OPC-sludge (c) OPC-CSF (d) OPC-FA (e) OPC-AC (f) OPC-MK and (g) OPC-RHA (continued)

In conclusion, the most obvious crystal formed in solidified sludges was calcite mineral. Calcite was formed as polymorph rhombohedron crystal with smooth surface. Calcite can incorporate several metals as insoluble solid products. Formation of calcite was accelerated by the presence of carbon in the incorporated sludge. Since the carbonation process occurred as post-hydration, a significant curvature in the strength change was observed at age 86 days where carbonation effect to increase the strength of W/C 0.45 in

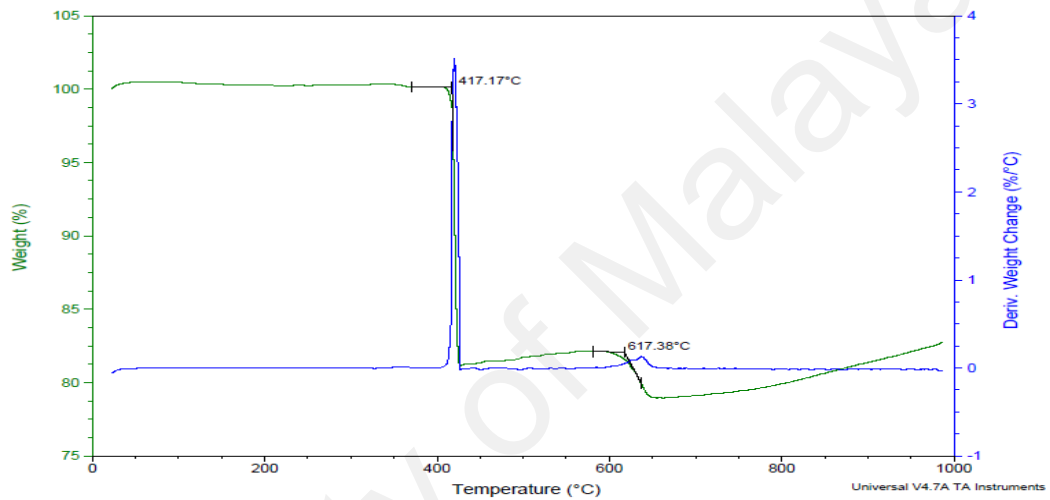
Figure 4.23(b). C-S-H surface was not seen due to its amorphous surface. Other common hydration products such as ettringite and CH were found in solidified sludge FA, AC and MK and well distributed in solidified OPC.

4.4.4.4 Thermogravimetry of solidified sludge

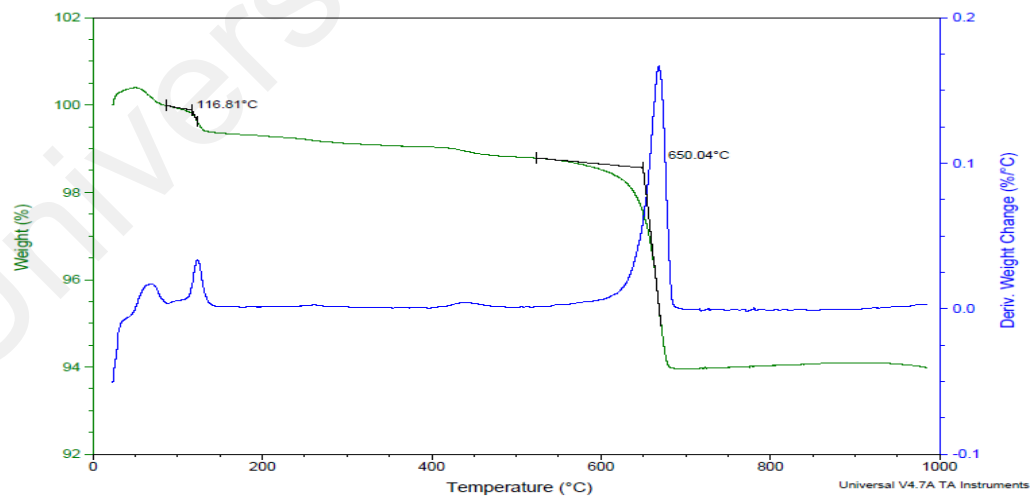
Thermogravimetry analysis of binder's material and solidified sludge was made using TA Instrument Q500 and analyzed by TA Universal Analysis 2000 software. About 10 mg of dry sample was used to measure the mass change as a function of temperature. Thermal change accompanying mass change includes decomposition, sublimation, reduction, desorption, absorption and vaporisation. Ca(OH)_2 was used as a reference sample to the raw and solidified binder's Ca(OH)_2 . The weight loss of Ca(OH)_2 , OPC and solidified OPC are illustrated in Figure 4.68(a), (b) and (c) accordingly. Thermogram analysis tabulated in Table 4.21 based on Figure 4.68(a) indicates the Ca(OH)_2 decarboxylation occurred at 351 to 500 °C. OPC thermal change mainly involved CaCO_3 decomposition lead to 4.78 % weight loss found at temperature of 500 to 800 °C as shown by Figure 4.68(b).

Thermal changes of hydrated cement generally occurred in four phases, namely gypsum and hemihydrates hydration at 100 to 200 °C, syngenite, $\text{K}_2\text{Ca(SO}_4)_2 \cdot \text{H}_2\text{O}$ decomposition at 250 to 300 °C, Ca(OH)_2 at 400 to 500 °C and decomposition of CaCO_3 by releasing CO_2 at 500 to 800 °C (Taylor, 1990). Dehydrated CSH and alumina occurred at temperature of up to 300 °C (Kakali, et al., 1998). Based on the thermogram of hydrated OPC shown in Figure 4.68(c) the extrinsic moisture was removed at temperature about 100 °C, Ca(OH)_2 decarboxylation caused 5.53 % weight loss and another 5.64 % for CaCO_3 /CSH/alumina decomposition. The hydrated OPC-sludge thermogram shows more

noise peaks to derivative weight change as the sludge content organics constituent which can be easily noticed by the increase of weight loss at temperature of 500 to 800 °C by 2.5 % due to decomposition of semivolatile, oil and grease and CaCO₃ decarbonation by removal of CO₂. Small portion of volatile is expected to vaporise at temperature below 100 to 200 °C.

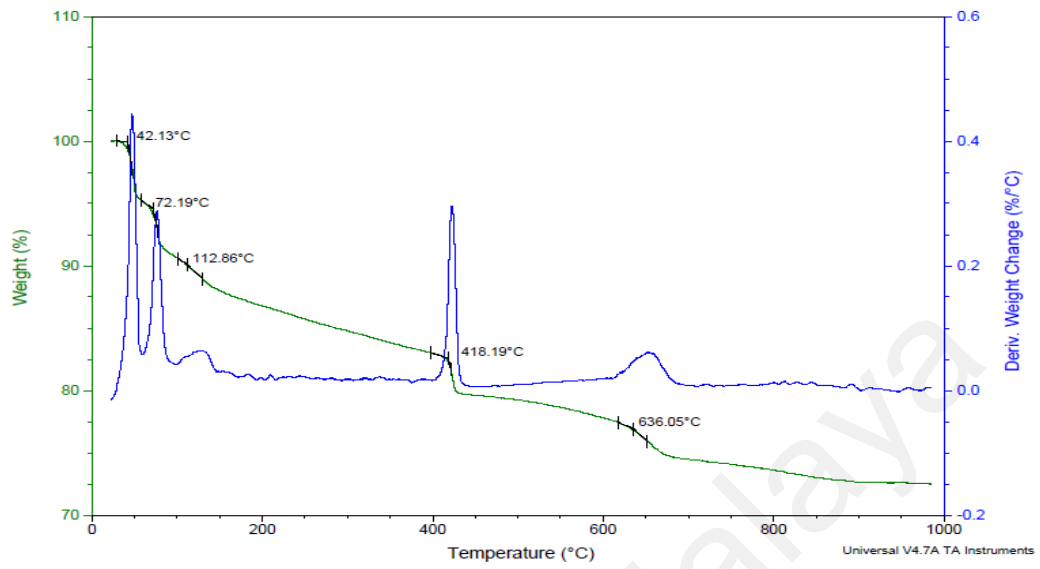


(a) Ca(OH)₂

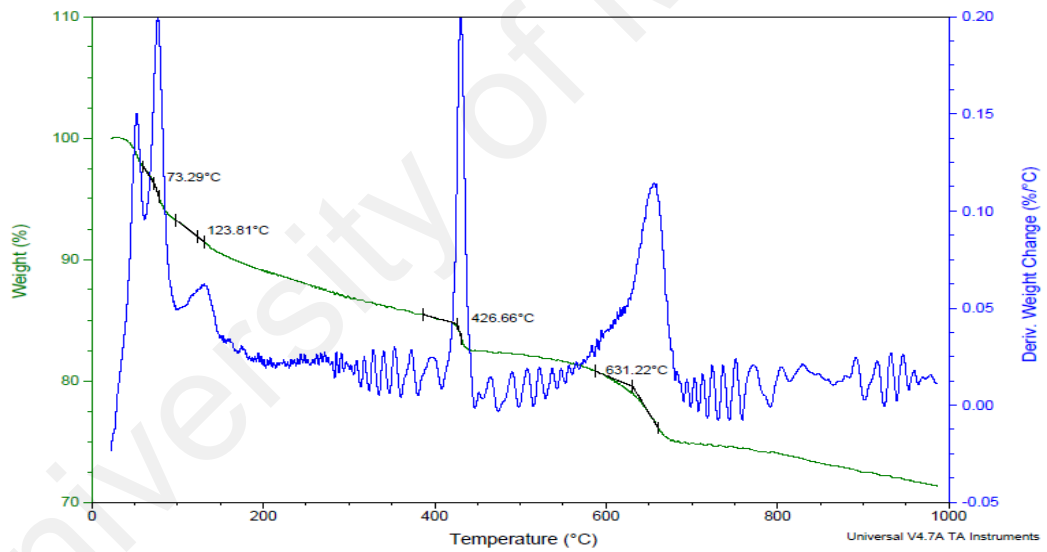


(b) OPC

Figure 4.68: Thermograms of (a) Ca(OH)₂ (b) OPC (c) hydrated OPC and (d) hydrated OPC-sludge



(c) Hydrated OPC



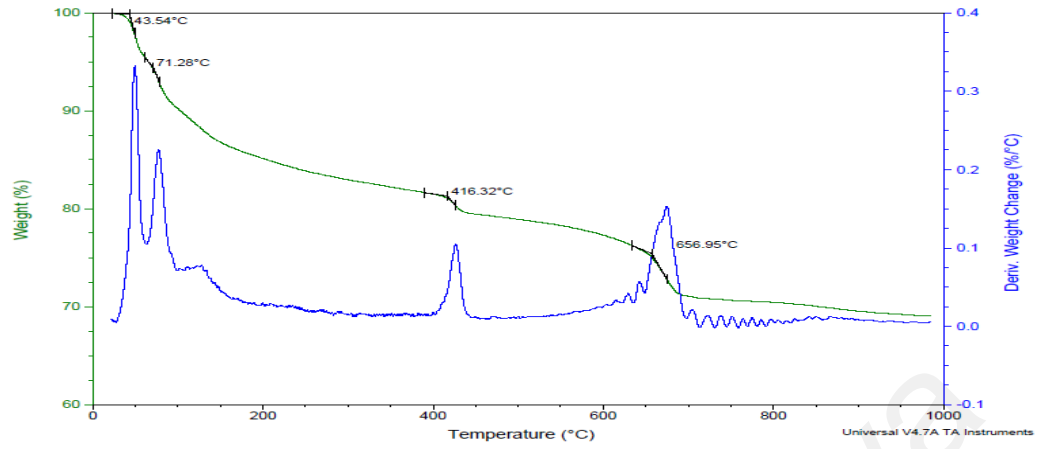
(d) Hydrated OPC-sludge

Figure 4.68: Thermogram of (a) $\text{Ca}(\text{OH})_2$ (b) OPC and (c) hydrated OPC (d) hydrated OPC-sludge (continued)

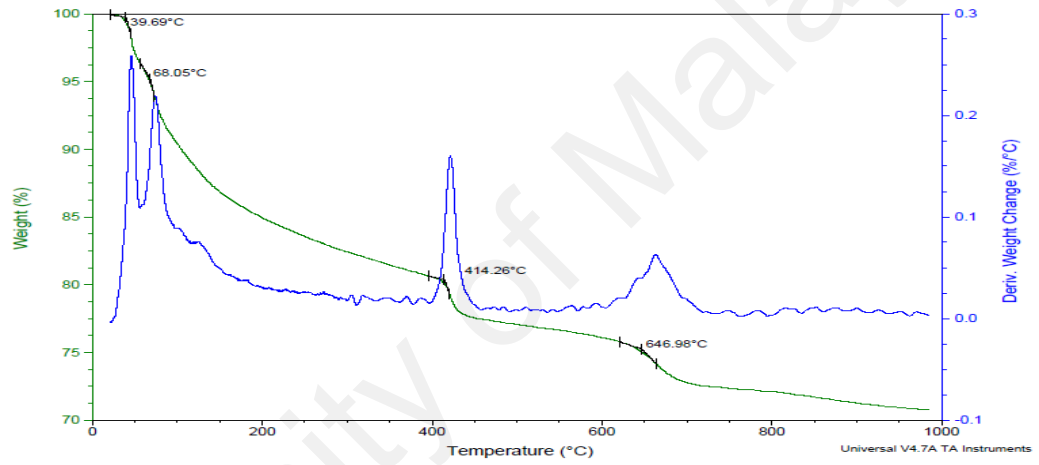
Table 4.21: Thermogravimetry data for Ca(OH)₂, OPC and hydrated OPC

| Sample | Temperature changes (°C) | Weight loss (%) | Thermal changes remark |
|---------------------|--------------------------|---|--|
| Ca(OH) ₂ | 351.59 - 500.00 | 18.60 | Decomposition of Ca(OH) ₂ |
| OPC | 75.62 - 100.15 | 0.07 | Moisture loss |
| | 100.15 - 199.50 | 0.63 | Gypsum and hemihydrates dehydration |
| | 199.50 - 300.07 | 0.17 | Syngenite, C-S-H & alumina |
| | 300.07 - 500.00 | 0.30 | Ca(OH) ₂ carboxylation |
| | 500.00 - 800.00 | 4.78 | CaCO ₃ decomposition |
| Hydrated OPC | 28.79 - 59.67 | 4.83 | Moisture loss |
| | 59.67 - 100.15 | 4.55 | Moisture loss |
| | 100.15 - 199.50 | 3.82 | Gypsum and hemihydrates dehydration |
| | 199.50 - 300.07 | 2.03 | Syngenite, C-S-H & alumina |
| | 300.07 - 500.00 | 5.53 | Ca(OH) ₂ carboxylation |
| 500.00 - 800.50 | 5.64 | CaCO ₃ decomposition/final C-S-H & alumina dehydration | |
| Hydrated OPC-Sludge | 22.42 - 62.12 | 2.54 | Moisture /volatile loss |
| | 62.12 - 100.15 | 4.32 | Moisture /volatile loss |
| | 100.15 - 199.50 | 4.03 | Gypsum and hemihydrates dehydration |
| | 199.50 - 300.07 | 2.19 | Syngenite, C-S-H & alumina decomposition |
| | 300.07 - 500.00 | 4.72 | Ca(OH) ₂ carboxylation |
| 500.00 - 800.50 | 8.13 | CaCO ₃ decomposition/final C-S-H & alumina dehydration/organic decomposition | |

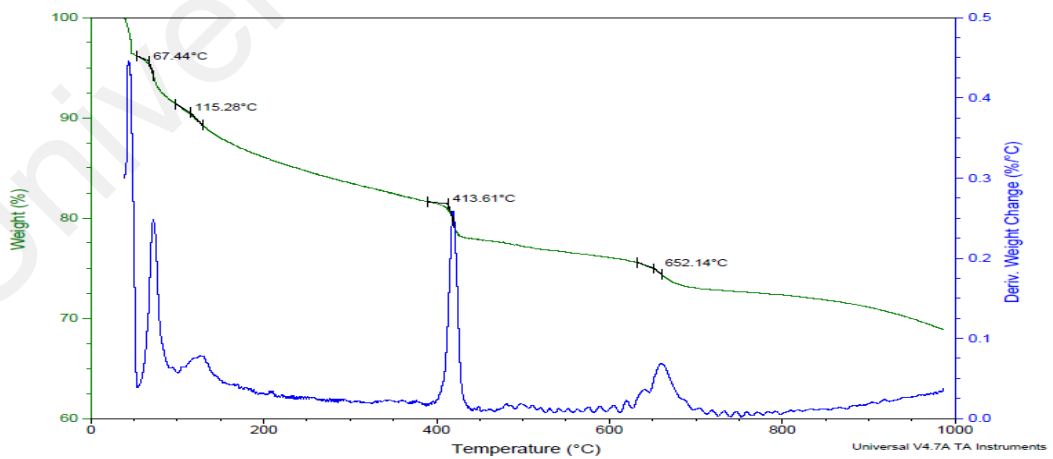
Thermograms for the OPC-Sludge with CRMs are depicted by Figure 4.69. The percent weight of Ca(OH)₂ in the samples are varied according to the available Ca(OH)₂ which reflected the pozzolanic activity in the hydrated OPC-Sludge with CRMs. Organic compound in the OPC-sludge may decompose at temperature of 500-800 °C where aliphatic or aromatic with C₂₀₊ reach to it critical temperature, T_c based on the increased of about 2.5 % weight loss compared to hydrated OPC, leaving the remaining portion as organic char and inert residue.



(a) CSF

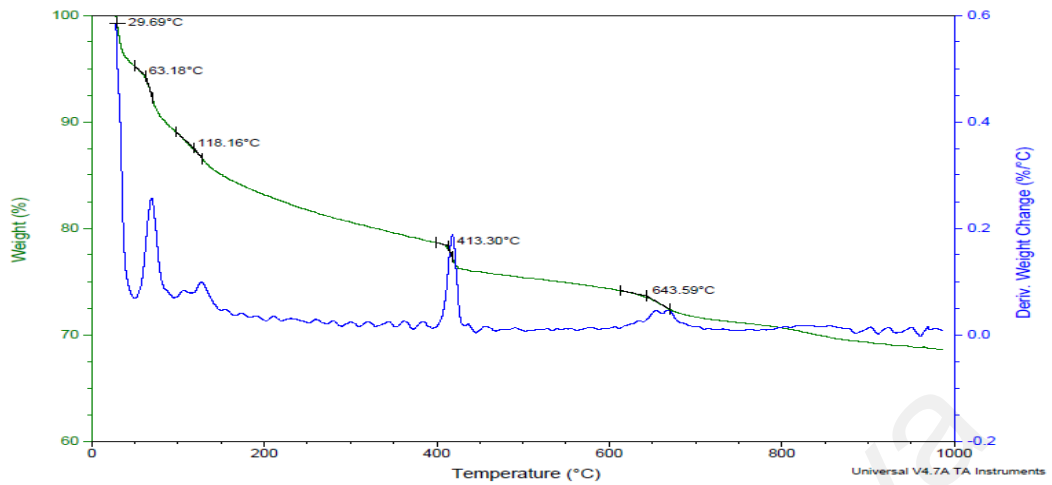


(b) FA

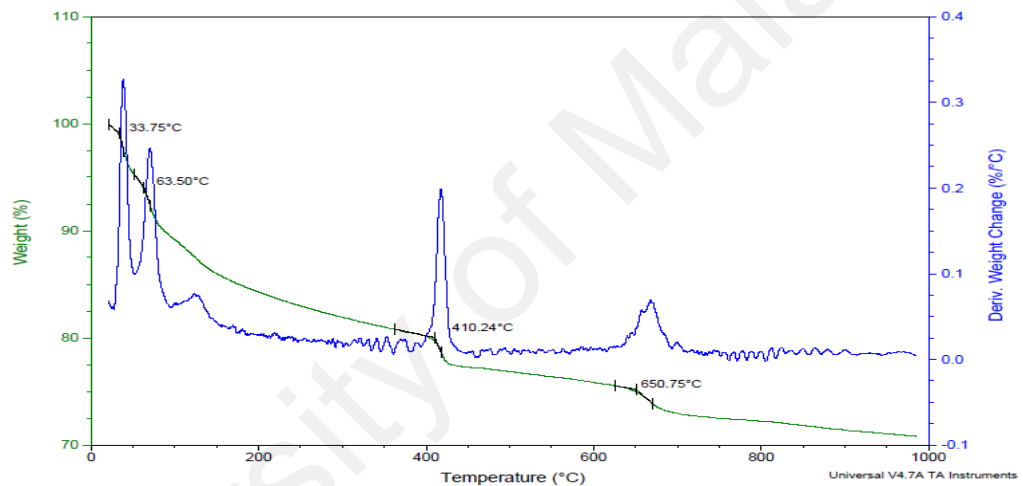


(c) AC

Figure 4.69: Thermograms of hydrated OPC-sludge with (a) CSF (b) FA (c) AC (d) MK and (e) RHA



(d) MK



(e) RHA

Figure 4.69: Thermograms of hydrated OPC-Sludge with (a) CSF (b) FA (c) AC (d) MK and (e) RHA (continued)

The weight changes accounted for the pozzolanic activity by the CRMs incorporation are tabulated in Table 4.22. In contrast to OPC-Sludge, all the $\text{Ca}(\text{OH})_2$ in OPC-Sludge with CRMs weight loss are smaller and insignificance noise of derivative weight change was observed. Organic was stabilized and adsorbed by the incorporation of CRMs that helped to bind the waste.

Weight change was split into seven steps. First and second steps involving temperature changes of up to about 100 °C indicate the moisture loss or volatile organics loss from the solidified cement. Accumulated weight losses of the first two steps are in range of 8 to 10 % forming largest portion compared to other steps.

Third weight change of about 5 % occurred at 100 to 200 °C was accounted to gypsum, hemihydrates dehydration and water removal from hydrated products. Syngenite decomposition, C-S-H and alumina dehydration can be found at 200 to 300 °C with amounted to 2.1 to 2.5 % weight loss.

The Ca(OH)_2 carboxylation involved weight loss of 4.0 to 6.3 % was estimated in the range of 300 to 500 °C. Final steps involving CaCO_3 decomposition and final C-S-H/alumina dehydration was observed at temperature of 500 to 800 °C. The organic residue like char and grease was also decomposed in this temperature range with weight loss of 4.6 to 8.4 %.

As a conclusion pozzolanic reaction was active in solidified sludge with CRMs as indicated by the weight loss of Ca(OH)_2 in all solidified sludge with CRMs generally lower than the solidified sludge since, the CH was consumed by the SiO_2 by converting to C-S-H.

The other significant weight loss was due to decarbonation at temperature 500 to 800 °C referring to the calcium carbonate formed from the reaction of carbon in the sludge with CH or C-S-H, which resulted in a lesser amount of both cement products in the solidified sludge or solidified sludge with CRMs due to the conversion to calcite.

Table 4.22: Thermogravimetry data for OPC-sludge with CRMs

| CRMs | Temperature changes (°C) | Weight loss (%) | Thermal changes remark |
|------|--------------------------|-----------------|---|
| CSF | 28 – 62 | 4.48 | Moisture /volatile loss |
| | 62 – 100 | 5.23 | Moisture /volatile loss |
| | 100 – 200 | 5.05 | Gypsum and hemihydrates dehydration |
| | 200 – 300 | 2.18 | Syngenite/C-S-H & alumina decomposition |
| | 300 – 500 | 4.03 | Ca(OH) ₂ carboxylation |
| | 500 – 800 | 8.49 | CaCO ₃ decomposition/final C-S-H & alumina dehydration/organic residue decomposition |
| FA | 30 – 55 | 3.39 | Moisture or volatile loss |
| | 55 - 100 | 6.12 | Moisture or volatile loss |
| | 100 - 200 | 5.42 | Gypsum and hemihydrates dehydration |
| | 200 - 300 | 2.53 | Syngenite/C-S-H & alumina decomposition |
| | 300 - 500 | 5.35 | Ca(OH) ₂ carboxylation |
| | 500 – 800 | 4.96 | CaCO ₃ decomposition/final C-S-H & alumina dehydration/organic residue decomposition |
| AC | 40 – 54 | 3.50 | Moisture /volatile loss |
| | 54 – 100 | 4.79 | Moisture /volatile loss |
| | 100 – 200 | 5.20 | Gypsum and hemihydrates dehydration |
| | 200 – 300 | 2.59 | Syngenite/C-S-H & alumina decomposition |
| | 300 – 500 | 6.28 | Ca(OH) ₂ carboxylation |
| | 500 – 800 | 4.86 | CaCO ₃ decomposition/final C-S-H & alumina dehydration/organic residue decomposition |
| MK | 28 - 48 | 4.61 | Moisture /volatile loss |
| | 48 - 100 | 6.47 | Moisture /volatile loss |
| | 100 - 200 | 5.72 | Gypsum and hemihydrates dehydration |
| | 200 - 300 | 2.59 | Syngenite/C-S-H & alumina decomposition |
| | 300 - 500 | 5.21 | Ca(OH) ₂ carboxylation |
| | 500 – 800 | 4.72 | CaCO ₃ decomposition/final C-S-H and alumina dehydration/organic residue decomposition |
| RHA | 22 – 52 | 4.64 | Moisture /volatile loss |
| | 52 - 100 | 6.07 | Moisture /volatile loss |
| | 100 - 200 | 4.87 | Gypsum and hemihydrates dehydration |
| | 200 - 300 | 2.38 | Syngenite/C-S-H & alumina decomposition |
| | 300 - 500 | 5.09 | Ca(OH) ₂ carboxylation |
| | 500 – 800 | 4.62 | CaCO ₃ decomposition/final C-S-H and alumina dehydration/organic residue decomposition |

4.4.4.5 Conclusions of microstructure properties

Several conclusions can be made based on the inspection of solidified sludge by SEM, FESEM, XRD and TGA analysis as summarized below:

1. SEM photomicrograph of metals and organic which formed high strength monolith depicts platy layers of precipitated metal hydroxide that enveloped the sludge granule.
2. SEM photomicrograph of solidified OPC exhibits the formation of ettringite and C-S-H as main products. Sludge inclusion showed lubricating effect to the cement surface with more interconnected C-S-H but lack of ettringite and less voids was observed.
3. FESEM EDAX elemental analysis has shown that the CRMs incorporation has reduced the calcium concurrent with the rise of carbon content.
4. Pozzolanic activity has caused slight reduction in Si content of the solidified sludge or sludge with CRMs compared to solidified OPC.
5. Solidified sludge with CSF exhibits ettringite surface due to abundant silica content.
6. AC incorporation in the solidified sludge has attributed to the finer surface of amorphous C-S-H due to large surface areas of AC for contaminant absorption.
7. Photomicrograph of solidified sludge with MK shows more void on the surface while photomicrographs of FA and RHA depict amorphous C-S-H surface with little ettringite needles.
8. The XRD diffractograms indicate major crystal formed was polymorph rhombohedron calcite as a result of carbonation reaction based on the reactants of CO₂ with either C-S-H or CH in all solidified sludge. Diffractogram of solidified

sludge with RHA indicates highest calcite crystal formation approaching 20 counts per second.

9. Thermograms of TGA analysis show that active pozzolanic reaction occurred in solidified sludge with CRMs as represented by significant weight loss of $\text{Ca}(\text{OH})_2$ at 300 to 500 °C recorded 4.0 to 6.3 %.
10. Carbonation product's decomposition also formed significant weight loss of 4.6 to 8.4 % observed at the temperature of 500 to 800 °C in thermograms of solidified sludge with CRMs.

4.4.5 Organic analysis

Volatile organics was performed by Shimadzu QP2010 GCMS. The solidified sludge and its leachate were analyzed for the organic compound by the USEPA SW-846, according to method for determination of extractable petroleum hydrocarbon (MADEP, 2004). The sample preparation methods are illustrated by a flowchart in Figure 4.70.

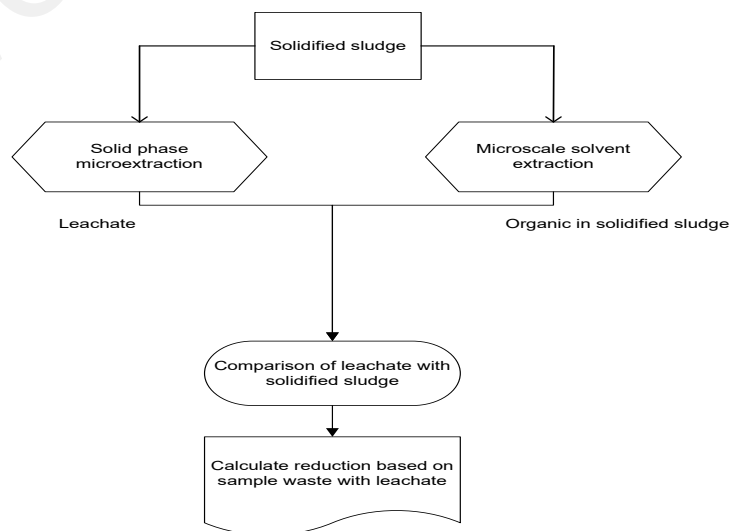


Figure 4.70: Organic analysis flowchart

4.4.5.1 Microscale solvent extraction

Solidified sludge organic compound in cement was determined by the microscale solvent extraction (MSE) according to USEPA SW-846 method 3570 (USEPA, 2006). Sample was immersed in Fluka Analytical methylene chloride and agitated by end-to-end rotary agitator for four hours. Solid was filtered from solvent by glass fiber filter to remove the solid material after the solvent formed a layer on top of the solid. The solvent was evaporated by pre-concentrate in 25 mL Supelco Kuderna Danish tube attached to a three ball synder column to trap analyte until 1 or 2 mL final volume. The extracted analyte was tested for organic compound using GCMS.

4.4.5.2 Solid phase microextraction

Solid phase microextraction (SPME) was developed by Pawliszyn and Belardi (1989). SPME was conducted based on two steps, the extraction and desorption of extracted compound as in Figure 4.71. In the first steps, fused silica rod with coated fiber was exposed to the analytes in headspace mediums. The fiber was injected into the Shimadzu QP2010Plus GCMS for desorption and quantitation. Fiber of 100 μm polymethylsiloxane (PDMS) was purchased from Supelco America (Bellefonte, PA) which has strong affinity for polar/nonpolar groups.

Operating parameters of the SPME analysis are as shown in Table 4.23, which include the splitless injection mode with injection temperature of 250 and 50 $^{\circ}\text{C}$ column oven temperature. The headspace adsorption time used was 25 minutes, and desorption time was 7 minutes in FID column. Column used was Rtx-5MS with 30 m length x 25 μm diameter. Post run of the sampling was 30 minutes for conditioning the fiber. Incubation period for the warming up of the sample prior to adsorption process was 5 minutes.

Headspace adsorption achieved faster equilibrium between the fiber and the headspace. Operating parameters was made based on the volatiles application method for SPME and GC of Supelco products.

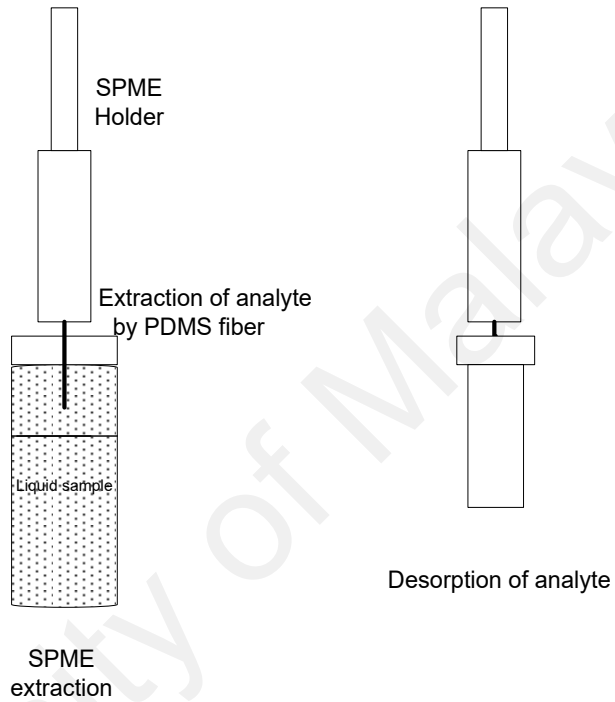


Figure 4.71: SPME extraction and desorption of analyte

The principle of SPME mass of analyte adsorbed equilibrium conditioned is represented by Equation 4-24.

$$n_f = \frac{K_{fx} V_f V_s C_0}{K_{fs} V_f + K_{hs} V_h + V_s} \quad \text{Eq. (4-24)}$$

where

n_f = mass of analyte adsorbed by coating

C_0 = initial concentration of analyte in sample

K_{fs} = partition coefficient for analyte between coating and aqueous phases

K_{hs} = partition coefficient for analyte between headspace and aqueous phases

V_f = volume of coating

V_s = volume of sample

V_h = volume of headspace

Table 4.23: SPME and GCMS operating parameters

| SPME operating parameter | Values |
|-----------------------------|---------------------|
| Column oven temperature, °C | 50 |
| Column Temperature, °C | 250 |
| Injection mode | Splitless |
| Absorption time, minute | 25 |
| Desorption time, minute | 7 |
| Incubation time, minute | 5 |
| Ion source | Electron ionization |
| Extraction agitation, rpm | 250 |

Based on the TIC chromatogram of GCMS, volatile organic compounds in the solidified cement matrix were determined based on the external standard calibration curve (Wang, 2001) for the targeted compounds of benzene, toluene, ethyl benzene, xylenes, naphthalene and phenanthrene. Calibration curves of target analyte were given in the Appendix D. None of the targeted aromatic compounds present in the solid sample since the aromatic form only 5 percent of the hydrocarbon content which already vaporized during the mixing process. Volatile organic compound in the sample was determined based on Equation 4-25 using the internal standard based on Method AK 102 for the determination of diesel range organics (Pilgrim, 2011). Organic compound found in the OPC-sludge and OPC-sludge leachate are shown in Table 4.24.

$$C_s = \frac{(A_x)(C_{st})(D)(V_t)}{(A_{st})(RF)(V_s)} \quad \text{Eq. (4-25)}$$

where

C_s = concentration of sample, mg/kg

A_x = response of sample, area

C_{st} = concentration of standard, $\mu\text{g/ml}$

RF = response factor of standard

A_{st} = response of standard, area

V_t = volume of final extract, mL

V_s = volume of sample extracted, L or kg

D = dilution factor, if no dilution was made use $D = 1$

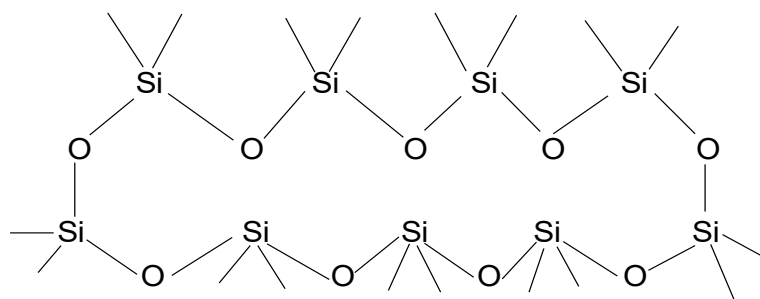
Hydrocarbon found in solidified sludge mainly contains the aliphatic group and ester acid. The main component includes tetracosane, hexatriacontane, hexadecane and octadecane; all are straight chain alkanes and 1, 2-Benzenedicarboxylic acid, diisooctyl ester. Branched alkanes was also found in the solidified sludge such as pentadecane, 2, 6, 10-trimethyl.

On the other end, leachate of OPC-sludge contained mainly organic acid and cyclic siloxane compound. Siloxane compound is a dissolution product of chemical reaction between silica in cement and organic compound by carboxylic acid.

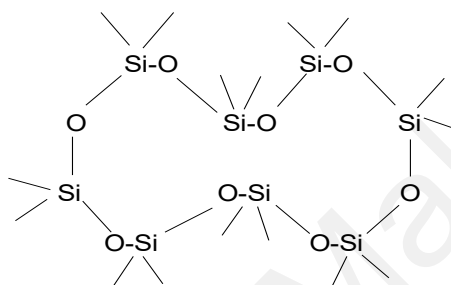
Table 4.24: Organic compound in the solidified sludge solid and leachate

| Sample | Organic compound | Concentration (mg/kg) | Formula |
|---------------------|--|-----------------------|--|
| OPC-sludge | Pentadecane | 38.95 | C ₁₅ H ₃₂ |
| | Hexadecane | 55.97 | C ₁₆ H ₃₄ |
| | Pentadecane, 2,6,10-trimethyl | 14.90 | C ₁₈ H ₃₈ |
| | Octadecane | 135.31 | C ₁₈ H ₃₈ |
| | Nanodecane | 89.28 | C ₁₉ H ₄₀ |
| | Hexadecane, 2,6,10,14-tetramethyl | 140.90 | C ₂₀ H ₄₂ |
| | Eicosane | 87.47 | C ₂₀ H ₄₂ |
| | Heneicosane | 86.08 | C ₂₁ H ₄₄ |
| | Docosane | 84.81 | C ₂₂ H ₄₆ |
| | 1,2-Benzenedicarboxylic acid, diisooctyl ester | 120.07 | C ₂₄ H ₃₈ O ₄ |
| | Tetracosane | 149.59 | C ₂₄ H ₅₀ |
| | Decanedioic acid, bis(2-ethylhexyl) ester | 23.30 | C ₂₆ H ₅₀ O ₄ |
| | Dotriacontane | 43.46 | C ₃₂ H ₆₆ |
| | Tetratriacontane | 69.94 | C ₃₄ H ₇₀ |
| | Hexatriacontane | 145.22 | C ₃₆ H ₇₄ |
| | Tetrapentacontane | 11.13 | C ₆₄ H ₁₁₀ |
| OPC-sludge leachate | Cycloheptasiloxane, tetradecamethyl | 2.15 | C ₁₄ H ₄₂ O ₇ Si ₇ |
| | Tetradecanoic acid | 2.10 | C ₁₄ H ₂₈ |
| | Propanoic acid, 2-methyl, 1-(1,1-dimethyl)-2-methyl-1,3-propanedyl ester | 12.18 | C ₁₆ H ₃₀ O ₄ |
| | Cyclooctasiloxane, hexadecamethyl | 1.09 | C ₁₆ H ₄₈ O ₈ Si ₈ |
| | Cyclononasiloxane, octadecamethyl | 4.26 | C ₁₈ H ₅₄ O ₉ Si ₉ |
| | Heneicosane | 1.88 | C ₂₁ H ₄₄ |
| | Squalane | 2.47 | C ₃₀ H ₅₀ |

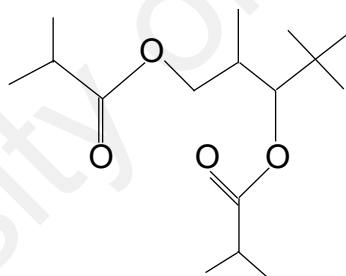
Organic leachate products from solidified sludge 8045 are in form of the reduced hydrocarbon ring such as C₁₄ and C₁₆ as a result of hydrocarbon in sludge reacts with acetate ions, or the chemical reaction of hydrocarbon with carbonic acid and silane forming cyclic siloxane hydrocarbon. The aliphatic hydrocarbon was also present in the leachate, but the value found was reduced tenfold of its concurrent solidified sludge, for instance, heneicosane. Hydrocarbon molecular structures in leachate are represented in Figure 4.72 from National Institute of Standard and Technology for GC database, NIST08s.Lib.



(a) cyclonanosiloxane octadecamethyl



(b) cyclooctasiloxane hexadecamethyl



(c) propanoic acid, 2-methyl, 1-(1,1-dimethyl)-2-methyl-1,3-propanedylester



(d) heneicosane

Figure 4.72: Structure of leachate products (a) cyclonanosiloxane octadecamethyl, (b) cyclooctasiloxane hexadecamethyl (c) propanoic acid, 2-methyl, 1-(1,1-dimethyl)-2-methyl-1,3-propanedyl ester and (d) heneicosane

As a conclusion, the organic compound found in the solidified sludge was in formed of linear or branched aliphatic hydrocarbon within C_{14} to C_{64} with long carbon chain, which

was quite resistant to decomposition of heavier hydrocarbon group origin. The leachate of solidified petroleum sludges are composed of cyclic siloxane or acid ester as a derivative product of leached silica reaction with hydrocarbon since silica has high affinity towards reverse charges and carboxylic acid reaction on hydrocarbon. Abundance of silica from cement hydration products facilitates the formation of cyclic siloxane similar like SiO₂ that formed sandy beaches. The regulated volatiles and semivolatiles TCLP was tabulated in Appendix E whereby none of the lists were found in the leachate.

4.4.5.3 Oil and grease

The oil and grease concentration and percent reduction of solidified sludge with CRMs leachate are represented in Figure 4.73. Liquid extraction is based on differences in solubilities of compounds in the extraction media. The analyte extracted equal to the concentration of analyte multiplied by volume of solvent. The distribution of solute between two phases is described by a distribution ratio, *D* as represented by Equation 4-26.

$$D = [\text{solvent}]/[\text{waste solution}] \quad \text{Eq. (4-26)}$$

Solidified sludge with CSF and FA release higher oil and grease than the control except 15 % FA, which associated to higher matrix mobility. Whereas solidified sludge in AC showed lowest mobility due to the sorbent capability with large micropore surface area that entrapped the oil and grease. Solidified sludge with CRMs leachate has an alkaline pH of 12.0 in comparison to control sample of 3.0. Reduction rate of oil and grease in solidified sludge with CRMs of AC, MK and RHA achieved about 99.5 %.

Based on the oil and grease immobilization, the suitable CRMs for oil and grease adsorption were AC, MK and RHA as shown by the higher reduction rate compared to FA

and CSF. The oil and grease in the leachate are well below the landfill acceptance criteria at 1000 mg/kg or 10 mg/L of Standard B industrial effluent.

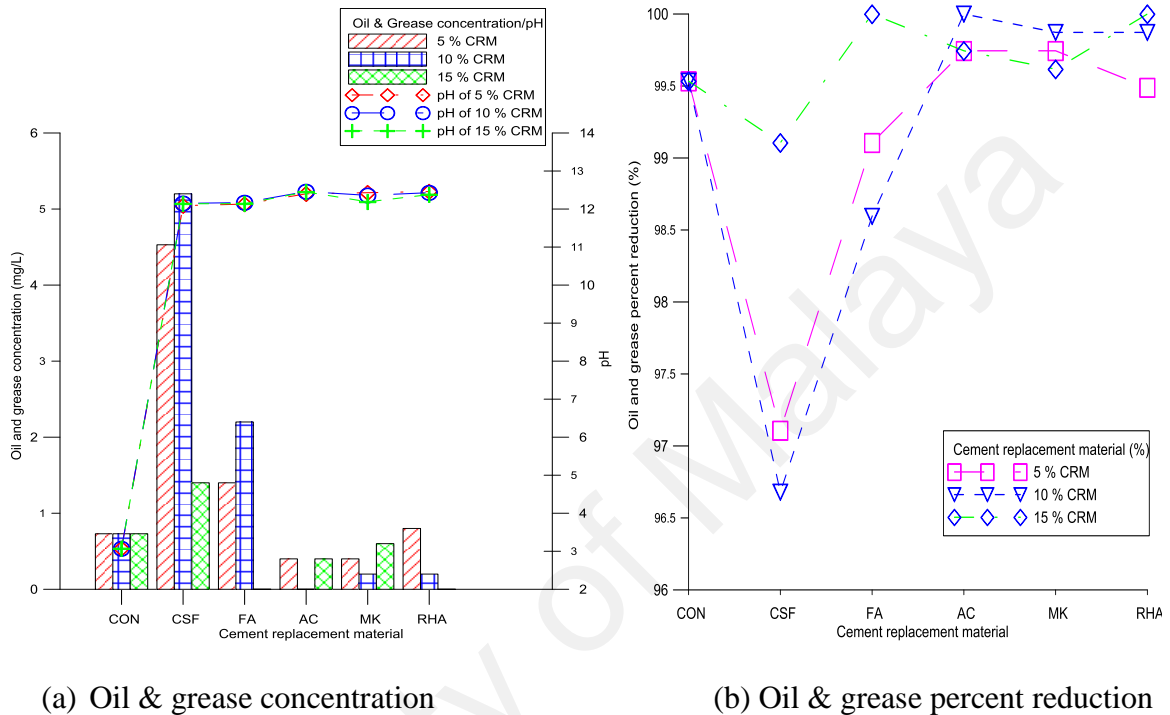


Figure 4.73: Oil and grease (a) concentration and (b) percent reduction in leachate

4.4.5.4 Nuclear magnetic resonance of ^1H and ^{13}C

FT-NMR at 400 MHz was used to investigate the absorption of ^1H and ^{13}C by Joel FT-NMR. The freeze dry extracted solidified sludge and leachate samples to remove moisture or solvent for ^1H proton and carbon-13 as NMR absorption was conducted in deuterium chloroform solvent, CDCl_3 . The chemical shift of the ^1H -NMR can determine the hydrogen that giving rise to the absorption. The ^1H chemical shift has a narrow range of 0 to 10 ppm (δ) and typical groups corresponding to its chemical shift are listed in Table

4.25. The ^1H solvent peak was found at 7.2 δ with singlet peak. The ^1H signal splitting was due to the influence of neighbouring non-equivalent hydrogen.

Table 4.25: Average chemical shifts of representative types of hydrogen (adopted from Brown, 2000)

| Type of hydrogen (<i>R</i> = alkyl, <i>Ar</i> = aryl) | Chemical shift (δ)* | Type of hydrogen (<i>R</i> = alkyl, <i>Ar</i> = aryl) | Chemical shift (δ)* |
|---|---------------------------------|---|---------------------------------|
| (CH ₃) ₄ Si | 0 | O | |
| RCH ₃ | 0.8-1.0 | | |
| RCH ₂ R | 1.2-1.4 | RCOCH ₃ | 3.7-3.9 |
| R ₃ CH | 1.4-1.7 | O | |
| R ₂ C=CRCHR ₂ | 1.6-2.6 | | |
| RC \equiv CH | 2.0-3.0 | RCOCH ₂ R | 4.1-4.7 |
| ArCH ₃ | 2.2-2.5 | RCH ₂ I | 3.1-3.3 |
| ArCH ₂ R | 2.3-2.8 | RCH ₂ Br | 3.4-3.6 |
| ROH | 0.5-6.0 | RCH ₂ Cl | 3.6-3.8 |
| RCH ₂ OH | 3.4-4.0 | RCH ₂ F | 4.4-4.5 |
| RCH ₂ OR | 3.3-4.0 | ArOH | 4.5-4.7 |
| R ₂ NH | 0.5-5.0 | R ₂ C=CH ₂ | 4.6-5.0 |
| O | | R ₂ C=CHR | 5.0-5.7 |
| | | ArH | 6.5-8.5 |
| RCCH ₃ | 2.1-2.3 | O | |
| O | | | |
| | | RCH | 9.5-10.1 |
| RCCH ₂ R | 2.2-2.6 | O | |
| | | | |
| | | RCOH | 10-13 |

*Values are approximates, other atom within molecule may cause the signal to appear outside these ranges

The ^1H proton chemical shifts of selected samples are tabulated in the Table 4.26 with the functional group of the proton. The area under NMR resonance is proportional to the number of hydrogen which that resonance represents. Integrating the different NMR resonance provides relative numbers of different hydrogen within a compound.

Tetramethylsilane, TMS is the reference compound normally resonance at 0 δ and other NMR spectrum's resonance relative to TMS. The ^1H NMR spectrums in the solidified sludge were found in the range of 0.83-0.89, 1.25 and 1.55 δ all referring to alkyl hydrogen.

Similar groups of alkyl hydrogen were found in solidified sludge with CRMs. The NMR spectrums of organic extracted from semi-dynamic leachate as represented by WBL1 to WBL5 indicate the alkanes proton and aromatic proton found at chemical shift of 1.18 or 1.44 and 7.16 δ respectively.

The ^1H -NMR spectrums showed that alkyl proton with functional groups of RCH_3 , RCH_2R and R_3CH were found in the solidified sludge. Similar ^1H groups were found in the leachate with additional aromatic proton. The compound was not predicted due to the potential of overlapping ^1H compounds. Oxidation of hydrocarbon may have occurred by the reaction of RCH_3 and R_3CH to RCOOH or $\text{R}_3\text{C}(\text{OH})$ accordingly as in Table 2.7. Hydrolysis of organic compound with water was also a common reaction which catalyzed by acidic or basic species of OH^- , H^+ or H_3O^+ .

Chemical shift in ^{13}C NMR has a wider range from 0-220 ppm. The ^{13}C solvent peak was found at 77.0-76.68 δ with triplet peak. It is generally possible to count the type of carbon atoms in a molecule. If without symmetrical substructure, molecular formula can be determined, but integral to the resonance to count on the number of carbon is not reliable. Multiplet splitting distinguished different functional groups such as $-\text{CH}$ (doublet in ^{13}C 1:1; ^1H 1:1 doublet), $-\text{CH}_2$ (^{13}C 1:2:1 triplet; ^1H 1:1 doublet), or $-\text{CH}_3$ (^{13}C 1:3:3:1 quartet; ^1H 1:1 doublet) (Marshall and Verdun, 1990).

The ^{13}C NMR carbon peak and chemical shift are tabulated in the Table 4.27 based on the count for identifiable peak that absorbed from 0 to 40 ppm, which was classified as straight chain alkane's carbon. Based on the NMR reference KBB-98 (Kalinowsky, et al., 1984) and straight chain hydrocarbon of the AC5 chemical shift, the skeleton structure is represented in Figure 4.74. The ^{13}C -NMR indicates the presence of 5 to 13 carbon types, which may constitute a single compound or overlapping compounds.

Table 4.26: ¹H-NMR proton chemical shifts in solidified sludge and leachate

| <i>Sample</i> | <i>Chemical shift (δ)</i> | <i>Proton groups</i> |
|---------------|---------------------------|---|
| 8045 | 0.07 (1) | TMS |
| | 0.83-0.89 (4) | RCH ₃ 0.89-CH ₃ |
| | 1.25 (1) | RCH ₂ R |
| | 1.55 (1) | R ₃ CH |
| WD50 | 0.81-0.88 (4) | RCH ₃ |
| | 1.20-1.23 (1) | RCH ₂ R 1.20-(CH ₃) ₃ COH; 1.23-CH ₂ |
| | 1.47-1.52 (1) | R ₃ CH |
| CSF5 | 0.70-0.96 (4) | RCH ₃ 0.7-CH ₃ SnPH ₃ ; 0.96-(CH ₃) ₄ |
| | 1.25 (1) | RCH ₂ R 1.25-CH ₃ -CH ₂ -CH ₃ |
| FA5 | 0.07 (1) | TMS |
| | 0.76-0.82 (4) | RCH ₃ |
| | 1.18 (1) | RCH ₂ R 1.18-CH ₃ CH ₂ OH |
| | 1.41-1.46 (1) | R ₃ CH 1.41-cyclopentane |
| AC5 | 0.83-0.89 (4) | RCH ₃ |
| | 1.25 (1) | RCH ₂ R |
| | 1.53 (1) | R ₃ CH |
| MK5 | 0.83-0.89 (4) | RCH ₃ |
| | 1.25 (1) | RCH ₂ R |
| | 1.49-1.54 (1) | R ₃ CH |
| RHA5 | 0.83-0.89 (4) | RCH ₃ |
| | 1.25 (1) | RCH ₂ R |
| | 1.53(1) | R ₃ CH |
| WBL1 | 1.18 | RCH ₂ R |
| | 1.44-1.47 | R ₃ CH |
| WBL2 | 7.19 | ArH |
| | 1.18 | RCH ₂ R |
| | 1.47 | R ₃ CH |
| WBL3 | 7.15-7.19 | ArH |
| | 1.18 | RCH ₂ R |
| | 1.47 | R ₃ CH |
| WBL4 | 7.16-7.19 | ArH |
| | 1.18 | RCH ₂ R |
| | 1.47 | R ₃ CH |
| WBL5 | 7.19 | ArH |
| | 1.18 | RCH ₂ R |
| | 1.44-1.47 | R ₃ CH |
| | 7.16-7.19 | ArH |

Table 4.27: ^{13}C -NMR in extracted solidified sludge

| <i>Sample</i> | <i>Carbon peak and chemical shift (δ)</i> |
|---------------|---|
| 8045 | 5 carbon types (31.89, 29.62-29.66, 29.33, 22.65 and 14.07) |
| WD50 | 5 carbon types (31.89, 29.62-29.66, 29.32, 22.65 and 14.07) |
| CSF5 | 11 carbon types (39.34, 37.37, 32.76, 31.89, 30.01, 29.63-29.67, 29.34, 27.94, 22.57-22.66, 19.70 and 14.06) |
| FA5 | 5 carbon types (31.94, 29.66-29.71, 29.37, 22.70 and 14.11). |
| AC5 | 6 carbon types (31.89, 29.62-29.66, 29.33, 27.94, 22.65 and 14.07) |
| MK5 | 13 Carbon types (39.40, 37.41, 32.78, 31.95, 30.07, 29.69-29.73, 29.39, 27.99, 24.82, 24.49, 22.62-22.71, 19.69 and 14.11) |
| RHA5 | 7 carbon types (39.39, 31.94, 29.67-29.71, 29.38, 27.99, 22.70 and 14.11) |

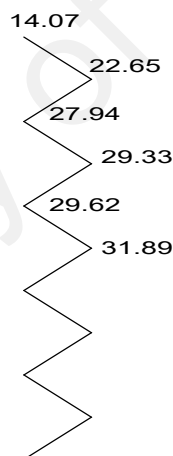


Figure 4.74: Straight chain hydrocarbon with ^{13}C chemical shift in δ for AC5

4.4.5.5 Conclusions of organic analysis

The salient points of organic analysis were summarized as follows:

1. Solidified sludge contained linear or branched aliphatic hydrocarbon of C_{14} to C_{64} with long chain carbon, which was quite resistant to biodegradation.

2. The leachate of solidified petroleum sludges were composed of cyclic siloxane or acid ester as a derivate product of leached silica reaction with hydrocarbon and carboxylic acid reaction on hydrocarbon. Silica has high affinity toward reverse charge's anion such as oxygen.
3. The aliphatic hydrocarbon was also present in the leachate, but the concentration was reduced tenfold of its concurrent solidified sludge, for instance, heneicosane.
4. AC, MK and RHA formed as suitable CRMs for solidified OPC-sludge as shown by the higher reduction rate of 99.5 % oil and grease compared to FA and CSF.
5. The NMR result showed that ^1H proton classified as alkyl group hydrogen of RCH_3 , RCH_2R and R_3CH were found in the solidified sludge while leachate was formed by similar ^1H groups with additional aromatic proton. The compound was not predicted due to the overlapping compound.
6. The ^{13}C -NMR indicates the presence of carbon-13 in formed of straight chain alkanes with 5 to 13 carbon types, which may constitute a single compound or overlapping compound.
7. Oil and grease in leachate were below the standard, and none of the volatile or semivolatile toxicity constituents were found in the leachate.

4.5 Applications of Solidified Sludge and Commercialization Potential

Long-term performance must be conducted before application of the waste into cement mixture by the waste generators. The excessive metals' content in the waste over the certain limit can inhibit hydration. Organic may interfere with the cement and form complex species in combination with the presence of metals. Satisfactory performance of solidified products achieved by 56-day ages may represent the long term result as the

longer curing did not significantly alter the monolith properties (Stegemann and Zhou, 2008).

The leachate released from solidified sludge must conform to the established standard such as the EU metal limit, USEPA TCLP, or UK authority guidelines limit. Monolith for specific purpose's material should meet the criteria set for the intended application area. Scheduled waste treatment and disposal or recycle for any final use must have a permission letter from local authority.

Conducted experimental works at the higher institution learning or research organization provides baseline data for practical utilization in manufacturing fabrication or for safe use in civil engineering practices. The waste treatment can simply be applied according to manufacturer plant design as the setup of batching plant can be made based on onsite or offsite application. The reasonable operating and capital costs are affordable to small and medium waste generators. Cost saving can be achieved at a shorter rate of return by avoiding treatment fees for sending bulk of hazardous waste to a license treatment plant.

Solidified product that able to meet the regulatory limit may be reused for to the following purposes:

1. Solidified waste for production of backfill materials, which normally employ FA as part of cement replacement material.
2. Pavement materials with enhanced aesthetic effect such as darker tone and bold textures. The waste and admixture may change the appearance according to the nature of material, which can provide a positive effect to the pavement without extra treatment to the solidified products. Incorporation of sand and gravel forming solidified mortar for the rough texture finished.

3. Bricks and concrete practically used in combination of admixture such as CSF for economic reasons. CSF can reduce the alkali effect in cement, and enhanced the durability of fresh and hardened state. CSF cement incorporated about 10 % weight of CSF will reduce diffusion coefficient and capillary pore. The brick made with clay has to meet the compressive strength of $\geq 50 \text{ N/mm}^2$ for engineering application B and $\geq 5 \text{ N/mm}^2$ for damp proof course or other application based on MS 27 1996.
4. Road and highway sub-based materials require high durability of cement to adsorb strong impact and vibration of mobile heavy pressure, which can be achieved by blending with organic polymer or rubbers.
5. Breakwater barrier requires cement with admixture to increase stiffening effect to chloride diffusivity such as CSF addition.
6. Solidified waste converted into the large cubes for embankment and surface realignment to ex-mining areas. The cement product can be used to cover the disturbed area from mineral extraction activities, especially in the dry and semi-arid region where leaching factors is decelerated.
7. Solidified waste formulated with water resistant can be used as riverbank erosion protection. Similar to breakwater barrier but the riverbank protection requires a better encapsulation cement mixture with less leaching capability since the leaching might have larger downstream impact since the river has smaller volume compared to ocean.

The Wastewater Technology Centre of Environment Canada (WTC) proposed evaluation protocol for final use of solidified waste. The evaluation protocol involve two

levels of testing, level 1 for chemical immobilization and level 2 for physical entrapment (Spence and Shi, 2004). The WTC proposed two utilization and two disposal scenarios based on the U.S.EPA maximum concentration limit and drinking water quality limit (DWQL) as follows:

1. Unrestricted utilization.

The unrestricted utilization would require the S/S material to have negligible leaching potential and can be considered for use in any way similar to natural material. The leachate concentration must meet the drinking water quality limit (DWQL).

2. Controlled utilization.

A controlled utilization requires the S/S material to have leaching potential acceptable for the specific usage. The leachate concentration achieved five times of DWQL.

3. Segregated landfill.

Solidified waste that fails to satisfy utilization is sent to segregated landfill which does not necessary have an engineered barrier or leachate collection system. The leachate concentration achieved ten times of DWQL. Solidified waste for disposal is also subjected to Malaysian landfill criteria as given in Table 2.12.

4. Sanitary landfill.

The S/S material can be sent for co-disposal with garbage material in sanitary landfill if the leachate meets the U.S.EPA TCLP maximum concentration limit.

Attractive cement features in waste S/S governed by the cement potential to perform the following mechanisms:

1. Ions absorption / adsorption on C-S-H surface.
2. Precipitation of insoluble hydroxide at high alkalinity.
3. Lattice incorporation into crystalline component of set cement.
4. Development of hydrous silicate and calcium salts.

Up scaling requires a detail design of engineering properties as the large scale will cause non ideal case to the kinetic of materials in process plant. Down scale will minimize the design parameters and might cause changes in the process performance. Full scale treatment plant of waste S/S can be employed based on the four treatment options:

1. In-drum mixing

Suitable for small quantity of toxic waste that been stored in drum but the option has relatively high cost compared to other options.

2. In-situ mixing

This option is more suitable for large volume of low reactivity and low solid content slurries or sludges. This method is the lowest-cost alternative.

3. Mobile plant

The on-site application of mobile plant is suitable for large volume of liquid, slurry or solid and permit transferable final disposal of cured waste.

4. Area mixing

Area mixing involves the spreading of waste and treatment agent in alternating layer at the on-site application. The alternative is more suitable for the treatment of high solid content waste or contaminated soils.

Cost element is tabulated in Table 4.28 as a comparison of the four alternatives quoted in U.S. dollars for a total of 2850 tons of waste by Portland cement and additive of sodium silicate (Barth, et al., 1990). In-situ mixing has the lowest-cost alternative with contracted price of \$32.28 per ton. Typical equipment required for the S/S work for in-drum mixing includes storage, chemical batching system, mixing system, and drum handling system.

Table 4.28: Cost estimation of waste S/S alternatives by Portland cement in U.S. dollar

(adopted from Barth, et al., 1990)

| <i>Cost element</i> | <i>In-drum mixing</i> | <i>In-situ mixing</i> | <i>Mobile mixing</i> | <i>Area mixing</i> |
|---|-----------------------|-----------------------|----------------------|--------------------|
| Capex: | | | | |
| Equipment rental | 8.48/ton | 1.38/ton | 3.93/ton | 4.07/ton |
| Opex: | | | | |
| Reagent | 20.50/ton | 20.50/ton | 20.50/ton | 20.50/ton |
| Material | 48.18/drum | - | - | - |
| Labour | 51.07/ton | 1.36/ton | 3.83/ton | 6.35/ton |
| Mobilization/ demobilization and site cleanup | 15.68/ton | 1.58/ton | 1.43/ton | 1.20/ton |
| Total cost | 172.57/ton | 24.83/ton | 29.69/ton | 32.11/ton |
| Overhead/ profit (30 %) | 51.72/ton | 7.45/ton | 8.91/ton | 9.63/ton |
| Total contracted price | 224.29/ton | 32.28/ton | 38.60/ton | 41.75/ton |

S/S treatment at the centralized treatment plant was rated at RM810/ton waste, which is considered acceptable to the large manufacturer but may cause a burden for small to the medium-size manufacturer. Landfill cost per ton is cheaper with RM495 compared to the incineration and physical-chemical treatment with RM2790 to RM3600 and RM3780 per ton accordingly.

The use of cement as an immobilization medium has numerous advantages, which may attract waste generators to consider S/S as one of the achievable methods for managing their waste. The associated advantages include the inertness of cement and fire resistant, corrosion resistant, simple batching plant, cheaper cost and ease of handling.

4.6 Application of S/S to Organic or Mixed Waste

The flowchart of Portland cement S/S for organic or mixed waste application is illustrated in Figure 4.75.

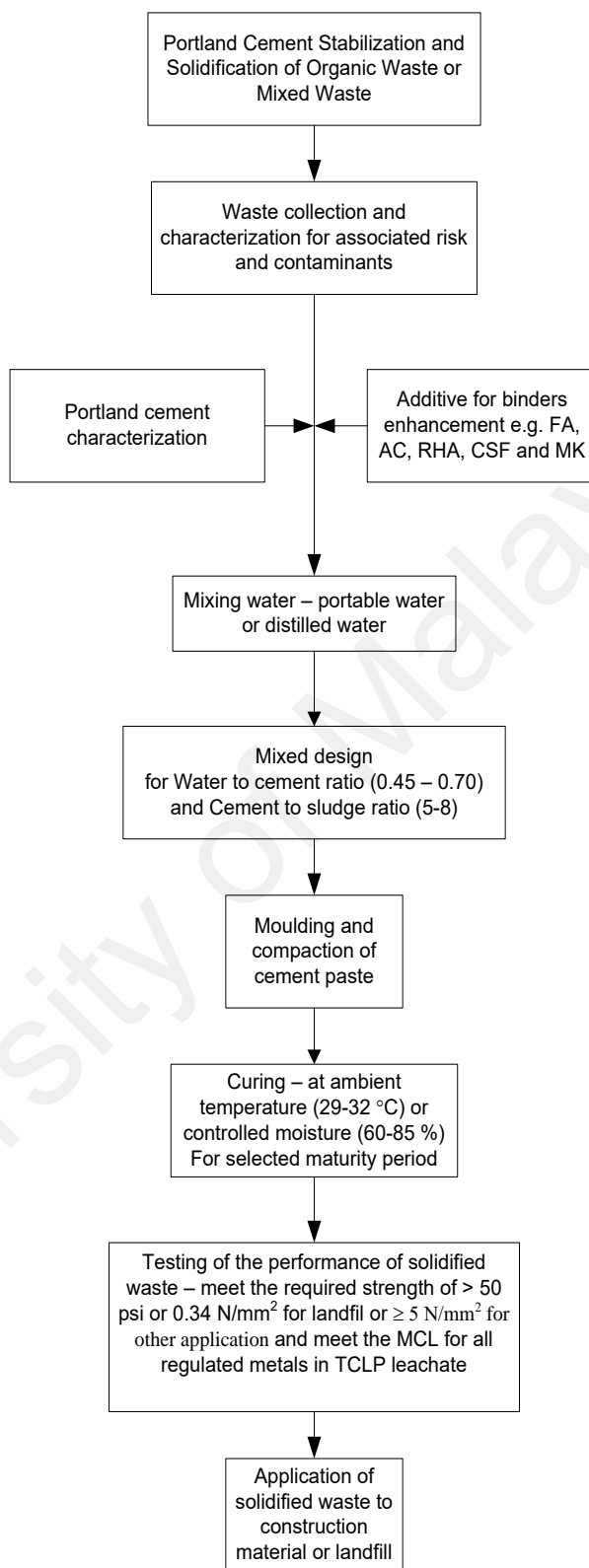


Figure 4.75: The application of S/S on organic or mixed waste

CHAPTER 5.1 CONCLUSIONS AND RECOMMENDATIONS

5.1 Conclusions

The objective of the study was to explore the potential of real petroleum sludge for S/S application using Portland cement as a main binder and selected CRMs namely CSF, FA, AC, MK and RHA. This work has investigated the optimum design parameters of water to cement ratio, cement to sludge ratio and the percentage of CRMs using the performance indicators of unconfined compressive strength of the monolith and leachability of the solidified sludge. The binder and solidified sludge properties were also investigated, which include physical, chemical and microstructure through numerous means of methods.

Based on the conducted experiments and results, the main conclusions can be made from a series of S/S performance parameter tests. The finding of the research can be classified into three areas, strengths, relationship of strength and porosity, leachability and microstructure. Leachability can be extended further to the inorganic metals and organic contaminants measurement.

The following objectives were met in this research:

1. Characterization of sludge and binders properties

The sludge was containing both inorganic and mostly organic contaminant, which indicates that the petroleum sludge was classified as toxic waste in nature. This includes benzene, classified as a known human carcinogen, at 21.0 mg/kg. The dried sludge has morphology of interconnected oily globules forming thick sludge layers.

Binder's property investigated include the cement component using the Bogue method showing that the main components were tricalcium silicate, C_3S and dicalcium silicate, C_2S . Most of the binder's physical and chemical properties may have direct influence to the performance parameters in immobilizing the sludge. The OPC was characterized by high conductivity with minimum reducing surface charge.

2. The optimum water to cement ratio and cement to the sludge ratio

The strength development in the OPC is controlled by the W/C. The solidified OPC of W/C 0.4 performed better at the 28-day period. The solidified sludge tested in narrowed range W/C ratio of 0.4 to 0.5 for an extended period of 180-day showed that the sample with W/C ratio 0.45 and C/Sd ratio of 8 gives the highest strength 38.16 N/mm^2 . The strength was slightly lower than the controlled OPC at the same W/C and curing period.

The addition of spike metals in the solidified sludge has contributed to the increased in strength value. Consequently the spike metals being transformed into metal hydroxides that encapsulated the sludge.

RHA was found to increase the strength up to day 90, thereafter the solidified sludge showed a sharp increased in the strength exceeding the CRMs strength at all percentage. The inclusion of 5 % weight CRMs has exhibited optimum strength than the higher percentage at 180-day. RHA recorded the highest strength value 28.34 N/mm^2 of all other CRMs. However, the solidified sludge without CRMs performed a better strength of 38.16 N/mm^2 . All strength values were well above the U.S.EPA stabilized material guideline of 0.24 N/mm^2 .

3. Effect of porosity to the strength, water to cement and cement to sludge

Permeable porosity was found to increase with the increased of cement to the sludge ratio. However, lower water to cement ratio indicate fewer permeable pores. The increased in CRMs percentage has exhibited a reduction in density. The AC, FA and CSF were less affected by permeable porosity.

The relationship of isostrength with porosity and cement to sludge showed contrast effect between solidified OPC and solidified sludge. Solidified OPC illustrates decreasing porosity with the strength but solidified sludge has an increasing porosity with strength for higher water to cement 0.45 and 0.5. However, at water to cement 0.4, rises in porosity has negatively affected the strength. The strength development was less affected by the cement to sludge at water to cement of 0.45.

The isostrength based on permeable pore and CRMs percentage depicts the maximum peaks were dominated by 5 % CRMs and lower porosity for all CRMs.

BET adsorption of solidified sludge followed the isotherm type IV with tapered/wedge hysteresis indicate the mesoporous monolith dominated by pore sizes of 20 to 500 Å. BJH cumulative adsorption pore volumes of solidified sludge with 5 % weight CSF, FA and MK exhibited the increased in micropore volume with the diameter of 10 to 20 Å.

The average pore diameter was increased by the incorporation of 5 % weight CRMs except FA. Accumulated pore volume in solidified sludge of 5 % weight of MK and RHA rise by 1.0 and 1.25 units higher compared to the solidified sludge.

4. Contaminant's immobilization by TCLP and semi-dynamic leaching tests

Solidified sludge showed minimum metals leached in TCLP extract with higher W/C of 0.5 having the lowest leaching values. No copper was found in the leachate for all samples of W/C ratios. pH of the leachate was in the range of 11.22 to 12.25. Solidified sludge with CRMs had the minimum leachability of metals. CRMs incorporation has increased the pH value 0.25 to 0.5 unit higher than solidified sludge.

Semi-dynamic leaching study indicates the leaching rate curve of most metal signify the diffusion leaching. The leaching dynamic of metal diffusion was under the pH control. Leaching achieved equilibrium at pH about 9.5 where acetate ions were dominating the solution and hydronium ion already depleted in reducing redox potential. Leachability indexes for most metals were above 6 for S/S utilization limit. Leaching mechanism of metals was governed by wash-off and diffusion. Fe and Pb formed lowest and highest diffusion coefficient accordingly, which are consistent with all CRMs. RHA5 performed the best average metal reduction in an acidic medium with 97.68 % while AC5 or MK5 formed the next-best options for organic sludge S/S. The TCLP and semi-dynamic metals were below the applicable standard.

5. Microstructure properties of solidified sludge

The morphology of solidified sludge exhibits the ettringite and C-S-H as the main products of cement hydration. However, sludge inclusion has changed the cement surface with lubricating effect of oily waste to the cement hydration products which formed more interconnected C-S-H with lack of ettringite and fewer voids.

Elemental analysis of solidified sludge indicates calcium as main element distributed as CH, C-S-H and ettringite. The CRMs incorporation has reduced the calcium concurrent with the rise of carbon content by converted into calcite. Pozzolanic activity has caused slight reduction of silica content in the solidified sludge or sludge with CRMs compared to solidified OPC. Solidified sludge with CSF exhibit ettringite surface due to its silica content while AC incorporation attributed to the finer surface due to it large surface area for contaminant absorption. MK inclusion indicates more voids but FA and RHA depicts amorphous C-S-H.

XRD diffractograms indicate major crystal formed was polymorph rhombohedron calcite as a result of carbonation reaction based on the reactants of CO_2 with either C-S-H or CH in all solidified sludges. TGA analysis showed that active pozzolanic reaction has occurred in solidified sludge with CRMs with significant weight loss of $\text{Ca}(\text{OH})_2$ at 300 to 500°C recorded 4.0 to 6.3 %. Carbonation product's decomposition also formed significant weight loss of 4.6 to 8.4 % observed at the temperature of 500 to 800°C in solidified sludge with CRMs.

6. Organic analysis

Solidified sludge contained linear or branched aliphatic hydrocarbon of C14 to C64 with long chain carbon, which was quite resistant to biodegradation. The leachate of solidified petroleum sludges were composed of cyclic siloxane or acid ester as a derivate product of leached silica reaction with hydrocarbon and carboxylic acid reaction on hydrocarbon. Silica has high affinity toward reverse charge's anion such as oxygen. The aliphatic hydrocarbon found in the leachate was reduced tenfold of its concurrent solidified sludge.

Oil and grease were reduced by 99.5 % in solidified sludge with 5 % AC, MK and RHA compared to other binders.

^1H -NMR proton in the solidified sludge was classified as alkyl group hydrogen of RCH_3 , RCH_2R and R_3CH while leachate was formed by similar ^1H groups with additional aromatic proton. The ^{13}C -NMR indicates the presence of carbon-13 in formed of straight chain alkanes composed of 5 to 13 carbon types, which may constitute a single compound or overlapping compounds. All organic contaminants in the leachate were below the standard, and none of the detected volatiles were toxicity constituents.

5.2 Recommendations

The current work has focus to certain aspects of S/S application. The immobilization of real petroleum sludge showed inhibition effect in a complex S/S system. The current work may be extended further with different focus or aspects, which complement the current works. Extended research works on waste S/S are recommended as follows:

1. The S/S should be tested to synthetic organic sludge for individual compound that presence in the real sludge. Interference caused by synergy effect of contaminants is under control, and the comparison can be made by conducting the combination of contaminants.
2. Different binders might work in a different way to immobilize organic sludge. Numerous binders are available for optimize the S/S process. The industrial by product as parts of CRMs are worth investigating since its can benefitted the waste material and economically viable.

3. Waste S/S should be conducted in the field instead of in the laboratory work environment. The weather effect under direct sunlight or rainfall might give different result compared to control laboratory media. The real field S/S placement will reduce the deviation in the output data for industrial application. This will minimize error in design parameters.
4. Development of propriety binders can be formulated by choosing the right proportion and compatible binders' material for waste S/S process. However, this will require a lot of trial series. The advantage was it can be made as a commercial product or patent.
5. The continuous leaching should be tested by simulate the flow through leaching to test on the contaminant migration in real environment.
6. The final recommendation was to study different type of parameters like the heat of hydration that may effects to the mechanistic of cement hydration. The durability of solidified waste subjected to certain force or application will attract the interested user in terms of its capability for reuse, recycle and reproduced as construction materials by manufacturers or stakeholders.

REFERENCES

- Abdullah, K., Hussin, M.W., Zakaria, F., Muhamad, R. and Abdul Hamid, Z. (2006) *POFA: A potential partial cement replacement material in aerated concrete*. Paper presented at 6th Asia-Pacific Structural Engineering and Construction Conference, Kuala Lumpur, Malaysia.
- Abdul Majid, Z., Shaaban, M. G. and Mahmud, H. (1996). *Cement-based Stabilization/solidification Technology in Hazardous Waste Stabilization: Review of Interference Mechanisms*. Paper presented at the Conference on Solid and Industrial Waste Management Systems, Kuala Lumpur, Malaysia.
- Abu Bakar, T. (2008). Special Waste Management, Department of Environment. Personal communication.
- ACI. (1998). Standard Practice for Selecting Proportions for Normal, Heavyweight, and Mass Concrete *Concrete Tools Proportioning and Handling Concrete* (Vol. 2, pp. 35). USA: ACI International American Concrete Institute.
- ACI. (1995). Guide to Shotcrete, ACI Committee 506 (Vol. 4, pp.8). USA: ACI International American Concrete Institute.
- ACI, C. R. (2003). Use of Fly Ash in Concrete (pp. 41): American Concrete Institute.
- ACI. (2006). Guide for the Use of Silica Fume in Concrete, 234R-06, A. C. (pp. 63): American Concrete Institute.
- Akhter, H., Cartledge, F. K., Roy, A. and Tittlebaum, M. E. (1997). Solidification/stabilization of arsenic salts: effects of long cure times. *J. of Hazardous materials*, 52, 247-264.
- Al-Tabba, A. and Perera, A. S. R. (2003). State of Practice Report. UK Stabilisation/Solidification Treatment and Remediation: Binders and Technology - Part II Research (E. Department, Trans.) (pp. 12). Cambridge: Cambridge University.
- Alonso, J. L. and Wesche, K. (1991). Characterization of Fly Ash. In K. Wesche (Ed.), *Rilem Report 7: Fly Ash in Concrete Properties and Performance* (pp. 3-23): RILEM.
- Ambroise, J., Maximilien, S. and Pera, J. (1994). Properties of metakaolin blended cements. *Advanced Cement Based Materials*, 1, 161-168.
- ANS. (2003). ANSI/ANS 16.1-2003 Measurement of the leachability of solidified low-level radioactive wastes by a short term procedure. La Grande Park, IL.
- APHA, AWWA and WEF. (1990). *Standard Test Method for the Analysis of Water and Wastewater* (20 ed.). Washington DC.

- Asavapisit, S., Nanthamontry, W. and Polprasert, C. (2001). Influence of condensed silica fume on the properties of cement-based solidified wastes. *Cement and Concrete Research*, 31, 1147-1152.
- Asbridge, A. H., Walters, G. V. and Jones, T. R. (2001). *Ternary blended concrete-OPC/GCFS/metakaolin*. Denmark.
- ASTM. (2005). Standard Test Methods for Time of Setting of Hydraulic Cement by Vicat Needle *Cement; Lime; Gypsum* (pp. 179-185): ASTM International.
- ASTM International. (2005a). ASTM C109-91 Standard Test Method for Compressive Strength of Hydraulic Cement Mortars *Cement, Lime, Gypsum* (pp. 76-81): ASTM International.
- ASTM International. (2005b). ASTM C642 Standard Test Method for Density, Absorption, and Voids in Hardened Concrete *Cement, Lime, Gypsum* (pp. 321-322).
- Ata, A. and Vipulanandan, C. (Eds.). (1997). *Silica Fume in Cement and Silicate Grouts and Grouted Sands*. New York: ASCE.
- Athenasious, K. K. and Evangelos, A. V. (2007). Cement-based Stabilization/solidification of Refinery Sludge: Leaching behaviour of alkanes and PAHs. *J. of Hazardous Materials*, 148, 122-135.
- AUSTROADS (2004). Pavement design – A guide to the structural design of road pavement. Austroads Inc.
- Badogiannis, E., Kakali, G., Dimopoulou, G., Chaniotakis, E. and Tsivilis, S. (2005). Metakaolin as a Main Cement Constituent: Exploitation of Poor Greek Kaolins. *Cement and Concrete Composites*, 27, 197-203.
- Barker, C., Robins, W. K., Hsu, C. S. and Drew, L. J. (2007). Petroleum Introduction *Petroleum Technology* (Vol. 1, pp. 1-42): Lewis.
- Barth, E. F., de Percin, P., Arozarena, M. M., Zieleniewski, J. L., Dosani, M., Maxey, H. R., Hokanson, S. A., Pryately, C. A. Whipple, T., Kravitz, R., Cullinane, M. J. R., Jones, L. W., Malone, P. G. and USEPA. (1990). *Stabilization and Solidification of Hazardous Wastes*. Park Ridge: Noyes Data Corporation.
- Beall, C. and Jaffe, R. (2003). *Concrete and Masonry Databook*: McGraw Hill.
- Bijen, J., Skalny, J. P. and Vazquez, E. (1991). Other Uses of Fly Ash. In K. Wesche (Ed.), *Rilem Report 7: Fly Ash in Concrete Properties and Performance* (pp. 160-178): Rilem.
- Bone, B. D., Barnard, L. H., Boardman, D. I., Carey, P. J., Jones, H. M., Macleod, C. L. and Tyrer, M. (2004). Review of scientific literature on the use of

stabilisation/solidification for the treatment of contaminated soil, solid waste and sludges (CASSST, Trans.). West Almondsbury, Bristol: Environment Agency.

- Brooks, J. J. and Johari, M. M. A. (2001). Effect of Metakaolin on Creep and Shrinkage of Concrete. *Cement & Concrete Composites*, 23, 495-502.
- Brown, W. H. (2000). *Introduction to Organic Chemistry* (2 ed.): Sander Collage Publishing.
- BSI. (1978). BS 4550 Part 3 Test for Heat of Hydration, Methods of Testing Cement, Physical Tests. London: British Standard Institution.
- BSI. (1983). BS 1881: Part 116 Method for Determination of Compressive Strength of Concrete Cubes *Testing Concrete*. London.
- Caijun, S. and Roger, S. (2004). Designing of Cement-Based Formula for Solidification/Stabilization of Hazardous, Radioactive, and Mixed Wastes. *Critical Reviews in Environmental Science and Technology*, 34, 391-417. doi: 10.1080/10643380490443281
- Caldarone, M. A., Gruber, K. A. and Burg, R. G. (1994). High-reactivity metakaolin: a new generation mineral admixture. *Concrete International*, 16(11), 37-40.
- Chen, Q. Y., Hills, C. D., Tyrer, M., Slipper, I., Shen, H. G. and Brough, A. (2007). Characterization of Products of Tricalcium Silicate Hydration in the Presence of Heavy Metals. *J. of Hazardous materials*, 147, 817-825.
- Cheng, K. Y. (1991). *Controlling Mechanisms of Metals Release from Cement-based Waste form in Acetic Acid Solution*. Ph.D, University of Cincinnati, U.S.
- CIRIA. (1995). Remedial Treatment for Contaminated Land *Ex-situ Remedial Methods for Soils, Sludges and Sediments* (Vol. VII): CIRIA.
- Cocke, D. L. and Mollah, M. Y. A. (1992). The Chemistry and Leaching Mechanisms of Hazardous Substances in Cementitious Solidification/Stabilization Systems. In R. D. Spence (Ed.), *Chemistry and Microstructure of Solidified Waste Forms* (pp. 187-242): Lewis Publishers.
- Conner, J. R. (1990). *Chemical Fixation and Solidification of Hazardous Wastes*. New York: Van Nostrand Reinhold.
- Conner, J. R. (1992). Chemistry of Cementitious Solidified/Stabilized Waste Form. In R. D. Spence (Ed.), *Chemistry and Microstructure of Solidified Waste Forms* (pp. 41-82): Lewis.
- Conner, J. R. (1994). Chemical Stabilization of Contaminated Soils. In D. J. Wilson & A. N. Clarke (Eds.), *Hazardous Waste Site Soil Remediation, Theory and Application of Innovative Technologies* (pp. 80-169). New York: Marcel and Dekker.

- Conner, J. R. (1996). Recent Findings on Immobilization of Organics as Measured by Total Constituent Analysis. *Waste Management*, 15(5/6), 359-369.
- Cote, P. (1986). *Contaminant Leaching from Cement-based Waste Forms under Acidic Conditions*. Ph.D, McMaster University, Ontario, Canada.
- Cote, P. and Isabel, D. (1984). Application of a dynamic leaching test to solidified hazardous wastes. In L. P. Jackson, A. R. Rohlik & R. A. Conways (Eds.), *Hazardous Industrial Solid Waste Testing: 3rd Symposium* (Vol. ASTM STP 851, pp. 48-60): ASTM.
- Cullinane, M. J. J. and Bricka, R. M. (1992). An Evaluation of Organic Materials That Interfere with Stabilization/Solidification Processes. In E. J. Calabrese and P. T. Kostecki (Eds.), *Principles and Practices for Petroleum Contaminated Soils* (pp. 349-385). Chelsea: Lewis.
- Cussler, E. L. (2009). *Diffusion Mass Transfer in Fluid Systems* (3 ed.): Cambridge University Press.
- de Groot, G. J. and van der Sloot, H. A. (Eds.). (1992). *Determination of Leaching Characteristic of Waste Materials Leading to Environmental Product Certification* (Vol. 1123). Philadelphia: ASTM.
- De Veaux, R. D., Velleman, P. F. and Bock, D. E. (2005). *Stat: Data and Models*: Pearson Education.
- DOE. (2008). Scheduled Waste Management. *Impact*, 1, 11.
- DOE. (2005). Environmental Quality (Scheduled Wastes) Regulations 2005, Section 7, Lawnet Percetakan National Malaysia Berhad, 1-38.
- Dutre, V., Kestens, C., Schaep, J. and Vandecasteele, C. (1998). Study of the remediation of a site contaminated with arsenic. *Sci. Total Environ.*, 220, 185-194.
- Dutre, V. and Vandecasteele, C. (1995). Solidification/stabilisation of hazardous arsenic containing waste from a copper refining process. *J. of Hazardous Materials*, 40, 55-68.
- Dutre, V., Vandecasteele, C. and Opdenakker, S. (1999). Oxidation of arsenic bearing fly ash as pretreatment before solidification. *J. of Hazardous Materials*, 68, 205-215.
- Eaton, H. C., Walsh, M. B., Tittlebaum, M. E., Cartledge, F. K., & Chalasani, D. (1987). Organic interference of solidified/stabilized hazardous wastes. *Environmental Monitoring and Assessment*, 9, 133-142.
- El-Kamash, A.M., El-Naggar, M.R. and El-Dessouky, M.I. (2006). Immobilization of cesium and strontium radionuclides in zeolite-cement blends. *J. of Hazardous Materials*, B136, 310-316.

- EPRI. (2004). In-Situ Solidification/ Stabilization (ISS) Bench-Scale Testing of Manufactured Gas Plant (MGP) Impacted Soils. Palo Alto: EPRI.
- Eskander, S.B., Abdel Aziz, S.M., El-Didamony, H. and Sayed, M.I. (2011). Immobilization of low and intermediate level of organic radioactive wastes in cement matrices. *J. of Hazardous Materials*, 190, 969-979.
- FIP. (1988). Condensed silica fume in concrete *State of the art report* (pp. 37). London: FIP.
- Frias, M. and Cabrera, J. (2000). Pore size distribution and degree of hydration of MK-cement pastes. *Cement and Concrete Research*, 30, 561-569.
- Fuessle, R. W. and Taylor, M. A. (2000). Stabilization of arsenic and barium-rich glass manufacturing waste. *J. of Environ. Eng.*, 126, 272-278.
- Fuessle, R. W. and Taylor, M. A. (2004). Stabilization of arsenite wastes with proir oxidation. *J. of Environ. Eng.*, 130, 1063-1066.
- Gani, M. S. J. (1997). *Cement and Concrete*. London: Chapman & Hall.
- Garrabrants, A. C. and Kosson, D. S. (2004). Leaching Processes and Evaluation Test for Inorganic Constituent Release from Cement-Based Matrices. In R. D. Spence & C. Shi (Eds.), *Stabilization and Solidification of Hazardous, Radioactive and Mixed Waste* (pp. 229-280): CRC Press.
- Ghosh, A. and Subbarao, C. (1998). Hydraulic conductivity and leachate characteristics of stabilized fly ash. *J. of Environ Eng.*, 124, 812-820.
- Gitipour, S., Bowers, M. T. and Bodocsi, A. (1997). The used of modified bentonite for removal of aromatic organics from contaminated soil. *J. of Colloid Interf. Sci.*, 196, 191-198.
- Glasser, F. P. (1993). Chemistry of Cement-Solidified Waste Forms. In R. Spence (Ed.), *Chemistry and Microstructure of Solidified Forms* (pp. 276). Lewis Publisher.
- Glasser, F. P. (1997). Fundamental aspects of cement solidification and stabilisation. *J. of Hazardous Materials*, 52, 151-170.
- Grasso, D. (1993). *Hazardous Waste Site Remediation: Source Control*: Lewis Publisher.
- Griesbaum, K., Behr, A., Biedenkapp, D., Voges, H. W., Garbe, D., Paetz, C., Colin, G., Mayer, D. and Hoke, H. (2007). Hydrocarbon *Petroleum Technology* (Vol. 2, pp. 591-651): John Wiley & Sons Inc.
- Hearn, N., Hooton, R. D. and Nokken, M. R. (2006). Pore Structure, Permeability, and Penetration Resistance Characteristics of Concrete. In J. F. Lamond and J. H. Peielert (Eds.), *Significance of Test and Properties of Concrete & Concrete-Making Materials* (pp. 238-252). West Conshohocken: ASTM International.

- Ho, C.E. (1998). A jet grout stabilized exclusion beneath on existing building. In L. Johnsen, and D. Berry (Eds.), *Grouts and grouting a potpourri of projects* (pp. 1-15). ASCE.
- IChemE. (2005). *Hazardous Substances in Refineries*. Rugby: Institution of Chemical Engineers.
- Ilic, M. R. and Polic, P. S. (2005). Solidification /Stabilization Technologies for the Prevention of Surface and Ground Water Pollution from Hazardous Wastes. In D. Barcelo and M. Petrovic (Eds.), *Handbook of Environ Chem* (Vol. 5, pp. 159-189). Berlin Heidelberg: Springer-Verlag.
- IPPC Bureau. (2001). Integrated Pollution Prevention and Control (IPPC) Reference Document on Best Available Techniques for Mineral Oil and Gas Refineries *Reference Document on Best Available Techniques for Mineral Oil and Gas Refineries* (pp. 379-390). Spain: IPPC.
- Jacob Consultancy Inc. (2002). Water Pollution Prevention Opportunities in Petroleum Refineries *Ecology Publication No. 02-07-017*. Texas: Washington State Department of Ecology.
- Jing, C., Korfiatis, G. P. and Meng, X. (2003). Immobilization mechanisms of arsenate in iron hydroxide sludge stabilized with cement. *J. of Environ. Sci. Technol.*, 37, 5050-5065.
- Jones, L. W. (1990). Interference Mechanisms in Waste Stabilization/Solidification Processes. *J. of Hazardous Materials*, 24, 83-88.
- Kakali, G., Tsivilis, S. and Tsialtas, A. (1998). Hydration of ordinary portland cement made from raw mix containing transition elements. *Cement and Concrete Research*, 28, 335-340.
- Kalb, P. D. (2004). Organic Polymers for Stabilization/Solidification. In R. D. Spence & C. Shi (Eds.), *Stabilization and Solidification of Hazardous, Radioactive and Mixed Wastes* (pp. 79-96): CRC Press.
- Kalinowsky, H. O., Berger, S. and Braun, S. (1984). ^{13}C NMR Spectroskopie. Available from Reich, H.J.-UWMadison NMR Spectra Retrieved Dec 2011, from Georg Thieme Verlag <http://www.chem.wisc.edu/areas/reich/handouts/nmr-h/hdata-cont.htm>
- Kamarudin, Z. and M Radzi, M. R. (2002). Energy Outlook of Malaysia (1985 - 2025) (E. Environment, Trans.) (pp. 30): Petroliam Nasional Berhad.
- Karamalidis, A. K. and Voudrias, E. A. (2007). Release of Zn, Ni, Cu, SO₄²⁻ and CrO₄²⁻ as a function of pH from cement-based stabilized/solidified refinery oily sludge and ash from incineration of oily sludge. *J. of Hazardous Materials*, 141, 591-606.

- Kualiti Alam Sdn Bhd. (2003). *Scheduled Waste Management Guide*. Kuala Lumpur.
- La Grega, M. D., Bungkingham, P. L., & Evans, J. C. (2001). *Hazardous Waste Management*: McGraw Hill.
- Lane, R. O. and Best, J. F. (1982). Properties and Use of Fly Ash in Portland Cement Concrete. *Concrete International*, 4(7), 81-92.
- Lee, D. J. (2004). *Solidification /Stabilization Mechanisms of Calcite on Solidified Waste Forms*. Ph.D, University of New South Wales, Australia.
- Leist, M., Casey, R. J. and Caridi, D. (2003). The fixation and leaching of cement stabilized arsenic. *Waste Management*, 23, 353-359.
- Linghong, Z., Lionel, J. J. C., Andrew, C. L. and Stephen, D. K. (2008). Effect of sucrose and sorbitol on cement-based stabilization/solidification of toxic metal waste. *J. of Hazardous Materials*, 151, 490-498.
- Lo, I. M. C. (1996). Solidification/Stabilization of Phenolic Waste using Organic Clay Complex. *J. of Environ Eng.*, 122, 850-855.
- MADEP. (2004). Method for the Determination of Extractable Petroleum Hydrocarbons (EPH) (pp. 60): MADEP.
- Malhotra, V. M. and Mehta, P. K. (1996). *Pozzolonic and Cementitious Materials - Advances in Concrete Technology* (Vol. 1): Taylor & Francis.
- Marcos, A. R. S., Liciana, M., Maria, M., Sauza, S., Albertina, X. R., Correa, R. S. and Claudemir, M. R. (2007). Small Hazardous Waste Generator in Developing Countries: Use of Stabilization/Solidification Process as an Economic Tool for Metal Wastewater Treatment and Appropriate Sludge Disposal. *J. of Hazardous materials*, 147, 986-990.
- Marshall, A. G. and Verdun, F. R. (1990). *Fourier Transform in NMR, Optical and Mass Spectrometry A User Handbook*. Netherlands: Elsevier Science Publisher.
- Martin, W. F., Lippitt, J. M. and Webb, P. J. (2000). *Hazardous Waste Handbook for Health and Safety* (3 ed.): Butterworth-Heinemann.
- Mattus, C. H. and Gilliam, T. M. (1994). A literature review of mixed waste components sensitives and effects upon solidification/stabilization in cement-based matrixes (Office of T. Development, Trans.). Washington: U.S. Department of Energy.
- Means, J. L., Smith, L. A., Nehring, K. W., Brauning, S. E., Gavaskar, A. R., Sass, B. M., Wiles, C.C. and Mashni, C. I. (1995). *The Application of Solidification/Stabilization to Waste Materials*: Lewis Publisher.

- Mehta, P. K. (1979). *The Chemistry and Technology of Cement Made from Rice Husk Ash*. Paper presented at the UNIDO/ESCAP/RCTT Workshop on Rice Husk Cements, Peshawar, Pakistan.
- Mehta, P. K. and Monteiro, P. J. M. (2006). *Concrete Microstructure, Properties and Materials* (3 ed.): McGraw-Hill.
- Merrit, S. D. (1996). *Immobilization of uranium and nickel Sludges treated by solidification and stabilization*. Ph.D, Texan A&M Univ. Texas.
- MIDA. (2007). Profit from Malaysia's Petrochemical Industries (pp. 11).
- Miller, J., Akhter, H., Cartledge, F. K. and McLearn, M. (2000). Treatment of arsenic contaminated soils. II Treatability study and remediation. *J. of Environ Eng.*, 126, 1004-1012.
- Minocha, A. K., Jain, N. and Varma, C. L. (2003). Effects of Organics Materials on the Solidification of Heavy Metal Sludge. *Construction and Building Materials*, 17, 77-81.
- Mohd Zain, A. and Amran, N. A. (2008). *Refinery Sludge Waste Stabilisation and Solidification by Concrete and Brick Development*. Paper presented at the Brownfield Asia, 21-23 October, Kuala Lumpur.
- Montgomery, D. M. (1991). Treatment of Organic-contaminated Industrial Waste Using Cement-Based Stabilization/Solidification – Microstructural Analysis of the Organophilic Clay as a pre solidification Adsorbent. *Waste Management and Research*, 9(1), 113-125.
- Montgomery, D. M., Sollars, C. J., Perry, R., Tarling, S. E., Barnes, P. and Henderson, E. (1991). Treatment of organic-contaminated industrial wastes using cement-based stabilizatio/solidification-III. Microstructural analysis of the organophilic clay as a pre-solidification adsorbent. *Waste Management*, 9, 113-125.
- Moon, D. H. and Dermatas, D. (2006). An evaluation of lead leachability from stabilized/solidified soils under modified semi-dynamic leaching conditions. *Engineering Geology*, 85, 67-74.
- Moon, D. H., Dermatas, D. and Menounou, N. (2004). Arsenic immobilization by calcium arsenic precipitates in lime treated soils. *Sci. Total Environ*, 330, 171-185.
- Morgan, I. L. and Bostik, W. D. (1992). Performance Testing of Grout-Based Waste Forms for the Solidification of Anion Exchange Resins. In T. M. Gilliam and C. C. Wiles (Eds.), *Solidification/Stabilization of Hazardous, Radioactive and Mixed Wastes*. (Vol. 2, pp. 133-149). Philadelphia: ASTM
- Navidi, W. C. (2010). *Principles of Statistic for Engineers and Scientists*: McGraw Hill.

- Palfy, P., Vircikova, E. and Molnar, L. (1999). Processing of arsenic waste by precipitation and solidification. *Waste Management*, 19, 55-59.
- Pamukcu, S. (1993). Additive Stabilization of Petroleum Contaminated Soils. In E. J. Calabrese and P. T. Kostecki (Eds.), *Principles and Practices for Petroleum Contaminated Soils* (pp. 367-385). Chelsea: Lewis.
- Paria, S. and Yuet, P. K. (2006). Solidification/Stabilization of Organic and Inorganic Contaminant using Portland Cement: A Literature Review. *Environmental Reviews*, 14, 217-255.
- Pawliszyn, J. and Belardi, R. P. (1989). The application of chemically modified fused silica fibers in the extraction of organics from water matrix samples and their rapid transfer to capillary columns. *Water Pollution Res*, 24, 179-191.
- Pera, J., Thevenin, G. and Chabannet, M. (1997). Design of a Novel System Allowing the Selection of an Adequate Binder for Solidification/ Stabilization of Wastes. *Cement and Concrete Research*, 27(10), 1533-1542.
- Perera, A. S. R., Al-Tabbaa, A., Reid, J. M. and Johnson, D. (2003). State of Practice Report UK Stabilisation/Solidification, Treatment and Remediation - Part V: Long Term Performance and Environment Impact (pp. 22). Cambridge: Cambridge University.
- Peyronnard, O. and Benzaazoua, M. (2012). Alternative by-product based binders for cemented mine backfill: Recipes optimization using Taguchi method. *Minerals Engineering*, 29, 28-38.
- Pilgrim, M. J. (2011). *Method AK 102 For Determination of Diesel Range Organics*. Version 04/08/02. Alaska. Retrieved at June 15, 2011 from <http://www.dec.state.ak.us/eh/docs/lab/cs/AK102.pdf>.
- Ponder, T. C. and Schmitt, D. (1991). Field Assessment of Air Emissions from Hazardous Waste Stabilization Operations. In: *Remedial Action, Treatment, and Disposal of Hazardous Waste*, Proceeding of the 17th Annual Hazardous Waste Research Symposium (pp. 532-542) Washington D.C: USEPA.
- Poon, C. S., Lio, K. W. and Tang, C. I. (2001). A systematic study of cement/PFA chemical stabilisation/ solidification process for the treatment of heavy metal waste. *Waste Management and Research*, 19, 276-283.
- Radojevic, M. and Baskin, V. N. (2006). *Practical Environmental Analysis* (2 ed.): RSC Publishing.
- Roy, M. and Scheetz, B. E. (Eds.). (1992). *The Chemistry of Cementitious Systems for Waste Management: The Penn State Experience*: Lewis Publishers.

- Royal Society of Chemistry. (2011). ChemSpider Chemical Database. Available from RSC Worldwide Ltd. ChemSpider. Retrieved at Nov 12, 2011 from RSC Worldwide Ltd <http://www.chemspider.com/Chemical.Structures-1108.html>.
- Rukzon, S. and Chindaprasirt, P. (2008). Development of Classified Fly Ash as a Pozzolonic Material. *Applied Science*, 8(6), 1097-1102.
- Safiuddin, M. and Hearn, N. (2005). Comparison of ASTM saturation techniques for measuring the permeable porosity of concrete. *Cement and Concrete Research*, 35, 1008-1013. doi: 10.1016/j.cemconres.2004.09.017
- Senapati, P.K. and Mishra, B.K. (2012). Design consideration for hydraulic backfilling with coal combustion products (CCPs) at high solids concentrations. *Powder Technology*, 229, 119-125.
- Shefali, S., Rubina, C. and Divya, K. (2008). Influence of pH, curing time and environmental stress on the immobilization of hazardous waste using activated fly ash. *Cement and Concrete Research*, 153, 1103-1109.
- Shaaban, M. G. (1993). Stabilization and Solidification (S/S) of Hazardous Wastes, Evaluation of Cement-Based Method. Short Course on Solid and Hazardous Waste Management, 1-24, Universiti Kebangsaan Malaysia, Bangi.
- Shi, C. (2004). Hydraulic Cement Systems for Stabilization/Solidification. In R. D. Spence and C. Shi (Eds.), *Stabilization and Solidification of Hazardous, Radioactive and Mixed Wastes* (pp. 49-77): CRC Press.
- Shih, C. J. and Lin, C. F. (2003). Arsenic contaminated site at an abandoned copper smelter plant: waste characterization and solidification/stabilization treatment. *Chemosphere*, 53, 691-703.
- Siddique, R. (2003). Effect of Fine Aggregate Replacement with Class F Fly Ash on the Mechanical Properties of Concrete. *Cement and Concrete Research*, 33(4), 539-547.
- Siddique, R. (2008). *Materials and By-Products in Concrete*. Berlin Heidelberg: Springer-Verlag.
- Sina, K. and Maassoumeh, B. (2012). Review of soft soils stabilization by grouting and injection methods with different chemical binders. *Scientific Research and Essays*, 7(24), 2104-2111.
- Smart, L. (Ed.). (2002). *Separation, Purification and Identification -The molecular world data book*. Cambridge: Royal Society of Chemistry.
- Smith, B. (1999). *Infrared spectral interpretation a systematic approach*: CRC Press.
- Sollars, C. J. and Perry, R. (1989). Cement Based Stabilization of Wastes: Practical and Theoretical Considerations. *J. Int. of Water Eng. Management*, 3, 125-134.

- Spence, R. D. (Ed.). (1992). *Chemistry and Microstructure of Solidified Waste Forms*: Lewis Publisher.
- Spence, R. D. and Caijun, S. (2004). *Stabilization and Solidification of Hazardous, Radioactives and Mixed Wastes*. New York: CRC Press.
- Stegemann, P. C. and Zhou, Q. (2008). Screening Test for Assessing Treatability of Inorganic Industrial Waste by Stabilized and Solidified Cement. *Journal of Hazardous Materials*. doi: 101016/ihazard 2008 03090
- Suthersan, S. S. (1999). *Remediation Engineering Design Concepts*: Chapman & Hall.
- Taylor, H. F. W. (1990). *Cement Chemistry*. New York: Academic Press Inc.
- Taylor, H. F. W. (1997). *Cement Chemistry* (2 ed.). London: Thomas Telford Press.
- Thomas, N. L., Jameson, D. A. and Double, D. D. (1981). The effect of lead nitrate on the early hydration of Portland cement. *Cement and Concrete Research*, 11, 143-153.
- Trussel, S. and Spence, R. D. (1994). A review of solidification/ stabilisation interferences. *Waste Management*, 14, 507-521.
- Tseng, D. H. and Ho, J. J. (1986). *Solidification/stabilization of hazardous industrial sludges*. Paper presented at the Regional Symposium on Management of Industrial Wastes in Asia and Pacific/ Malaysian Chemical Congress, 17-20 November, Kuala Lumpur.
- U.S. Department of Transportation (2012). Fly ash facts for highway engineers. Federal Highway Administration. Retrieved at Dec 31, 2012 from <http://www.fhwa.dot.gov/pavement/recycling/facho1.cfm>.
- USEPA. (1986). Handbook for Stabilization/Solidification of Hazardous Wastes. H. W. E. R. Laboratory, Trans., Cincinnati, Ohio: U.S. Environmental Protection Agency
- USEPA. (1989). Solidification Process, Douglassville, PA (Office of Research & Dev., Risk Reduction Engineering Laboratory, Trans.) *Application Analysis Report* (pp. 51). Cincinnati, Ohio, U.S. Environmental Protection Agency.
- USEPA. (1990a). International Waste Technologies, Geo-Con Insitu Stabilization and Solidification, Applications of Analysis Report (Office of Research & Dev., Risk Reduction Engineering Laboratory, Trans.). Cincinnati, Ohio: U.S. Environmental Protection Agency.
- USEPA. (1990b). Soliditech, Inc. Solidification/Stabilization Process, Applications of Analysis Report (Off. of Research Dev., Risk Reduction Engineering Laboratory, Trans.). Cincinnati, Ohio: U.S. Environmental Protection Agency.

- USEPA. (1991). Chemfix Technologies, Inc. Solidification/Stabilization Process Application Analysis Report (Office of Research Dev. Risk Reduction Engineering Laboratory, Trans.). Cincinnati, Ohio: U.S. Environmental Protection Agency.
- USEPA. (1992). Study Innovative Treatment Technologies: Semi Annual Status Report. Office of Solid Waste and E. Response, Trans. (3 ed.). Washington DC.: U.S. Environmental Protection Agency.
- USEPA. (1993). Technical Resource Document: Solidification/ Stabilization and its Application to Waste Materials. Off. of Research and Development, Trans., Washington D.C.: U.S. Environmental Protection Agency.
- USEPA. (1996). SW-846 *Test Methods for Evaluating Waste, Physical/Chemical*. U.S.: U.S. Environmental Protection Agency.
- USEPA. (2000). Solidification/Stabilization Use at Superfund Sites. H. W. I. D. Office of Solid Waste, Trans., (pp. 9). Cincinnati, Ohio: U.S. Environmental Protection Agency.
- Vandecasteele, C., Dutre, V., Geysen, D. and Wauters, G. (2002). Solidification/stabilisation of arsenic bearing fly ash from the metallurgical industry. Immobilisation mechanism of arsenic. *Waste Management*, 22, 143-146.
- Vial, J. and Jardey, A. (2001). Quantitation by Internal Standard. In J. Cazes (Ed.), *Encyclopedia of Chromatography* (pp. 693-695), Marcel Dekker Inc.
- Vipulanandan, C. (1995). Effects of clays and cement on the solidification/stabilization of phenol-contaminated soils. *Waste Management*, 15, 399-406.
- Vipulanandan, C. and Krishnan, S. (1990). Solidification/Stabilization of phenolic waste with cementitious and polymeric materials. *Hazardous Materials*, 24, 123-136.
- Voigt, D. E., Brantley, S. L. and Hennes, R. J. C. (1996). Chemical fixation of arsenic in contaminated soils. *Appl. Geochem*, 11, 633-643.
- Wang, T. (2001). Quantitation by External Standard. In J. Cazes (Ed.), *Encyclopedia of Chromatography* (pp. 927): Marcel Dekker Inc.
- Wild, S., Khatib, J. M. and Jones, A. (1996). Relative Strength, Pozzolanic Activity and Cement Hydration in Superplasticised Metakaolin Concrete. *Cement and Concrete Research*, 26(10), 1537-1544.
- Wilk, C. M. (1997). Stabilisation of Heavy Metals with Portland Cement: Research Synopsis (P. W. Department, Trans.) *Waste Management Information*: Portland Cement Association, Skokie IL.
- Yin, C. Y., Mahmud, H. and Shaaban, M. G. (2006). Stabilization / Solidification of Lead-Contaminated Soil Using Cement and Rice Husk Ash. *Hazardous Materials*, B137, 1758-1764.

- Ying, T. S. and Yung, W. S. (1987). *Analisis Kuantitatif* (4 ed.): USM.
- Young, J. F. (1972). A Review of the Mechanisms of Set-Retardation in Portland Cement Pastes Containing Organic Admixtures. *Cement and Concrete Research*, 2, 415-433.
- Yu, Q., Sawayama, K., Sugita, S., Shoya, M. and Isojima, Y. (1999). The Reaction Between Rice-Husk Ash and $\text{Ca}(\text{OH})_2$ solution and the Nature of Its Products. *Cement and Concrete Research*, 29(1), 37-43.
- Zhang, M. H., Lastra, R. and Malhotra, V. M. (1996). Rice-Husk Ash Paste and Concrete: Some aspects of Hydration and the Microstructure of the Interfacial Zone Between the Aggregate and Paste. *Cement and Concrete Research*, 26(6), 963-977.
- Zhu, L., Chen, B. and Shen, X. (2000). Sorption of phenol p-nitrophenol, aniline to dual cation organobentonites from water. *Environ. Sci. Technol.*, 34, 468-475.

APPENDIX A: Physical properties of petroleum waste

Table A-1: pH

| Sample No | pH |
|-----------|------|
| 1 | 6.86 |
| 2 | 7.23 |
| 3 | 7.09 |
| Average | 7.06 |

Table A-2: Moisture Content (APHA 2540G)

| Sample No. | Container weight | Crucible + Sludge (wet) | Crucible + Sludge (dry) | Sludge (wet) | Sludge (dry) | Water Content |
|------------|------------------|-------------------------|-------------------------|--------------|--------------|---------------|
| | (g) | (g) | (g) | (g) | (g) | (%) |
| 1 | 86.80 | 111.83 | 97.28 | 25.02 | 10.48 | 58.14 |
| 2 | 95.71 | 121.74 | 108.14 | 26.02 | 12.43 | 52.23 |
| 3 | 93.21 | 118.30 | 105.48 | 25.08 | 12.27 | 51.07 |
| Average | | | | 25.37 | 11.73 | 53.81 |

$$\text{Moisture content} = (\text{Wet weight} - \text{dry weight}) / \text{Wet weight} \times 100 = 53.81\%$$

Table A-3: Total Solid (APHA 2540G), Volatile Solid and Fixed Solid

| Sample No. | Crucible | Crucible + Sludge (wet) | Crucible + Sludge (dry) | Crucible + Sludge (furnace dry) | Total Solid (%) | Volatile Solid (%) | Fixed Solid (%) |
|------------|----------|-------------------------|-------------------------|---------------------------------|-----------------|--------------------|-----------------|
| | B (g) | C (g) | A (g) | D (g) | | | |
| 1 | 86.80 | 111.83 | 97.28 | 87.64 | 41.88 | 92.0 | 7.99 |
| 2 | 95.71 | 121.74 | 108.14 | 96.68 | 47.76 | 92.19 | 7.80 |
| 3 | 93.21 | 118.30 | 105.48 | 94.18 | 48.92 | 92.05 | 7.94 |
| Average | | | | | 46.19 | 92.08 | 7.91 |

$$\text{Total solid} = (A - B) / (C - B) \times 100 = 46.19\%$$

$$\text{Volatile solid} = (A - D) / (A - B) \times 100 = 92.08\%$$

$$\text{Fixed solid} = (D - B) / (A - B) \times 100 = 7.91\%$$

Table A-4: Specific Gravity (APHA 2710F)

| Sample No. | Container, W | Container + Sludge, S | Container + Distilled water at 4°C, R | Distilled Water | Sludge | Specific Gravity |
|------------|--------------|-----------------------|---------------------------------------|-----------------|--------|------------------|
| | (g) | (g) | (g) | (g) | (g) | |
| 1 | 18.25 | 66.79 | 68.69 | 50.44 | 48.54 | 0.95 |
| 2 | 18.25 | 66.87 | 68.69 | 50.43 | 48.62 | 0.95 |
| 3 | 17.80 | 66.19 | 67.94 | 50.14 | 48.39 | 0.96 |
| Average | | | | 50.34 | 48.52 | 0.95 |

$$\text{Sludge temperature} = 25^\circ\text{C} (F=0.9975)$$

$$\text{Specific Gravity (SG)} = (S - W) / (R - W) \times F = 0.9596$$

APPENDIX B: Chemical properties of petroleum sludge

Table B-1: Oil & grease (APHA 5520E)

| Sample | Sample 1 | Sample 2 | Sample 3 | Average |
|---|----------|----------|----------|----------|
| Wet weight of sludge, g | 20.1880 | 20.0258 | 20.2148 | |
| Initial weight (wet sludge + flask) , g | 104.6987 | 104.6988 | 104.7569 | |
| Final weight, (residue + flask), g | 112.0468 | 112.2900 | 113.5301 | |
| Oil and grease, g | 7.3481 | 7.5912 | 8.7732 | |
| Dry Solid fraction | 0.3284 | 0.3284 | 0.3284 | |
| % of O&G as dry solid fraction | 110.8300 | 115.4200 | 132.1500 | 119.4667 |
| % of O&G | 36.3984 | 37.9071 | 43.3999 | 39.2351 |

Table B-2: Organic contaminant

| Organic Component | Concentration, mg/kg | |
|---------------------|----------------------|--------------------|
| Benzene | 21.0 | USEPA 5030B, 8260B |
| Toulene | 139.0 | USEPA 5030B, 8260B |
| Ethyl benzene | 23.0 | USEPA 5030B, 8260B |
| m-Xylene & p-Xylene | 325.0 | USEPA 5030B, 8260B |
| o-Xylenes | 98.0 | USEPA 5030B, 8260B |
| Naphthalene | 1,960.0 | USEPA 3570, 8270C |
| Phenanthrene | 251.0 | USEPA 3570, 8270C |

Table B-3: Total petroleum hydrocarbon (TPH)

| Component | Concentration (mg/kg) | Method |
|------------|-----------------------|--------------------|
| TPH | | |
| C6-C9 | 2,030.0 | USEPA 5030B, 8260B |
| C10-C14 | 270,000.0 | USEPA 3570, 8015B |
| C15-C28 | 537,000.0 | USEPA 3570, 8015B |
| C29-C36 | 21,900.0 | USEPA 3570, 8015B |
| TPH Total | 830,930.0 | |

Table B-4: Inorganic analysis using Nitric acid digestion APHA 3030E (mg/L)

| Element | Sample 1 | Sample 2 | Sample 3 | Ave |
|---------|----------|----------|----------|-------|
| Pb | ND | ND | ND | ND |
| Ni | 0 | 0 | 0 | 0.00 |
| Fe | 15.49 | 17.91 | 3.45 | 12.28 |
| Mn | ND | ND | ND | ND |
| Cr | ND | ND | ND | ND |
| Cu | ND | ND | ND | ND |
| Zn | ND | ND | ND | ND |
| Al | 12.48 | 15.11 | 2.808 | 10.13 |

APPENDIX C: Radar plots of TCLP leachate

Figure C-1: Radar plots of metal concentration in TCLP extract for solidified sludge (mg/L)

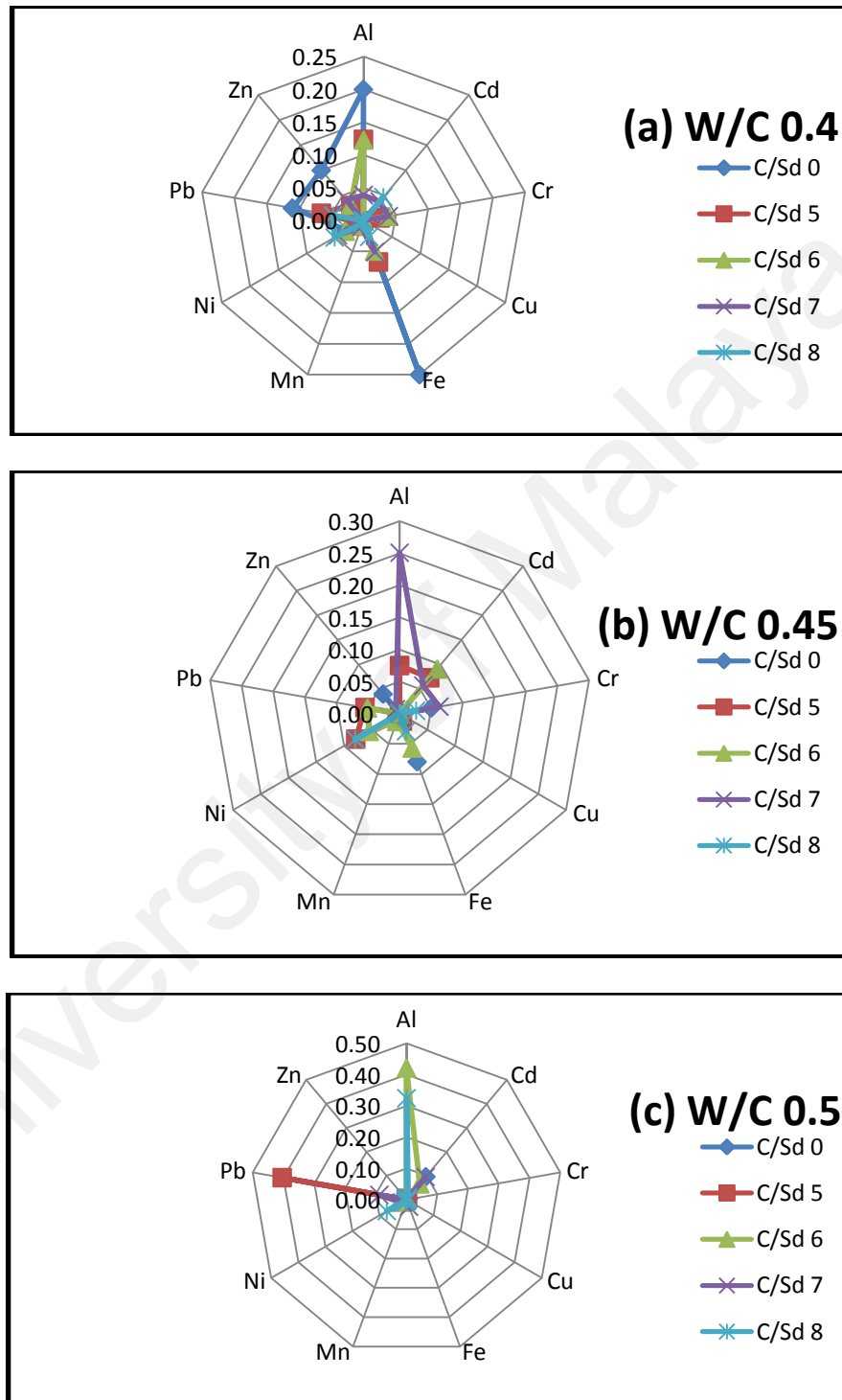
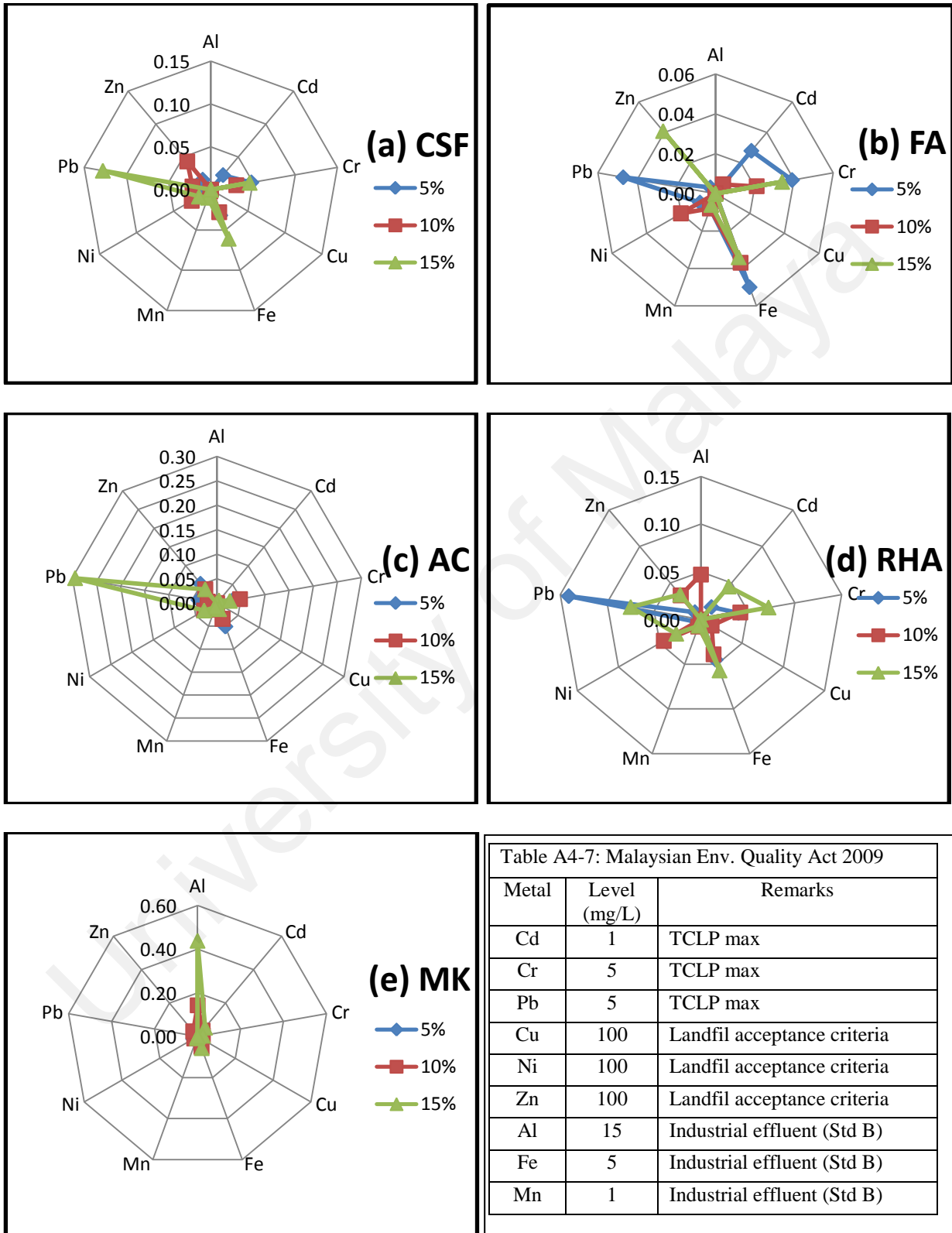
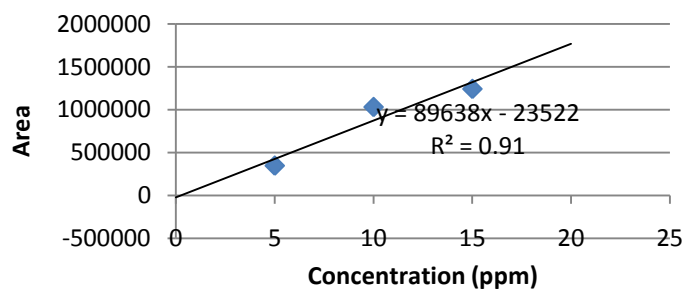


Figure C-2: Radar plots of metal concentration in TCLP extract for solidified sludge with CRMs (mg/L) and Malaysian Environmental Quality Act 2009



APPENDIX D: Calibration curves of volatiles organic analysis

Benzene



Benzene

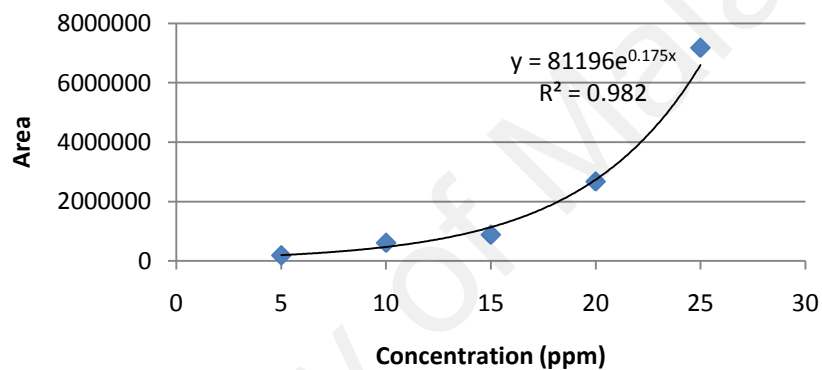
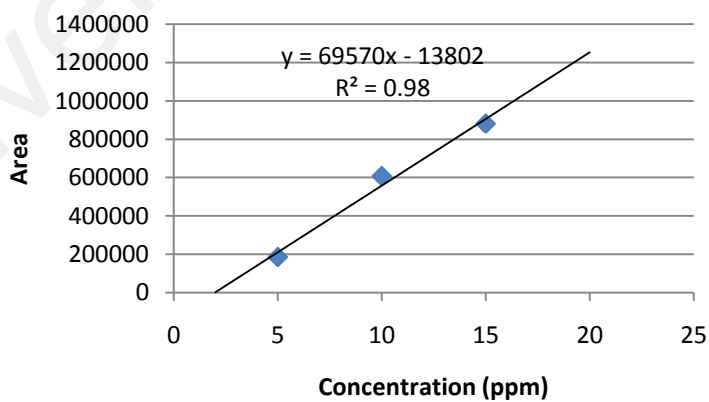


Figure D-1: Benzene calibration curves

Toulene



Toulene

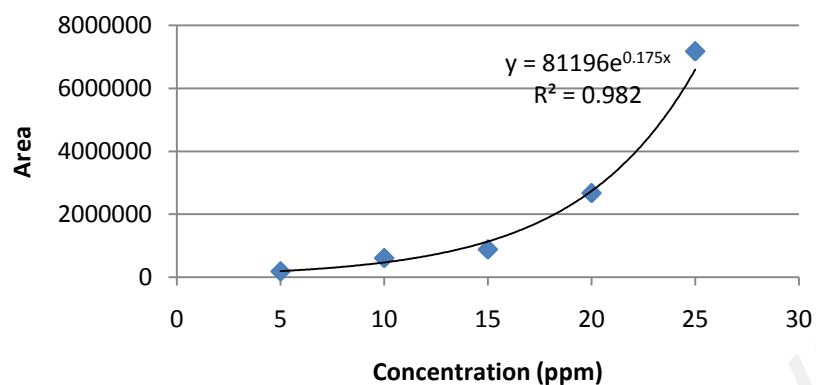
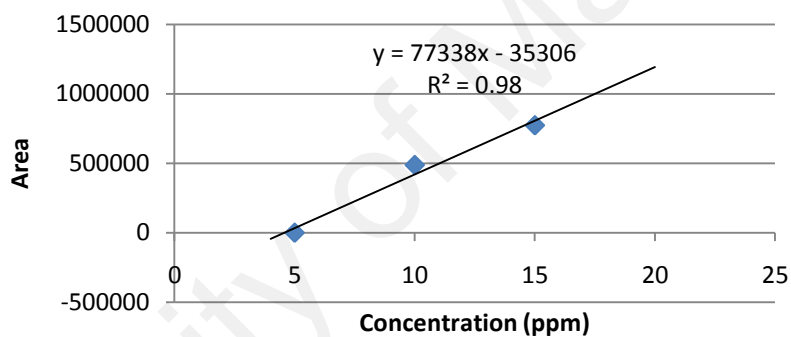


Figure D-2: Toulene calibration curves

Ethylbenzene



Ethylbenzene

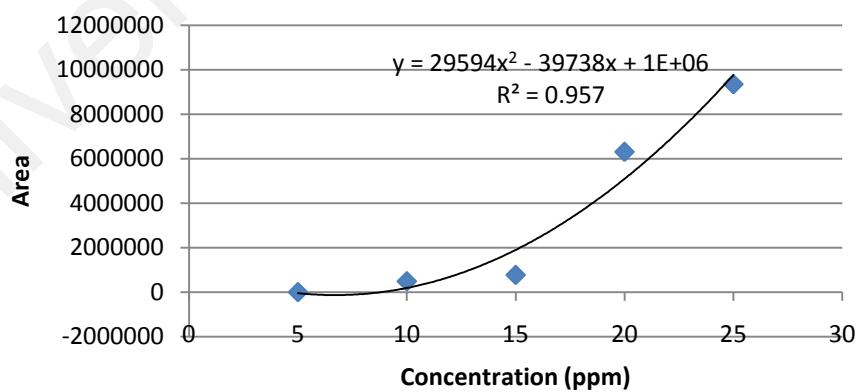
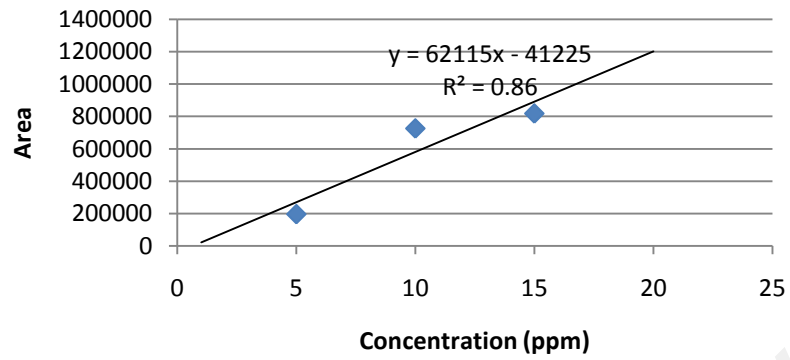


Figure D-3: Ethylbenzene calibration curves

o-Xylene



o-Xylene

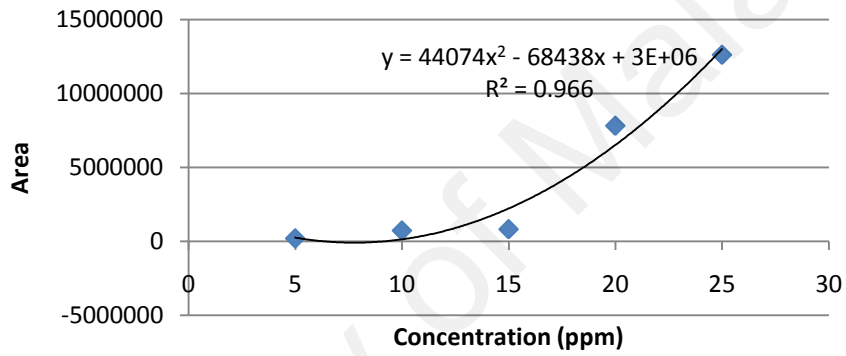
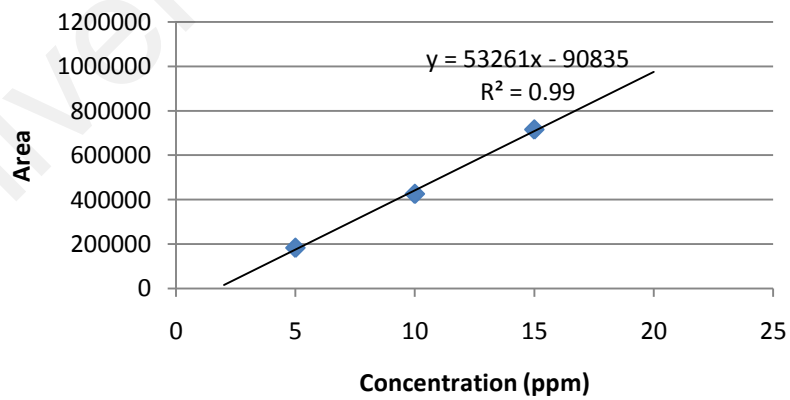


Figure D-4: o-Xylene calibration curves

m-Xylene



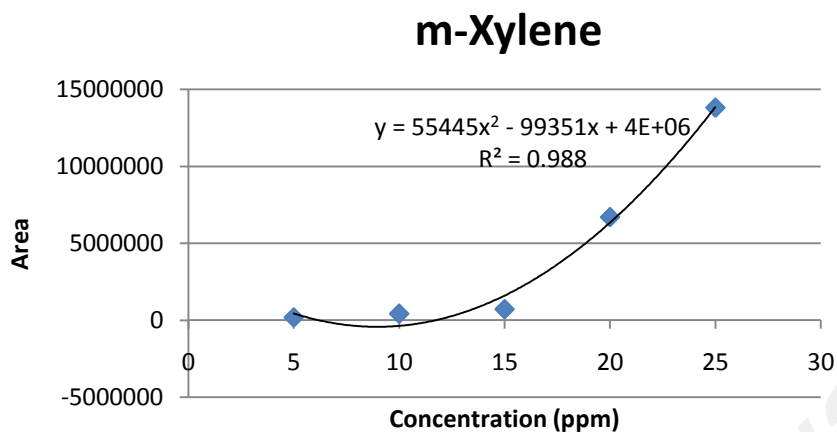


Figure D-5: m-Xylene calibration curves

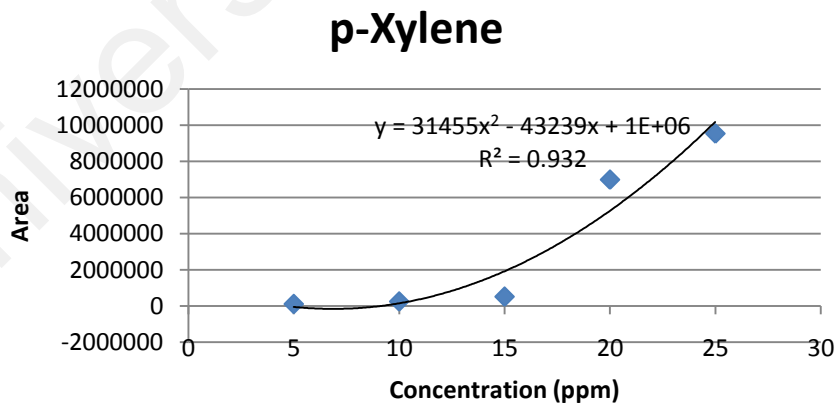
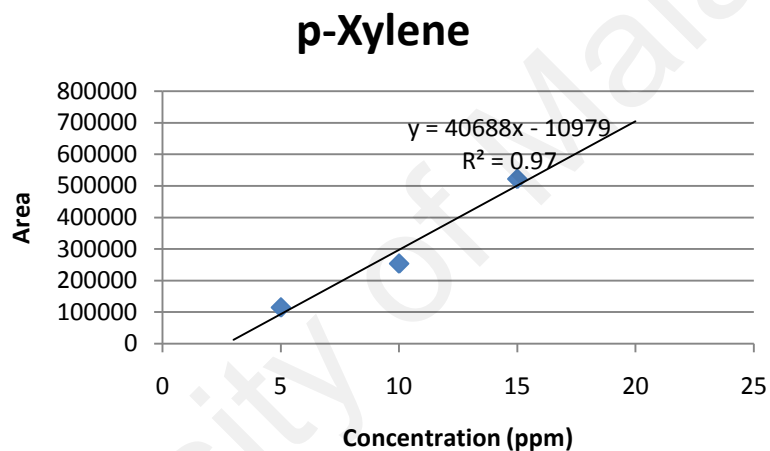


Figure D-6: p-Xylene calibration curves

Napthalene

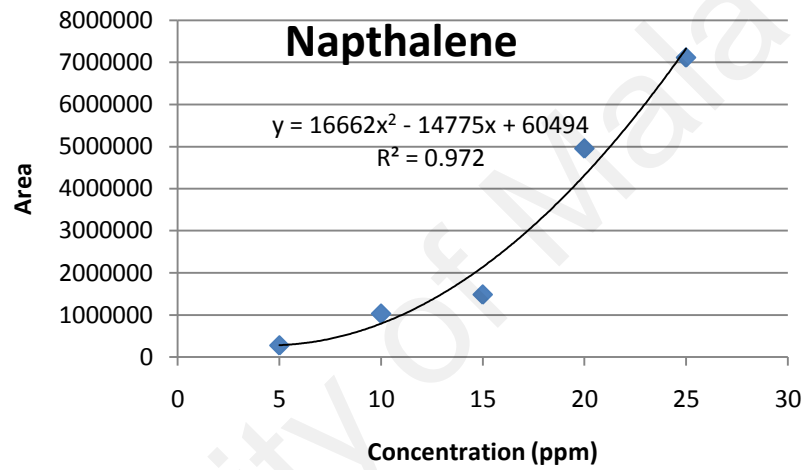
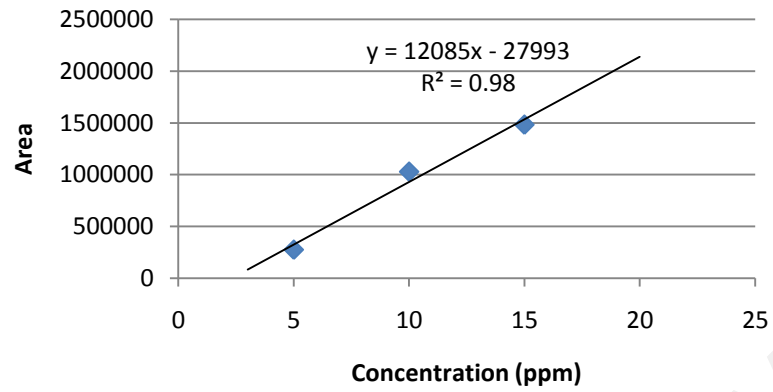
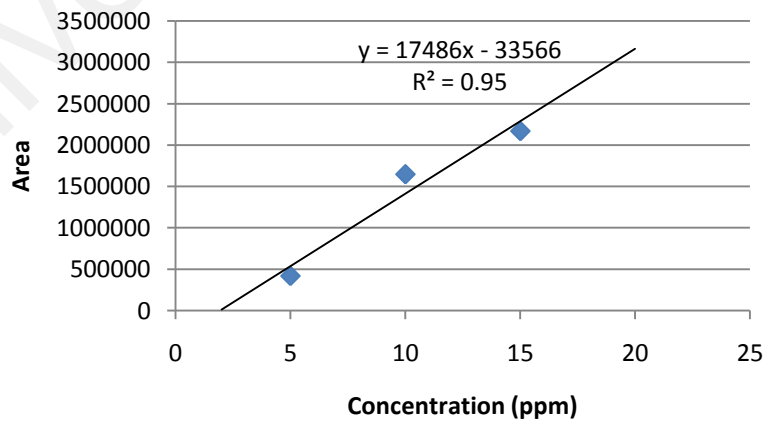


Figure D-7: Napthalene calibration curves

Phenanthrene



Phenanthrene

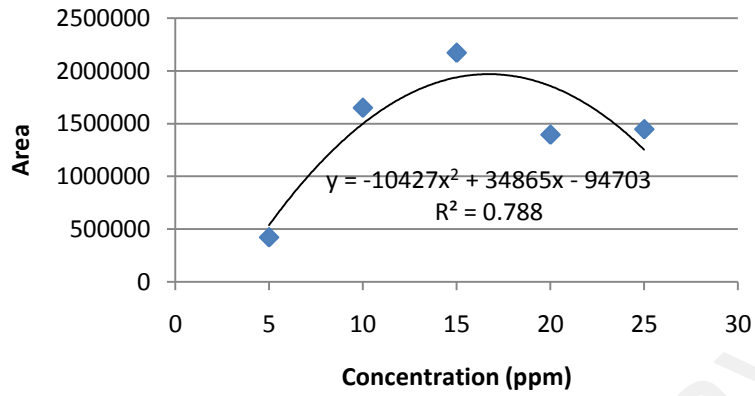


Figure D-8: Phenanthrene calibration curves

Chlorobenzene-d5

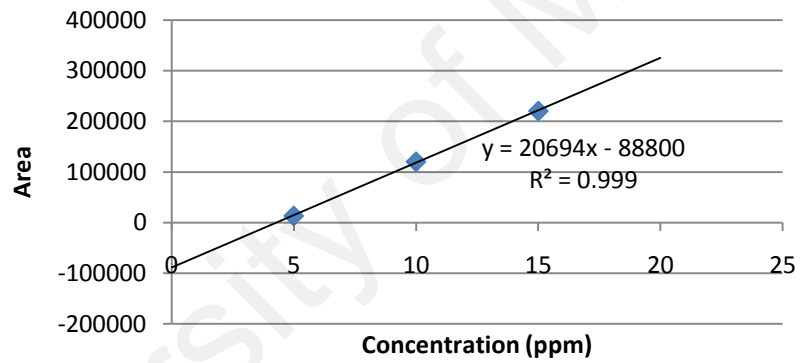


Figure D-9: Chlorobenzene-d5 calibration curve

Crysene-d12

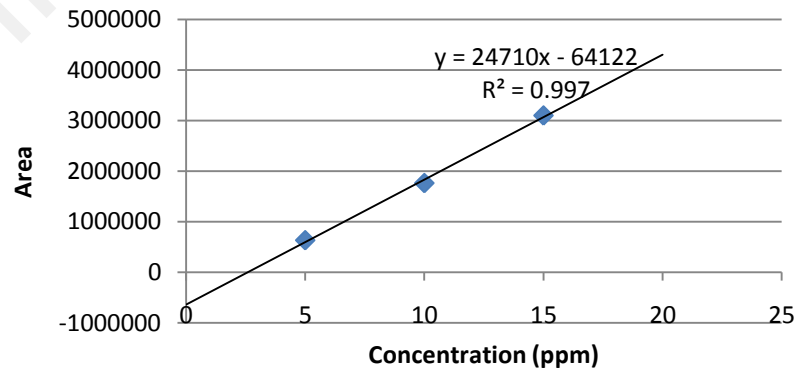


Figure D-10: Crysene-d12 calibration curve

Perylene-d12

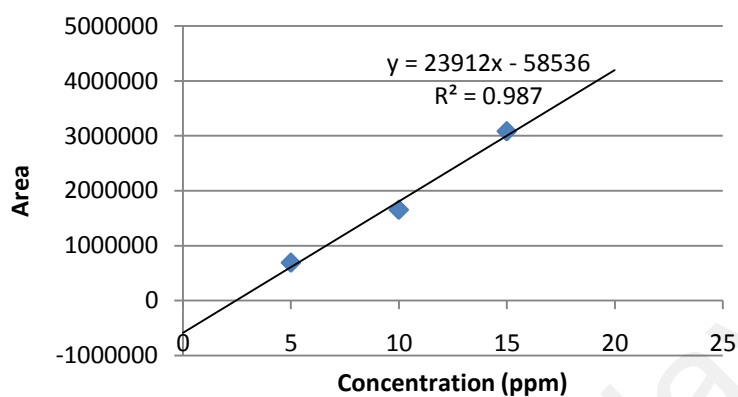


Figure D-11: Perylene-d12 calibration curve

Phenanthrene-d10

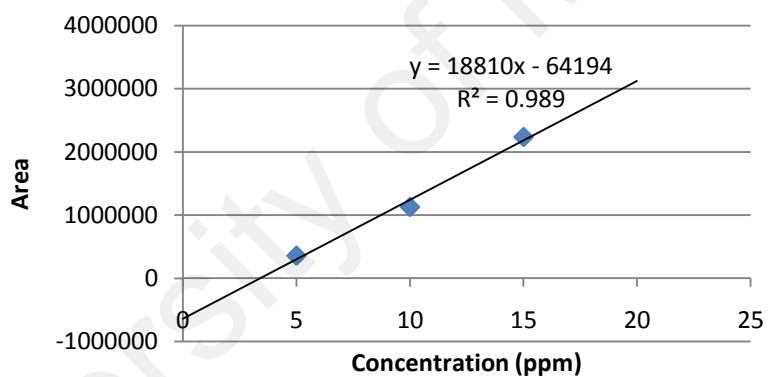


Figure D-12: Phenanthrene-d10 calibration curve

Pentafluorobenzene

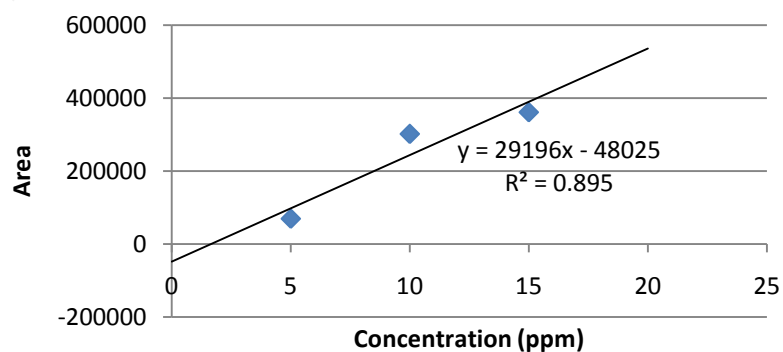


Figure D-13: Pentafluorobenzene calibration curve

1-4 Difluorobenzene

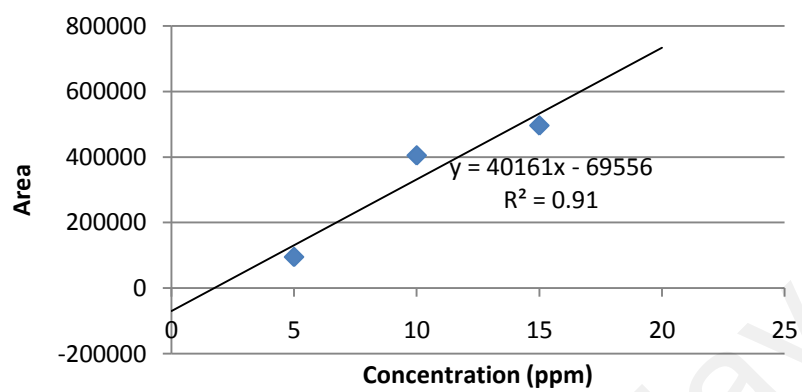


Figure D-14: 1-4-Difluorobenzene calibration curve

University of Malaya

APPENDIX E: Toxicity characteristic of constituents

Table E-1: Toxicity characteristics constituents U.S. EPA TCLP regulatory level (mg/L) –
Source 40 CFR 261.24

| Types | Contaminants | Regulatory level (mg/L) |
|---------------------------------|-------------------------|-------------------------|
| Metals: | Arsenic | 5.0 |
| | Barium | 100.0 |
| | Cadmium | 1.0 |
| | Chromium | 5.0 |
| | Lead | 5.0 |
| | Mercury | 0.2 |
| | Selenium | 1.0 |
| | Silver | 5.0 |
| Volatiles organic compounds: | Benzene | 0.5 |
| | Carbon tetrachloride | 0.5 |
| | Chlorobenzene | 100.0 |
| | Chloroform | 6.0 |
| | 1, 2-Dichloroethane | 0.5 |
| | 1, 1-Dichloroethylene | 0.7 |
| | Methyl ethyl ketone | 200.0 |
| | Tetrachloroethylene | 0.7 |
| | Trichloroethylene | 0.5 |
| | Vinyl chloride | 0.2 |
| Semivolatile volatile organics: | o-Cresol | 200.0 |
| | m-Cresol | 200.0 |
| | p-Cresol | 200.0 |
| | Cresol | 200.0 |
| | 1, 4-Dichlorobenzene | 7.5 |
| | 2, 4-Dinitrotoulene | 0.13 |
| | Hexachlorobenzene | 0.13 |
| | Hexachlorobutadiene | 0.5 |
| | Hexachloroethane | 3.0 |
| | Nitrobenzene | 2.0 |
| | Pentachlorophenol | 100.0 |
| | Pyridine | 5.0 |
| | 2, 4, 5-Trichlorophenol | 400.0 |
| 2, 4, 6-Trichlorophenol | 2.0 | |

APPENDIX F: List of publications

1. Mohd Zain, A., Shaaban, M.G and Mahmud, H., Waste Stabilization and Solidification Techniques by Cement as a Main Binder, TECHPOS, Int. Conf. for Technical Postgraduates 2009, 14-15 Dec 2009, Legend Hotel, KL, pp. 1-5.
2. Mohd Zain, A, Shaaban, M.G. and Mahmud, H., Petroleum Sludge Stabilization and Solidification by Ordinary Portland Cement, World Eng., Science and Technology Congress (EASTCON), Int. Conf. on Process Eng & Adv. Material/24th Symposium of Malaysian Chemical Engineers 2010, 15-17 June 2010 KLCC, pp. 1-4.
3. Mohd Zain, A, Shaaban, M.G. and Mahmud, H., Petroleum Sludge Stabilization and Solidification- An alternative treatment using ordinary Portland cement and rice husk ash, 2nd. Int. Conference on Biological, Chemical and Environmental Engineering (ICBEE 20101), 2-4 Nov 2010, Cairo, Egypt, pp. 1-5.
4. Mohd Zain, A, Shaaban, M.G. and Mahmud, Immobilization of petroleum sludge incorporating Portland cement and rice husk ash, International Journal of Chemical Engineering and Application, Vol 1 No. 3, IACSIT, 2010 Singapore pg 1-5.
5. Mohd Zain, A, Shaaban, M.G. and Mahmud, H., Organic compounds in solidified petroleum sludge and leachate, World Eng., Science and Technology Congress (EASTCON), Int. Conf. on Process Eng & Adv. Material 2012, 12-13 June 2012 KLCC, pp. 1-4.
6. Mohd Zain, A, Shaaban, M.G. and Mahmud, H., Leachability of Solidified Petroleum Sludge, Submitted to J. Applied Science. Nov 2012.